frontiers | Research Topics

Central vertigo and dizziness

Edited by
David Samuel Zee, Dominik Straumann,
Ji Soo Kim and Miriam Welgampola

Published in
Frontiers in Neurology

ISSN 1664-8714
ISBN 978-2-83250-841-1
DOI 10.3389/978-2-83250-841-1

About Frontiers

Frontiers is more than just an open access publisher of scholarly articles: it is a pioneering approach to the world of academia, radically improving the way scholarly research is managed. The grand vision of Frontiers is a world where all people have an equal opportunity to seek, share and generate knowledge. Frontiers provides immediate and permanent online open access to all its publications, but this alone is not enough to realize our grand goals.

Frontiers journal series

The Frontiers journal series is a multi-tier and interdisciplinary set of open-access, online journals, promising a paradigm shift from the current review, selection and dissemination processes in academic publishing. All Frontiers journals are driven by researchers for researchers; therefore, they constitute a service to the scholarly community. At the same time, the *Frontiers journal series* operates on a revolutionary invention, the tiered publishing system, initially addressing specific communities of scholars, and gradually climbing up to broader public understanding, thus serving the interests of the lay society, too.

Dedication to quality

Each Frontiers article is a landmark of the highest quality, thanks to genuinely collaborative interactions between authors and review editors, who include some of the world's best academicians. Research must be certified by peers before entering a stream of knowledge that may eventually reach the public - and shape society; therefore, Frontiers only applies the most rigorous and unbiased reviews. Frontiers revolutionizes research publishing by freely delivering the most outstanding research, evaluated with no bias from both the academic and social point of view. By applying the most advanced information technologies, Frontiers is catapulting scholarly publishing into a new generation.

What are Frontiers Research Topics?

Frontiers Research Topics are very popular trademarks of the *Frontiers journals series*: they are collections of at least ten articles, all centered on a particular subject. With their unique mix of varied contributions from Original Research to Review Articles, Frontiers Research Topics unify the most influential researchers, the latest key findings and historical advances in a hot research area.

Find out more on how to host your own Frontiers Research Topic or contribute to one as an author by contacting the Frontiers editorial office: frontiersin.org/about/contact

Central vertigo and dizziness

Topic editors

David Samuel Zee — Johns Hopkins University, United States
Dominik Straumann — University of Zurich, Switzerland
Ji Soo Kim — Seoul National University, South Korea
Miriam Welgampola — The University of Sydney, Australia

Citation

Zee, D. S., Straumann, D., Kim, J. S., Welgampola, M., eds. (2023). *Central vertigo and dizziness*. Lausanne: Frontiers Media SA. doi: 10.3389/978-2-83250-841-1

Table of contents

frontiers in Neurology

ORIGINAL RESEARCH
published: 31 March 2022
doi: 10.3389/fneur.2022.818533

Cerebral Small Vessel Disease in Elderly Patients With Vestibular Neuritis

Fieke K. Oussoren[1,2], Louise N. F. Poulsen[3], Joost J. Kardux[3], Tjard R. Schermer[1], Tjasse D. Bruintjes[1,2] and Roeland B. van Leeuwen[1]*

[1] Apeldoorn Dizziness Centre, Gelre Hospital, Apeldoorn, Netherlands, [2] Department of Otorhinolaryngology, Leiden University Medical Center, Leiden, Netherlands, [3] Department of Radiology, Gelre Hospital, Apeldoorn, Netherlands

Background: Acute audiovestibular loss is a neurotologic emergency of which the etiology is frequently unknown. In vestibular neuritis a viral genesis is expected, although there is insufficient evidence to support viruses as the only possible etiological factor. In sudden deafness, a vascular etiology has been proposed in elderly patients, since cardiovascular risk factors are more frequently present and a higher risk of developing a stroke was seen compared to the general population. So far, very little research has been carried out on vascular involvement in elderly patients with vestibular neuritis. Cardiovascular risk factors have a positive correlation with cerebral small vessel disease, visible as white matter hyperintensities, brain infarctions, microbleeds and lacunes on MRI. The presence of these characteristics indicate a higher risk of developing a stroke.

Aim: We investigated whether elderly patients with vestibular neuritis have a higher prevalence of vascular lesions on MRI compared to a control cohort.

Materials and Methods: Patients of 50-years and older, diagnosed with vestibular neuritis in a multidisciplinary tertiary referral hospital, were retrospectively reviewed and compared to a control cohort. The primary outcome was the difference in cerebral small vessel disease on MRI imaging, which was assessed by the number of white matter hyperintensities using the ordinal Fazekas scale. Secondary outcomes were the presence of brain infarctions on MRI and the difference in cardiovascular risk factors.

Results: Patients with vestibular neuritis ($N = 101$) had a 1.60 higher odds of receiving a higher Fazekas score than the control cohort ($N = 203$) ($p = 0.048$), there was no difference in presence of brain infarctions ($p = 1.0$). Hyperlipidemia and atrial fibrillation were more common in patients experiencing vestibular neuritis.

Conclusion: We found a positive correlation of white matter hyperintensities and VN which supports the hypothesis of vascular involvement in the pathophysiology of vestibular neuritis in elderly patients. Further prospective research is necessary to confirm this correlation.

Keywords: stroke, vestibular neuritis (VN), MRI, white matter hyper intensities, vascular etiology

OPEN ACCESS

Edited by:
Ji Soo Kim,
Seoul National University, South Korea

Reviewed by:
Giovanna Viticchi,
Marche Polytechnic University, Italy
Richard Ibitoye,
Imperial College London, United Kingdom

****Correspondence:***
Fieke K. Oussoren
f.oussoren@gelre.nl

Specialty section:
This article was submitted to Neuro-Otology, a section of the journal Frontiers in Neurology

Received: *19 November 2021*
Accepted: *21 February 2022*
Published: *31 March 2022*

Citation:
Oussoren FK, Poulsen LNF, Kardux JJ, Schermer TR, Bruintjes TD and van Leeuwen RB (2022) Cerebral Small Vessel Disease in Elderly Patients With Vestibular Neuritis. Front. Neurol. 13:818533. doi: 10.3389/fneur.2022.818533

INTRODUCTION

Acute audiovestibular loss is a neurotologic emergency. The cause of vestibular neuritis (VN), sudden sensorineural hearing loss (SSNHL) or labyrinthitis is unknown in a significant number of cases (1, 2).

Recently, research has focused on a possible vascular cause of audio and vestibular loss (3–6). An acute onset of symptoms and frequently unilateral presentation resemble acute cardiovascular diseases.

Very little information is available on vascular involvement in VN. It is believed to be an inflammatory disorder of viral origin (7). However, patients do not show clinical benefit from antiviral therapy or corticosteroid use (8, 9). The question is whether VN might have a different etiology and, consequently, a different therapy should be applied.

Because of its relatively high incidence, SSNHL has been studied frequently. Compared to the general population, cardiovascular risk factors are more frequently present in patients with SSNHL (3, 10, 11). Subsequently, several authors have investigated the chance of developing a stroke in patients with SSNHL. These studies show that, after correction for age and other cardiovascular risk factors, patients with sudden hearing loss have a 1.26–2.02 higher chance of developing a stroke than the general population (12–15).

A vascular compromised brain raises the chance of developing a stroke. On magnetic resonance imaging (MRI) imaging, cerebral small vessel disease (CSVD), visible as white matter hyperintensities (silent), brain infarctions and microbleeds have shown to be indicative of developing stroke (16–19).

With this study we investigated whether patients with VN have more CSVD on MRI compared suggesting a vascular involvement in the pathophysiology of VN.

MATERIALS AND METHODS

Setting

This retrospective case-control study was based upon hospital records from patients either visiting the emergency departments of Gelre Hospital Apeldoorn and Zutphen, the outpatient neurology clinic or the Apeldoorns Dizziness Centre (ADC), located in Gelre hospital. The ADC serves as a tertiary referral center that specializes in the diagnostic and therapeutic workup of dizziness. It is a multidisciplinary center involving the Neurology, Clinical neurophysiology and Otorhinolaryngology departments of the Gelre Hospital Apeldoorn. This retrospective cohort study gained ethical approval from the local ethics committee at Gelre Hospital Apeldoorn.

Cohorts

A study cohort was compiled of patients diagnosed with vestibular neuritis between January 2010 and March 2021 who received an MRI cerebrum. Patients either presented at the emergency departments of both Gelre hospitals or at the outpatient Apeldoorn dizziness centre.

Vestibular neuritis was defined as a single episode of acute, severe vertigo lasting for at least 24 h in the absence of auditory symptoms or neurological symptoms, with or without loss of vestibular function measured with caloric testing. VN was distinguished from acute stroke either by a positive head impulse test, by the presence of unidirectional horizontal nystagmus, by the absence of skew deviation (HINTS) or by the absence of an infarction on MRI. At the emergency departments patients the diagnostic tests were performed by different physicians.

The control cohort was compiled of patients who either visited the outpatient neurological department with facial pain, suspected for trigeminal neuralgia, or patients who visited the ADC with recurrent episodes of spontaneous vertigo lasting several seconds, suggestive of vestibular paroxysmia. All patients received an MRI cerebrum to rule out the presence of an intracranial neoplasm.

Exclusion criteria were age 49 years or younger and a history of cerebrovascular accident or transient ischemic attack. If during follow-up the type of dizziness changed and did not meet the aforementioned criteria of VN, these patients were excluded. Patients were also excluded if the MRI was performed more than a year after presentation at either the emergency department or the outpatient dizziness clinic.

MRI Protocol

An MRI was suitable for radiological assessment of white matter hyperintensities and brain infarctions if at least one sequence of the entire brain, either FLAIR or T2, was available. The imaging was performed using a 1.5 Tesla MRI scanner. The cerebral sequence was depicted with a slice thickness of 5 mm. Twenty-three MRI scans were performed elsewhere and uploaded in the Gelre Hospital database, two of these scans had a slice thickness of 4 mm, and the remaining had a slice thickness of 5 mm. The type of MRI scanner used for these external MRIs could not be retrieved.

Outcomes

The primary outcome was the degree of cerebral vascular damage assessed on MRI imaging by measuring the Fazekas score. The Fazekas score is a validated diagnostic tool for assessing the severity of white matter hyper-intensities both periventricular and in the deep white matter with a possible score from 0 to 6, where 0 means no hyperintensities present, (see **Figure 1**).

A secondary outcome was the presence of brain infarctions on MRI imaging. Brain infarctions were defined by lesions of the brain of at least 3 mm with a cerebrospinal fluid appearance on all MRI sequences, differentiable from leukariosis and dilated Virchow-Robinson spaces that did not result in prior neurological deficits (20).

Another secondary outcome was the difference in the presence of the cardiovascular risk factors; smoking, hypertension, hyperlipidemia, diabetes, a history of myocardial infarction and atrial fibrillation between the SSNHL and control cohort. The following assumptions were made in the identification of cardiovascular risk factors. Hypertension and diabetes were defined as being present either by having a positive medical history or if medication for these conditions were used. In case

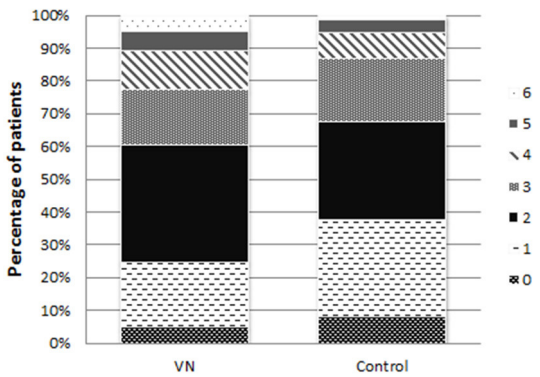

FIGURE 1 | Fazekas scale for MRI imaging. The figure displays hyperintensities in the deep white matter (upper row) and periventricular (lower row).

no complete medical history had been obtained, the variable was defined as missing. Hyperlipidemia was defined as being present when the patient had a positive medical history of dyslipidemia, used statins, or had an elevated total cholesterol level of >4.9 mmol/L within a month before or after presentation at our dizziness centre.

Assessment

MRI imaging was assessed by two radiologists separately, LP and JK. The two radiologists involved in this study have multiple years of experience in examining MRI imaging of the head and neck. To limit observer bias, both radiologists were blinded for the patients' characteristics or study arm.

If there was a difference in Fazekas rating between the two raters, the following rules were applied. If the difference was 1 rank, the highest rank was then applied. If the difference was 2 ranks or more, the radiologists reviewed the case together until consensus was reached.

Baseline characteristics, data from diagnostic tests and MRI ratings were gathered and de-identified in a Castor electronic database (CastorECD, Amsterdam, The Netherlands).

Rater Reliability Testing

Inter- and intra-rater reliability for the two radiologists was assessed for the Fazekas rating scale using the present control cohort plus a cohort of patients who suffered from sudden sensorineural hearing loss. All patients were rated by the same raters involved in the present study. Sample size calculation showed that thirty patients had to be rated twice by both raters to evaluate the intra-rater reliability. A weighted Cohens' kappa coefficient was calculated using linear weighting, where the difference between low and high ratings is of equal importance.

Statistical Analysis

Continuous variables were described using the following summary descriptive statistics: number of non-missing values, mean and standard deviation in case of normally distributed data or median and interquartile ranges in case of non-normally distributed data.

Categorical variables were described using frequencies and percentages. Percentages were calculated on the number of non-missing observations.

Ninety-five confidence intervals were calculated when applicable. Statistical testing was performed two-sided at a 0.05 significance level.

Differences in the ordinal ranking of the Fazekas scale between the two cohorts were calculated using the Mann-Whitney U test for ordinal non-paired data.

Because the presence of brain infarctions is a binary variable, the difference between the cohorts was compared using the Chi-square test.

Ordinal logistic regression analysis was performed to compare the outcomes between the cohorts while adjusting for the potential confounders: age, hypertension, hyperlipidemia, diabetes, a medical history of MI, smoking, gender, an outpatient or inpatient presentation, the presence of vestibular loss with an abnormal video head impulse testing or abnormal caloric testing and the type of MRI sequence used.

RESULTS

Patient Characteristics

A total of 101 patients with VN were included. The control cohort consisted of 203 patients, 149 suspected cases of trigeminal neuralgia and 54 suspected cases of vestibular paroxysmia. In the vestibular neuritis cohort, 50 patients were diagnosed upon presentation at the emergency department while 51 patients were diagnosed at the outpatient clinic of the Apeldoorn Dizziness Centre. None of the VN patients demonstrated bilateral vestibular dysfunction.

Baseline characteristics of both cohorts are displayed in **Table 1**. The mean age did not differ significantly between both cohorts. Both study cohorts consisted of more women than men.

In patients with VN, hyperlipidemia and atrial fibrillation were significantly more common. Also a medical history of myocardial infarction, smoking and hypertension were more frequently present in the VN cohort, though not statistically significant. Diabetes was more frequently present in the control cohort, also not statistically significant.

In case of presentation at the emergency department, the MRI was made after 24 h in only six cases. All other patients received an MRI within 24 h up to several days after the onset of symptoms. The MRI of 31 (30.7%) patients in the VN cohort was assessed using a T2 sequence compared to 106 (52.2%) in the control cohort ($p < 0.001$).

Rater-Reliability Testing

All 328 MRI scans were reviewed by both raters. In 201 cases both radiologists gave the same Fazekas score, in 103 cases they differed one point and in 24 cases the difference in score given was two points or more. This resulted in a kappa-coefficient of 0.74 for inter-rater reliability.

TABLE 1 | Patient characteristics.

	VN ($N = 101$)	Control ($N = 203$)	Missing	*P*-value
Age [mean, (SD)]	64 (9.8)	63 (9.4)	0	0.423
*50–60	42 (41.6)	100 (49.3)	0	0.469
*61–70	28 (27.7)	56 (27.6)	0	
*71–80	28 (27.7)	41 (20.2)	0	
* >80	3 (3.0)	6 (3.0)	0	
Gender			0	0.460
Male	56 (55.4)	123 (60.6)		
Female	45 (44.6)	80 (39.4)		
Prior myocardial infarction	4 (4.0)	7 (3.4)	0	1.000
Anticoagulant use	12 (11.9)	21 (10.3)	0	0.700
Smoking			27	0.073
Former	21 (22.6)	25 (13.6)		
Yes	6 (6.5)	23 (12.5)		
Hypertension	35 (36)	67 (33.3)	6	0.700
Hyperlipidemia	52 (51.5.0)	63 (31.0)	0	0.001
Diabetes	7 (6.9)	20 (9.9)	0	0.522
Atrial fibrillation	8 (7.9)	4 (2.0)	0	0.023

*Patient characteristics of 101 patients with vestibular neuritis and a control cohort of 203 patients displayed in numbers and percentages. For age the mean and standard deviation are displayed. N, number; SD, standard deviation; VN, vestibular neuritis. * Age stratified by decades.*

Thirty subjects were rated twice by each rater, which resulted in a weighted kappa-coefficient of 0.80 and 0.82 for rater 1 and 2, respectively, suggesting a near-perfect agreement for each rater.

Fazekas Score

The distribution of Fazekas ratings in both cohorts is displayed in **Figure 2**.

The modus of the Fazekas score was 2 in both cohorts. The group that received Fazekas 5 and 6 form a larger proportion of cases in the VN cohort than in the control cohort. Therefore, the ordinal differed statistically significant ($p = 0.023$).

Ordinal Regression Analysis

Table 2 displays the results of the ordinal regression analysis. In a univariate regression analysis only the variables neuritis, hypertension and age all significantly increased the risk of a higher Fazekas score. The remaining cardiovascular risk factors and diagnostic characteristics did not influence the Fazekas score.

After adding hypertension and age to the model, patients with vestibular neuritis had a 1.60 (95%CI 1.01–2.42, $p = 0.048$) higher odds of having a higher Fazekas score. Age also significantly increased the odds of white matter hyperintensities on MRI.

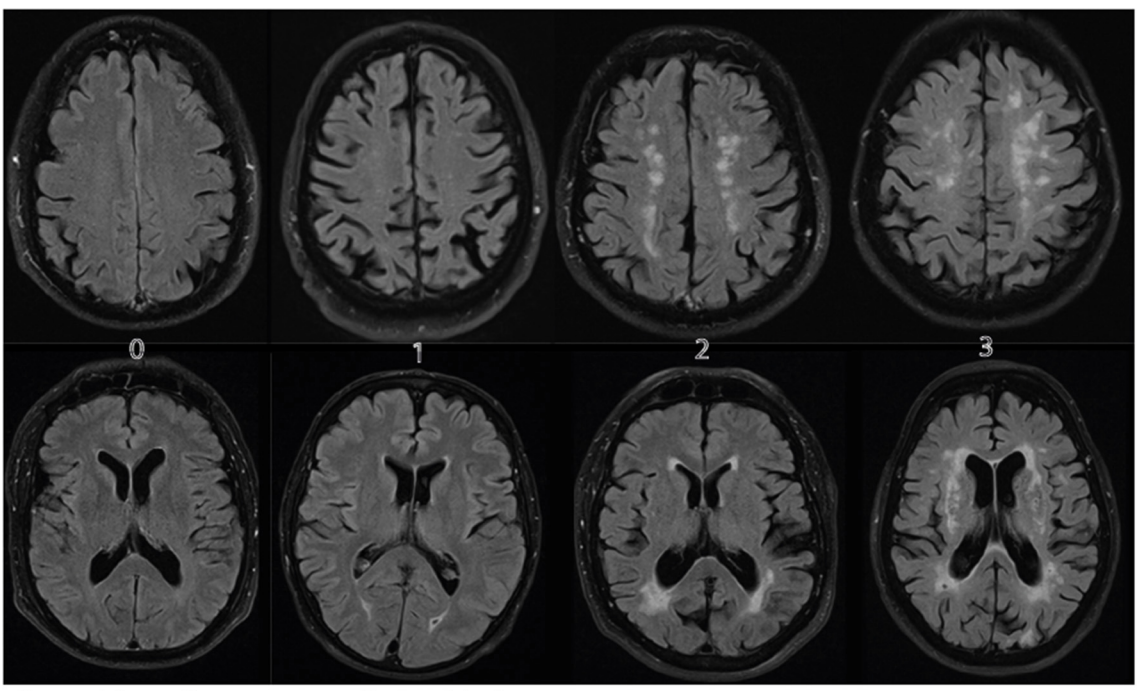

FIGURE 2 | Fazekas distribution. The distribution of the Fazekas scale score 1 up to 6 over the both cohorts displayed in percentages. VN, vestibular neuritis.

TABLE 2 | Ordinal regression analysis.

Variable	Univariate			Multivariate		
	Odds	Sig	95% CI	Odds	Sig	95% CI
Neuritis	2.10	0.012*	1.26–3.83	1.6	0.048*	1.01–2.42
Age	1.11	0.000*	1.08–1.13	1.10	0.000*	1.07–1.13
Diabetes	0.96	0.909	0.47–1.94			
Gender	1.11	0.628	0.74–1.66			
History of MI	2.46	0.100	0.84–7.15			
Hyperlipidemia	1.22	0.358	0.81–1.85			
Hypertension	2.48	0.000*	1.60–3.84	1.52	0.067	0.97–2.39
Smoking	1.00	0.997	0.73–1.37			
Abnormal caloric testing	1.02	0.928	0.63–1.66			
Abnormal video-HIT	1.17	0.717	0.50–2.73			
Outpatient presentation	0.85	0.648	0.42–1.71			
MRI Sequence (FLAIR)	1.48	0.058	0.99–2.22			

*Regression analysis for Fazekas score. FLAIR, Fluid Attenuated Inversion Recovery; HIT, head impulse test; CI, Confidence interval; MI, myocardial infarction; MRI, Magnetic Resonance Imaging; Sig, significance; * Significant at level $p < 0.05$.*

Brain Infarctions

Brain infarctions were present in 10 (9.9%) cases with VN and 21 (10.4%) cases in the control cohort. The difference between the two cohorts was not significant (p-value = 1.0).

In both cohorts, most brain infarctions were located in the deep white matter, in five patients from the VN cohort and seven from the control cohort. The cerebellum was affected in three patients with VN and seven controls. In five control patients an infarction was located in the basal ganglia, while none of the patients with VN had lesions in this region. In only one patient with vestibular neuritis a cortical infarction was seen, compared to four patients in the study cohort. In both cohorts the brainstem was not affected. Due to the limited number of cerebral infarctions, a regression analysis was not performed.

DISCUSSION

We found a positive correlation between VN and CSVD on MRI imaging. Patients with VN had a 1.60 odds of receiving a higher Fazekas rating compared to the control cohort. Very few brain infarctions were seen in both groups resulting in no significant difference between the study cohorts. All cardiovascular risk factors, apart from diabetes, were more frequently present in the study cohort. However, the difference in prevalence was only statistically significant for hyperlipidemia and atrial fibrillation.

Literature on vascular involvement in the pathophysiology of VN is limited. We based our hypothesis upon the following train of thought. VN is generally expected to be the result of inflammation secondary to viral infection. VN often has a viral prodrome and latent herpes simplex virus type 1 has been detected in human vestibular ganglia with PCR (21). Also, postmortem studies showed atrophy of the vestibular nerve and sensory epithelium, similar to pathological alterations seen in inner ear infections with measles (22–25). Nevertheless, corticosteroid and antiviral therapy have failed to show clinical benefit in the treatment of VN (8, 9).

The current treatment in the Netherlands is symptomatic with vestibular suppressants and anti-emetics. The question is whether VN can be solely contributed to a viral infection or if a different pathophysiology is probable. Since the ear and vestibular organ have limited collateral blood supply, it is particularly vulnerable to blood pressure dysregulation or acute occlusion.

Blood pressure dysregulation (BPD) in the vestibulocochlear blood circulation was first described by Fisch et al. (26). Cochlear atherosclerosis, related to cardiovascular risk factors as age, hypertension, diabetes, hyperlipidemia and smoking, results in a pathologic alteration in the composition of the arteries and arterioles. Hyalinosis causes thickening of the tunica adventitia, while the number of fibromuscular cells is reduced, which induces a decrease in adrenergic regulation (27). Meanwhile, due to arteriosclerosis, the internal caliber of the arteriole is reduced. This combination of blood pressure dysregulation secondary to reduced adrenergic regulation and shrinking of the arterial lumen results in damage to the vestibular nerve fibers (28, 29).

Acute onset vertigo or sudden sensorineural hearing loss, with or without vertigo, can also be caused by acute occlusion somewhere along the course of the anterior inferior cerebellar artery. After studying the vascular structure of the inner ear, Tange et al. came up with a theoretical flowchart depicting obstruction lines and the expected symptoms caused by this obstruction (30). In case of acute arterial occlusion, one would expect a patient to present with combined audiovestibulopathy, because of the common vascular supply to the cochlea and vestibule by the internal auditory artery.

A third argument supporting a vascular hypothesis of VN is based upon microvascular occlusion secondary to inflammation either due to viral infection or auto-immune response. Freedman et al. found a significantly elevated expression of CD40 positive monocytes and macrophages in patients with VN (31). These cells are known to cause platelet-monocytes aggregates that might cause thrombotic changes in the vascular system. A significantly increased expression of cyclooxygenase−2 (COX-2) was also found in patients with VN (32). This enzyme is responsible for vasodilatation and is generally present in the peripheral blood mononuclear cells (PBMC's) of patients with cardiovascular comorbidity (32, 33). It is suggested that the proinflammatory activation of PBMC's and elevation of CD 40 expression reduces the microvascular perfusion of the vestibular organ by increased thrombotic events, resulting in loss of function of the vestibular organ.

Since the cochlea is supplied by the same vascular system as the vestibular organ, a similar hypothesis of vascular compromise in the origin SSNHL has gained considerable attention. Hypoperfusion due to arteriosclerosis and BPD is thought to result in damage of the stria vascularis and subsequent hearing loss. Ciorba et al. and Fusconi et al. have investigated the presence of white matter hyperintensities as an indicator of cerebral small vessel disease in patients with SSNHL (34, 35). Ciorba et al. found no difference in the incidence of WMH, they did, however, find a correlation between more WMH and a poorer hearing recovery (34). Fusconi et al. found more WMH in individuals aged 40–60 in the SSNHL subset and also correlated this to a poorer rearing recovery (35). Several other authors found

a higher incidence of stroke following SSNHL than in the general population (12, 14, 15).

Oron et al. investigated the presence of cardiovascular risk factors in patients with VN compared to the general population (36). They found a significantly higher presence of dyslipidemia, hypertension, diabetes, ischemic heart disease, prior CVA/TIA, cigarettes smoking, and obesity when compared to healthy controls. Their study cohort consisted of 160 patients with VN with a mean age of 56 years old, which is a larger but also younger study populations than our cohort. Age was a significant contributor of the prevalence in cardiovascular risk factors. For this exact reason our study population consisted only of patients 50 years of age or older. Since age is known to be an important risk factor for both CSVD and the risk of developing stroke, we corrected for age in a multivariate regression analysis. After correction, patients in the VN cohort still had increased odds of having a higher degree of white matter hyperintensities.

Chung et al. also investigated a possible vascular etiology in VN (37). They compared metabolic syndrome scores and arterial stiffness, using brachial ankle pulse wave velocity, between patients with VN and controls (37). They found an increased arterial stiffness and hypothesized that this increase might reflect endothelial dysfunction and microvascular compromise in patients with VN. Since arterial stiffness can affect small vessel in the brain it could lead to cerebral small vessel disease (38).

Adamec et al. previously demonstrated that white matter supratentorial lesions and older age reduced the odds of clinical recovery after VN (39). They speculated that because of interaction with central compensatory mechanisms, white matter lesions can influence the clinical recovery after VN (39).

This is the first study to compare cerebral small vessel disease in elderly patients with VN to a control cohort. The positive association that was found could have significant clinical implications since cerebral vascular damage increases the risk of developing cardiovascular disease. According to Fazekas et al. cerebral microbleeds, white matter hyperintensities, silent brain infarctions and lacunes are indicators of cognitive impairment and stroke (16–18). The presence of these indicators in patients with VN should henceforth caution the physician for vascular involvement in VN.

We need to address some limitations that are unavoidable as a consequence of the retrospective study design. As explained in the method section, several assumptions were made in the recording of cardiovascular risk factors. This could have resulted in some underestimation of the presence of these risk factors. However, there is no reason to suspect that this underestimation differed between both cohorts.

Also, we did not use a standardized sequence schedule for MRI assessment. In some patients, the Fazekas score and presence of brain infarctions were evaluated on a FLAIR sequence, while in others a T2 sequence was used. White matter hyperintensities and brain infarctions can be seen on both sequences and the slice-thickness did not differ between patients. Furthermore, the type of MRI sequence used did not correlate with the Fazekas score in the regression analysis.

As opposed to Menière's disease or vestibular migraine, there are no universally accepted criteria for the clinical diagnosis of vestibular neuritis. HINTS was proven to be superior to MRI in differentiating VN from a stroke in the acute phase (40). The accuracy of diagnosing VN is determined predominantly by the physicians' experience in performing and interpreting these diagnostic tests. Since the patients presenting in the emergency departments were diagnosed by different physicians with different levels of competence in performing these diagnostic tests, this might have influenced the selected study cohort. In a univariate regression analysis, the outpatient presentation did not influence the degree of white matter hyper intensities in patients with vestibular neuritis.

Also, not all patients with VN receive an MRI. An MRI is usually performed to exclude a central cause of the dizziness. Patients who received an MRI might have had more severe dizziness than patients who did not receive imaging or had an unclear diagnosis at first. This might have resulted in some selection bias.

Finally, resilience, the capacity to cope with brain pathology is a factor that can be influenced by cerebral small vessel disease (28). Patients with a high degree of cerebral small vessel disease might develop more severe symptoms after vestibular neuritis than patients with limited small vessel disease, since they have limited brain reserve, i.e., white matter structural integrity, to compensate the loss of vestibular function. While high cognitive reserve, i.e., educational attainment and IQ, can attenuate the effect of cerebral small vessel disease on cognitive function (41). In this study the premorbid cognitive ability was not tested and could therefore be a confounder. Future prospective studies should implement a baseline cognitive function test.

Regardless of these limitations, patients with vestibular neuritis presented more often with CSVD than the control cohort, supporting the hypothesis of vascular involvement in the pathophysiology of VN in a subset of elderly patients. These results, however, cannot be extrapolated to younger patients.

The next step would be to confirm a positive correlation of VN with cardiovascular risk factors and CSVD in a prospective setting, without the limitations of a retrospective study design. The time course of vertigo should be determined in prospective work, since a sudden onset would favor a vascular hypothesis whereas acute onset with evolution to peak intensity over 1 up to 3 days would better support a post-infectious or inflammatory mechanism.

Further research should then focus on whether elderly patients with vestibular neuritis have a higher chance of developing cardiovascular disease and should receive cardiovascular risk management or anticoagulant therapy.

DATA AVAILABILITY STATEMENT

The original contributions presented in the study are included in the article/supplementary files, further inquiries can be directed to the corresponding author/s.

ETHICS STATEMENT

The studies involving human participants were reviewed and approved by Local Ethics Committee Gelre Hospital Apeldoorn. Written informed consent for participation was not required for

this study in accordance with the national legislation and the institutional requirements.

AUTHOR CONTRIBUTIONS

FO is responsible for the data collection, data analysis, and overall integrity of the paper. LP and JK are responsible for the radiological assessment and the integrity of the radiological part of the materials and method section. TS is responsible, together with FO, for the statistical analysis and the integrity of this section in the paper. TB and RL are responsible, together with FO, for the study design, writing the article, and overall integrity of the paper. All authors contributed to the article and approved the submitted version.

REFERENCES

1. Stokroos RJ, Albers FW. The etiology of idiopathic sudden sensorineural hearing loss. a review of the literature. *Acta Otorhinolaryngol Belg.* (1996) 50:69–76.
2. Chau JK, Lin JRJ, Atashband S, Irvine RA. Systematic review of the evidence for the etiology of adult sudden sensorineural hearing loss. *Laryngoscope.* (2010) 120:1011–21. doi: 10.1002/lary.20873
3. Kim C, Sohn J-H, Jang MU, Hong S-K, Lee J-S, Kim H-J, et al. Ischemia as a potential etiologic factor in idiopathic unilateral sudden sensorineural hearing loss: analysis of posterior circulation arteries. *Hear Res.* (2016) 331:144–51. doi: 10.1016/j.heares.2015.09.003
4. Kim H-A, Lee H. Recent advances in understanding audiovestibular loss of a vascular cause. *J stroke.* (2017) 19:61–6. doi: 10.5853/jos.2016.00857
5. Hsu Y-H, Hu H-Y, Chiu Y-C, Lee F-P, Huang H-M. Association of sudden sensorineural hearing loss with vertebrobasilar insufficiency. *JAMA Otolaryngol Head Neck Surg.* (2016) 142:672–5. doi: 10.1001/jamaoto.2016.0845
6. Doijiri R, Uno H, Miyashita K, Ihara M. How commonly is stroke found in patients with isolated vertigo or dizziness attack? *J Stroke Cerebrovasc Dis.* (2016) 25:2549–52. doi: 10.1016/j.jstrokecerebrovasdis.2016.06.038
7. Jeong SH, Kim HJ, Kim JS. Vestibular neuritis. *Semin Neurol.* (2013) 33:185–94. doi: 10.1055/s-0033-1354598
8. Marcucci R, Alessandrello Liotta A, Cellai AP, Rogolino A, Berloco P, Leprini E, et al. Cardiovascular and thrombophilic risk factors for idiopathic sudden sensorineural hearing loss. *J Thromb Haemost.* (2005) 3:929–34. doi: 10.1111/j.1538-7836.2005.01310.x
9. Wegner I, van Benthem PPG, Aarts MCJ, Bruintjes TD, Grolman W, van der Heijden GJMG. Insufficient evidence for the effect of corticosteroid treatment on recovery of vestibular neuritis. *Otolaryngol Neck Surg.* (2012) 147:826–31. doi: 10.1177/0194599812457557
10. Lodigiani C, Lorusso R, Ferrazzi P, Libre L, Rota RR. Sudden sensorineural hearing loss: a possible role of thrombophilia and cardiovascular risk factors. *J Thromb Haemost.* (2011) 9(Suppl. 2):875.
11. Mosnier I, Stepanian A, Baron G, Bodenez C, Robier A, Meyer B, et al. Cardiovascular and thromboembolic risk factors in idiopathic sudden sensorineural hearing loss: a case-control study. *Audiol Neurootol.* (2011) 16:55–66. doi: 10.1159/000312640
12. Chang T-P, Wang Z, Winnick AA, Chuang H-Y, Urrutia VC, Carey JP, et al. Sudden hearing loss with vertigo portends greater stroke risk than sudden hearing loss or vertigo alone. *J Stroke Cerebrovasc Dis.* (2018) 27:472–8. doi: 10.1016/j.jstrokecerebrovasdis.2017.09.033
13. Chang C-F, Kuo Y-L, Chen S-P, Wang M-C, Liao W-H, Tu T-Y, et al. Relationship between idiopathic sudden sensorineural hearing loss and subsequent stroke. *Laryngoscope.* (2013) 123:1011–5. doi: 10.1002/lary.23689
14. Kim J-Y, Hong JY, Kim D-K. Association of sudden sensorineural hearing loss with risk of cardiocerebrovascular disease: a study using data from the Korea National Health Insurance Service. *JAMA Otolaryngol Head Neck Surg.* (2018) 144:129–35. doi: 10.1001/jamaoto.2017.2569
15. Lin H-C, Chao P-Z, Lee H-C. Sudden sensorineural hearing loss increases the risk of stroke: a 5-year follow-up study. *Stroke.* (2008) 39:2744–8. doi: 10.1161/STROKEAHA.108.519090
16. Park J-H, Heo SH, Lee MH, Kwon HS, Kwon SU, Lee JS. White matter hyperintensities and recurrent stroke risk in patients with stroke with small-vessel disease. *Eur J Neurol.* (2019) 26:911–8. doi: 10.1111/ene.13908
17. Fazekas F, Kapeller P, Schmidt R, Offenbacher H, Payer F, Fazekas G. The relation of cerebral magnetic resonance signal hyperintensities to Alzheimer's disease. *J Neurol Sci.* (1996) 142:121–5. doi: 10.1016/0022-510X(96)00169-4
18. Fazekas F, Kleinert R, Offenbacher H, Schmidt R, Kleinert G, Payer F, et al. Pathologic correlates of incidental MRI white matter signal hyperintensities. *Neurology.* (1993) 43:1683–9. doi: 10.1212/WNL.43.9.1683
19. Fazekas F, Chawluk JB, Alavi A, Hurtig HI, Zimmerman RA. MR signal abnormalities at 15 T in Alzheimer's dementia and normal aging. *Am J Roentgenol.* (1987) 149:351–6. doi: 10.2214/ajr.149.2.351
20. Zhu Y-C, Dufouil C, Tzourio C, Chabriat H. Silent brain infarcts: a review of MRI diagnostic criteria. *Stroke.* (2011) 42:1140–5. doi: 10.1161/STROKEAHA.110.600114
21. Arbusow V, Schulz P, Strupp M, Dieterich M, von Reinhardstoettner A, Rauch E, et al. Distribution of herpes simplex virus type 1 in human geniculate and vestibular ganglia: implications for vestibular neuritis. *Ann Neurol.* (1999) 46:416–9. doi: 10.1002/1531-8249(199909)46:3<416::AID-ANA20>3.0.CO;2-W
22. Strupp M, Brandt T. Vestibular neuritis. *Adv Otorhinolaryngol.* (1999) 55:111–36. doi: 10.1159/000059060
23. Bronstein AM, Lempert T. Management of the patient with chronic dizziness. *Restor Neurol Neurosci.* (2010) 28:83–90. doi: 10.3233/RNN-2010-0530
24. Baloh RW. Vestibular neuritis. *N Engl J Med.* (2003) 348:1027–32. doi: 10.1056/NEJMcp021154
25. Baloh RW, Ishyama A, Wackym PA, Honrubia V. Vestibular neuritis: clinical-pathologic correlation. *Otolaryngol Neck Surg.* (1996) 114:586–92. doi: 10.1016/S0194-5998(96)70251-6
26. Fisch U, Dobozi M, Greig D. Degenerative changes of the arterial vessels of the internal auditory meatus during the process of aging. A histological study. *Acta Otolaryngol.* (1972) 73:259–66. doi: 10.3109/00016487209138940
27. Kidwell CS, Rosand J, Norato G, Dixon S, Worrall BB, James ML, et al. Ischemic lesions, blood pressure dysregulation, and poor outcomes in intracerebral hemorrhage. *Neurology.* (2017) 88:782–8. doi: 10.1212/WNL.0000000000003630
28. Wardlaw JM, Smith C, Dichgans M. Small vessel disease: mechanisms and clinical implications. *Lancet Neurol.* (2019) 18:684–96. doi: 10.1016/S1474-4422(19)30079-1
29. Guseva AL. Pal'chun VT. Clinical diagnosis and treatment of chronic dizziness. *Zhurnal Nevrol i Psikhiatrii Im SS Korsakova.* (2020) 120:131–7. doi: 10.17116/jnevro2020120121131
30. Tange RA. Vascular inner ear partition: a concept for some forms of sensorineural hearing loss and vertigo. *J Otorhinolaryngol Relat Spec.* (1998) 60:78–84. doi: 10.1159/000027569
31. Freedman JE, Loscalzo J. Platelet-monocyte aggregates: bridging thrombosis and inflammation. *Circulation.* (2002) 105:2130–2. doi: 10.1161/01.CIR.0000017140.26466.F5
32. Bonaterra GA, Hildebrandt W, Bodens A, Sauer R, Dugi KA, Deigner H-P, et al. Increased cyclooxygenase-2 expression in peripheral blood mononuclear cells of smokers and hyperlipidemic subjects. *Free Radic Biol Med.* (2005) 38:235–42. doi: 10.1016/j.freeradbiomed.2004.10.021
33. Greco A, Macri GF, Gallo A, Fusconi M, De Virgilio A, Pagliuca G, et al. Is vestibular neuritis an immune related vestibular neuropathy inducing vertigo? *J Immunol Res.* (2014) 2014:459048. doi: 10.1155/2014/459048
34. Ciorba A, Bianchini C, Crema L, Ceruti S, Ermili F, Aimoni C, et al. White matter lesions and sudden sensorineural hearing loss. *J Clin Neurosci.* (2019) 65:6–10. doi: 10.1016/j.jocn.2019.04.037

35. Fusconi M, Attanasio G, Capitani F, Di Porto E, Diacinti D, Musy I, et al. Correction to: is there a relation between sudden sensorineural hearing loss and white matter lesions? *Eur Arch Otorhinolaryngo*. (2019) 276:3521. doi: 10.1007/s00405-019-05622-2
36. Oron Y, Shemesh S, Shushan S, Cinamon U, Goldfarb A, Dabby R, et al. Cardiovascular risk factors among patients with vestibular neuritis. *Ann Otol Rhinol Laryngol*. (2017) 126:597–601. doi: 10.1177/0003489417718846
37. Chung JH, Lee SH, Park CW, Jeong JH, Shin J-H. Clinical significance of arterial stiffness and metabolic syndrome scores in vestibular neuritis. *Otol Neurotol*. (2017) 38:737–41. doi: 10.1097/MAO.0000000000001352
38. Bae J-H, Kim J-M, Park K-Y, Han S-H. Association between arterial stiffness and the presence of cerebral small vessel disease markers. *Brain Behav*. (2021) 11:e01935. doi: 10.1002/brb3.1935
39. Adamec I, Krbot Skorić M, HandŽić J, Habek M. Incidence, seasonality and comorbidity in vestibular neuritis. *Neurol Sci*. (2015) 36:91–5. doi: 10.1007/s10072-014-1912-4
40. Kattah JC, Talkad AV, Wang DZ, Hsieh Y-H, Newman-Toker DE. HINTS to diagnose stroke in the acute vestibular syndrome: three-step bedside oculomotor examination more sensitive than early MRI diffusion-weighted imaging. *Stroke*. (2009) 40:3504–10. doi: 10.1161/STROKEAHA.109.551234
41. Banerjee G, Jang H, Kim HJ, Kim ST, Kim JS, Lee JH, et al. Total MRI small vessel disease burden correlates with cognitive performance, cortical atrophy, and network measures in a memory clinic population. *J Alzheimers Dis*. (2018) 63:1485–97. doi: 10.3233/JAD-170943

Conflict of Interest: The authors declare that the research was conducted in the absence of any commercial or financial relationships that could be construed as a potential conflict of interest.

Publisher's Note: All claims expressed in this article are solely those of the authors and do not necessarily represent those of their affiliated organizations, or those of the publisher, the editors and the reviewers. Any product that may be evaluated in this article, or claim that may be made by its manufacturer, is not guaranteed or endorsed by the publisher.

frontiers | Frontiers in Neurology

ORIGINAL RESEARCH
published: 29 April 2022
doi: 10.3389/fneur.2022.814518

Non-contrast MRI of Inner Ear Detected Differences of Endolymphatic Drainage System Between Vestibular Migraine and Unilateral Ménière's Disease

Yangming Leng[1], *Ping Lei*[2]*, *Cen Chen*[2], *Yingzhao Liu*[1], *Kaijun Xia*[1] and *Bo Liu*[1]*

[1] Department of Otorhinolaryngology, Union Hospital, Tongji Medical College, Huazhong University of Science and Technology, Wuhan, China, [2] Department of Radiology, Union Hospital, Tongji Medical College, Huazhong University of Science and Technology, Wuhan, China

OPEN ACCESS

Edited by:
Dominik Straumann,
University of Zurich, Switzerland

Reviewed by:
Vincenzo Marcelli,
Local Health Authority Naples 1 Center, Italy
Rafael da Costa Monsanto,
University of Minnesota Twin Cities, United States

***Correspondence:**
Ping Lei
leiping_rosemary@126.com
Bo Liu
liuboent@hust.edu.cn

Specialty section:
This article was submitted to Neuro-Otology, a section of the journal Frontiers in Neurology

Received: 13 November 2021
Accepted: 30 March 2022
Published: 29 April 2022

Citation:
Leng Y, Lei P, Chen C, Liu Y, Xia K and Liu B (2022) Non-contrast MRI of Inner Ear Detected Differences of Endolymphatic Drainage System Between Vestibular Migraine and Unilateral Ménière's Disease. Front. Neurol. 13:814518. doi: 10.3389/fneur.2022.814518

Objective: We aimed to evaluate the diagnostic performance of some anatomical variables with regard to endolymphatic sac (ES) and duct (ED), measured by non-contrast three-dimensional sampling perfection with application-optimized contrasts using different flip angle evolutions (3D-SPACE) magnetic resonance imaging (MRI), in differentiating vestibular migraine (VM) from unilateral Ménière's disease (MD).

Methods: In this study, 81 patients with VM, 97 patients with unilateral MD, and 50 control subjects were enrolled. The MRI-visualized parameters, such as the distance between the vertical part of the posterior semicircular canal and the posterior fossa (MRI-PP distance) and visibility of vestibular aqueduct (MRI-VA), were measured bilaterally. The diagnostic value of the MRI-PP distance and MRI-VA visibility for differentiating VM from unilateral MD was examined.

Results: (1) Compared with the VM patients, patients with unilateral MD exhibited shorter MRI-PP distance and poorer MRI-VA visibility. No differences in the MRI-PP distance and MRI-VA visibility were detected between patients with VM and control subjects. (2) No significant interaural difference in the MRI-PP distance and MRI-VA visibility was observed in patients with VM and those with unilateral MD, respectively. (3) Area under the curve (AUC) showed a low diagnostic value for the MRI-PP distance and MRI-VA visibility, respectively, in differentiating between the VM and unilateral MD.

Conclusions: Based on non-enhanced MRI-visualized measurement, anatomical variables with regard to the endolymphatic drainage system differed significantly between the patients with VM and those with unilateral MD. Further investigations are needed to improve the diagnostic value of these indices in differentiating VM from unilateral MD.

Keywords: vestibular migraine, Ménière's disease, magnetic resonance imaging, endolymphatic sac, endolymphatic duct

INTRODUCTION

Two distinct clinical entities, vestibular migraine (VM) and Ménière's disease (MD), remain the frequent causes of the episodic vestibular syndrome (1, 2). VM is a relatively new disorder that is characterized by episodic vertigo or dizziness and coexisting migraine. MD is presented as the episodic vertigo attack, fluctuating sensorineural hearing loss (SNHL), tinnitus, and aural fullness, and the pathology of MD is characterized by endolymphatic hydrops (ELH). The linkage between migraine and MD was proposed as early as 1861 until the recent establishment of a definitive association (3). Considerable overlap of symptoms has been reported in MD and VM, such as vertigo, migraine, hearing loss, and tinnitus (2). Ghavami et al. found that, in patients with definite MD, 95% had one or more features of migraine, 51% had migraine headaches, and 48% met the diagnostic criteria of VM (4). Various objective approaches have been reported to identify VM and MD, such as caloric response, video head impulse test (5), vestibular evoked myogenic potentials (VEMPs) (6), biological markers (7), motion perception thresholds (8), and gadolinium-enhanced magnetic resonance imaging (MRI) of the inner ear (9). Even so, there are no pathognomonic findings for VM or MD, and no clinical test can fully differentiate between these two conditions. For instance, the shifts of VEMPs threshold and tuning can be found both in patients with MD and those with VM, which suggests that VM might share a common pathophysiology with MD (10–12). Additionally, about 8–25% of patients with VM have unilateral vestibular hyporeflexia to caloric irrigation (13–16), while the incidence of attenuated caloric response in patients with MD ranges somewhere between 45 and 75% (15, 17–20). Recently, by using the intratympanic (21) or the intravenous (22) route of contrast agent application, MRI of the inner ear has been used to visualize ELH *in vivo* for patients with MD. However, this ELH *in vivo* can also be observed in the patients with VM (23, 24). Therefore, the clinical discrimination between VM and MD remains challenging due to the overlapping clinical criteria and the lack of selective and sensitive diagnostic tools (25–27).

The pathophysiology of VM and MD has yet to be completely elucidated. The variability of symptoms and clinical findings both during and between attacks in patients with VM suggests that migraine affects the vestibular system at multiple levels. The presumed mechanisms comprised the cortical spreading depression, genetic defects, neurotransmitters modulation, the reciprocal connections between the trigeminal and vestibular nuclei, and etc. (28). Alternatively, the pathological hallmark of MD is ELH. At present, it is generally believed that ELH arises from the increased endolymph production or decreased endolymph absorption. Many factors have been proposed as leading to the development of ELH, which involve anatomical abnormalities, ionic imbalance, genetic predisposition, autoimmune reactions, viral infection, vascular irregularities, allergic responses, among others (29, 30). As for the anatomical variations of the inner ear, histopathological studies have revealed that patients with MD have significantly smaller vestibular aqueducts (VA) and endolymphatic sacs (ES) than healthy individuals (31, 32). Moreover, numerous radiological studies using MRI and computerized tomography (CT) have confirmed the presence of anatomical variations of inner ear in patients with MD (33, 34). These radiological variations include a significantly reduced distance between the vertical part of the posterior semicircular canal and the posterior fossa (33, 35), less visibility of VA and endolymphatic duct (ED) (34), poorer periaqueductal pneumatization (36), higher prevalence of jugular bulb abnormalities (37), retro-vestibular bony hypoplasia (38), and so on. The anatomical abnormalities of the inner ear do not seem to correspond to the existing pathophysiology of VM.

Previous studies have analyzed the differences between patients with VM and MD in terms of clinical presentation, audio-vestibular function, and inner ear MRI with gadolinium (5–7, 9). However, until now, to our knowledge, no study has examined the significance of the anatomical variations of inner ear associated with the ES and ED in differentiating between these two diseases. In this retrospective study, we looked into the radiological indices of inner ear based on the MRI-visualized measurement in patients with VM, unilateral MD, and control subjects. We sought to determine whether these radiological variations are helpful for differentiating VM from MD.

MATERIALS AND METHODS

Participants

This retrospective study was conducted in the Union Hospital of Tongji Medical College, Huazhong University of Science and Technology, Wuhan, China.

In this study, eighty-one patients with VM and ninety-seven patients with unilateral definitive MD were enrolled between August 2016 and July 2020. Definite and probable VM was diagnosed against the International Headache Society (IHS) (25) and Bárány Society criteria (26), respectively. Furthermore, the diagnosis of unilateral definitive MD was in accordance with the diagnostic criteria proposed by the Bárány Society (39). For all patients, a thorough history investigation, otoscopy, neurotological examinations (audiometry, impedance, videonystagmography, caloric test, etc.), and imaging evaluations were conducted for differential diagnosis. In addition, fifty control subjects without audio-vestibular symptoms were enrolled.

Exclusion criteria were: (1) VM and MD co-morbidities; (2) middle or inner ear infections (otitis media, mastoiditis, labyrinthitis, etc.); (3) middle or inner ear anomaly (common cavity malformation, semicircular canal dysplasia, enlarged vestibular aqueduct, etc.); (4) bilateral MD; (5) having received previous otologic surgery or intratympanic injections; (6) retro-cochlear lesions (vestibular schwannoma, internal acoustic canal stenosis, etc.); and (7) head trauma.

This study was conducted according to the tenets of the Declaration of Helsinki. Informed consent was obtained from each patient and control. The project was approved by the ethical committee of the Tongji Medical College of Huazhong University of Science and Technology.

Audio-Vestibular Evaluations

All patients received audio-vestibular evaluations during the interictal period, such as the pure tone audiogram and caloric test. Within 48 h before testing, all subjects were instructed to refrain from alcohol, caffeine, or medications (sedative, anti-depressant drugs, etc.) that would affect the results of vestibular tests.

Radiological Evaluations

All participants received MRI examinations by the Verio or Magnetom Trio 3T scanners (Siemens, Erlangen, Germany) with a 12-element phased array coil. T1-weighted and T2-weighted imaging were applied. Three-dimensional sampling perfection with application optimized contrasts using different flip angle evolutions (3D-SPACE) was used to measure the distance between the vertical part of the posterior semicircular canal and the posterior fossa (**Supplementary Table 1**).

The protocol of radiological evaluations has been detailed in our most recent report (40). All radiological data were transferred to the workstations, and imaging analyses were performed on a Picture Archiving and Communication System (PACS) workstation (Carestream Client, Carestream Health, Rochester, NY, USA). Radiological data of all subjects were intermixed and reviewed by two senior neuroradiologists who were blinded to the clinical data (L.P with an experience of over 10 years and C.C over 5 years). In this study, the involved anatomical variables by MRI-visualized measurement included the distance between the vertical part of the posterior semicircular canal and the posterior fossa (MRI-PP distance, as presented in **Figure 1**) and visualization of VA (MRI-VA visibility). Visibility of VA refers to a linear or dot-like high intensity that is visualized continuously on more than one MRI sections in the direction of common crus to the posterior edge of the temporal bone. **Figures 2**, **3** presented the typical examples of visualization and non-visualization of VA in 3D-SPACE, respectively.

Statistical Analysis

Statistical analyses were performed by using software SPSS (version 22.0). All continuous variables are presented as means ± standard deviations (SDs) or median and interquartile range (IQR 25–75th percentiles) after verification of normal distribution. Categorical variables are presented as counts and percentages. Data were tested for normal distribution using the Shapiro–Wilk test. The Mann–Whitney *U*-test was used for comparison between two groups and the Kruskal–Wallis *H*-test for more than two groups. A chi-square test was performed for categorical variables. The interobserver agreement for MRI-measurement was determined using the intraclass correlation coefficient (ICC). The agreement was generally interpreted as: poor, ICC $<$ 0.20; fair, 0.2 $<$ ICC $\leq$ 0.40; moderate, 0.4 $<$ ICC $\leq$ 0.60; good, 0.6 $<$ ICC $\leq$ 0.80; and excellent, 0.8 $<$ ICC $\leq$ 1.0. The significance level was set at 0.05.

The diagnostic value of the radiological data was characterized by using a receivers operating characteristic (ROC) curve. When a significant cutoff value was observed, the sensitivity, specificity of MRI-PP distance, and MRI-VA visibility for differentiating the affected sides of MD, VM, and those of control subjects were calculated. Area under the curve (AUC) and 95% confidence intervals (*CI*s) were estimated for the diagnostic value of radiological data. The meaning of AUC is defined as: no diagnostic value if AUC $<$ 0.5, low diagnostic value if AUC is between 0.5 and 0.7, moderate diagnostic value if AUC is between 0.7 and 0.9, and high diagnostic value if AUC $>$ 0.9.

FIGURE 1 | A 0.5-mm axial 3D-SPACE MRI scan showing detailed image of the right ear at the level of the measured distance between the vertical part of the posterior semicircular canal **(a)** and the posterior fossa **(b)**. *3D-SPACE,* three-dimensional sampling perfection with application optimized contrasts using different flip angle evolutions.

RESULTS

Demographic Characteristics of the Participants

In the VM group, 81 patients (57 cases of definitive VM and 24 cases of probable VM) were included, of which 70 (86.4%) were women and 11 (13.6%) were men. The average age was 42.93 ± 10.45 years old. Of these patients with VM, 48 cases (59.3%) that manifested episodic vertigo, 31 cases (38.3%) who had positional vertigo, and 37 cases (45.7%) had intolerance to head movement. In addition, 28 cases (34.6%) exhibited cochlear symptoms (subjective hearing loss, tinnitus, or aural fullness), 54 patients (66.7%) had photophobia, 52 patients (64.2%) showed phonophobia, and 51 case (63.0%) experienced motion sickness. All patients with VM underwent caloric test, and 20 cases (24.7%) showed an abnormal canal paresis (CP) value in one ear.

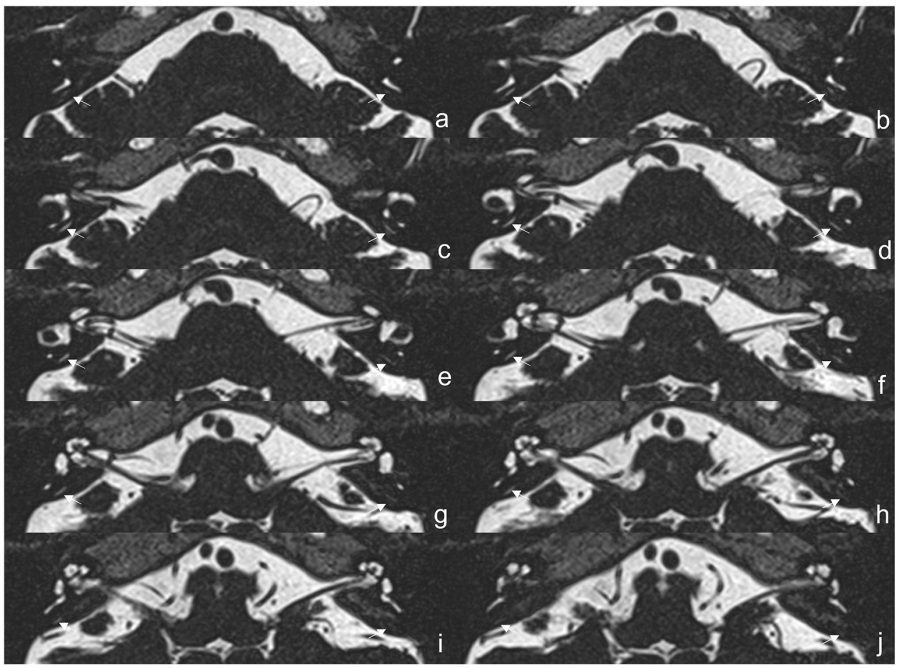

FIGURE 2 | The 3D-SPACE MRI images of a 57-year-old female with vestibular migraine (VM). **(a–j)** Axial, high-resolution, and T2-weighted MRI scan showing visualization of the vestibular aqueduct on both sides. *3D-SPACE,* three-dimensional sampling perfection with application optimized contrasts using different flip angle evolutions, *VM,* vestibular migraine.

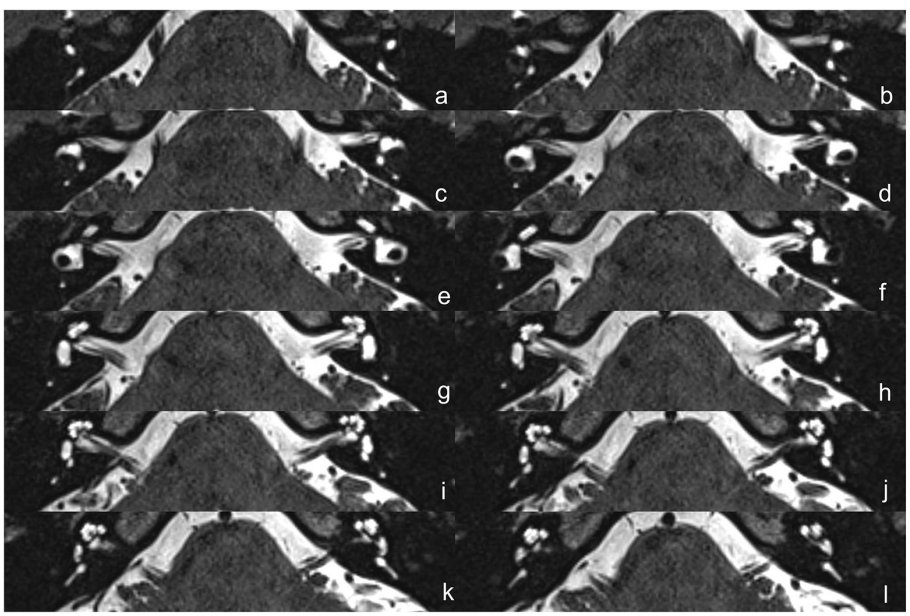

FIGURE 3 | The 3D-SPACE MRI images of a 48-year-old female with VM. **(a–l)** Axial, high-resolution, and T2-weighted MRI scan showing non-visualization of the vestibular aqueduct on both sides. *3D-SPACE,* three-dimensional sampling perfection with application optimized contrasts using different flip angle evolutions, *VM,* vestibular migraine.

In the unilateral definitive MD group, 97 patients were involved, of which 53 (54.6%) were women and 44 (45.4%) were men. The average age was 48.20 ± 12.55 years old. Furthermore, 50 healthy subjects (40 women and 10 men) were enrolled as a control group, with an average age of 50.44 ± 12.59 years old.

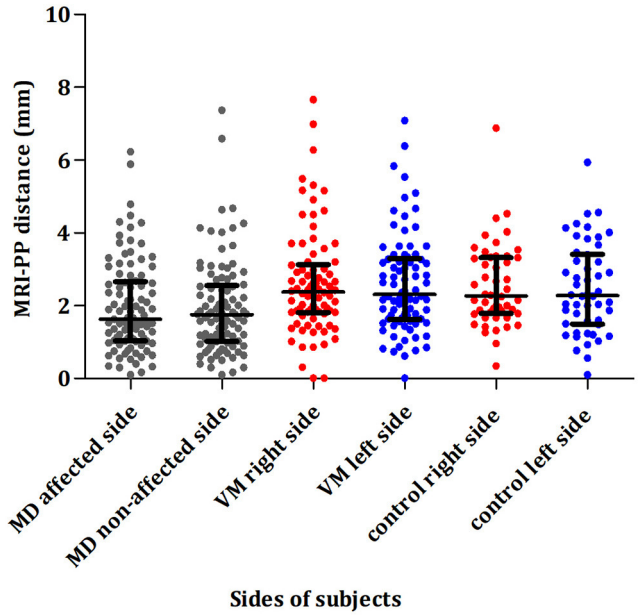

FIGURE 4 | Comparison of the distance between the vertical part of the posterior semicircular canal and the posterior fossa (MRI-PP) distance in patients with unilateral MD (affected and non-affected side), patients with VM (right and left side), and control subjects (right and left side). *MD,* Ménière's disease; *VM,* vestibular migraine.

In this study, the interobserver agreement for radiological assessment was excellent for MRI-PP distance (ICC = 0.981) and MRI-VA visibility (ICC = 0.846), respectively. Therefore, the results evaluated by one neuroradiologist were used randomly for further analyses.

Radiological Variations in Patients With VM and Unilateral MD

Of 81 patients with VM, the left and right ears had a median MRI-PP distance of 2.26 (1.61, 3.276) and 2.36 (1.805, 3.06) mm, respectively. The percentage of MRI-VA visibility in the left and right sides was 42% (34/81) and 37% (30/81), respectively. As shown in **Figure 4**, there was no significant interaural difference in MRI-PP distance or MRI-VA visibility in patients with VM ($Z = 0.559$, $p = 0.576$ and $\chi^2 = 0.500$, $p = 0.481$).

Of 97 patients with unilateral MD, the median MRI-PP distance in the affected and non-affected ears was 1.63 (1.04, 2.66) and 1.75 (1.02, 2.56) mm, respectively. The percentage of MRI-VA visibility in the affected and non-affected sides was 15.5% (15/97) and 19.6% (19/97), respectively. As shown in **Figure 4**, no significant differences in MRI-PP distance or MRI-VA visibility were found between the affected and non-affected side in patients with unilateral MD ($Z = 0.103$, $p = 0.918$ and $\chi^2 = 0.643$, $p = 0.424$).

Of 50 control subjects, the left and right ears had a median MRI-PP distance of 2.27 (1.79, 3.32) and 2.28 (1.50, 3.42) mm, respectively. The percentage of MRI-VA visibility in the left and right sides was 30% (15/50) and 28% (14/50), respectively. No significant interaural difference in MRI-PP distance or MRI-VA visibility was observed in control subjects ($Z = 0.729$, $p = 0.466$ and $\chi^2 = 0.000$, $p = 1.000$).

Comparison of Anatomical Variations Among Three Groups

For comparison of the radiological indices, the left side of patients with VM and the left side of control subjects were randomly selected, along with the affected side of patients with MD. As for the MRI-PP distance, group comparison revealed significant difference among these three groups ($\chi^2 = 13.250$, $p = 0.001$). The results of pairwise comparisons between each two groups were as follows: (1) patients with MD showed shorter MRI-PP distance in the affected ears, compared with the left side of patients with VM ($p = 0.002$) and control subjects ($p = 0.026$), respectively. (2) No significant differences in MRI-PP distance were found between left side of VM and that of control subjects ($p = 1.000$). As for the MRI-VA visibility, group comparison revealed significant difference among these three groups ($\chi^2 = 10.773$, $p = 0.005$). Pairwise comparisons between each two groups were performed with a Bonferroni correction using an alpha level of 0.05/3 = 0.0167 and the results were as follows: (1) patients with MD showed poorer visibility of MRI-VA in the affected ears, compared with the left side of patients with VM ($p = 0.001$). (2) No significant differences in MRI-VA visibility were found between the left side of VM and that of control subjects ($p = 0.293$) and between the affected side of MD and left side of control subjects ($p = 0.038$).

The Differential Diagnostic Value of Radiological Variations

When comparing the MD-affected side and the left side of VM, the AUC with 95% *CI* estimated for MRI-PP distance was 0.646 (0.566, 0.727). The ideal cutoff point was 1.56 mm, with sensitivity and specificity being 48.5 and 77.8%, respectively (**Figure 5a**). When comparing the MD-affected side and the right side of VM, the diagnostic value of the MRI-PP distance was also low with an AUC of 0.645 (0.564, 0.726). The cutoff MRI-PP distance of 1.7 mm had a sensitivity of 52.6% and specificity of 77.8% (**Figure 5b**).

When comparing the MD-affected side and the left side of VM, the AUC with 95% *CI* estimated for MRI-VA visibility was 0.630 (0.547, 0.713). The ideal cutoff point was 0.5, with sensitivity and specificity being 84.5 and 41.5%, respectively (**Figure 5c**). When comparing the MD-affected side and the right side of VM, the diagnostic value of the MRI-VA visibility was also low with an AUC of 0.589 (0.472, 0.707). The cutoff MRI-VA visibility of 0.5 had a sensitivity of 84.5% and specificity of 33.3% (**Figure 5d**).

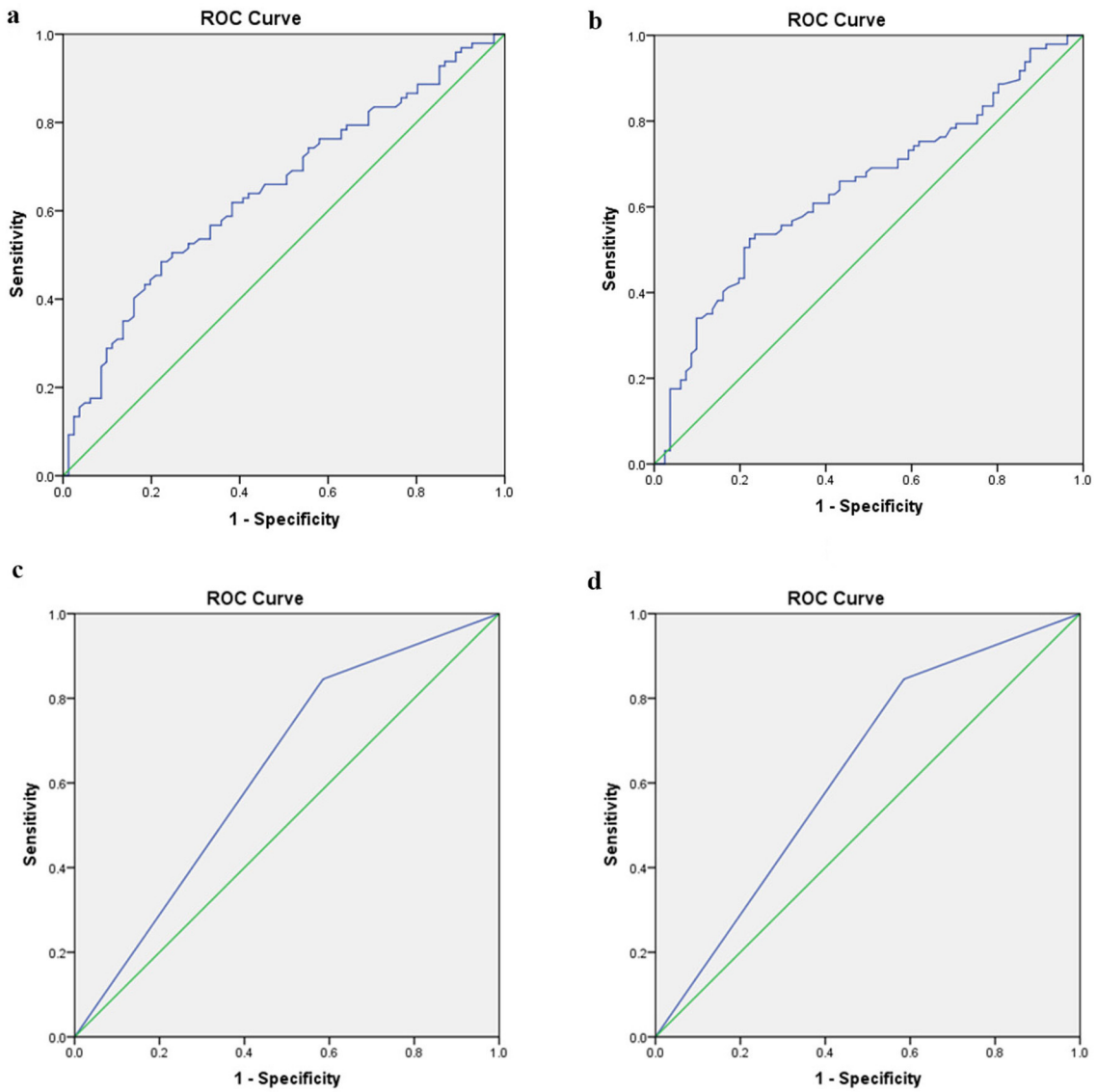

FIGURE 5 | Receiver operating characteristic curves for the two radiological variables that showed significant difference between unilateral MD and VM. **(a)** Difference of MRI-PP distance between the affected side of MD and left side of VM. **(b)** Difference of MRI-PP distance between the affected side of MD and right side of VM. **(c)** Difference of MRI-VA visibility between the affected side of MD and left side of VM. **(d)** Difference of MRI-VA visibility between the affected side of MD and right side of VM. ROC, receivers operating characteristic; MD, Ménière's disease; VM, vestibular migraine; PP distance, distance between the vertical part of the posterior semicircular canal and the posterior fossa; VA, vestibular aqueduct.

DISCUSSION

Differences of Radiological Variations of Inner Ear Between VM and MD

The present study showed that, compared with VM patients and control subjects, patients with unilateral MD had shorter MRI-PP distance and poorer MRI-VA visibility in both affected and non-affected ears. Meanwhile, no difference was found in MRI-PP distance and MRI-VA visibility between patients with VM and control subjects.

Anatomical variations of inner ear have been shown to play a role in the pathogenesis of MD (33, 34, 36–38), and morphological analysis by histopathological and radiological studies has confirmed hypoplasia of ED and ES as one of the predisposing factors. Radiologically, a short PP distance may suggest a small ES and poor ES function in patients with MD (33). In this study, another radiological variable was the visibility of VA in MRI. Previous histological studies have demonstrated hypoplasia of the VA and narrowing of the lumen of the ED in patients with MD, which may implicate

congenital or developmental abnormality of the VA/ED as a likely predisposing factor for the development of ELH in patients with MD (32, 41, 42). Similar findings have been highlighted by 2D CT, 3D-Cone beam CT as well as by MRI (43–45). Another hypothesis to explain the calcification and narrowing of VA is calcium ion (Ca^{2+}) augmentation in hydropic ears, as demonstrated in biological samples (46) and more recently with mineralized cells around the VA in histopathological analysis (47). ES and ED, as part of the endolymphatic drainage system, may play an essential role in maintaining endolymph homeostasis. Pathophysiologically, the hypoplasia of ES and ED has been assumed to compromise endolymph absorption, which could induce ELH in MD. To our knowledge, our study was the first to find a difference of MRI-visualized measurement in the endolymphatic drainage system between these two episodic vestibular syndromes, which indicated that the diminished endolymph absorption resulted from hypoplasia of the endolymphatic drainage system can be regarded as a predisposing factor in the pathogenesis of MD rather than VM.

As for the pathophysiology of VM, recent electrophysiological findings of caloric reflex and VEMP showed dysfunction of inner ear (10, 13, 48), which may be, at least partly, attributed to the neurogenic inflammation in the inner ear. Trigeminal nerve endings have been found in the blood vessels of the inner ear (49). Migraine attack or serotonin provocation could induce plasma extravasation from dural and labyrinth vessels, causing transient inflammation not only in the dura mater but also in the inner ear (50). Additionally, the migraine-associated nociceptive receptor has been observed in the human ES (51) and the absorption of the endolymph in the ES might be compromised in migraineurs. Furthermore, MRI-demonstratable ELH has been observed in the cochlear and/or vestibule of patients with VM (24, 52). These observations led to the hypothesis that MD and VM may share a common pathophysiology, i.e., ELH (10). From a radiological and anatomical perspective, our results supported these earlier findings by implying that different pathophysiological mechanisms are involved in the common condition ELH. Some factors other than a compromised endolymphatic drainage system may contribute to the pathogenesis of VM, as VM may affect the vestibular system at multiple levels, especially the central pathways (53). Based on these imaging discrepancies in the peripheral rather than the central vestibular system, our findings suggest that anatomical variations in the inner ear may play differential roles in the pathogenesis of VM and MD. These results might be used to develop more pathologically oriented diagnostic algorithms and strategies for treating these two conditions in the future.

Differential Diagnostic Value of Radiological Variations Between VM and MD

The current study, from the ROC analyses, showed that the MRI-PP distance has a low diagnostic accuracy for discriminating unilateral MD from VM or controls, which means this radiological variation is not yet a suitable tool in the differential diagnosis between these two episodic vestibular syndromes.

Many studies have attempted to establish a method to distinguish MD from VM, which includes the history investigation, audio-vestibular testing, and imaging evaluation (5, 6, 9, 10, 54). But so far, no definite diagnostic test can reliably distinguish between these two entities. During the past two decades, high-resolution MRI with intravenous or intratympanic application of gadolinium as the contrast agent has provided direct evidence of ELH in the inner ear *in vivo* (21, 22), which was also used to differentiate VM from MD (9, 24, 52). Nakada et al. demonstrated that ELH *in vivo* was present in the vestibule in two out of seven patients with VM. Meanwhile, a significant unilateral or bilateral ELH can be found in the vestibule of all patients with MD (52). In addition, Sun et al. reported that the MRI-demonstratable ELH were observed in the cochlea and vestibule in the affected ears of patients with MD, while only suspicious cochlear hydrops and no vestibular hydrops was noted in the patients with VM (9). Nevertheless, Gürkov et al. found that 21% (4/19) patients with VM exhibited evidence of cochlear and vestibular ELH by enhanced MRI of the inner ear (24). The presence of MRI-demonstratable ELH *in vivo* in a small proportion of patients with VM could be attributed to neurogenic inflammation in VM, which could induce inner ear dysfunction and ELH. Another explanation might be the comorbidity of VM and MD.

Recent studies using other imaging modalities, such as position-emission tomography (PET) (55), blood-oxygen-level dependent functional MRI (BOLD-fMRI) (56), and MRI-based voxel-based morphometry (57), found that the enhanced vestibular organ perception and its interactions with the brainstem, thalamus, and cortex may underlie the pathogenesis of VM (58, 59). Furthermore, radiomics of the inner ear has been suggested as a promising tool in the diagnosis of MD (60). These findings, together with our results, implicated that although non-contrast MRI-based evaluations of the inner ear provides limited information in discriminating VM from MD, the radiological evidence of inner ear variations offers deeper insight into the pathophysiological differences of these two episodic vestibular syndromes. Future radiomic studies are expected to provide additional imaging evidence for the differential diagnosis of these two entities.

Our study has several limitations. First, this is a retrospective study and is potentially subjected to selection bias and information bias. Second, we did not analyze the radiological indices based on phenotypes of unilateral MD. The following five distinctive clinical subtypes have been identified by the Ménière's Disease Consortium (61): Type 1 included patients without a familial history of MD, migraine, or autoimmune comorbidity; Type 2 had delayed MD characterized by SNHL which antedated the vertigo episodes; Type 3 included all familial cases of MD; Type 4 was associated with migraine with or without aura, and Type 5 was defined by a concurrent autoimmune disorder (61). Recently, Diao et al. found that some radiological variables differed between patients with MD with and without migraine, including the poorer mastoid pneumatization and the shorter distance between the sigmoid sinus and posterior wall

of the external acoustic canal (62). Then, it is reasonable to suppose that the anatomical variations may play inconsistent roles in different subtypes of unilateral MD. Large-scale study including full spectrum of MD subtypes are warranted in the future.

CONCLUSIONS

Compared with VM patients, patients with definitive unilateral MD had a shorter MRI-PP distance and poorer visibility of MRI-VA in both affected and non-affected ears. The differences in these radiological indices between VM and MD may reflect different mechanisms underlying these two disease entities. However, these indices only showed low diagnostic value in differentiating VM from MD, which needs to be improved by further investigations.

DATA AVAILABILITY STATEMENT

The original contributions presented in the study are included in the article/**Supplementary Material**, further inquiries can be directed to the corresponding authors.

ETHICS STATEMENT

The studies involving human participants were reviewed and approved by the Ethical Committee of Tongji Medical College of Huazhong University of Science and Technology. The patients/participants provided their written informed consent to participate in this study.

AUTHOR CONTRIBUTIONS

YLe: patient consultation, interpretation of data, drafting, and critical revision of the manuscript. PL and CC: data collection, image extraction, and analysis. YLi and KX: patient recruitment, data collection, and statistical analysis. BL: study conception and design, patient consultation, interpretation of data, and critical revision of the manuscript. All authors contributed to the article and approved the submitted version.

FUNDING

This work was supported by grants from the National Natural Science Foundation of China (NSFC No. 81670930), the Natural Science Foundation of Hubei Province, China (No. 2016CFB645), and the Fundamental Research Funds for the Central Universities, China (No. 2016YXMS240).

ACKNOWLEDGMENTS

We appreciate Prof. Meixia Lu for statistical consultation and analysis.

SUPPLEMENTARY MATERIAL

The Supplementary Material for this article can be found online at: https://www.frontiersin.org/articles/10.3389/fneur.2022.814518/full#supplementary-material

REFERENCES

1. Liu YF, Xu H. The intimate relationship between vestibular migraine and meniere disease: a review of pathogenesis and presentation. *Behav Neurol.* (2016) 2016:3182735. doi: 10.1155/2016/3182735
2. Lopez-Escamez JA, Dlugaiczyk J, Jacobs J, Lempert T, Teggi R, von Brevern M, et al. Accompanying symptoms overlap during attacks in meniere's disease and vestibular migraine. *Front Neurol.* (2014) 5:265. doi: 10.3389/fneur.2014.00265
3. Radtke A, Lempert T, Gresty MA, Brookes GB, Bronstein AM, Neuhauser H. Migraine and Meniere's disease: is there a link? *Neurology.* (2002) 59:1700–4. doi: 10.1212/01.WNL.0000036903.22461.39
4. Ghavami Y, Mahboubi H, Yau AY, Maducdoc M, Djalilian HR. Migraine features in patients with Meniere's disease. *Laryngoscope.* (2016) 126:163–8. doi: 10.1002/lary.25344
5. Blodow A, Heinze M, Bloching MB, von Brevern M, Radtke A, Lempert T. Caloric stimulation and video-head impulse testing in Meniere's disease and vestibular migraine. *Acta Otolaryngol.* (2014) 134:1239–44. doi: 10.3109/00016489.2014.939300
6. Zuniga MG, Janky KL, Schubert MC, Carey JP. Can vestibular-evoked myogenic potentials help differentiate Meniere disease from vestibular migraine? *Otolaryngol Head Neck Surg.* (2012) 146:788–96. doi: 10.1177/0194599811434073
7. Flook M, Frejo L, Gallego-Martinez A, Martin-Sanz E, Rossi-Izquierdo M, Amor-Dorado JC, et al. Differential proinflammatory signature in vestibular migraine and Meniere disease. *Front Immunol.* (2019) 10:1229. doi: 10.3389/fimmu.2019.01229
8. Bremova T, Caushaj A, Ertl M, Strobl R, Bottcher N, Strupp M, et al. Comparison of linear motion perception thresholds in vestibular migraine and Meniere's disease. *Eur Arch Otorhinolaryngol.* (2016) 273:2931–9. doi: 10.1007/s00405-015-3835-y
9. Sun W, Guo P, Ren T, Wang W. Magnetic resonance imaging of intratympanic gadolinium helps differentiate vestibular migraine from Meniere disease. *Laryngoscope.* (2017) 127:2382–8. doi: 10.1002/lary.26518
10. Murofushi T, Ozeki H, Inoue A, Sakata A. Does migraine-associated vertigo share a common pathophysiology with Meniere's disease? Study with vestibular-evoked myogenic potential. *Cephalalgia.* (2009) 29:1259–66. doi: 10.1111/j.1468-2982.2009.01860.x
11. Rauch SD, Zhou G, Kujawa SG, Guinan JJ, Herrmann BS. Vestibular evoked myogenic potentials show altered tuning in patients with Meniere's disease. *Otol Neurotol.* (2004) 25:333–8. doi: 10.1097/00129492-200405000-00022
12. Jerin C, Berman A, Krause E, Ertl-Wagner B, Gurkov R. Ocular vestibular evoked myogenic potential frequency tuning in certain Meniere's disease. *Hear Res.* (2014) 310:54–9. doi: 10.1016/j.heares.2014.02.001
13. Dieterich M, Brandt T. Episodic vertigo related to migraine (90 cases): vestibular migraine? *J Neurol.* (1999) 246:883–92. doi: 10.1007/s004150050478
14. Teggi R, Colombo B, Bernasconi L, Bellini C, Comi G, Bussi M. Migrainous vertigo: results of caloric testing and stabilometric findings. *Headache.* (2009) 49:435–44. doi: 10.1111/j.1526-4610.2009.01338.x
15. Shin JE, Kim CH, Park HJ. Vestibular abnormality in patients with Meniere's disease and migrainous vertigo. *Acta Otolaryngol.* (2013) 133:154–8. doi: 10.3109/00016489.2012.727469
16. Celebisoy N, Gokcay F, Sirin H, Bicak N. Migrainous vertigo: clinical, oculographic and posturographic findings. *Cephalalgia.* (2008) 28:72–7. doi: 10.1111/j.1468-2982.2007.01474.x

17. de Sousa LC, Piza MR, da Costa SS. Diagnosis of Meniere's disease: routine and extended tests. *Otolaryngol Clin North Am.* (2002) 35:547–64. doi: 10.1016/S0030-6665(02)00029-4
18. Carey JP, Minor LB, Peng GC, Della Santina CC, Cremer PD, Haslwanter T. Changes in the three-dimensional angular vestibulo-ocular reflex following intratympanic gentamicin for Meniere's disease. *J Assoc Res Otolaryngol.* (2002) 3:430–43. doi: 10.1007/s101620010053
19. Limviriyakul S, Luangsawang C, Suvansit K, Prakairungthong S, Thongyai K, Atipas S. Video head impulse test and caloric test in definite Meniere's disease. *Eur Arch Otorhinolaryngol.* (2020) 277:679–86. doi: 10.1007/s00405-019-05735-8
20. Fukushima M, Oya R, Nozaki K, Eguchi H, Akahani S, Inohara H, et al. Vertical head impulse and caloric are complementary but react opposite to Meniere's disease hydrops. *Laryngoscope.* (2019) 129:1660–6. doi: 10.1002/lary.27580
21. Nakashima T, Naganawa S, Sugiura M, Teranishi M, Sone M, Hayashi H, et al. Visualization of endolymphatic hydrops in patients with Meniere's disease. *Laryngoscope.* (2007) 117:415–20. doi: 10.1097/MLG.0b013e31802c300c
22. Naganawa S, Yamazaki M, Kawai H, Bokura K, Sone M, Nakashima T. Visualization of endolymphatic hydrops in Meniere's disease with single-dose intravenous gadolinium-based contrast media using heavily T(2)-weighted 3D-FLAIR. *Magn Reson Med Sci.* (2010) 9:237–42. doi: 10.2463/mrms.9.237
23. Kirsch V, Becker-Bense S, Berman A, Kierig E, Ertl-Wagner B, Dieterich M. Transient endolymphatic hydrops after an attack of vestibular migraine: a longitudinal single case study. *J Neurol.* (2018) 265:51–3. doi: 10.1007/s00415-018-8870-3
24. Gurkov R, Kantner C, Strupp M, Flatz W, Krause E, Ertl-Wagner B. Endolymphatic hydrops in patients with vestibular migraine and auditory symptoms. *Eur Arch Otorhinolaryngol.* (2014) 271:2661–7. doi: 10.1007/s00405-013-2751-2
25. Headache Classification Committee of the International Headache Society (IHS). The International Classification of Headache Disorders, 3rd edition. *Cephalalgia*. (2018) 38:1–211. doi: 10.1177/0333102417738202
26. Lempert T, Olesen J, Furman J, Waterston J, Seemungal B, Carey J, et al. Vestibular migraine: diagnostic criteria. *J Vestib Res.* (2012) 22:167–72. doi: 10.3233/VES-2012-0453
27. Committee on Hearing and Equilibrium guidelines for the diagnosis and evaluation of therapy in Meniere's disease. American Academy of Otolaryngology-Head and Neck Foundation, Inc. *Otolaryngol Head Neck Surg.* (1995) 113:181–5. doi: 10.1016/S0194-5998(95)70102-8
28. Ashina M. Migraine. *N Engl J Med.* (2020) 383:1866–76. doi: 10.1056/NEJMra1915327
29. Merchant SN, Adams JC, Nadol JB Jr. Pathophysiology of Meniere's syndrome: are symptoms caused by endolymphatic hydrops? *Otol Neurotol.* (2005) 26:74–81. doi: 10.1097/00129492-200501000-00013
30. Rizk HG, Mehta NK, Qureshi U, Yuen E, Zhang K, Nkrumah Y, et al. Pathogenesis and etiology of Meniere disease: a scoping review of a century of evidence. *JAMA Otolaryngol Head Neck Surg.* (2022) 148:360–8. doi: 10.1001/jamaoto.2021.4282
31. Sando I, Ikeda M. The vestibular aqueduct in patients with Meniere's disease. A temporal bone histopathological investigation. *Acta otolaryngol.* (1984) 97:558–70. doi: 10.3109/00016488409132934
32. Ikeda M, Sando I. Endolymphatic duct and sac in patients with Meniere's disease. A temporal bone histopathological study. *Ann Otol Rhinol Laryngol.* (1984) 93:540–6. doi: 10.1177/000348948409300603
33. Mateijsen DJ, Van Hengel PW, Krikke AP, Van Huffelen WM, Wit HP, Albers FW. Three-dimensional Fourier transformation constructive interference in steady state magnetic resonance imaging of the inner ear in patients with unilateral and bilateral Meniere's disease. *Otol Neurotol.* (2002) 23:208–13. doi: 10.1097/00129492-200203000-00017
34. Mainnemarre J, Hautefort C, Toupet M, Guichard JP, Houdart E, Attye A, et al. The vestibular aqueduct ossification on temporal bone CT: an old sign revisited to rule out the presence of endolymphatic hydrops in Meniere's disease patients. *Eur Radiol.* (2020) 30:6331–8. doi: 10.1007/s00330-020-06980-w
35. Albers FW, Van Weissenbruch R, Casselman JW. 3DFT-magnetic resonance imaging of the inner ear in Meniere's disease. *Acta Otolaryngol.* (1994) 114:595–600. doi: 10.3109/00016489409126111
36. Hall SF, O'Connor AF, Thakkar CH, Wylie IG, Morrison AW. Significance of tomography in Meniere's disease: periaqueductal pneumatization. *Laryngoscope.* (1983) 93:1551–3. doi: 10.1288/00005537-198312000-00006
37. Redfern RE, Brown M, Benson AG. High jugular bulb in a cohort of patients with definite Meniere's disease. *J Laryngol Otol.* (2014) 128:759–64. doi: 10.1017/S0022215114001820
38. Yazawa Y, Kitahara M. Computerized tomography of the petrous bone in Meniere's disease. *Acta Otolaryngol Suppl.* (1994) 510:67–72. doi: 10.3109/00016489409127306
39. Lopez-Escamez JA, Carey J, Chung WH, Goebel JA, Magnusson M, Mandala M, et al. Diagnostic criteria for Meniere's disease. *J Vestib Res.* (2015) 25:1–7. doi: 10.3233/VES-150549
40. Lei P, Leng Y, Li J, Zhou R, Liu B. Anatomical variation of inner ear may be a predisposing factor for unilateral Meniere's disease rather than for ipsilateral delayed endolymphatic hydrops. *Eur Radiol.* (2022). doi: 10.1007/s00330-021-08430-7. [Epub ahead of print].
41. Hebbar GK, Rask-Andersen H, Linthicum FH Jr. Three-dimensional analysis of 61 human endolymphatic ducts and sacs in ears with and without Meniere's disease. *Ann Otol Rhinol Laryngol.* (1991) 100:219–25. doi: 10.1177/000348949110000310
42. Monsanto RD, Pauna HF, Kwon G, Schachern PA, Tsuprun V, Paparella MM, et al. A three-dimensional analysis of the endolymph drainage system in Meniere disease. *Laryngoscope.* (2017) 127:E170–E5. doi: 10.1002/lary.26155
43. Miyashita T, Toyama Y, Inamoto R, Mori N. Evaluation of the vestibular aqueduct in Meniere's disease using multiplanar reconstruction images of CT. *Auris Nasus Larynx.* (2012) 39:567–71. doi: 10.1016/j.anl.2011.11.005
44. Tanioka H, Kaga H, Zusho H, Araki T, Sasaki Y. MR of the endolymphatic duct and sac: findings in Meniere disease. *AJNR Am J Neuroradiol.* (1997) 18:45–51.
45. Yamane H, Konishi K, Sakamaoto H, Yamamoto H, Matsushita N, Oishi M, et al. Practical 3DCT imaging of the vestibular aqueduct for Meniere's disease. *Acta Otolaryngol.* (2015) 135:799–806. doi: 10.3109/00016489.2015.1034879
46. Salt AN, DeMott J. Endolymph calcium increases with time after surgical induction of hydrops in guinea-pigs. *Hear Res.* (1994) 74:115–21. doi: 10.1016/0378-5955(94)90180-5
47. Michaels L, Soucek S, Linthicum F. The intravestibular source of the vestibular aqueduct: Its structure and pathology in Meniere's disease. *Acta Otolaryngol.* (2009) 129:592–601. doi: 10.1080/00016480802342416
48. Iwasaki S, Ushio M, Chihara Y, Ito K, Sugasawa K, Murofushi T. Migraine-associated vertigo: clinical characteristics of Japanese patients and effect of lomerizine, a calcium channel antagonist. *Acta Otolaryngol Suppl.* (2007) 559:45—9. doi: 10.1080/03655230701596491
49. Vass Z, Shore SE, Nuttall AL, Miller JM. Direct evidence of trigeminal innervation of the cochlear blood vessels. *Neuroscience.* (1998) 84:559–67. doi: 10.1016/S0306-4522(97)00503-4
50. Koo JW, Balaban CD. Serotonin-induced plasma extravasation in the murine inner ear: possible mechanism of migraine-associated inner ear dysfunction. *Cephalalgia.* (2006) 26:1310–9. doi: 10.1111/j.1468-2982.2006.01208.x
51. Taguchi D, Takeda T, Kakigi A, Takumida M, Nishioka R, Kitano H. Expressions of aquaporin-2, vasopressin type 2 receptor, transient receptor potential channel vanilloid (TRPV)1, and TRPV4 in the human endolymphatic sac. *Laryngoscope.* (2007) 117:695–8. doi: 10.1097/mlg.0b013e318031c802
52. Nakada T, Yoshida T, Suga K, Kato M, Otake H, Kato K, et al. Endolymphatic space size in patients with vestibular migraine and Meniere's disease. *J Neurol.* (2014) 261:2079–84. doi: 10.1007/s00415-014-7458-9
53. Furman JM, Marcus DA, Balaban CD. Vestibular migraine: clinical aspects and pathophysiology. *Lancet Neurol.* (2013) 12:706–15. doi: 10.1016/S1474-4422(13)70107-8
54. Ishiyama G, Ishiyama A, Baloh RW. Drop attacks and vertigo secondary to a non-meniere otologic cause. *Arch Neurol.* (2003) 60:71–5. doi: 10.1001/archneur.60.1.71
55. Shin JH, Kim YK, Kim HJ, Kim JS. Altered brain metabolism in vestibular migraine: comparison of interictal and ictal findings. *Cephalalgia.* (2014) 34:58–67. doi: 10.1177/0333102413498940
56. Russo A, Marcelli V, Esposito F, Corvino V, Marcuccio L, Giannone A, et al. Abnormal thalamic function in patients with vestibular migraine. *Neurology.* (2014) 82:2120–6. doi: 10.1212/WNL.0000000000000496

57. Obermann M, Wurthmann S, Steinberg BS, Theysohn N, Diener HC, Naegel S. Central vestibular system modulation in vestibular migraine. *Cephalalgia.* (2014) 34:1053–61. doi: 10.1177/0333102414527650
58. Schwedt TJ, Chong CD, Chiang CC, Baxter L, Schlaggar BL, Dodick DW. Enhanced pain-induced activity of pain-processing regions in a case-control study of episodic migraine. *Cephalalgia.* (2014) 34:947–58. doi: 10.1177/0333102414526069
59. Tabet P, Saliba I. Meniere's disease and Vestibular Migraine: updates and review of the literature. *J Clin Med Res.* (2017) 9:733–44. doi: 10.14740/jocmr3126w
60. van den Burg EL, van Hoof M, Postma AA, Janssen AM, Stokroos RJ, Kingma H, et al. An exploratory study to detect Meniere's disease in conventional MRI scans using radiomics. *Front Neurol.* (2016) 7:190. doi: 10.3389/fneur.2016.00190
61. Frejo L, Martin-Sanz E, Teggi R, Trinidad G, Soto-Varela A, Santos-Perez S, et al. Extended phenotype and clinical subgroups in unilateral Meniere disease: a cross-sectional study with cluster analysis. *Clin Otolaryngol.* (2017) 42:1172–80. doi: 10.1111/coa.12844
62. Diao T, Han L, Jing Y, Wang Y, Ma X, Yu L, et al. The clinical characteristics and anatomical variations in patients with intractable unilateral Meniere's Disease with and without migraine. *J Vestib Res*. (2021) 32:57–67. doi: 10.3233/VES-190755

Conflict of Interest: The authors declare that the research was conducted in the absence of any commercial or financial relationships that could be construed as a potential conflict of interest.

Publisher's Note: All claims expressed in this article are solely those of the authors and do not necessarily represent those of their affiliated organizations, or those of the publisher, the editors and the reviewers. Any product that may be evaluated in this article, or claim that may be made by its manufacturer, is not guaranteed or endorsed by the publisher.

frontiers | Frontiers in Neurology

ORIGINAL RESEARCH
published: 16 May 2022
doi: 10.3389/fneur.2022.845707

Significance of Vertigo, Imbalance, and Other Minor Symptoms in Hyperacute Treatment of Posterior Circulation Stroke

Min Kim[1], *So Young Park*[1], *Sung Eun Lee*[2], *Jin Soo Lee*[1], *Ji Man Hong*[1] *and Seong-Joon Lee*[1*†]

[1] Department of Neurology, Ajou University Medical Center, Ajou University School of Medicine, Suwon, South Korea, [2] Department of Emergency Medicine, Ajou University Medical Center, Ajou University School of Medicine, Suwon, South Korea

Background: This study aimed to determine the clinical significance of acute vestibular syndrome (AVS)/acute imbalance syndrome (AIS) in posterior circulation stroke (PCS) and how it should be addressed in the thrombolysis code.

Methods: Our institution has recently changed its thrombolysis code from one that is generous to AVS/AIS to one that is exclusive. The subjects in this study were patients with PCS who presented before this transition (May 2016 to April 2018, period 1) and those who presented after (January 2019 to December 2020, period 2) with an onset-to-door time of 4.5 h. Hyperacute stroke treatment was compared between the two periods. The clinical significance of AVS/AIS was evaluated by dichotomizing the patients' clinical severity to minor or major deficits, then evaluating the significance of AVS/AIS in each group. Presenting symptoms of decreased mental alertness, hemiparesis, aphasia (anarthria), or hemianopsia were considered major PCS symptoms, and patients who did not present with these symptoms were considered minor PCS.

Results: In total, 114 patients presented in period 1 and 114 in period 2. Although the code activation rate was significantly lower in period 2 (72.8% vs. 59.7%), $p = 0.04$, there were no between-group differences in functional outcomes (mRS score at 3 months; 1 [0–3] vs. 0 [0–3], $p = 0.18$). In 77 patients with PCS and AVS/AIS, the difference in code activation rate was not significant according to changes in thrombolysis code. In minor PCS, AVS/AIS was associated with lower NIHSS scores, lower early neurological deterioration rates, and favorable outcomes. In major PCS, while AVS/AIS was not associated with outcomes, the majority of cases were prodromal AVS/AIS which simple vertigo and imbalance symptoms were followed by a major PCS symptom.

Conclusions: This study failed to show differences in outcome in patients with PCS according to how AVS/AIS is addressed in the stroke thrombolysis code. In patients with minor PCS, AVS/AIS was associated with a benign clinical course. Prompt identification of prodromal AVS/AIS is essential.

Keywords: posterior circulation ischemic stroke, thrombolysis code, thrombolysis, vertigo, disequilibrium

OPEN ACCESS

Edited by:
David Samuel Zee, Johns Hopkins University, United States

Reviewed by:
Alexander A. Tarnutzer, University of Zurich, Switzerland
Eun-Jae Lee, University of Ulsan, South Korea
Georgios Mantokoudis, Bern University Hospital, Switzerland

***Correspondence:**
Seong-Joon Lee
editisan@gmail.com

Specialty section:
This article was submitted to Neuro-Otology, a section of the journal Frontiers in Neurology

Received: *30 December 2021*
Accepted: *25 April 2022*
Published: *16 May 2022*

Citation:
Kim M, Park SY, Lee SE, Lee JS, Hong JM and Lee S-J (2022) Significance of Vertigo, Imbalance, and Other Minor Symptoms in Hyperacute Treatment of Posterior Circulation Stroke. Front. Neurol. 13:845707. doi: 10.3389/fneur.2022.845707

INTRODUCTION

About 12–19% of all strokes treated by intravenous thrombolysis (IVT) are posterior circulation stroke (PCS) (1, 2), and ∼10% of large vessel occlusion strokes involve the vertebrobasilar artery (3). However, clinical evidence of hyperacute stroke treatment in the posterior circulation lags behind anterior circulation strokes. The differences in safety and outcomes of thrombolysis between the anterior and posterior circulation is continuously being investigated (4) while the treatment effect of mechanical thrombectomy is still debated in the posterior circulation (3, 5, 6). Two randomized trials failed to prove benefit for endovascular therapy compared to medical therapy in patients with vertebrobasilar occlusion (3, 5), while one non-randomized cohort study showed better functional outcomes and reduced mortality (6). Hyperacute treatment of PCS is complicated by a number of reasons.

First, patients with PCS differ from those with anterior circulation ischemic stroke (ACS) in terms of presenting symptoms and signs, contributing to delay in diagnosis (7). A key symptom is dizziness and vertigo. Acute dizziness accounts for 3.5–11% of all patient visits to the emergency department (ED) (8, 9). Stroke accounts for 3–5% of all presentations to the ED with vertigo and dizziness (10, 11), while symptoms of dizziness or vertigo occur in 47–75% of patients with PCS (12). Accordingly, PCS patients may present as acute vestibular syndrome (AVS: vertigo, nystagmus, nausea/vomiting) or as acute imbalance syndrome (AIS: dizziness, sudden unsteadiness of stance and/or gait, no nystagmus) (13). Identification of stroke in AVS/AIS is a diagnostic challenge. While there have been numerous studies focusing on identification of central vertigo, it is still not appropriately addressed, resulting in misdiagnosis (11, 14).

Second, the symptoms of PCS is under-represented in scales evaluating stroke severity (15). The National Institutes of Health Stroke Scale (NIHSS) is the tool most widely used to evaluate the severity of acute stroke and focuses on the status of the anterior circulation. However, symptoms of PCS such as vertigo, nystagmus, and truncal ataxia, which are components of AVS/AIS are not fully included in the NIHSS, which complicates thrombolysis for PCS (16). Moreover, According to a previous study, the prognosis may be poorer in patients with PCS than in those with ACS, even with a low NIHSS score of $\leq$4 (17). Furthermore, according to the National Institute of Neurological Disorders and Stroke criteria, symptoms that arise in the brainstem, such as vertigo, dizziness, and dysarthria, are not defined as transient ischemic attacks (18). Therefore, the clinical severity of PCS may be underrated.

Stroke centers capable of providing thrombolysis and endovascular reperfusion treatment implement critical pathway and formal protocols to accelerate the delivery of hyperacute stroke treatments (19). Thus, when a patient suspected of stroke arrives to the ED, emergency medicine physicians or emergency nurses are able to activate the institutional thrombolysis code, calling for stroke physicians to determine thrombolysis eligibility, while enabling neurointerventional team members to prepare for possible endovascular thrombectomy (20). How the institutional thrombolysis code addresses acute vertigo/imbalance may have significant influences on hyperacute management of PCS, and according clinical outcomes of this population. Considering that only 3–5% of stroke patients present with dizziness, indiscriminate referrals and code activation will result in unnecessary costs and wasted manpower (10, 11, 21). On the contrary, neglection of AVS/AIS in the thrombolysis code may result in neglected treatment and resultant early neurological deterioration (END).

Recently, we had the opportunity to address such concerns, for we have recently modified our thrombolysis code from one that is generous to AVS/AIS to a more strict code that focuses on major deficits. We hypothesized that modifications in thrombolysis code to one that is exclusive to AVS/AIS will be detrimental to PCS stroke outcomes by causing delays in critical treatment. Such influence on outcome may differ according to whether the patient presented with AVS/AIS or not, and also if the patient presented with accompanying major neurological deficits, which would justify thrombolysis by itself, or minor neurological deficits. To confirm this hypothesis, using the institutional posterior circulation stroke database, we compared clinical outcomes in patients with PCS according to changes in stroke thrombolysis code. Using the same population, we also aimed to evaluate the clinical significance of AVS/AIS in PCS patients after dividing the patients to minor and major neurological deficits. Through this analysis, we further sought to identify patients that are likely to deteriorate or result in poor outcomes, who might benefit through faster and more proactive treatment.

METHODS

Study Participants and Changes to the Thrombolysis Activation Code

This retrospective, single-center, observational study was approved by the Institutional Review Board of Ajou University Hospital, Suwon, Korea and was conducted in accordance with the Declaration of Helsinki (AJIRB-MED-MDB-21-613). The requirement for informed consent was waived in view of the retrospective nature of the research.

Patient data were obtained from our institutional stroke registry, which contains information on all patients admitted with ischemic stroke. The institutional stroke thrombolysis code was modified in April 2018 to reflect the relative importance of the thrombolysis code to detect large vessel occlusion strokes (22), and to prepare for increases in thrombolysis code activation triggered by success of the late window thrombectomy trials (23, 24), aiming for efficient use of resources and manpower in our hospital. Before then, a thrombolysis code based on "sudden, side, symptoms" with more permissive symptomatology was utilized. "Sudden" was classified as an abrupt neurological deficit within 6 h from onset to arrival in the emergency room (ER). "Side" was defined as unilateral weakness affecting the face, an arm, or a leg. "Symptoms" that activated the thrombolysis code were as follows: difficulty walking, dysarthria or aphasia, motor weakness, abnormal behavior, sensory changes, visual disturbance, or others, in which vertigo could be incorporated

(**Table 1**). After May 2018 (period 2), we used a thrombolysis code that focused on major deficits and prohibited activation for isolated vertigo or disequilibrium. This thrombolysis code used the modified Face Arm Speech Time test (25). Relevant indications for activation of the thrombolysis code were two or more of consecutive unilateral hemiplegia of the face, arms, and legs, aphasia, and loss of consciousness without other clear causes within 8 h from onset to arrival in the ER. Symptoms of mono limb paresis, bilateral paresis without change in mental status, amnesia, vertigo, disequilibrium, and sensory change were contraindications to activation of the thrombolysis code (**Table 1**). In this study, data for all PCS patients who presented to the ED within 4.5 h of onset of symptoms between May 2016 and April 2018 (period 1) or between January 2019 and December 2020 (period 2) were analyzed. The diagnosis of PCS was confirmed by MRI. Stroke lesions were classified into medulla, pons, midbrain, anterior inferior cerebellar artery, posterior inferior cerebellar artery, superior cerebellar artery, thalamus, and posterior cerebral artery lesions excluding thalamus, in which diffusion restriction was confirmed on MRI. Patients with simultaneous PCS and anterior circulation stroke were excluded. The 8 months in between was considered a transitional period and not included in the analysis. In Period 1, 1,592 patients were hospitalized for ischemic stroke, of which 457 had PCS. Of the patients with PCS, 114 patients with PCS visited the ED within 4.5 h of symptoms. Likewise, in period 2, 1,508 patients were hospitalized for ischemic stroke, and among them, 475 patients with PCS were admitted for ED. Among them, 114 patients who visited to ED within 4.5 h of symptom onset were enrolled in the study in period 2.

TABLE 1 | Thrombolysis code according to study periods.

Study period	Model	
Period 1 (May 2016 to April 2018)	3S cube model (Sudden, Side, Symptom)	
	Sudden	Within 6 h
	Side	Unilateral weakness in an arm, a leg, or the face
	Symptom	1) Gait difficulty 2) Dysarthria or aphasia 3) Motor weakness 4) Abnormal behavior 5) Sensory change 6) Visual disturbance 7) Other (including vertigo and disequilibrium)
Period 2 (January 2019 to December 2020)	FAST model	
	Time	Within 8 h
	Symptom	1) Unilateral hemiplegia in an arm, a leg, or the face 2) Aphasia 3) Loss of consciousness without clear causes
	Exclusion	1) Weakness in one limb 2) Bilateral paresis without change in mental status 3) Amnesia 4) Vertigo 5) Disequilibrium 6) Sensory changes

Period 1: Thrombolysis code focusing on "sudden, side, symptoms" with more permissive symptomatology (May 2016 to April 2018) Period 2: Thrombolysis code focusing on major deficits and prohibited its activation for isolated vertigo or disequilibrium (January 2019 to December 2020).

Clinical Variables and Classification of Major and Minor PCS

Patient data regarding hyperacute management of stroke such as onset to visit time, code activation rate, door to neurologist referral time, median NIHSS scores, reperfusion treatment rate, END rate, and neurological outcomes were collected. According to the TOAST classification, the etiology of stroke was classified as large artery atherosclerosis, cardioembolism, small vessel occlusion, stroke of other determined etiology, or stroke of undetermined etiology (26).

Reperfusion therapy was defined as endovascular treatment (EVT) or IVT. Symptoms were confirmed through the NIHSS recorded in the medical record. Presenting symptoms of decreased mental alertness (defined as a level of consciousness subset score of $\geq$1 on the NIHSS), hemiparesis involving at least two compartments (face, upper limb, lower limb), aphasia (anarthria), or hemianopsia were considered major neurological deficits and patients with according deficits were termed major PCS, and patients who did not present with these symptoms were considered to present with minor deficits, and termed minor PCS (13). This classification was based on the idea that major deficits are usually regarded clearly disabling, and justify reperfusion treatments in itself, while there may be considerable uncertainty for AVS/AIS accompanied by minor deficits, and management of this subgroup would more likely be influenced by changes in thrombolysis code. END was defined as an increase of two or more points from the initial NIHSS after admission.

In patients with minor PCS, we defined an unfavorable outcome as that corresponding to a modified Rankin Scale (mRS) score of 2–6 at 3 months or END during hospitalization and an excellent outcome indicated by a mRS score of 0–1 and no END. In patients with major PCS, a good outcome was defined as a mRS score of 0–2 and a poor outcome as a mRS score of 3–6 at 3 months.

Evaluation of Vertigo, Imbalance, and Central Oculomotor Findings

The electronic medical records were retrospectively reviewed to identify PCS patients who presented with vertigo or imbalance. These symptoms were subclassified as follows: AVS (vertigo, nausea, vomiting, with or without spontaneous nystagmus, and continuously present at the time of ED presentation); acute imbalance syndrome (AIS, acute onset of unsteadiness in stance and gait that persisted at ED presentation without spontaneous nystagmus); transient AVS/AIS (resolution of symptoms before presentation to the ER); or prodromal AVS/AIS (vertigo or imbalance followed by major neurological deficits [as classified in the above section] that led to presentation to

TABLE 2 | Demographics, hyperacute treatments, and dizziness classification of enrolled patients.

	All patients ($n = 228$)			AVS/AIS ($n = 77$)			Minor PCS ($n = 96$)		
	Period 1 ($n = 114$)	Period 2 ($n = 114$)	*p*-value	Period 1 ($n = 39$)	Period 2 ($n = 38$)	*p*-value	Period 1 ($n = 53$)	Period 2 ($n = 43$)	*p*-value
Age (years)	65 ± 14	67 ± 12	0.30	61 ± 15	65 ± 13	0.21	63 ± 13	63 ± 11	0.86
Sex (male, %)	69 (60.5%)	74 (64.9%)	0.58	28 (71.8%)	26 (68.4%)	0.94	37 (69.8%)	30 (69.8%)	>0.99
Onset to visit time (min)	111 ± 66	126 ± 66	0.10	115 ± 66	124 ± 57	0.53	122 ± 67	142 ± 70	0.16
Door to neurology department referral time (min)	51 ± 123	75 ± 95	0.11	104 ± 193	128 ± 115	0.50	80 ± 169	119 ± 107	0.17
Code activation, *n* (%)	83 (72.8%)	68 (59.7%)	0.04	20 (51.3%)	17 (44.7%)	0.73	31 (58.5%)	12 (27.9%)	0.005
IVT, *n* (%)	24 (21.1%)	19 (17.0%)	0.54	5 (12.8%)	4 (11.1%)	>0.99	2 (3.8%)	0 (0.0%)	0.57
Door to needle time (min)	53 ± 22	74 ± 48	0.10	73 ± 37	67 ± 41	0.82	46 ± 0.71	–	
EVT, *n* (%)	26 (22.8%)	17 (15.0%)	0.19	7 (18.0%)	6 (16.2%)	>0.99	1 (1.9%)	1(2.3%)	>0.99
Door to groin puncture time (min)	120 ± 38	154 ± 162	0.40	134 ± 49	214 ± 276	0.52	95	60	–
Initial NIHSS, median	3 [1–13]	5 [2–10]	0.44	2 [1–6]	2 [1–5]	0.95	1 [0–3]	2 [0.5–2]	0.73
3 months mRS, median	1 [0–3]	1 [0–3]	0.18	1 [0–2.5]	1 [0–1]	0.34	1 [0–1]	0 [0–1]	0.09
3 months mRS 0–1, n (%)	65 (57.0%)	73 (64.0%)	0.34	25 (64.1%)	29 (76.3%)	0.36	45 (84.9%)	41 (95.4%)	0.18
3 months mRS 0–2, *n* (%)	74 (64.9%)	82 (71.9%)	0.32	29 (74.4%)	31 (81.6%)	0.62	47 (88.7%)	41 (95.4%)	0.42
END, *n* (%)	20 (17.5%)	19 (16.7%)	>0.99	4 (10.3%)	6 (15.8%)	0.70	6 (11.3%)	4 (9.3%)	>0.99
Dizziness classification			0.24			0.16			0.46
None, *n* (%)	75 (65.8%)	76 (66.7%)		0 (0.0%)	0 (0.0%)		31 (58.5%)	20 (46.5%)	
AVS, *n* (%)	11 (9.7%)	14 (12.3%)		11 (28.2%)	14 (36.8%)		10 (18.9%)	11 (25.6%)	
AIS, *n* (%)	9 (7.9%)	13 (11.4%)		9 (23.1%)	13 (34.2%)		7 (13.2%)	10 (23.3%)	
Prodromal AVS, *n* (%)	15 (13.2%)	7 (6.1%)		15 (38.5%)	7 (18.4%)		1 (1.9%)	0 (0.0%)	
Prodromal AIS, *n* (%)	0 (0.0%)	2 (1.8%)		0 (0.0%)	2 (5.3%)		0 (0.0%)	0 (0.0%)	
Transient AVS/AIS, *n* (%)	4 (3.5%)	2 (1.8%)		4 (10.3%)	2 (5.3%)		4 (7.6%)	2 (4.7%)	

AIS, acute imbalance syndrome; AVS, acute vestibular syndrome; END, early neurological deterioration; EVT, endovascular treatment; IVT, intravenous thrombolysis; NIHSS, National Institutes of Health Stroke Scale; mRS, modified Rankin Scale; PCS, posterior circulation ischemic stroke.

the ER). Horizontal/vertical gaze-evoked nystagmus, vertical or purely torsional spontaneous nystagmus, or ophthalmoparesis (27) were considered central oculomotor signs. PCS patients without symptoms of vertigo or imbalance were subclassified as non-AVS/AIS group. Our institution routinely performs CT angiography to patients with neurological deficits suspected of stroke, and also to patients that present with AVS/AIS. For the analysis on the relationship between stenosis or occlusion and prognosis, vertebrobasilar steno-occlusion was defined as the presence of significant occlusion or stenosis of more than 50% in the basilar artery or both vertebral arteries (28–30).

Statistical Analysis

For the first part of the study, the total PCS population was dichotomized according to changes in thrombolysis code as patients that presented in period 1 and those that presented in period 2 (**Table 1**). The two groups were compared to clarify whether a change in the thrombolysis code that excludes minor neurological deficits such as vertigo resulted in delays in treatment and changes in outcome. This analysis was also performed in the subgroup of patients with PSC who presented with AVS/AIS, and subgroup of patients that presented with minor PCS. Next, the clinical significance of AVS/AIS in PCS was evaluated. Given the likelihood that obvious major neurological deficits may be more disabling for the patient and influence clinical triage, the patients were divided according to whether PCS was major or minor. Univariate and multivariate analyses were performed to clarify the significance of vertigo and acute imbalance on the clinical characteristics and prognosis of minor and major PCS.

Continuous variables are summarized as the mean ± standard deviation, number (percentage), or median (interquartile range) and categorical variables as counts and percentages as appropriate. For comparing two groups, Continuous variables were compared using the Student's *t*-test and Mann-Whitney *U* test and categorical variables using the chi-square test. For comparison of three groups, continuous variables were compared using one-way ANOVA and *post hoc* Tamhane's test, and categorical variables by using the chi-square test. Multiple logistic regression was performed to identify predictors of outcome, including clinically relevant variables. Associations are presented as the odds ratio (OR) with the corresponding 95% confidence interval (CI). Statistical analyses were performed using R statistical software (version 3.6.3; R Foundation for Statistical Computing, Vienna, Austria) and the IBM SPSS package (version 25.0 for Windows; IBM Corp., Armonk, NY, USA). A p-value of <0.05 was considered statistically significant.

TABLE 3 | Demographics and clinical characteristics of patients with minor posterior circulation stroke.

	None-AVS/AIS ($n = 51$)	AVS/AIS ($n = 45$)	*p*-value
Age (years)	63 ± 10	63 ± 14	0.90
Onset to visit time (min)	139 ± 74	123 ± 63	0.26
Door to neurology department referral time (min)	51 ± 72	152 ± 186	0.001
Code activation, *n* (%)	32 (62.8%)	11 (24.4%)	<0.001
Reperfusion therapy, *n* (%)	2 (3.9%)	1 (2.2%)	>0.99
Initial NIHSS, median	2 [1–3]	1 [0–2]	0.04
3 month mRS, median	1 [0–1]	0 [0–1]	0.16
3 month mRS 0–1, *n* (%)	43 (84.3%)	43 (95.6%)	0.14
3 month mRS 0–2, *n* (%)	45 (88.2%)	43 (95.6%)	0.36
END, *n* (%)	9 (17.7%)	1 (2.2%)	0.03
Unfavorable outcome, *n* (%)	14 (27.5%)	3 (6.7%)	0.02
Dysarthria, *n* (%)	29 (56.9%)	17 (37.8%)	0.10
Facial palsy, *n* (%)	11 (21.6%)	9 (20.0%)	>0.99
Central oculomotor sign, *n* (%)	1 (2.0%)	8 (17.8%)	0.02
Vertebrobasilar steno-occlusion, *n* (%)	17 (33.3%)	7 (15.6%)	0.09
TOAST classification, *n* (%)			0.13
LAA	16 (31.4%)	16 (35.6%)	
CAE	5 (9.8%)	7 (15.6%)	
SVO	22 (43.10%)	10 (22.2%)	
OD	1 (2.0%)	5 (11.1%)	
UN	7 (13.7%)	7 (15.6%)	

AIS, acute imbalance syndrome; AVS, acute vestibular syndrome; CAE, cardioembolism; END, early neurological deterioration; LAA, large artery atherosclerosis; OD, stroke of other determined etiology; SVO, small vessel occlusion; TOAST classification; UN, stroke of undetermined etiology.

TABLE 4 | Clinical predictors of a good outcome in patients with minor posterior circulation stroke.

Parameter	Multivariate analysis	
	OR (95% CI)	*p*-value
AIS/AVS	7.8 [1.5–39.4]	0.01
Age	1.0 [0.9–1.1]	0.74
Code activation	0.9 [0.2–3.8]	0.91
Dysarthria	0.1 [0.01–0.5]	0.005
Facial palsy	6.2 [1.1–35.4]	0.04
Vertebrobasilar steno-occlusion	19.4 [1.9–194.6]	0.01

AIS, acute imbalance syndrome; AVS, acute vestibular syndrome; CI, confidence interval; OR, odds ratio.

RESULTS

Differences in Code Activation and Treatment Outcomes According to Changes in Stroke Code

Of 228 patients diagnosed to have PCS between May 2016 and December 2020, 114 presented in period 1 (age, 65 ± 14 years; male, 69 [60.5%]) and 114 presented in period 2 (age, 67 ± 12 years; male, 74 [64.9%]). The rates of thrombolysis code activation were significantly lower in period 2 (72.8% vs. 59.7%, $p = 0.04$). However, there was no significant difference in time to door (111 ± 66 min vs. 126 ± 66 min, $p = 0.10$), ED door to neurology department referral time (51 ± 123 min vs. 75 ± 95 min, $p = 0.11$), median initial NIHSS score (3 [1–13] vs. 5 [2–10], $p = 0.44$), intravenous thrombolysis rate (21.1% vs. 17.0%, $p = 0.54$), and frequency of EVT (22.8% vs. 15.0%, $p = 0.19$). Also, there was no significant difference in door to needle time (53 ± 22 min vs. 74 ± 48, $p = 0.10$) and door to groin puncture time (120 ± 38 min vs. 154 ± 162, $p = 0.40$). Furthermore, there was no difference in the frequency of a mRS score of 0–1 (57.0% vs. 64.0%, $p = 0.34$) or 0–2 (64.9% vs. 71.9%, $p = 0.32$) at 3 months, or frequency of END (17.5% vs. 16.7%, $p > 0.99$) between the two periods (**Table 2**).

Accompanying symptoms of acute vertigo or imbalance syndrome were present in 39 patients (34.2%) during period 1 and in 38 (33.3%) during period 2. Analysis of the AVS/AIS group according to time period did not reveal any significant difference in patient age (61 ± 15 years vs. 65 ± 13 years, $p = 0.21$), sex distribution (male, 28 [71.8%] vs. 26 [68.4%], $p = 0.94$), code activation rate (51.3% vs. 44.7%, $p = 0.73$), initial NIHSS score (2 [1–6] vs. 2 [1–5], $p = 0.95$), or mRS score at 3 months (1 [0–2.5] vs. 1 [0–1], $p = 0.34$) between the time periods (**Table 2**).

In the minor PCS sub-analysis, there was no significant difference in time to door (122 ± 67 vs. 142 ± 70 min, $p = 0.16$) and ED door to neurology referral time (80 ± 170 vs. 120 ± 108 min, $p = 017$) between two periods, but the code activation rate was significantly higher in period 1 (58.5% vs. 27.9%, $p = 0.005$). Also, there was no significant difference in functional outcome, as indicated by the mRS score at 3 months, between the two groups (1 [0–1] vs. 0 [0–1], $p = 0.09$) (**Table 2**).

In the non–AVS/AIS group, there was no significant between-period difference in patient age (67 ± 13 years vs. 68 ± 12 years, $p = 0.76$), sex distribution (male, 41 [54.7%] vs. 48 [63.2%], $p = 0.37$), initial NIHSS score (5 [2–15] vs. 6 [3–12], $p = 0.35$), or mRS score at 3 months (1 [1–4] vs. 1 [0–4], $p = 0.33$). However, a high code activation rate was observed in period 1 in the non-AVS/AIS group (84.0% vs. 67.1%, $p = 0.03$) (**Supplementary Table 1**).

There was no statistical difference between dizziness classification and stroke lesion according to period. When stroke lesions were compared according to AVS/AIS regardless of period and stroke severity, midbrain (18.5% vs. 31.7%, $p = 0.05$) and PICA lesions (20.5% vs. 41.6%, $p = 0.001$) were more frequently involved in PCS with AVS/AIS.

Clinical Significance of AVS/AIS in Patients With Minor PCS

Compared to the non-AVS/AIS subgroup, patients with AVS/AIS in the group with minor PCS (**Table 3**) revealed a lower rate of unfavorable outcome (mRS score ≥2 or END; 27.5% vs. 6.7%, $p = 0.02$). According to the mRS score at 3 months, there was no significant between-group difference in functional outcome (1 [0–1] vs. 0 [0–1], $p = 0.16$). In the AVS/AIS group, there was a significantly lower code activation rate (62.8% vs. 24.4%,

TABLE 5 | Demographics and clinical characteristics of patients with major posterior circulation stroke.

	None-AVS/AIS ($n = 100$)	AVS/AIS ($n = 9$)	Prodromal ($n = 23$)	*p*-value
Age (years)	70 ± 13	68 ± 15	63 ± 14	0.18
Onset to visit time (min)	108 ± 63	144 ± 57	103 ± 60	0.20
Door to neurology department referral time (min)	29 ± 50	143 ± 108	35 ± 64	0.02
Code activation, *n* (%)	82 (82.0%)	5 (55.6%)	21 (91.3%)	0.06
Reperfusion therapy, *n* (%)	47 (47.0%)	3 (33.3%)	14 (60.9%)	0.32
Door to needle time (min)	61 ± 38	128	63 ± 31	–
Door to groin puncture time (min)	118 ± 30	467 ± 433	123 ± 45	0.63
Initial NIHSS, median	10 [5–18.25]	5 [4–9]	8 [3–20.5]	0.09
3 month mRS, median	2 [1–5]	2 [1–3]	2 [1–5]	0.53
3 month mRS 0–2, *n* (%)	51 (51.0%)	5 (55.6%)	12 (52.2%)	0.96
END, *n* (%)	20 (20.0%)	1 (11.1%)	8 (34.8%)	0.22
Dysarthria, *n* (%)	86 (86.0%)	7 (77.8%)	16 (69.6%)	0.16
Facial palsy, *n* (%)	64 (64.0%)	7 (77.8%)	18 (78.3%)	0.33
Central oculomotor sign, *n* (%)	2 (3.0%)	2 (22.2%)	7 (43.8%)	<0.001
Decreased mental alertness, *n* (%)	52 (52.0%)	1 (11.1%)	12 (52.2%)	0.06
Hemiparesis (2 or more), *n* (%)	86 (86.0%)	6 (66.7%)	17 (73.9%)	0.17
Vertebrobasilar steno-occlusion, *n* (%)	60 (60.0%)	3 (33.3%)	15 (65.2%)	0.24
TOAST classification, *n* (%)				0.003
LAA	32 (32.0%)	1 (11.1%)	14 (60.9%)	
CAE	28 (28.0%)	4 (44.4%)	2 (8.7%)	
SVO	21 (21.0%)	2 (22.2%)	4 (17.4%)	
OD	1 (1.0%)	1 (11.1%)	3 (13.0%)	
UN	18 (18.0%)	1 (11.1%)	0 (0.0%)	

AIS, acute imbalance syndrome; AVS, acute vestibular syndrome; CAE, cardioembolism; END, early neurological deterioration; LAA, large artery atherosclerosis; NIHSS, National Institutes of Health Stroke Scale; mRS, modified Rankin Scale; OD, stroke of other determined etiology; SVO, small vessel occlusion; TOAST classification; UN, stroke of undetermined etiology.

$p < 0.001$) and a significantly longer ED door to neurology department referral time (51 ± 72 min vs. 152 ± 186 min, $p = 0.001$). There was no significant between-group difference in the frequency of focal neurological symptoms, such as dysarthria and facial palsy, or vertebrobasilar insufficiency confirmed by CT. There was a significantly higher rate of accompanied central oculomotor signs in patients with AVS (2.0% vs. 17.8%, $p = 0.02$) (**Table 3**).

In the multivariable analysis, AVS/AIS (OR 7.8, CI 1.5–39.4; $p = 0.01$), facial palsy (OR 6.2, CI 1.1–35.4; $p = 0.04$), and vertebrobasilar steno-occlusion (OR 19.4, CI 1.9–194.6; $p = 0.01$) were associated with good outcomes. Dysarthria was negatively correlated (OR 0.1, CI 0.01–0.5; $p = 0.005$), with age and code activation rate as covariates (**Table 4**).

Clinical Significance of AVS/AIS and Central Oculomotor Signs in Patients With Major PCS

In the group with major PCS, AVS/AIS was frequently prodromal (23/32, 71.8%). Accordingly, patients with major PCS were divided into three groups: non-AVS/AIS group ($n = 100$, 75.8%), those with AVS/AIS ($n = 9$, 6.8%), and those with prodromal AVS/AIS ($n = 23$, 17.4%) (**Table 5**). There was no significant difference in patient age (70 ± 13 years vs. 68 ± 15 years vs. 63 ± 14 years, $p = 0.18$) or onset to visit time (108 ± 63 min vs. 144 ± 57 min vs. 103 ± 60 min, $p = 0.20$) between the three groups. However, the ED door to neurology department referral time was shorter in non-AVS/AIS group and prodromal AVS/AIS group when comparing with AVS/AIS group (non-AVS/AIS vs. AVS/AIS vs. prodromal AVS/AIS, listed in this order here-on; 29 ± 50 vs. 143 ± 108 vs. 35 ± 64 min, $p = 0.02$). In the AVS/AIS group, there was a lower code activation rate compared to non-AVS/AIS group, and prodromal AVS/AIS group (82.0% vs. 55.6% vs. 91.3%, $p = 0.06$). Central oculomotor signs were significantly more common in the AVS/AIS and prodromal AVS/AIS groups than in the non-AVS/AIS group (3.0% vs. 22.2% vs. 43.8%, $p < 0.001$). When etiology was analyzed by TOAST classification, large artery atherosclerosis was significantly more common in the group with prodromal AVS/AIS than in the other groups (32.0% vs. 11.1% vs. 60.9%, $p = 0.003$) and CAE was less common in the prodromal AVS/AIS group than in the other groups (28.0% vs. 44.4% vs. 8.7%, $p = 0.003$). While the rate of reperfusion treatment was highest in the prodromal AVS/AIS group, it did not reach clinical significance (47.0% vs. 33.3% vs. 60.9%, $p = 0.32$). There was no significant difference in functional outcome, as indicated by the mRS score at 3 months, between the three groups (2 [1–5] vs. 2 [1–3] vs. 2 [1–5], $p = 0.53$) (**Table 5**). In multivariable analysis, there was no association of presence of

TABLE 6 | Clinical predictors of a good outcome in patients with major posterior circulation stroke.

Parameter	Multivariate analysis	
	OR (95% CI)	*p*-value
Presence of AVS/AIS		0.71
None	Reference	
AVS/AIS	0.5 [0.1–2.6]	0.43
Prodromal	0.8 [0.3–2.4]	0.70
Age	0.96 [0.9–0.99]	0.01
Decreased mental alertness	0.4 [0.2–0.98]	0.04
Hemiparesis	0.3 [0.1–1.04]	0.06
EVT	0.5 [0.2–1.4]	0.17
Vertebrobasilar steno-occlusion	0.9 [0.3–2.2]	0.73

AIS, acute imbalance syndrome; AVS, acute vestibular syndrome; EVT, endovascular treatment.

AVS/AIS with a good outcome ($p = 0.71$) when age, mental status, hemiparesis, reperfusion treatments, and vertebrobasilar steno-occlusion were incorporated as covariates (**Table 6**).

The time from the onset of AVS/AIS to the major neurological deficits in patients with prodromal AVS/AIS was median 630 (Interquartile range: 56–1,440) min. Regarding their temporal profile, among 23 patients with prodromal AVS/AIS, 9 (39.1%) patients worsened with occurrence of major deficits within 3 h, 18 (78.2%) patients worsened within 24 h, and 20 patients worsened within 3 days (87.0%) with prodromal AVS/AIS. Regarding prior medical care before deterioration, 12 (52.2%) experienced deterioration before seeking medical care, and 1 (4.3%) deteriorated while presenting to a clinic for AVS/AIS symptoms. Eleven patients (47.8%) patients deteriorated after emergency medical care, in which 8 patients deteriorated while admitted to primary hospitals due to vertigo, 1 presented to our ED due to vertigo but deteriorated before clinical assessment, and 1 patient presented to our ED for AVS 3 days before the stroke event, but was discharged.

The following is an example of the last patient who presented with prodromal AVS (**Figure 1**). A 50 year-old man with a past history of schizophrenia visited the ER with a 6 day history of dizziness, headache, and vomiting. The patient did not show any focal neurological deficits. CT angiography was performed in the ER and revealed calcified plaque with stenosis in the dominant left vertebral artery. The patient did not agree to further evaluation and management and was discharged. Three days later, the patient revisited the ER with central oculomotor signs, dysarthria, facial palsy, and an NIHSS score of 13. CT angiography showed occlusion of the vertebral and basilar arteries, and mechanical thrombectomy was needed for arterial reperfusion.

DISCUSSION

In this study, we failed to show that differences in how AVS/AIS is addressed in the stroke thrombolysis code would influence the quality of hyperacute treatment and affect clinical outcomes. In the minor PCS group, AVS/AIS was associated with good outcomes. In the major PCS group, while AVS/AIS was not associated with clinical outcomes, a clinically significant group of PCS patients presenting with prodromal vertigo could be identified.

Our results did not show differences in PCS stroke outcomes according to changes in institutional thrombolysis code despite actual changes in the percentage of patients referred to the neurology department for possible thrombolysis. The decreases in code activation was not associated with poorer functional outcomes, but it was also not associated with decreased rates of reperfusion therapy. There may be two explanations. First, even with changes in thrombolysis code, this change may have not been sufficient to lead to a clinically significant change in medical practice, especially because AVS/AIS patients were excluded from thrombolysis code, not the other way around. If clinical differences in outcomes were to occur between the two time periods, it would most likely be led by a larger number of minor PCS patients presenting with AVS/AIS, referred early to neurologists, and treated with hyperacute stroke treatments such as IVT or EVT. However, differences in thrombolysis code was not associated with changes in rates of reperfusion therapy. Scarce scientific evidence for reperfusion therapy in AVS/AIS seemed to limit radical changes regarding management of this population. Second, while our study results do not directly address the issue of IVT in AVS/AIS, which is still uncertain (13, 31), it may present indirect supporting evidence that treatment effects of aggressive screening of isolated AVS/AIS patients for thrombolysis may not be cost-effective. However, while the current study judged the cost-effectiveness of thrombolysis protocol based on the rate of time metrics, reperfusion treatments, and clinical outcome, it may be reasonable to also evaluate the rate of false-positive code activations and false-negative code activations in future studies. As this study included only patients with PCS, according data could not be shown in this study. We hope to address this issue in future studies.

Our study results do not claim against reperfusion therapy in PCS patients with AVS/AIS. While isolated AVS/AIS is often not considered disabling to justify IVT (31), a recent study involving a small number of PCS patients presenting with dizziness found IVT to be associated with salvage of brain tissues (13), which is encouraging. More sensitive neurological scales may be needed for prompt identification of PCS patients presenting with AVS/AIS, and to include them for future thrombolysis trials. This is evidenced by longer referral time for the AVS/AIS group compared to the non-AVS/AIS group in both minor and major PCS group. Prompt detection of PCS patients may be limited by the NIHSS, which is not known to be very sensitive in PCS (32), and under-estimates stroke severity and following functional neurological deficits (15). A previous study evaluating IVT in isolated AVS/AIS also faced similar issues, as decision for IVT was largely led by focal neurological deficits previously known to be disabling, and higher NIHSS stroke scales (33). In this regard, the use of extended clinical scales such as the e-NIHSS, which adds specific elements in existing items to explore signs or symptoms of posterior circulation stroke, may improve the sensitivity of PCS

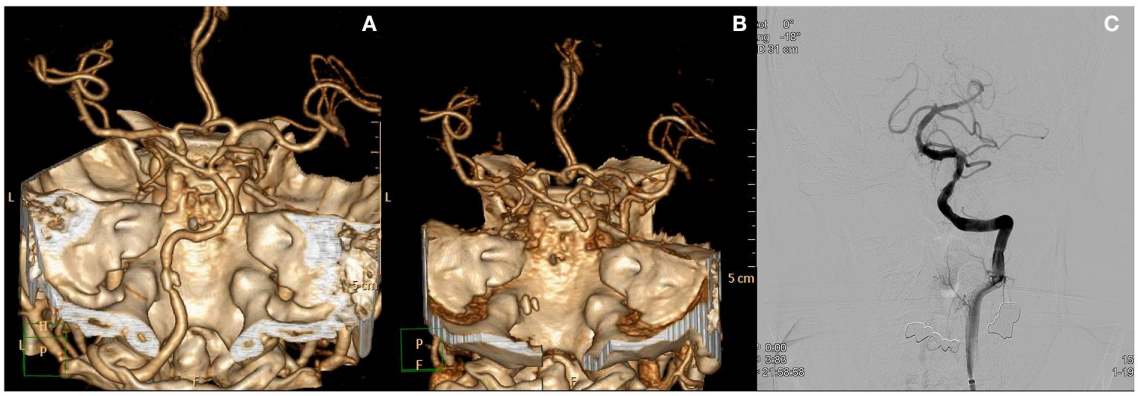

FIGURE 1 | Case of a patient who presented with prodromal acute vestibular syndrome. **(A)** Initial CT angiography revealed focal calcified plaque at the left distal vertebral artery with stenosis. The patient was discharged from the ED. Three days later, the patient revisited the ED with newly onset major neurological deficits. **(B)** CT angiography at that time show occlusion from the left vertebral artery to the distal basilar artery. **(C)** Recanalization of basilar and vertebral arteries after endovascular treatment.

detection, and may aid future studies regarding reperfusion therapy in PCS (32).

Our data shows the importance of identifying prodromal AVS/AIS, which was the dominant AVS/AIS pattern in major PCS. In this group, large artery atherosclerosis was more common, and over half the patients underwent reperfusion therapy. They also experienced END in 1/3 of the patients. In addition, the time interval from AVS/AIS to major deficits were within 3 days for the majority of the patients. It will be important to identify prodromal AVS/AIS patients in the prodromal stage without major deficits. To achieve this goal, careful description of vertigo characteristics in this prodromal group must be performed. A recent literature described that transient vestibular symptoms preceding PCS occurred in 12% during the 3 previous 3 months, which is usually vertigo with or without imbalance, with durations usually seconds to minutes (34). Similar studies should be further performed to identify the population of prodromal vertigo. The HINTS (Head-Impulse, Nystagmus, Test-of-Skew) may be helpful to differentiate prodromal vertigo. The HINTS has been extensively verified for its ability to distinguish central vertigo rather than peripheral vertigo among patients with AVS (35, 36). The ability of HINTS to identify patients at high risk for neurological deterioration needs to be confirmed in future studies. Also, presence of upbeat or downbeat nystagmus, which indicates vestibular imbalance in the pitch plane and bilateral vestibular structure involvement, may be signs that suggest global hypoperfusion and impending neurological aggravation (37). Imaging modalities for patient screening in the emergency department should also focus in identification of this potentially critical population. The presence of vertebrobasilar steno-occlusion in over half of this population emphasizes the importance of arterial imaging in acute vertigo and imbalance. This may be further aided by perfusion imaging (38), which may detect brain tissue that may be salvaged with hyperacute stroke treatments (13). Due to the high rates of large artery atherosclerosis in this population, dual antiplatelets and high dose statins to stabilize atherosclerotic plaque (39) may be the preferred treatment in this population. In the meantime, the clinical characteristics of this potentially grave population identified in this study may provide evidence for the length of hospital admission for those patients in which central vertigo is suspected, but not yet confirmed by imaging findings.

In patients with minor PCS, AVS/AIS was associated with lower NIHSS scores, lower rates of END, and better outcomes. There may be two possible explanations. First, compared to PCS patients with other minor symptoms, disabling neurological deficits may be less likely accompanied, or less likely to occur in the treatment course in PCS patients with AVS/AIS. Sustained vertigo with direction specific falls is associated with lesions of the vestibular nuclei and vestibular cerebellum causing vestibular toner imbalance in the yaw plane (40). Commonly accompanied oculomotor findings such as ocular tilt reaction or lateropulsion is caused by vestibular imbalance in the roll plane. Such vestibular asymmetry in the yaw or roll plane point to a unilateral disease of the brainstem, and usually do not indicate a progressive infratentorial stroke (41). Furthermore, corticospinal tract is located in the medial brainstem, while lesions causing isolated dizziness and vertigo is usually localized to the lateral brainstem (37). The finding that dysarthria, a sign of corticobular and corticospinal tract involvement (42), was associated with poor clinical outcomes, is supportive of this view. Second, vertigo, imbalance itself as a disabling symptom may be less significant, as vestibular tone imbalance due to central lesions are known to resolve within 2–4 weeks as a compensatory process (43). The cerebellum takes role in this compensatory mechanism within weeks, unless the patients have lesions in specific regions within the cerebellar hemispheres which might hinder compensatory processes (44, 45). However, care should be noted in interpretation of the current findings because previous studies have found non-lacunar mechanisms in half of stroke patients presenting with AVS (46), and heterogenous stroke etiologies are also seen in our study.

In our study, vertebrobasilar steno-occlusion and facial palsy were also identified as a good prognostic factor in patients with minor PCS. In the minor deficit subgroup, most of the vertebrobasilar steno-occlusion would have been chronic, and collateral vessels may have been well-developed due to longstanding hypoperfusion (47), contributing to better outcomes. The facial motor nucleus is located in the lateral brainstem (48), rather than the medial brainstem in which the corticospinal tract is located, and which would be a key determinant of functional outcomes if involved by a stroke lesion. These findings and corresponding mechanisms need to be validated in future studies.

Previous literature had classified acute AVS patients as isolated AVS and non-isolated AVS (49). It is clinically important to differentiate isolated vascular vertigo (37) from benign causes of AVS such as vestibular neuritis. However, the main focus of the current study was influence of vertigo on thrombolysis, and we chose to classify their symptoms by presence of AVS/AIS, and also by clinical severity as major and minor deficits (13). Furthermore, another important focus of our study was whether changes in thrombolysis code will cause delays in acute stroke treatment. This would usually be more dominant in patients without obvious major neurological deficits, and caused by delayed neurologist referral by emergency physicians due to uncertainty in diagnosis, and neurologists pondering over therapeutic benefits. This is another reason we classified their symptoms into major and minor deficits.

Our study has several limitations. First, as this analysis was performed through analysis of a stroke database, worsened clinical outcomes due to misdiagnosis of central vertigo may not be appropriately represented. However, such patients are at least partly represented by the prodromal vertigo group in this study, and we believe that our study results is distinguished from analysis of AVS/AIS patients because the clinical course of all PCS patients is described. Second, due to the retrospective observational design the classification of dizziness information regarding central oculomotor signs may be inaccurate. However, as all patients were admitted with multiple neurological exams performed by stroke staff, neurology residents, and stroke nurse in the stroke unit, it is unlikely that symptoms were omitted to a large degree. Third, there still remains a gap between minor AVS/AIS group and prodromal vertigo group, as END was infrequent in minor AVS/AIS. Thus, in future studies, risk factors of END in minor AVS/AIS should be identified, such as incomplete occlusions or distal basilar involvements that have predicted END in vertebrobasilar occlusions (50, 51).

In conclusion, an emphasis on AVS/AIS in the stroke thrombolysis code was not associated with higher thrombolysis rates nor with differences in clinical outcomes. In PCS patients presenting with AVS/AIS without severe focal neurological deficits, the clinical course seems to be usually benign. However, a substantial percentage of patients presented with prodromal AVS/AIS in major PCS, and care should be taken to identify this subgroup in the prodromal phase.

DATA AVAILABILITY STATEMENT

The raw data supporting the conclusions of this article will be made available by the authors, without undue reservation.

ETHICS STATEMENT

The studies involving human participants were reviewed and approved by Ethics Committee and Institutional Review Board of Ajou University Hospital. Written informed consent for participation was not required for this study in accordance with the national legislation and the institutional requirements.

AUTHOR CONTRIBUTIONS

MK: data interpretation, drafted the work, revised the draft critically for important intellectual content, and approved the final version of the paper. SP, SL, JL, and JH: data interpretation, revised the draft critically for important intellectual content, and approved the final version of the paper. S-JL: conceptualization and supervision of the study, data interpretation, revised the draft critically for important intellectual content, and approved the final version of the paper.

FUNDING

This work was supported by the Basic Science Research Program through the National Research Foundation of Korea (NRF) funded by the Ministry of Education (NRF-2021R1I1A1A01048331; S-JL).

SUPPLEMENTARY MATERIAL

The Supplementary Material for this article can be found online at: https://www.frontiersin.org/articles/10.3389/fneur.2022.845707/full#supplementary-material

REFERENCES

1. Dornák T, Král M, Hazlinger M, Herzig R, Veverka T, Burval S, et al. Posterior vs. anterior circulation infarction: demography, outcomes, and frequency of hemorrhage after thrombolysis. *Int J Stroke.* (2015) 10:1224–8. doi: 10.1111/ijs.12626
2. Dornák T, Král M, Šanák D, Kanovský P. Intravenous thrombolysis in posterior circulation stroke. *Front Neurol.* (2019) 10:417. doi: 10.3389/fneur.2019.00417
3. Langezaal LCM, van der Hoeven E, Mont'Alverne FJA, de Carvalho JJF, Lima FO, Dippel DWJ, et al. Endovascular therapy for stroke due to basilar-artery occlusion. *N Engl J Med.* (2021) 384:1910–20. doi: 10.1056/NEJMoa2030297
4. Keselman B, Gdovinova Z, Jatuzis D, Melo TPE, Vilionskis A, Cavallo R, et al. Safety and outcomes of intravenous thrombolysis in posterior versus anterior circulation stroke: results from the safe implementation of treatments in stroke registry and meta-analysis. *Stroke.* (2020) 51:876–82. doi: 10.1161/STROKEAHA.119.027071

5. Liu X, Dai Q, Ye R, Zi W, Liu Y, Wang H, et al. Endovascular treatment versus standard medical treatment for vertebrobasilar artery occlusion (best): an open-label, randomised controlled trial. *Lancet Neurol.* (2020) 19:115–22. doi: 10.1016/S1474-4422(19)30395-3
6. Zi W, Qiu Z, Wu D, Li F, Liu H, Liu W, et al. Assessment of endovascular treatment for acute basilar artery occlusion via a nationwide prospective registry. *JAMA Neurol.* (2020) 77:561–73. doi: 10.1001/jamaneurol.2020.0156
7. Burns JD, Rindler RS, Carr C, Lau H, Cervantes-Arslanian AM, Green-LaRoche DM, et al. Delay in diagnosis of basilar artery stroke. *Neurocrit Care.* (2016) 24:172–9. doi: 10.1007/s12028-015-0211-0
8. Crespi V. Dizziness and vertigo: an epidemiological survey and patient management in the emergency room. *Neurol Sci.* (2004) 25(Suppl. 1):S24–5. doi: 10.1007/s10072-004-0212-9
9. Lammers W, Folmer W, Van Lieshout EM, Mulligan T, Christiaanse JC, Den Hartog D, et al. Demographic analysis of emergency department patients at the Ruijin Hospital, Shanghai. *Emerg Med Int.* (2011) 2011:748274. doi: 10.1155/2011/748274
10. Newman-Toker DE. Missed stroke in acute vertigo and dizziness: it is time for action, not debate. *Ann Neurol.* (2016) 79:27–31. doi: 10.1002/ana.24532
11. Kerber KA, Brown DL, Lisabeth LD, Smith MA, Morgenstern LB. Stroke among patients with dizziness, vertigo, and imbalance in the emergency department: a population-based study. *Stroke.* (2006) 37:2484–7. doi: 10.1161/01.STR.0000240329.48263.0d
12. Nouh A, Remke J, Ruland S. Ischemic posterior circulation stroke: a review of anatomy, clinical presentations, diagnosis, and current management. *Front Neurol.* (2014) 5:30. doi: 10.3389/fneur.2014.00030
13. Machner B, Choi JH, Neumann A, Trillenberg P, Helmchen C. What guides decision-making on intravenous thrombolysis in acute vestibular syndrome and suspected ischemic stroke in the posterior circulation? *J Neurol.* (2021) 268:249–64. doi: 10.1007/s00415-020-10134-9
14. Tarnutzer AA, Lee SH, Robinson KA, Wang Z, Edlow JA, Newman-Toker DE. Ed Misdiagnosis of cerebrovascular events in the era of modern neuroimaging: a meta-analysis. *Neurology.* (2017) 88:1468–77. doi: 10.1212/WNL.0000000000003814
15. Hoyer C, Szabo K. Pitfalls in the diagnosis of posterior circulation stroke in the emergency setting. *Front Neurol.* (2021) 12:682827. doi: 10.3389/fneur.2021.682827
16. Martin-Schild S, Albright KC, Tanksley J, Pandav V, Jones EB, Grotta JC, et al. Zero on the Nihss does not equal the absence of stroke. *Ann Emerg Med.* (2011) 57:42–5. doi: 10.1016/j.annemergmed.2010.06.564
17. Inoa V, Aron AW, Staff I, Fortunato G, Sansing LH. Lower Nih stroke scale scores are required to accurately predict a good prognosis in posterior circulation stroke. *Cerebrovasc Dis.* (2014) 37:251–5. doi: 10.1159/000358869
18. Paul NL, Simoni M, Rothwell PM. Transient isolated brainstem symptoms preceding posterior circulation stroke: a population-based study. *Lancet Neurol.* (2013) 12:65–71. doi: 10.1016/S1474-4422(12)70299-5
19. Ko SB, Park HK, Kim BM, Heo JH, Rha JH, Kwon SU, et al. 2019 Update of the Korean clinical practice guidelines of stroke for endovascular recanalization therapy in patients with acute ischemic stroke. *J Stroke.* (2019) 21:231–40. doi: 10.5853/jos.2019.00024
20. Kim DH, Kim B, Jung C, Nam HS, Lee JS, Kim JW, et al. Consensus statements by Korean Society of Interventional Neuroradiology and Korean Stroke Society: hyperacute endovascular treatment workflow to reduce door-to-reperfusion time. *Korean J Radiol.* (2018) 19:838–48. doi: 10.3348/kjr.2018.19.5.838
21. Saber Tehrani AS, Coughlan D, Hsieh YH, Mantokoudis G, Korley FK, Kerber KA, et al. Rising annual costs of dizziness presentations to US emergency departments. *Acad Emerg Med.* (2013) 20:689–96. doi: 10.1111/acem.12168
22. McTaggart RA, Holodinsky JK, Ospel JM, Cheung AK, Manning NW, Wenderoth JD, et al. Leaving no large vessel occlusion stroke behind: reorganizing stroke systems of care to improve timely access to endovascular therapy. *Stroke.* (2020) 51:1951–60. doi: 10.1161/STROKEAHA.119.026735
23. Nogueira RG, Jadhav AP, Haussen DC, Bonafe A, Budzik RF, Bhuva P, et al. Thrombectomy 6 to 24 hours after stroke with a mismatch between deficit and infarct. *N Engl J Med.* (2018) 378:11–21. doi: 10.1056/NEJMoa1706442
24. Albers GW, Marks MP, Kemp S, Christensen S, Tsai JP, Ortega-Gutierrez S, et al. Thrombectomy for stroke at 6 to 16 hours with selection by perfusion imaging. *N Engl J Med.* (2018) 378:708–18. doi: 10.1056/NEJMoa1713973
25. Kothari RU, Pancioli A, Liu T, Brott T, Broderick J. Cincinnati prehospital stroke scale: reproducibility and validity. *Ann Emerg Med.* (1999) 33:373–8. doi: 10.1016/S0196-0644(99)70299-4
26. Adams HP, Jr., Bendixen BH, Kappelle LJ, Biller J, Love BB, et al. Classification of subtype of acute ischemic stroke. Definitions for use in a multicenter clinical trial. TOAST. Trial of Org 10172 in acute stroke treatment. *Stroke.* (1993) 24:35–41. doi: 10.1161/01.STR.24.1.35
27. Machner B, Choi JH, Trillenberg P, Heide W, Helmchen C. Risk of acute brain lesions in dizzy patients presenting to the emergency room: who needs imaging and who does not? *J Neurol.* (2020) 267:126–35. doi: 10.1007/s00415-020-09909-x
28. Moufarrij NA, Little JR, Furlan AJ, Leatherman JR, Williams GW. Basilar and distal vertebral artery stenosis: long-term follow-up. *Stroke.* (1986) 17:938–42. doi: 10.1161/01.STR.17.5.938
29. Schneider PA, Rossman ME, Bernstein EF, Ringelstein EB, Torem S, Otis SM. Noninvasive evaluation of vertebrobasilar insufficiency. *J Ultrasound Med.* (1991) 10:373–9. doi: 10.7863/jum.1991.10.7.373
30. Chimowitz MI, Lynn MJ, Howlett-Smith H, Stern BJ, Hertzberg VS, Frankel MR, et al. Comparison of warfarin and aspirin for symptomatic intracranial arterial stenosis. *N Engl J Med.* (2005) 352:1305–16. doi: 10.1056/NEJMoa043033
31. Lee SH, Kim JS. Acute diagnosis and management of stroke presenting dizziness or vertigo. *Neurol Clin.* (2015) 33:687–98, xi. doi: 10.1016/j.ncl.2015.04.006
32. Olivato S, Nizzoli S, Cavazzuti M, Casoni F, Nichelli PF, Zini A. E-Nihss: an expanded national institutes of health stroke scale weighted for anterior and posterior circulation strokes. *J Stroke Cerebrovasc Dis.* (2016) 25:2953–7. doi: 10.1016/j.jstrokecerebrovasdis.2016.08.011
33. Shi T, Zhang Z, Jin B, Wang J, Wu H, Zheng J, et al. Choice of intravenous thrombolysis therapy in patients with mild stroke complaining of acute dizziness. *Am J Emerg Med.* (2021) 52:20–4. doi: 10.1016/j.ajem.2021.11.020
34. Kim HA, Oh EH, Choi SY, Choi JH, Park JY, Lee H, et al. Transient vestibular symptoms preceding posterior circulation stroke: a prospective multicenter study. *Stroke.* (2021) 52:e224–8. doi: 10.1161/STROKEAHA.120.032488
35. Kattah JC, Talkad AV, Wang DZ, Hsieh YH, Newman-Toker DE. Hints to diagnose stroke in the acute vestibular syndrome: three-step bedside oculomotor examination more sensitive than early Mri diffusion-weighted imaging. *Stroke.* (2009) 40:3504–10. doi: 10.1161/STROKEAHA.109.551234
36. Newman-Toker DE, Kerber KA, Hsieh YH, Pula JH, Omron R, Saber Tehrani AS, et al. Hints outperforms Abcd2 to screen for stroke in acute continuous vertigo and dizziness. *Acad Emerg Med.* (2013) 20:986–96. doi: 10.1111/acem.12223
37. Lee H. Isolated vascular vertigo. *J Stroke.* (2014) 16:124–30. doi: 10.5853/jos.2014.16.3.124
38. Choi JH, Park MG, Choi SY, Park KP, Baik SK, Kim JS, et al. Acute transient vestibular syndrome: prevalence of stroke and efficacy of bedside evaluation. *Stroke.* (2017) 48:556–62. doi: 10.1161/STROKEAHA.116.015507
39. Kim JS, Bang OY. Medical treatment of intracranial atherosclerosis: an update. *J Stroke.* (2017) 19:261–70. doi: 10.5853/jos.2017.01830
40. Brandt T, Dieterich M. The dizzy patient: don't forget disorders of the central vestibular system. *Nat Rev Neurol.* (2017) 13:352–62. doi: 10.1038/nrneurol.2017.58
41. Dieterich M, Brandt T. The bilateral central vestibular system: its pathways, functions, and disorders. *Ann N Y Acad Sci.* (2015) 1343:10–26. doi: 10.1111/nyas.12585
42. Kwon HG, Lee J, Jang SH. Injury of the corticobulbar tract in patients with dysarthria following cerebral infarct: diffusion tensor tractography study. *Int J Neurosci.* (2016) 126:361–5. doi: 10.3109/00207454.2015.1020536
43. Baier B, Dieterich M. Ocular tilt reaction: a clinical sign of cerebellar infarctions? *Neurology.* (2009) 72:572–3. doi: 10.1212/01.wnl.0000342123.39308.32
44. Baier B, Müller N, Rhode F, Dieterich M. Vestibular compensation in cerebellar stroke patients. *Eur J Neurol.* (2015) 22:416–8. doi: 10.1111/ene.12475

45. Zwergal A, Möhwald K, Salazar López E, Hadzhikolev H, Brandt T, Jahn K, et al. A prospective analysis of lesion-symptom relationships in acute vestibular and ocular motor stroke. *Front Neurol.* (2020) 11:822. doi: 10.3389/fneur.2020.00822
46. Saber Tehrani AS, Kattah JC, Mantokoudis G, Pula JH, Nair D, Blitz A, et al. Small strokes causing severe vertigo: frequency of false-negative Mris and nonlacunar mechanisms. *Neurology.* (2014) 83:169–73. doi: 10.1212/WNL.0000000000000573
47. Romero JR, Pikula A, Nguyen TN, Nien YL, Norbash A, Babikian VL. Cerebral collateral circulation in carotid artery disease. *Curr Cardiol Rev.* (2009) 5:279–88. doi: 10.2174/157340309789317887
48. Gates P. The rule of 4 of the brainstem: a simplified method for understanding brainstem anatomy and brainstem vascular syndromes for the non-neurologist. *Intern Med J.* (2005) 35:263–6. doi: 10.1111/j.1445-5994.2004.00732.x
49. Choi JH, Kim HW, Choi KD, Kim MJ, Choi YR, Cho HJ, et al. Isolated vestibular syndrome in posterior circulation stroke: frequency and involved structures. *Neurol Clin Pract.* (2014) 4:410–8. doi: 10.1212/CPJ.0000000000000028
50. Koh S, Lee SE, Jung WS, Choi JW, Lee JS, Hong JM, et al. Predictors of early neurological deterioration in stroke due to vertebrobasilar occlusion. *Front Neurol.* (2021) 12:696042. doi: 10.3389/fneur.2021.696042
51. Koh S, Park JH, Park B, Choi MH, Lee SE, Lee JS, et al. Prediction of infarct growth and neurological deterioration in patients with vertebrobasilar artery occlusions. *J Clin Med.* (2020) 9:3759. doi: 10.3390/jcm9113759

Conflict of Interest: The authors declare that the research was conducted in the absence of any commercial or financial relationships that could be construed as a potential conflict of interest.

Publisher's Note: All claims expressed in this article are solely those of the authors and do not necessarily represent those of their affiliated organizations, or those of the publisher, the editors and the reviewers. Any product that may be evaluated in this article, or claim that may be made by its manufacturer, is not guaranteed or endorsed by the publisher.

frontiers | Frontiers in Neurology

ORIGINAL RESEARCH
published: 12 July 2022
doi: 10.3389/fneur.2022.920357

Videooculography "HINTS" in Acute Vestibular Syndrome: A Prospective Study

*Athanasia Korda[1], Wilhelm Wimmer[1,2], Ewa Zamaro[1], Franca Wagner[3], Thomas C. Sauter[4], Marco D. Caversaccio[1] and Georgios Mantokoudis[1]**

[1] Department of Otorhinolaryngology, Head and Neck Surgery, Inselspital, University Hospital Bern and University of Bern, Bern, Switzerland, [2] Hearing Research Laboratory, ARTORG Center, University of Bern, Bern, Switzerland, [3] University Institute of Diagnostic and Interventional Neuroradiology, Inselspital, University Hospital Bern and University of Bern, Bern, Switzerland, [4] Department of Emergency Medicine, Inselspital, University Hospital Bern and University of Bern, Bern, Switzerland

Objective: A three-step bedside test ("HINTS": Head Impulse-Nystagmus-Test of Skew), is a well-established way to differentiate peripheral from central causes in patients with acute vestibular syndrome (AVS). Nowadays, the use of videooculography gives physicians the possibility to quantify all eye movements. The goal of this study is to compare the accuracy of VOG "HINTS" (vHINTS) to an expert evaluation.

Methods: We performed a prospective study from July 2015 to April 2020 on all patients presenting at the emergency department with signs of AVS. All the patients underwent clinical HINTS (cHINTS) and vHINTS followed by delayed MRI, which served as a gold standard for stroke confirmation.

Results: We assessed 46 patients with AVS, 35 patients with acute unilateral vestibulopathy, and 11 patients with stroke. The overall accuracy of vHINTS in detecting a central pathology was 94.2% with 100% sensitivity and 88.9% specificity. Experts, however, assessed cHINTS with a lower accuracy of 88.3%, 90.9% sensitivity, and 85.7% specificity. The agreement between clinical and video head impulse tests was good, whereas for nystagmus direction was fair.

Conclusions: vHINTS proved to be very accurate in detecting strokes in patients AVS, with 9% points better sensitivity than the expert. The evaluation of nystagmus direction was the most difficult part of HINTS.

Keywords: HINTS, videooculography, acute unilateral vestibulopathy, stroke, vertigo

OPEN ACCESS

Edited by:
Ji Soo Kim,
Seoul National University, South Korea

Reviewed by:
Christine Rogers,
University of Cape Town, South Africa
Peter Müller-Barna,
München Hospital, Germany

****Correspondence:***
Georgios Mantokoudis
georgios.mantokoudis@insel.ch

Specialty section:
This article was submitted to Neuro-Otology, a section of the journal Frontiers in Neurology

Received: *14 April 2022*
Accepted: *02 June 2022*
Published: *12 July 2022*

Citation:
Korda A, Wimmer W, Zamaro E, Wagner F, Sauter TC, Caversaccio MD and Mantokoudis G (2022) Videooculography "HINTS" in Acute Vestibular Syndrome: A Prospective Study. Front. Neurol. 13:920357. doi: 10.3389/fneur.2022.920357

INTRODUCTION

Acute vestibular syndrome (AVS) consists of vertigo, nausea/vomiting, and gait unsteadiness together with head motion intolerance and nystagmus lasting from days to weeks (1). The most common cause of this syndrome is acute unilateral vestibulopathy (AUVP). However, some patients with AVS can suffer from brainstem or cerebellar strokes that mimic AUVP (2). There is a high prevalence of dizziness in the emergency department (ED) (3, 4) with a large proportion of strokes (3)[1].

[1]Nikles F, Kerkeni H, Zamaro E, Korda A, Sauter TC, Kalla R, et al. Do stroke patients with dizziness present a vestibular syndrome without nystagmus? An underestimated entity (2022).

The Head-Impulse-Nystagmus-Test-of-Skew ("HINTS") battery proved to be more accurate in detecting strokes than MRI scan of the brain, especially if it is performed in the beginning of symptoms (5). However, the accuracy of "HINTS" can vary and depends on the experience of the physician (6). Moreover, although "HINTS," since its first description is thought to have been established in the clinical practice and a bedside three-step examination seems to be a very fast and easy way to detect a stroke, physicians in the ED are still not so familiar with this examination (7–9). In addition, the sensitivity and specificity of head impulse varies with experience, and even experts have difficulties (10) and need a learning curve (11).

Nowadays, the use of VOG devices assists physicians to quantify eye movements. These devices are easy to use (11) and they can serve in the near future with telemedicine and machine learning (12) for remote areas or in pandemic times (13, 14) as a diagnostic tool for acute dizziness and as a support for physicians in the ED analog to an "Eye-ECG"(15). Although there are many studies that show the superiority of video head impulse test (vHIT), there are no studies that assess the aggregated results of all the other steps of the HINTS battery using VOG.

In this study, we sought to assess and compare the diagnostic accuracy of VOG "HINTS" (vHINTS) and of clinical "HINTS"(cHINTS) in predicting a stroke in the ED. Furthermore, we wanted to calculate the concordance between clinical and VOG-assisted tests for each of the three steps of the "HINTS" examination.

MATERIALS AND METHODS

Patient Characteristics

In this prospective, cross-sectional study, data from patients with AVS (convenience sample) were collected in the ED between July 2015 and April 2020 and were part of a larger study (DETECT: Dizziness Evaluation Tool for Emergent Clinical Triage) (16–18). The inclusion and exclusion criteria have been described previously (18). The accuracy of vHIT, video test of skew, and nystagmus test for discriminating vestibular strokes as a single stand-alone test, has been evaluated and previously published (16, 19). Here, we present the data from patients with AVS who received all the three tests clinically (cHINTS) and with VOG (vHINTS) at the bedside. A neurootologist (expert) with 2 years of experience in the field, performed the physical examination with cHINTS assessment and vHINTS testing in all the enrolled patients. We performed caloric testing in all the patients as an additional examination at the time of ED presentation either in the ED or in our vertigo center. All the patients received an acute MRI either within 48 h in the ED or a second, delayed MRI (3–10 days after onset of symptoms) if there was no acute MRI indicated based on clinical grounds or if the first acute MRI was non-diagnostic with regard to the question of a stroke. The delayed MRI served as a gold standard for stroke detection. Patients with a negative acute and/or delayed MRI and a pathological caloric test were diagnosed as having acute unilateral vestibulopathy (AUVP)/vestibular neuritis. Additionally, we collected information on age and gender. All the enrolled patients gave written consent. The local ethics committee (IRB) approved this study (KEK # 047/14).

Abbreviations: AVS, acute vestibular syndrome; AUVP, acute unilateral vestibulopathy; "HINTS", Head-Impulse-Nystagmus-Test-of-Skew; ED, emergency department; VOG, videooculography, vHIT, video head impulse test; cHINTS, clinical HINTS; vHINTS, VOG "HINTS".

MR Protocol

The patients were scanned at one of our six MR scanners either on a 1.5 T scanner (Siemens MAGNETOM Avanto and Siemens MAGNETOM Aera; Siemens Medical Solutions, Erlangen, Germany) or a 3 T scanner (Siemens MAGNETOM; Siemens Medical Solutions, Erlangen, Germany). Our standard MRI protocol for all the patients included axial diffusion-weighted imaging (DWI) with apparent diffusion coefficient (ADC) [5 mm slice thickness (SL)], axial fluid-attenuated inversion recovery (FLAIR) (5 mm SL), axial susceptibility-weighted imaging (SWI) (1.6 mm slice thickness), and time of flight (TOF) angiography (0.5 mm slice thickness). Optional and depending on the clinical symptoms, axial brainstem diffusion-weighted imaging (DWI) with apparent diffusion coefficient (ADC) (3 mm SL) and axial T2-weighted imaging over the brainstem (3 mm SL) were added. After the application of intravenous gadobutrol (Gadovist; Bayer Schering Pharma, Berlin, Germany) in an antecubital vein with a 5-ml/s injection rate, we acquired a standard dynamic susceptibility contrast (DSC) MRI perfusion (5 mm slice thickness) as well as a contrast-enhanced T1 turbo spin echo (TSE)-weighted sequence (slice thickness 5 mm SL). Finally, contrast-enhanced magnetic resonance angiography (CE MRA) of the head and neck vessels was acquired after injection of a second bolus of gadobutrol with a 3-ml/s injection rate. If indicated, follow-up MR imaging was performed using the same MR scanner and field strength with the same MRI protocol or a short native variant of the MR protocol without acquisition of sequences with contrast.

vHINTS

We recorded vHINTS with a VOG device (EyeSeeCam, Munich) and measured head and eye movement velocity (head impulse test), nystagmus slow phase velocity (SPV), and vertical ocular misalignment (test of skew) with a head-mounted infrared high-speed camera (monocular, 250 Hz) connected to a laptop by USB (**Figures 1A–C**). The high-speed infrared camera was calibrated by projecting dots on a TV screen or a tablet with a predefined distance.

vHIT was performed by fast passive horizontal head movements (high frequency, 10–20° head excursion in 100–300 m/s corresponding to 1,000–6,000°/s^2 acceleration) in room light during visual target fixation at more than 1 m distance. VOR gain values were derived from eye velocity divided by head velocity at 60 ms after HIT onset.

For nystagmus quantification (beating direction and SPV), we used three fixation lights as a target for straight-ahead gaze and for eccentric gaze positions of 15 ± 5 deg to the right and left. We recorded an average SPV for 10 s in each target position (tablet: distance eyes to target: 260 mm, target size: 4 mm, luminosity: 6.17 Lux, angular size: 0.89 degrees; TV screen: distance eyes to

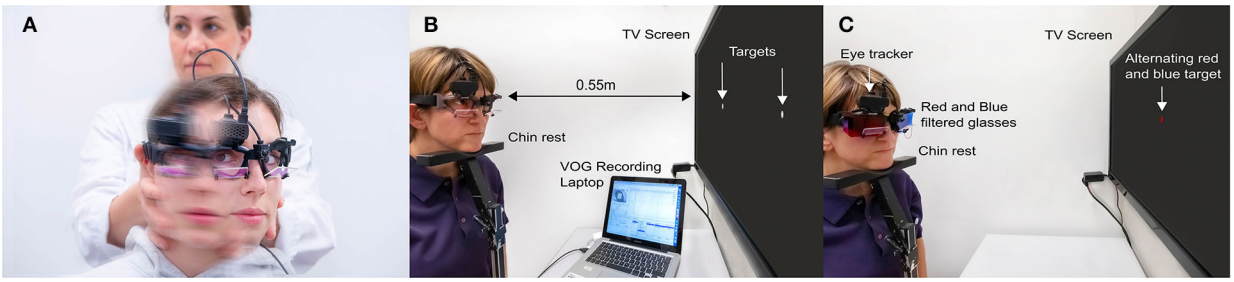

FIGURE 1 | Illustration of all parts of the Head Impulse-Nystagmus-Test of Skew (HINTS) battery by videooculography (VOG). **(A)** Video head impulse test, **(B)** videonystagmography, and **(C)** video test of skew.

target: 55 cm, target Size: 5 mm, luminosity: 11.8 Lux., angular size: 0.23 degrees).

Vertical ocular misalignment was tested by fixating an alternating colored dot (red/blue) displayed for 2 s in the center of the TV screen or the tablet while synchronizing with VOG. We used color-filtered glasses on both eyes (red filter for the left eye and blue filter for the right eye), allowing only a monochromatic view of the target dot. Skew deviation was quantitatively reported in degrees (eye position) or converted into prism diopters. Details about automated skew deviation calculation have been described elsewhere (20). Here, we report skew deviation in degrees (vertical misalignment) throughout the manuscript.

Statistical Analysis

All statistics were reported using the SPSS statistical software (IBM SPSS Statistics for Windows, Version 25.0. Armonk, NY, IBM Corp.). We classified the patients into central or peripheral "HINTS" (binary outcome) based on vHINTS or cHINTS exams. We used VOG cut-off values for vHINTS classification derived from previous studies: head impulses with bilateral vHIT VOR gain larger than >0.685 (17) and/or skew deviation larger than 3.3 deg (16) and/or any change in nystagmus beating direction (19) were classified as central. We conducted cross-tabulations to assess the specificity (Spec) and sensitivity (Sens) for tests such vHIT alone, combination of vHIT and videonystagmography (vHINT), or all the three tests including video test of skew (vHINTS). Accuracy, Sens. and Spec. were also calculated for cHIT (clinical HIT), cHINT (clinical HIT and nystagmus test), and cHINTS. Cohen's Kappa was calculated for the assessment of agreement between expert's evaluation and VOG.

RESULTS

vHINTS vs. cHINTS

We analyzed the data from 46 patients (21 women and 25 men aged between 30 and 78, mean 55 ±15 y) with a diagnosis of stroke or AUVP and who completed cHINTS and vHINTS measurements (35 with AUVP and 11 with stroke) (**Figure 2**). Details of patient diagnosis, vascular territories of strokes, and findings of the clinical tests are shown in **Supplementary Table S1**.

Figures 3, **4** show the VOG eye recordings of a patient with AUVP and a patient with stroke. Typically, a patient with AUVP has an abnormal head impulse test with asymmetrical VOR gain and corrective saccades, unidirectional nystagmus, and no skew deviation (**Figure 3**). On the other side, a patient with stroke can appear with a normal VOR gain bilaterally without corrective saccades or direction changing nystagmus or skew deviation (**Figure 4**). Any of these signs are red flags for stroke.

Figure 5 shows the receiver operator characteristic (ROC) curve for the overall "HINTS" (clinically and video-assisted) sensitivity and specificity for stroke in patients with AVS. It also shows the sensitivity of the HIT alone (vHIT sensitivity was 91% and specificity 89%) or in conjunction with the assessment of nystagmus beating direction at eccentric gaze (vHINT/cHINT). Overall, cHINTS sensitivity was 90.9% and specificity was 85.7%, whereas vHINTS sensitivity was 100% and specificity was 88.9%. False positive rate was 14.3%, and false negative rate was 9.1 % for clinical evaluation. False positive rate was 11.1%, and false negative rate was 0% for VOG. Accuracy was 88.3% for clinical evaluation and 94.2% for the VOG.

There was a perfect agreement between clinical test of skew and video test of skew ($k = 1$) and a good agreement for head impulse test (cHIT vs. vHIT) ($k = 0.63$). Physicians had more difficulties in detecting direction-changing nystagmus, which was clearly detectable with videonystagmography resulting in a fair agreement ($k = 0.284$).

DISCUSSION

Our study demonstrates that vHINTS has a perfect sensitivity in predicting posterior circulation strokes and proved to be even better than the expert. On the other side, VOG is not the gold standard test to recognize AUVP, and almost 11% of peripheral cases can be misclassified as strokes. Evaluation of direction-changing nystagmus was the most challenging of the three HINTS steps.

Video HIT alone has a 91% sensitivity, which is, according to the literature, even better than an early DWI MRI (5). The specificity of vHIT is 89%, and it does not change if we add nystagmus or test of skew, as there is a case of AUVP with normal vHIT but hypofunction in caloric test. Dissociation between abnormal calorics and normal vHIT can also be seen in patients

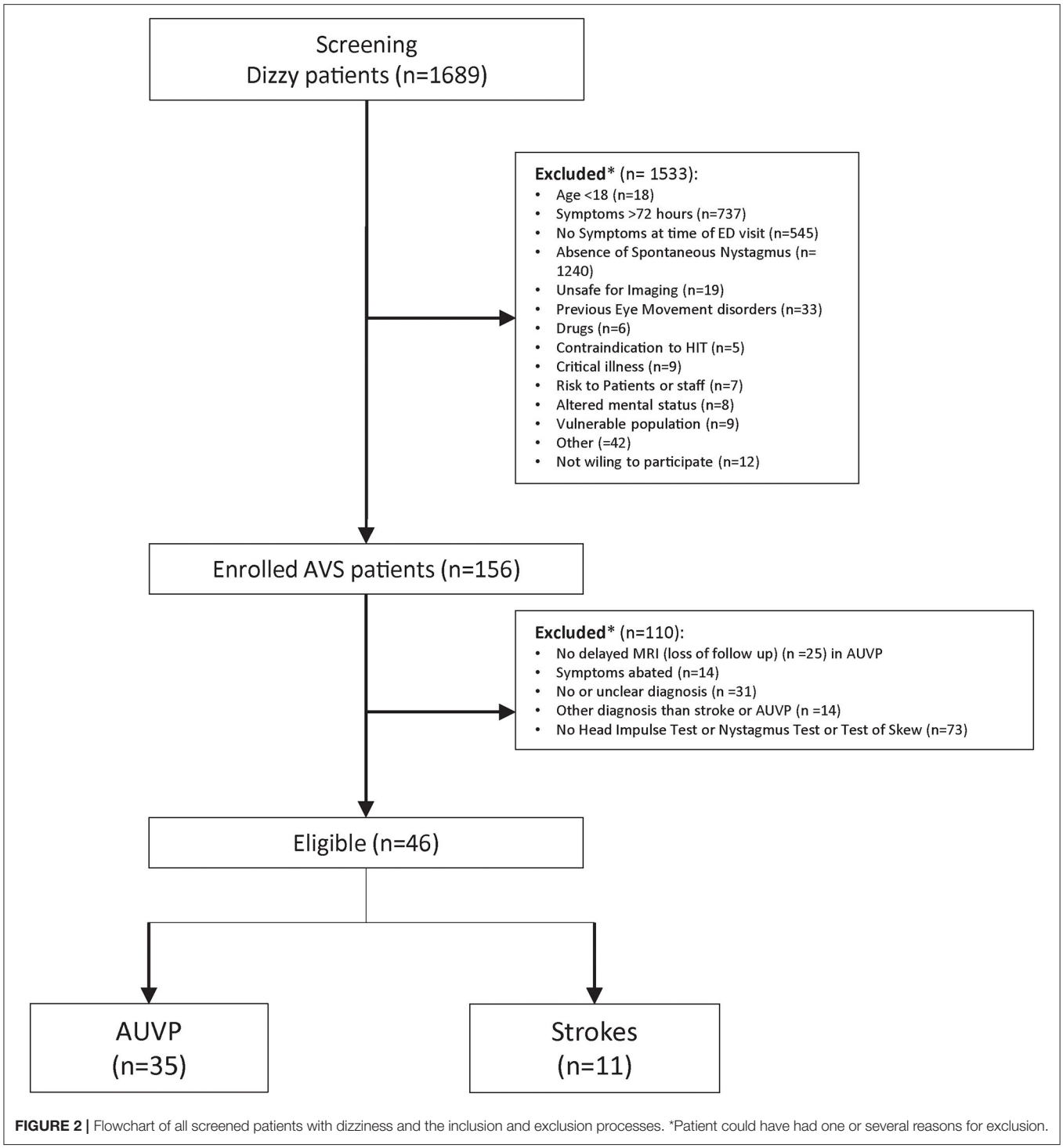

FIGURE 2 | Flowchart of all screened patients with dizziness and the inclusion and exclusion processes. *Patient could have had one or several reasons for exclusion.

with mild vestibular hypofunction. Thus, patients presenting with a clinical picture of AVS, with a normal delayed MRI (3–10 days after symptom onset) and a normal vHIT, would be good candidates for further investigations by calorics (17).

On the other hand, cHIT showed a good agreement with vHIT. Its execution and test result evaluation remains challenging even for experts (10). There are many reasons for this. First and foremost, it is not always easy to perform large head acceleration on patients with acute dizziness. What is more, spontaneous nystagmus and covert saccades make things more complicated. With regard to HIT, the use of VOG is mandatory.

However, our study results showed that detection and interpretation of nystagmus continue to pose challenges. Discernment of nystagmus seems to be difficult because of

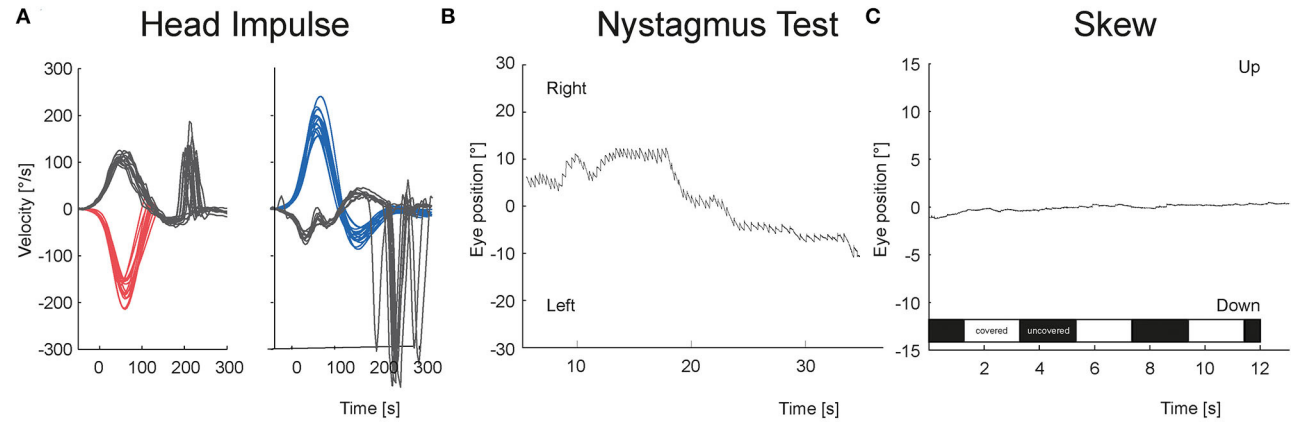

FIGURE 3 | VOG eye recordings of a patient with AUVP are shown. **(A)** vHIT is abnormal to the left with corrective saccades. **(B)** Nystagmus is unidirectional at all gaze directions. Panel **(C)** There is no vertical eye movement in test of skew regardless of whether the right eye was covered (white bar) or uncovered (black bar).

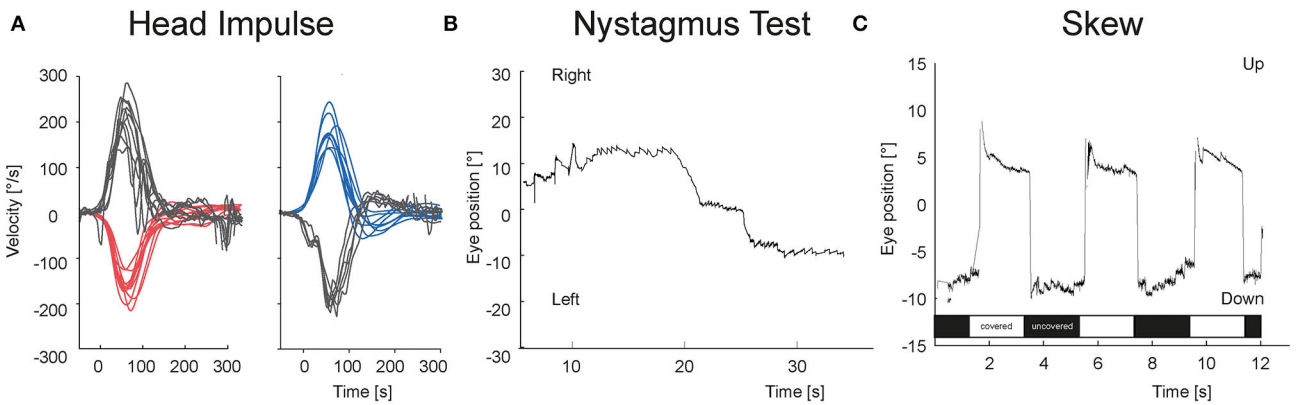

FIGURE 4 | VOG eye recordings of a patient with stroke. **(A)** vHIT is bilaterally normal without any corrective saccades. **(B)** Nystagmus is changing the beating direction at right and left gaze. **(C)** There is a vertical eye movement of 11 degrees in the test of skew during the transition from covered (white bar) to uncovered (black bar) right eye and vice versa.

low-intensity nystagmus in patients with stroke (18), which is sometimes evaluated as physiologic gaze-evoked nystagmus (GEN). VOG distinguishes physiologic GEN from pathologic GEN by calculation of time constant. Time constant is defined as the reciprocal value of the increase in SPV (drift) per increase in degree of gaze eccentricity, and reflects the fidelity of the neural gaze-holding integrator (19). In addition, VOG can quantify more accurately the nystagmus suppression test, which is an additional useful test for stroke detection (18). Frenzel glasses are much less sensitive than VOG (21).

Furthermore, we showed that the test of skew in the HINTS test is the simplest step to perform clinically in the ED, since there was a perfect agreement between clinical test of skew and video test of skew. This is not surprising, because only large skews are considered as a red flag for stroke and are discernable/visible to the examiner without any VOG support (16).

STRENGTHS AND LIMITATIONS

The examiner who performed the VOG measurements is an expert in the field. It is still unclear whether or not the results can be generalized for non-experts. As we have shown in our previous studies, although the detection of a saccade is challenging even for very experienced examiners (10), the performance of a vHIT seems to be easy after a brief instruction by an expert (11).

We used a non-commercial VOG system with projected and synchronized gaze targets on a screen that are not available in current VOG systems in the market. There is clear superiority in detecting strokes using VOG; however, current available systems do not offer an automated quantitative analysis of all three HINTS steps, and there is no automated interpretation of test results.

Another limitation of our study is the high proportion of exclusions (**Figure 2**). Many patients without a clear diagnosis

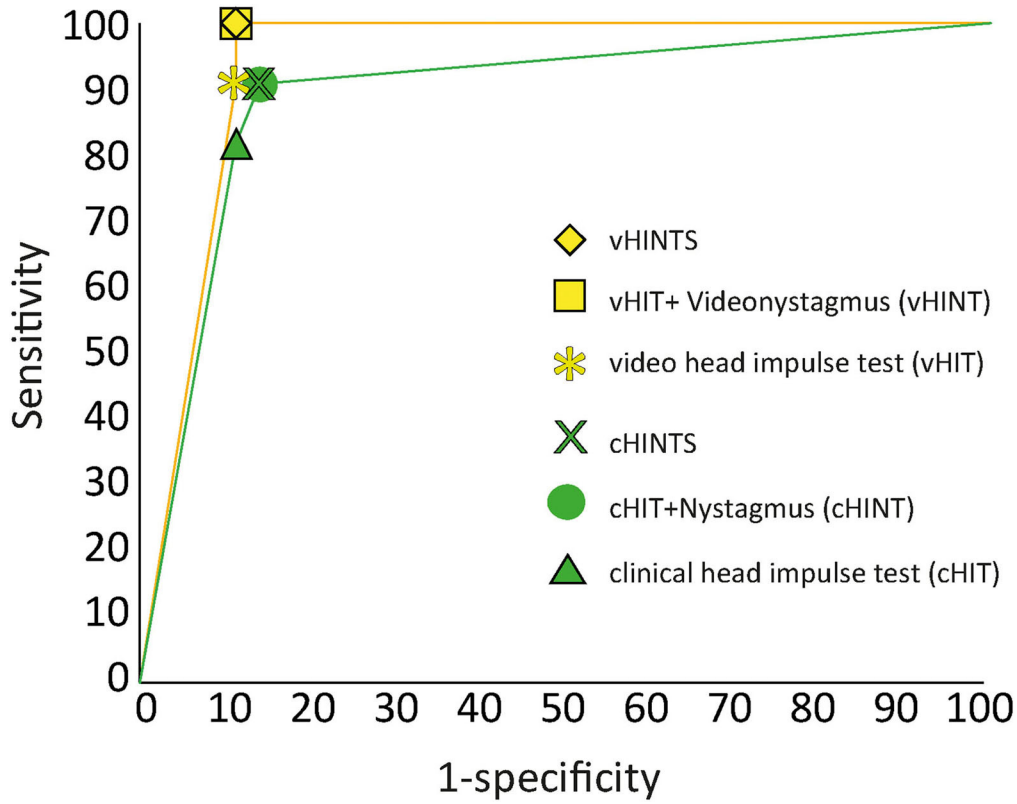

FIGURE 5 | ROC analysis for stroke diagnosis of clinical (green) vs. video "HINTS" (yellow). We report here the sensitivity/specificity of the head impulse tests alone (HIT) or in conjunction with the other two components of the "HINTS" battery (HINT or HINTS).

and with missing or invalid VOG results were excluded. This may lead to potential selection bias; thus, we should be prudent when generalizing the results. However, technical issues and invalid recordings happened randomly in unselected patients.

Since 2009, when Newman-Toker first recommended the use of VOG devices as an ECG analog for the eyes, many studies have proved the accuracy and feasibility of using these devices (9, 16, 17, 19, 22, 23).

Non-experts might benefit even more from vHIT (9), since it offers a standard examination less dependent of the examiners' experience; however, it remains operator-dependent because eye-tracking systems are susceptible to artifacts (24, 25). Non-experts struggle with the use of such systems and its interpretation. Here, telemedicine can solve the problems as long as there are no automated systems in the market (26, 27). This may overcome the lack of expertise outside metropolitan areas. Furthermore, intensive educational courses for ED physicians through vertigo experts are an option. Application of artificial intelligence on big patient's data in the future can lead to development of an accurate automated interpretation of VOG results (12, 24, 28).

IMPLICATIONS FOR CLINICIANS

Our findings have practical implications for clinical care. Clinical HINTS may not always be diagnostic for vestibular stroke in patients with AVS in the ED because of its lower sensitivity than vHINTS. We therefore strongly recommend the use of a VOG device for all the three parts of the "HINTS" protocol. vHINTS could be a potent and cost-efficient diagnostic tool for smaller community hospitals without 24-h MRI service with no experts available, in rural hospitals, in underserved areas, or in resource-poor nations.

ED physicians should become familiar with the application and interpretation of vHINTS in order to minimize diagnostic errors. We also recommend the implementation of a dizziness telemedicine service to support ED physicians in the diagnostic process.

CONCLUSIONS

vHINTS had a high accuracy in detecting central causes of AVS. Its accuracy exceeds that of expert's clinical examination. Nystagmus evaluation was the most difficult part of the three-step test without the use of the VOG device. VOG devices should be used in the future in EDs.

DATA AVAILABILITY STATEMENT

The original contributions presented in the study are included in the article/**Supplementary Material**,

further inquiries can be directed to the corresponding author/s.

ETHICS STATEMENT

The studies involving human participants were reviewed and approved by KEK Bern, #047/14. The patients/participants provided their written informed consent to participate in this study. Written informed consent was obtained from the individual(s) for the publication of any potentially identifiable images or data included in this article.

AUTHOR CONTRIBUTIONS

AK and EZ collected and processed the data. GM and AK conceived the study, analyzed, interpreted the data, and wrote the draft. MC, TS, WW, and FW were involved in the interpretation of the data and in the review. All authors discussed the results, commented on the manuscript, read, and approved the final version.

FUNDING

This study was supported by the Swiss National Science Foundation (#320030_173081).

ACKNOWLEDGMENTS

EyeSeeTec GmbH loaned the VOG goggles. We thank Miranda Morrison for the English editing and also like to thank Mr. Gianni Pauciello photographer for the photos.

SUPPLEMENTARY MATERIAL

The Supplementary Material for this article can be found online at: https://www.frontiersin.org/articles/10.3389/fneur.2022.920357/full#supplementary-material

REFERENCES

1. Hotson JR, Baloh RW. Acute vestibular syndrome. *N Engl J Med*. (1998) 339:680–5. doi: 10.1056/NEJM199809033391007
2. Tarnutzer AA, Berkowitz AL, Robinson KA, Hsieh YH, Newman-Toker DE. Does my dizzy patient have a stroke? A systematic review of bedside diagnosis in acute vestibular syndrome. *Cmaj*. (2011) 183:E571–92. doi: 10.1503/cmaj.100174
3. Goeldlin M, Gaschen J, Kammer C, Comolli L, Bernasconi CA, Spiegel R, et al. Frequency, aetiology, and impact of vestibular symptoms in the emergency department: a neglected red flag. *J Neurol*. (2019) 266:3076–86. doi: 10.1007/s00415-019-09525-4
4. Comolli L, Goeldlin M, Gaschen J, Kammer C, Sauter TC, Caversaccio MD, et al. [Dizziness and vertigo in a tertiary ENT emergency department]. *Hno*. (2020) 68:763–72. doi: 10.1007/s00106-020-00857-6
5. Kattah JC, Talkad AV, Wang DZ, Hsieh YH, Newman-Toker DE. HINTS to diagnose stroke in the acute vestibular syndrome: three-step bedside oculomotor examination more sensitive than early MRI diffusion-weighted imaging. *Stroke*. (2009) 40:3504–10. doi: 10.1161/STROKEAHA.109.551234
6. Quimby AE, Kwok ESH, Lelli D, Johns P, Tse D. Usage of the HINTS exam and neuroimaging in the assessment of peripheral vertigo in the emergency department. *J Otolaryngol Head Neck Surg*. (2018) 47:54. doi: 10.1186/s40463-018-0305-8
7. Warner CL, Bunn L, Koohi N, Schmidtmann G, Freeman J, Kaski D. Clinician's perspectives in using head impulse-nystagmus-test of skew (HINTS) for acute vestibular syndrome: UK experience. *Stroke Vasc Neurol*. (2021) 7:172–5. doi: 10.1136/svn-2021-001229
8. Ohle R, Montpellier RA, Marchadier V, Wharton A, McIsaac S, Anderson M, et al. Can emergency physicians accurately rule out a central cause of vertigo using the HINTS examination? A systematic review and meta-analysis. *Acad Emerg Med*. (2020) 27:887–96. doi: 10.1111/acem.13960
9. Machner B, Erber K, Choi JH, Trillenberg P, Sprenger A, Helmchen C. Usability of the head impulse test in routine clinical practice in the emergency department to differentiate vestibular neuritis from stroke. *Eur J Neurol*. (2020) 28:1737–44. doi: 10.1111/ene.14707
10. Korda A, Carey JP, Zamaro E, Caversaccio MD, Mantokoudis G. how good are we in evaluating a bedside head impulse test? *Ear Hear*. (2020) 41:1747–51. doi: 10.1097/AUD.0000000000000894
11. Korda A, Sauter TC, Caversaccio MD, Mantokoudis G. Quantifying a learning curve for video head impulse test: pitfalls and pearls. *Front Neurol*. (2020) 11:615651. doi: 10.3389/fneur.2020.615651
12. Ahmadi SA, Vivar G, Navab N, Möhwald K, Maier A, Hadzhikolev H, et al. Modern machine-learning can support diagnostic differentiation of central and peripheral acute vestibular disorders. *J Neurol*. (2020) 267:143–52. doi: 10.1007/s00415-020-09931-z
13. Newman-Toker DE, Kerber KA, Hsieh YH, Pula JH, Omron R, Saber Tehrani AS, et al. HINTS outperforms ABCD2 to screen for stroke in acute continuous vertigo and dizziness. *Acad Emerg Med*. (2013) 20:986–96. doi: 10.1111/acem.12223
14. Green KE, Pogson JM, Otero-Millan J, Gold DR, Tevzadze N, Saber Tehrani AS, et al. Opinion and special articles: remote evaluation of acute vertigo: strategies and technological considerations. *Neurology*. (2021) 96:34–8. doi: 10.1212/WNL.0000000000010980
15. Newman-Toker DE, Curthoys IS, Halmagyi GM. Diagnosing stroke in acute vertigo: the HINTS family of eye movement tests and the future of the "Eye ECG". *Semin Neurol*. (2015) 35:506–21. doi: 10.1055/s-0035-1564298
16. Korda A, Zamaro E, Wagner F, Morrison M, Caversaccio MD, Sauter TC, et al. Acute vestibular syndrome: is skew deviation a central sign? *J Neurol*. (2021) 269:1396–403. doi: 10.1007/s00415-021-10692-6
17. Morrison M, Korda A, Zamaro E, Wagner F, Caversaccio MD, Sauter TC, et al. Paradigm shift in acute dizziness: is caloric testing obsolete? *J Neurol*. (2021) 269:853–60. doi: 10.22541/au.161748699.99609461/v1
18. Mantokoudis G, Wyss T, Zamaro E, Korda A, Wagner F, Sauter TC, et al. Stroke prediction based on the spontaneous nystagmus suppression test in Dizzy patients: a diagnostic accuracy study. *Neurology*. (2021) 97:e42–51. doi: 10.1212/WNL.0000000000012176
19. Mantokoudis G, Korda A, Zee DS, Zamaro E, Sauter TC, Wagner F, et al. Bruns' nystagmus revisited: a sign of stroke in patients with the acute vestibular syndrome. *Eur J Neurol*. (2021) 28:2971–9. doi: 10.1111/ene.14997
20. Morrison M, Kerkeni H, Korda A, Räss S, Caversaccio MD, Abegg M, et al. Automated alternate cover test for 'HINTS' assessment: a validation study. *Eur Arch Otorhinolaryngol*. (2021) 279:2873–9. doi: 10.22541/au.162220958.82500368/v1
21. West PD, Sheppard ZA, King EV. Comparison of techniques for identification of peripheral vestibular nystagmus. *J Laryngol Otol*. (2012) 126:1209–15. doi: 10.1017/S0022215112002368
22. Machner B, Erber K, Choi JH, Sprenger A, Helmchen C, Trillenberg P. A simple gain-based evaluation of the video head impulse test reliably detects normal vestibulo-ocular reflex indicative of stroke in patients with acute vestibular syndrome. *Front Neurol*. (2021) 12:741859. doi: 10.3389/fneur.2021.741859

23. Mantokoudis G, Tehrani AS, Wozniak A, Eibenberger K, Kattah JC, Guede CI, et al. VOR gain by head impulse video-oculography differentiates acute vestibular neuritis from stroke. *Otol Neurotol*. (2015) 36:457–65. doi: 10.1097/MAO.0000000000000638
24. Mantokoudis G, Otero-Millan J, Gold DR. Current concepts in acute vestibular syndrome and video-oculography. *Curr Opin Neurol*. (2021) 35:75–83. doi: 10.1097/WCO.0000000000001017
25. Mantokoudis G, Saber Tehrani AS, Wozniak A, Eibenberger K, Kattah JC, Guede CI, et al. Impact of artifacts on VOR gain measures by video-oculography in the acute vestibular syndrome. *J Vestib Res*. (2016) 26:375–85. doi: 10.3233/VES-160587
26. Müller-Barna P, Hubert ND, Bergner C, Schütt-Becker N, Rambold H, Haberl RL, et al. TeleVertigo: diagnosing stroke in acute dizziness: a telemedicine-supported approach. *Stroke*. (2019) 50:3293–8. doi: 10.1161/STROKEAHA.119.026505
27. Chari DA, Wu MJ, Crowson MG, Kozin ED, Rauch SD. Telemedicine algorithm for the management of dizzy patients. *Otolaryngol Head Neck Surg*. (2020) 163:857–9. doi: 10.1177/0194599820935859
28. Kabade V, Hooda R, Raj C, Awan Z, Young AS, Welgampola MS, et al. Machine learning techniques for differential diagnosis of vertigo and dizziness: a review. *Sensors*. (2021) 21:7565. doi: 10.3390/s21227565

Conflict of Interest: The authors declare that the research was conducted in the absence of any commercial or financial relationships that could be construed as a potential conflict of interest.

Publisher's Note: All claims expressed in this article are solely those of the authors and do not necessarily represent those of their affiliated organizations, or those of the publisher, the editors and the reviewers. Any product that may be evaluated in this article, or claim that may be made by its manufacturer, is not guaranteed or endorsed by the publisher.

frontiers | Frontiers in Neurology

TYPE Original Research
PUBLISHED 05 August 2022
DOI 10.3389/fneur.2022.945764

OPEN ACCESS

EDITED BY
Dominik Straumann,
University of Zurich, Switzerland

REVIEWED BY
Aravind Ganesh,
University of Calgary, Canada
Fazil Necdet Ardiç,
Pamukkale University, Turkey

*CORRESPONDENCE
Frederik Kragerud Goplen
frederik.kragerud.goplen@helse-bergen.no

†These authors have contributed equally to this work

SPECIALTY SECTION
This article was submitted to Neuro-Otology, a section of the journal Frontiers in Neurology

RECEIVED 16 May 2022
ACCEPTED 07 July 2022
PUBLISHED 05 August 2022

CITATION
Berge JE, Goplen FK, Aarstad HJ, Storhaug TA and Nordahl SHG (2022) The Romberg sign, unilateral vestibulopathy, cerebrovascular risk factors, and long-term mortality in dizzy patients.
Front. Neurol. 13:945764.
doi: 10.3389/fneur.2022.945764

The Romberg sign, unilateral vestibulopathy, cerebrovascular risk factors, and long-term mortality in dizzy patients

Jan Erik Berge[1,2,3†], Frederik Kragerud Goplen[1,2,3*†], Hans Jørgen Aarstad[2,3], Tobias Andre Storhaug[3,4] and Stein Helge Glad Nordahl[1,3]

[1]Norwegian National Advisory Unit for Vestibular Disorders, Haukeland University Hospital, Bergen, Norway, [2]Department of Otorhinolaryngology and Head and Neck Surgery, Haukeland University Hospital, Bergen, Norway, [3]Department of Clinical Medicine, University of Bergen, Bergen, Norway, [4]Department of Anesthesiology and Intensive Care, Vestre Viken Hospital Trust, Drammen, Norway

Objectives: Describe the relationship between unsteadiness, canal paresis, cerebrovascular risk factors, and long-term mortality in patients examined for dizziness of suspected vestibular origin.

Study design: Observational cohort with prospective collection of survival data.

Setting: University clinic neurotological unit.

Patients: Consecutive patients aged 18–75 years examined in the period 1992–2004 for dizziness of suspected vestibular origin.

Outcome measures: Overall survival. Standardized mortality ratio (SMR). Factors: Unsteadiness, canal paresis, age, sex, patient-reported diabetes, hypertension, heart disease, stroke, or TIA/minor stroke. Patients were classified as steady or unsteady based on static posturography at baseline compared to normative values.

Results: The study included 1,561 patients with mean age 48 years and 60 % females. Mean follow-up was 22 years. Unsteadiness was associated with higher age, heart disease, diabetes, hypertension, and cerebrovascular dizziness. There were 336 deaths over 31,335 person-years (SMR 0.96; 95 % confidence interval: 0.86–1.07). Canal paresis was not related to unsteadiness (chi square: $p = 0.46$) or to mortality (unadjusted Cox hazard ratio: 1.04, 95% CI: 0.80–1.34). Unsteadiness was an independent predictor of mortality (adjusted Cox hazard ratio: 1.44, 95% CI: 1.14–1.82).

Conclusions: Unsteadiness measured by static posturography is associated with higher age, known cerebrovascular risk factors, and with increased long-term mortality, but not with canal paresis in patients evaluated for dizziness. The study highlights the importance of evaluating patients with conspicuous postural instability for non-vestibular causes.

KEYWORDS

survival, posturography, dizziness, vertigo, vestibular disorders, caloric response, balance

Introduction

The Romberg sign (Moritz Romberg 1795–1873) is present when a patient tends to sway or fall while standing with feet together and eyes closed. It was first described in the 19th century as a useful indicator of proprioceptive loss due to neurosyphilis (tabes dorsalis) (1). Romberg himself was probably unaware that a similar disruption of balance may be caused by vestibular loss (2). This ambiguity complicates the interpretation of the Romberg sign in clinical practice.

In patients with acute vestibular symptoms, commonly seen in emergency departments, oculomotor signs denoted by the acronym "HINTS" are more suitable than the Romberg test to single out patients with a central lesion–for example due to a posterior circulation stroke–as opposed to more common benign peripheral vestibular disorders (3). Marked postural sway may be present in both central and peripheral lesions. However, in patients with severe truncal ataxia who are unable to sit or stand without support, a central lesion is usually suspected (4).

In patients with episodic or chronic vestibular symptoms, commonly seen in outpatient clinics, the spectrum of possible causes is even wider, and even advanced posturographic systems, have been found to have limited diagnostic value (5). If the simple Romberg test is to be used at all in this setting, the clinician would be right to ask whether marked postural instability with eyes closed should be interpreted as a sign of a peripheral vestibular problem, or rather of a proprioceptive or central nervous disease and whether this finding has implications for the prognosis of the patient, for example with respect to long-term survival.

Patients suffering from dizziness or vertigo are often found to have benign disorders of the peripheral vestibular system (6), and severe underlying conditions have, to some extent, been ruled out by referring physicians (7). Nevertheless, a considerable proportion suffers from disorders of unclear or complex etiology, and some may have more serious underlying disorders including cerebrovascular disease. Dizziness and unsteadiness are sometimes indicators of serious disease. In a large population-based study, Corrales et al. (8) found a near doubling of mortality (OR 1.7, 95% CI 1.4–2.2) in adult Americans reporting dizziness or balance problems after adjusting for age, sex, education, ethnicity, race, diabetes, cardiovascular or cerebrovascular disease, and cancer. This study did not differentiate between dizziness and unsteadiness. Other studies have shown that postural instability, quantified by different clinical scoring systems, is associated with increased mortality in elderly (9) and middle-aged persons (10).

In a previous study, we found that standardized mortality ratio in patients examined for dizziness of suspected vestibular origin was the same as in the general population (11). This implies that vestibular symptoms *per se* are not necessarily a sign of serious underlying disease. On the contrary, such symptoms are often caused by benign vestibular disorders, the most common being benign paroxysmal positional vertigo, vestibular migraine, and persistent postural-perceptual dizziness. However, increased mortality was found in a subgroup of patients reporting unsteadiness between dizziness attacks. This suggests that it is of importance to differentiate the symptoms of dizziness/vertigo from that of unsteadiness.

The purpose of this study was to examine the value of an objective measure of standing balance, a version of the Romberg test–static posturography with eyes closed–with respect to its ability to discriminate patients with unilateral vestibulopathy–as measured by the caloric test–from patients with more serious underlying disorders–as measured by comorbidity and long-term mortality.

Materials and methods

Patients and setting

This is a study of survival data gathered prospectively from a cohort of consecutive patients aged 18–75 years examined between 1992 and 2004 in a neurotological laboratory at the Department of Otorhinolaryngology and Head and Neck Surgery at Haukeland University Hospital in Bergen. The subjects were mostly outpatients referred for suspected vestibular disorder. For patients seen more than once during the study period, only data from the first examination was included in the study.

Ethics

The study was approved by the Regional Committee for Medical and Health Research Ethics of Western Norway (2012/1075/REK vest).

Survival data

Survival data were obtained from the Norwegian National Population Register and updated as per 31 January 2021. Standardized mortality ratios (SMR) were calculated based on life tables by sex and age published by Statistics Norway (12).

Static posturography

All patients underwent static posturography as described previously (13). Briefly, the patient was asked to stand quietly on a static force platform (Cosmogamma®, AC International, Cento, Italy) for 60 s with eyes open and then for 60 s with eyes closed. The visual surroundings were kept constant and the room quiet. The platform contained three strain gauge transducers connected to a computer that calculated the

TABLE 1 Descriptive data of participants ($n = 1,561$).

Parameter	Values
Age (years); *mean, SD*	48.4, 14.0
18–39 years; *n*	444
40–49 years; *n*	369
50–59 years; *n*	391
60–75 years; *n*	357
Female; *n, %*	934, 59.8
Posturography	
Unsteady patients; *n, %*	357, 22.9
Path length (mm)*; *quartiles (25%, 50%, 75%)*	521, 724, 1,069
Caloric test; *n*	1,326
Canal paresis; *n, %*	378, 28.5
Patient-reported comorbidities	
Diabetes; *n, %*	30, 1.9
Hypertension; *n, %*	213, 13.6
Heart disease; *n, %*	84, 5.4
Stroke or TIA; *n, %*	26, 1.7
10-year survival (percent)	
Observed, lower CI, upper CI	93.9, 92.7, 95.0

TIA, transitory ischemic attack; n, count; SD, standard deviation; mm, millimeters; CI, 95 % confidence interval.
*Arithmetic mean of path length with eyes open and eyes closed.

TABLE 2 Clinical diagnoses in 1,561 patients examined in a university clinic for suspected vestibular disorder.

Diagnosis	Count	Percent
Peripheral vestibular		
Benign paroxysmal positional vertigo	209	13.4 %
Vestibular neuritis	184	11.8 %
Labyrinthitis	26	1.7 %
Menière's disease	175	11.2 %
Vestibular schwannoma	63	4.0 %
Other ear and hearing disorders		
Otosclerosis	8	0.5 %
Sudden deafness	8	0.5 %
Chronic otitis media	1	0.1 %
Other middle ear disease	11	0.7 %
Hearing loss NOS	15	1.0 %
Trauma		
Perilymphatic fistula	7	0.4 %
Skull fracture	13	0.8 %
Head injury without fracture	24	1.5 %
Whiplash	11	0.7 %
Decompression sickness	6	0.4 %
Barotrauma	4	0.3 %
Neurological disorders		
Cerebrovascular	106	6.8 %
Central vestibular NOS*	148	9.5 %
Multiple sclerosis	6	0.4 %
Borreliosis	1	0.1 %
Epilepsy	3	0.2 %
Other		
Drug induced	4	0.3 %
ME	1	0.1 %
Postinfectious	29	1.9 %
Cervicogenic	136	8.7 %
Congenital	2	0.1 %
Psychogenic	15	1.0 %
Non-otogenic NOS	274	17.6 %

NOS, not otherwise specified; ME, myalgic encephalopathy; CNS, central nervous system.
*Including vestibular migraine.

center of pressure (COP) exerted by the patient's feet on the platform while maintaining balance. The length of the curve in millimeters (path length) described by the COP during each examination was used as the main parameter indicating postural instability. The path length may vary from zero–the theoretical result of an immovable object being placed on the platform–to several thousands, indicating severe postural instability. Normative values were taken from a previous study (13). Path lengths >895 millimeters with eyes open or 1,665 millimeters with eyes closed were considered abnormal.

Caloric testing

All patients underwent bithermal (44 and 30 degrees centigrade) caloric testing after static posturography, and caloric asymmetry was calculated according to Jongkees' formula. Caloric asymmetry >25 % was considered abnormal and defined as a canal paresis.

Clinical data and covariates

The clinical diagnoses were reviewed retrospectively by two of the co-authors (FG, SHGN). Patients were divided into four age groups (18–39, 40–49, 50–59, and 60–75 years). Cardio-vascular comorbidities were evaluated clinically based on information given by the patient and examining physicians. Included covariates were canal paresis, patient-reported hypertension, diabetes, history of stroke, TIA/minor stroke (TIA, transitory ischemic attack), or heart disease. In addition, some of the patients received a diagnosis of dizziness of suspected cerebrovascular origin. This was a clinical diagnosis made by an otorhinolaryngologist and not based on explicit criteria or imaging. It was rarely indicative of an acute stroke since most patients were seen in an elective, outpatient setting. However, since dizziness of cerebrovascular origin may

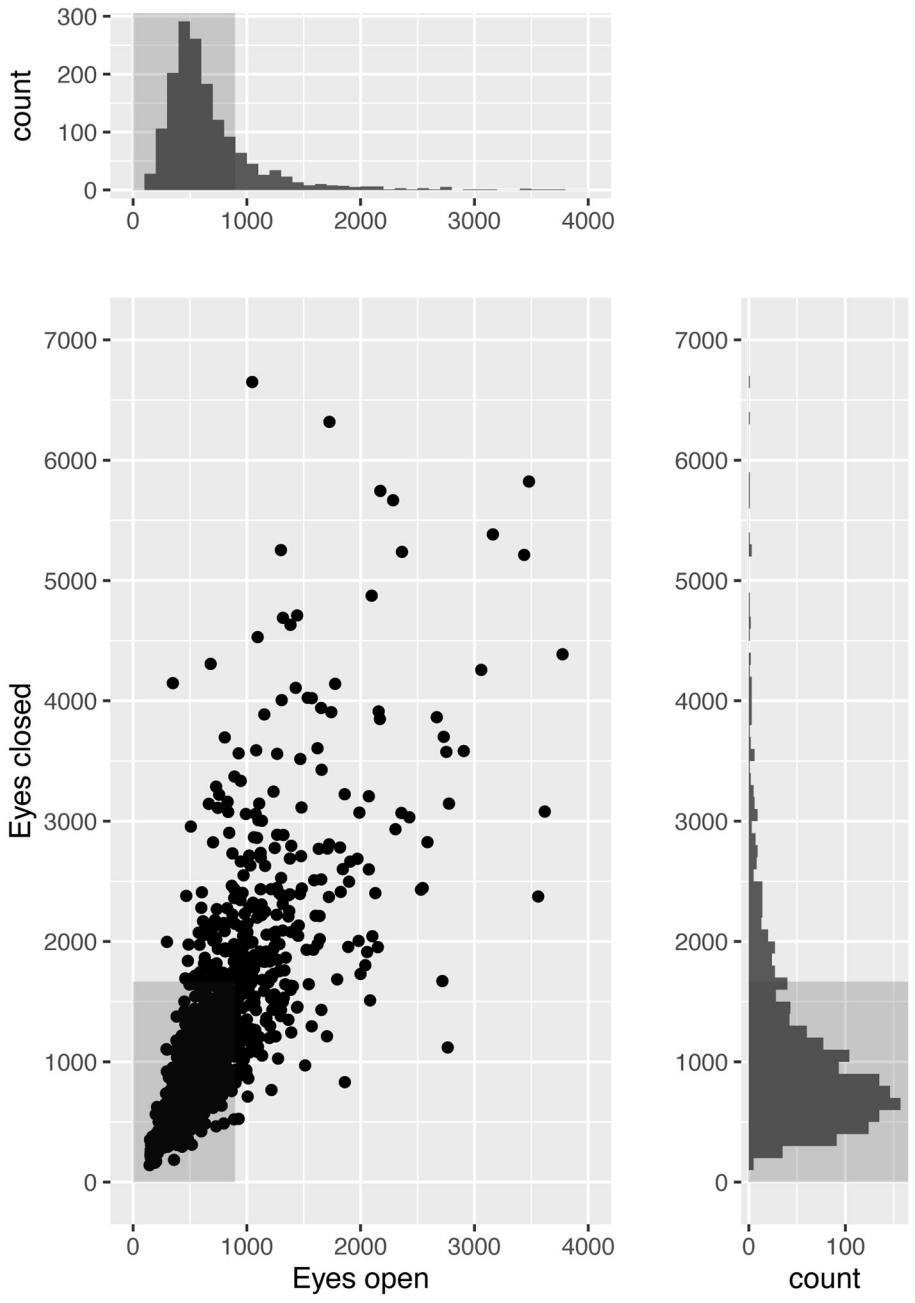

FIGURE 1
Static posturography results in 1,561 patients examined for dizziness of suspected vestibular origin. Scatterplot with marginal histograms showing postural sway while standing quietly on a static force platform for 60 s with eyes open and closed. Plotted values are the length in millimeters of the path described by the center of pressure under the patient's feet. Gray boxes indicate normal limits.

influence survival, this diagnosis was included among the risk factors in the study.

Statistical analysis

For statistical analysis and data interpretation, two variables of postural sway were used. First, a continuous variable was made by averaging path length with eyes open and eyes closed. This variable was then stratified by quartiles to four levels indicating low, low-median, median-high, or high postural instability. Second, a dichotomized variable was created using previously published normative data (13). If the path length was outside normal limits either with eyes open or closed, the patient was characterized as "unsteady." Otherwise, the patient was considered "steady."

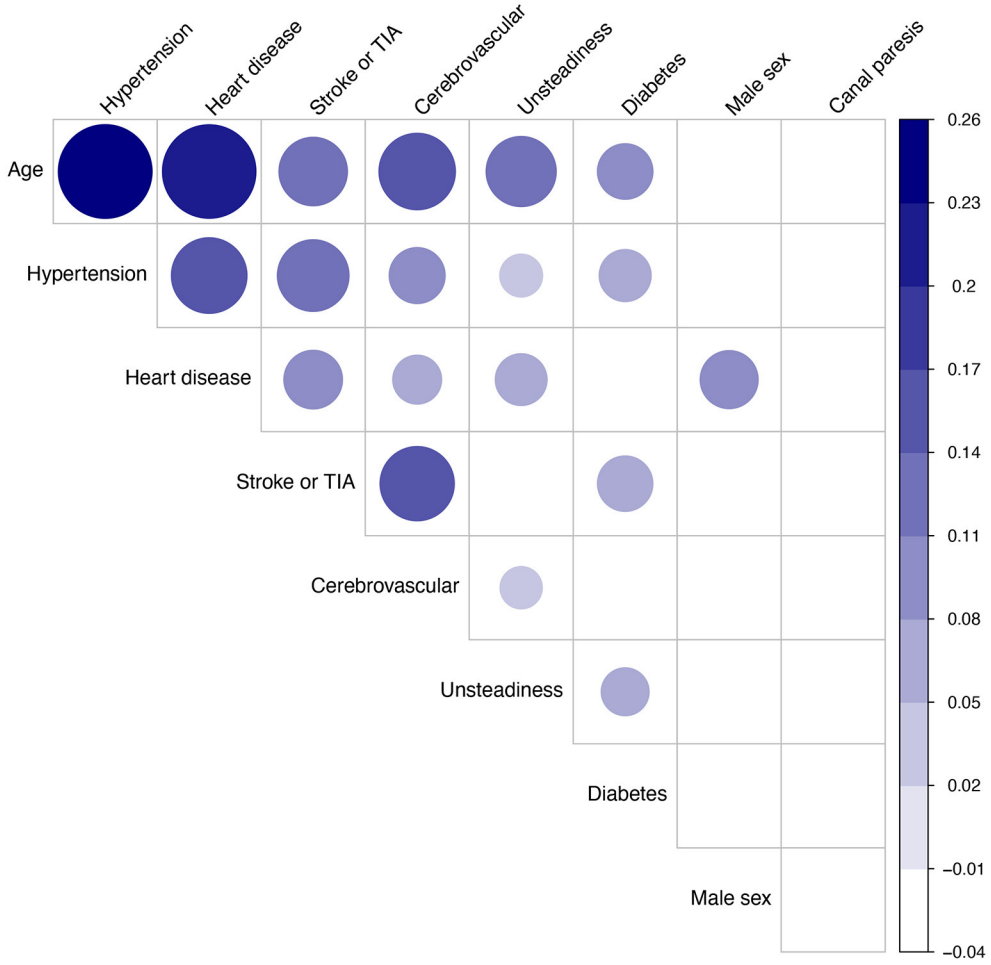

FIGURE 2
Correlation matrix analysis of nine candidate factors, prior to survival analysis, in 1,561 patients examined for dizziness of suspected vestibular origin. Dots indicate significant correlations ($p < 0.05$). Dot size and darkness indicate strength of correlation (Pearson's R). Factor ordering: first principal component order.

Cox proportional hazards regressions models were used to calculate crude and adjusted hazard ratios for survival predicted by age, sex, postural instability, diabetes, hypertension, heart disease, stroke, TIA/minor stroke, and dizziness of cerebrovascular origin. Adjusted hazard ratios were reported after backward stepwise elimination of non-significant factors. Follow-up time was defined as the time interval between the first examination and the last update of survival data (31 January 2021).

Statistical analysis was performed using R 4.0.3 (R Foundation for Statistical Computing, Vienna, Austria), the Epi (14) and popEpi packages (15). Two-sided p-values < 0.05 were considered significant.

Results

Out of 1,796 patients with complete data on posturography and clinical covariates, 84 patients were excluded due to missing consent or unknown vital status, and further 151 due to being outside the age-range 18–75 years at baseline. Descriptive data for the remaining 1,561 participants are presented in Table 1 with clinical diagnoses in Table 2. Results from the caloric test were available for 1,326 patients of which 28.5% had a canal paresis. Dizziness of suspected cerebrovascular origin was noted in 106 (6.8%) of the patients. Posturography results are shown in Figure 1 and the correlation matrix between risk factors is shown in Figure 2.

Follow-up time ranged from 17 to 29 years (mean 22, SD 2.9 years). The observed number of deaths in the study population was 336 over a total of 31,335 person-years, which did not differ significantly from the expected number of 350 deaths in the Norwegian general population matched for age, sex, and calendar years (standardized mortality ratio: 0.96, 95 % confidence interval: 0.86–1.07).

Results of the Cox regression analysis are shown in Table 3. Unsteadiness on static posturography was a significant predictor of mortality independent on age, sex, self-reported

10.3389/fneur.2022.945764

TABLE 3 Cox regression analysis of long-term survival in 1,561 patients examined for dizziness of suspected vestibular origin.

	Univariate 95% CI				Adjusted 95% CI			
Factor	HR	lower	upper	*p*	HR	lower	upper	*p*
Age								
18–39 yr	reference				reference			
40–49 yr	5.878	2.605	13.26	<0.0001	5.685	2.519	12.828	<0.0001
50–59 yr	12.548	5.769	27.29	<0.0001	11.416	5.244	24.854	<0.0001
60–75 yr	65.342	30.765	138.78	<0.0001	59.857	28.141	127.322	<0.0001
Sex								
Male	1.384	1.117	1.714	0.00298	1.379	1.111	1.711	0.00350
Self-reported comorbidity								
Diabetes	4.162	2.618	6.618	<0.0001	2.089	1.307	3.340	0.00207
Hypertension	2.630	2.059	3.358	<0.0001				
Heart disease	4.339	3.210	5.865	<0.0001				
Stroke or TIA/minor stroke	4.615	2.869	7.424	<0.0001	2.034	1.256	3.295	0.00392
Clinical diagnosis								
Dizziness of cerebrovascular origin	2.179	1.566	3.032	<0.0001				
Static posturography								
Unsteady*	1.831	1.453	2.306	<0.0001	1.438	1.138	1.815	0.00229

Univariate and adjusted hazard ratios after backward stepwise elimination of non-significant factors.
CI, confidence interval; HR, hazard ratio.
*Path length outside normative values with eyes open or closed.

comorbidities, and clinical diagnosis of dizziness of suspected cerebrovascular origin with an adjusted hazard ratio of 1.438 (95% CI: 1.138–1.815). Self-reported diabetes and stroke or TIA/minor stroke were also significant predictors in the adjusted analysis.

Kaplan-Meier analysis of survival related to four increasing levels of postural instability is shown in Figure 3. The two groups with median-high or high postural sway had decreased survival compared to the group with low postural sway (Cox regression, $p < 0.005$).

The presence of a canal paresis (caloric asymmetry >25 %) was not associated with postural instability (chi square: $p = 0.44$), nor with mortality (HR 1.036, 95% CI: 0.8002–1.34).

Discussion

In this cohort of patients examined for dizziness of suspected vestibular origin, postural instability was not associated with unilateral vestibulopathy, but rather with increasing age, cerebrovascular risk factors and increased long-term mortality. Unsurprisingly, a canal paresis was not associated with mortality. To the best of our knowledge, this is the first study to show the relationship between an objective measure of postural sway and long-term survival in dizzy patients. Combined with the patient-reported comorbidities, a relatively simple measure of postural instability may provide prognostic information in patients undergoing evaluation for dizziness. This finding underscores the importance of evaluating unsteadiness, and of differentiating this from dizziness and vertigo, in patients with vestibular symptoms.

Cerebrovascular risk factors contributed significantly to mortality, which was expected since stroke is one of the leading causes of death in Europe (16). In the acute setting, dizziness and vertigo are sometimes caused by a posterior circulation stroke (17), and even when this has been excluded, a study has indicated increased risk of a cerebrovascular event after hospital discharge (18). Moreover, a recent study provides evidence that transient isolated vertigo or dizziness may sometimes be symptoms of TIA (19). However, the present study was performed in an elective setting, and patients with suspected cerebrovascular cause of their symptoms had presumably been screened out, to some extent, by referring physicians. The diagnosis of dizziness of suspected cerebrovascular origin did not contribute to the prognosis after adjustment for patient-reported comorbidities. The reason for this may be that the major risk factors of stroke–i.e., age and patient-reported diabetes, hypertension, atrial fibrillation, and previous stroke or TIA/minor stroke–were accounted for in the adjusted analysis. Hence, the clinical diagnosis of cerebrovascular dizziness without additional objective information, such as biochemical markers, MRI or Doppler imaging findings, did not provide additional prognostic value. It is nevertheless interesting that

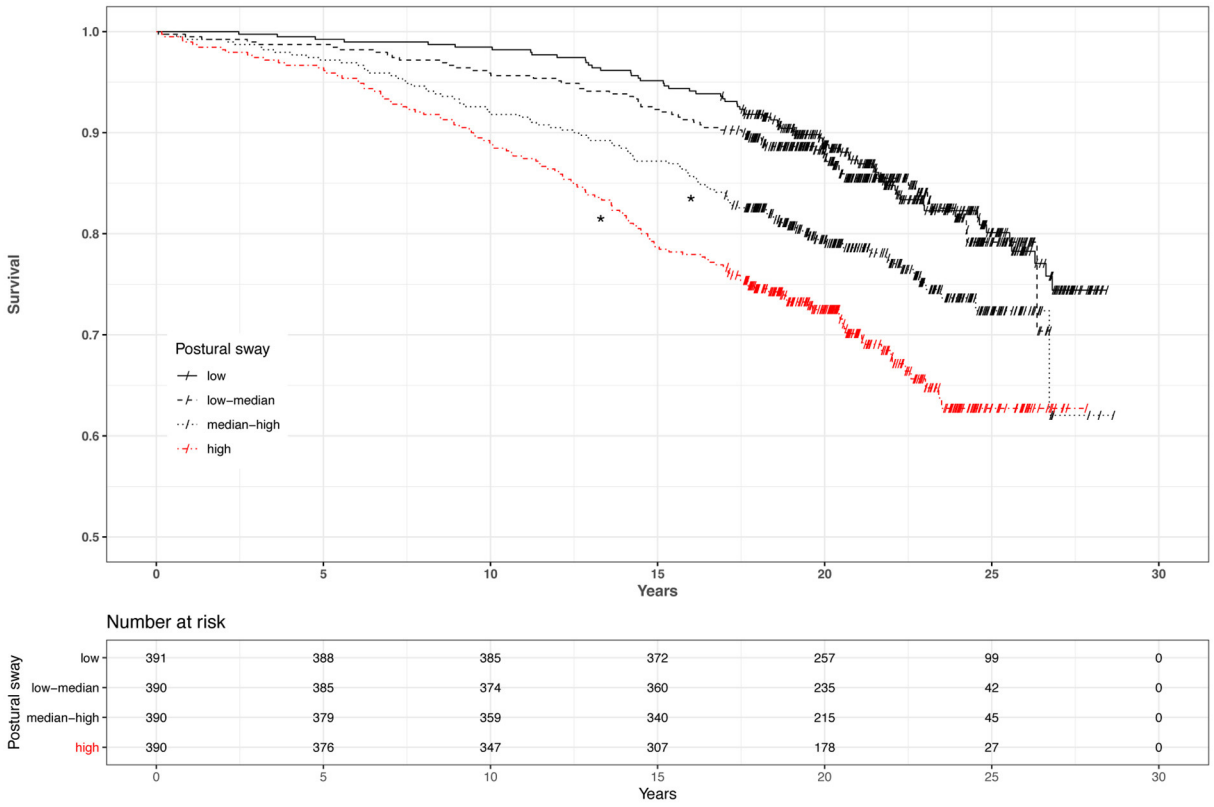

FIGURE 3
Kaplan-Meier survival in 1,561 dizzy patients and postural instability stratified by quartiles. Postural sway measured while standing quietly on a force platform for 60 s with eyes open and closed. Movement of the center of pressure was measured in millimeters, and results with eyes open and closed were averaged. Censoring events are marked with a slash (/). *Significant (Cox regression, $p < 0.005$).

posturography remained a significant predictor even after correction for these factors.

Previous studies have documented mortality in patients suffering from vestibular symptoms (8, 9, 20). In a large population-based study, Corrales et al. (8) found a near doubling of mortality (OR 1.7, 95% CI 1.4–2.2) in adult Americans reporting dizziness or balance problems after adjusting for age, sex, education, ethnicity, race, diabetes, cardiovascular or cerebrovascular disease, and cancer. In our study of dizzy patients, the standardized mortality rate was the same as in the general population. This may be explained by patient selection and screening by referring physicians, since the main purpose of the examination was to uncover vestibular disorders. The benign nature of these disorders is supported by our finding that caloric asymmetry was not associated with increased mortality. Van Vugt et al. (20) found a 40.5% 10-year mortality in a group of elderly patients with dizziness in primary care. This was not compared to standardized mortality rates. Moreover, the patients had a mean age of 79 years at inclusion, which is considerably higher than in our study. The finding by van Vugt et al. (20) that patients with vertigo had lower mortality than those with dizziness of other types is interesting, and agrees with a previous study from our group (7). In the latter study, patient-reported unsteadiness between dizziness episodes was associated with higher mortality.

Other studies have found that gait and balance problems can be used to predict mortality. Blain et al. (21) studied a population of community-dwelling women aged ≥75 years and found that 8-year survival was related to balance and walking speed after adjusting for a wide range of covariates. Cooper et al. (10) found that all-cause mortality in a group of 2,766 53-year-olds was related to measures of physical capability, specifically grip strength, chair rise speed and standing balance time. The authors found some evidence that the timed one-leg stance test with eyes closed was the factor most strongly associated with survival. A linear relationship between this test and path length from posturography has been reported in a previous study (22) indicating a partial overlap between these two methods.

A similar-sized study from Finland reported no association between posturographic unsteadiness and long-term mortality in a population-based cohort of 1,568 women (23). A positive association was found in the crude analysis between mortality

and anteroposterior, mediolateral and total maximum amplitude of the COP. However, the association was lost after adjustment for age, parents' hip fracture, smoking and leg-extension strength. The study also found postural sway to be associated with osteoporotic fractures. Possible explanations for the difference in outcomes may include different sway parameters (maximum sway amplitude vs. total path length), test conditions (eyes open vs. average between eyes open and closed) and patient selection (population sample of women vs. dizzy patients of both sexes). However, since the crude analysis revealed similar results in the two studies, the difference may also be explained by the difference in covariates. The authors of the Finnish study suggested that the association between postural sway and mortality is indirect, and that "sway is more of an indicator for general health status." This is in line with our study, finding sway to be mostly correlated with age and other cerebrovascular risk factors.

The lack of association between postural sway and caloric asymmetry is not surprising (11). Most of the patients were seen in an elective setting due to chronic or episodic symptoms. While a vestibular lesion leading to canal paresis typically causes marked unsteadiness in the acute phase, the symptoms tend to improve due to central vestibular compensation. Thus, a disease leading to asymmetric caloric function, for example a sequela to vestibular neuritis or vestibular schwannoma, may sometimes lead to less postural unsteadiness than an episodic disorder with symmetric caloric response, like BPPV or Menière's disease, or a chronic neurological or orthopedic problem.

Apart from underlying cardio- and cerebrovascular disorders, possible causal relationships between unsteadiness and mortality could involve general frailty and risk of falling. In a study of relatively active home-dwelling elderly persons with mean age 70 years, Tuunainen et al. (24) concluded that vertigo and poor postural stability constituted the major reasons for falling. Falls are a major cause of morbidity in the elderly population (25, 26), and even though vertigo of peripheral vestibular origin may not be associated with increased all-cause mortality–as our study indicates–falls rank among the leading causes of death (26). Part of the excess mortality in patients with postural instability might therefore be explained by falls.

Strengths of the present study include the objective measuring of postural balance and caloric asymmetry, the long follow-up (mean 22 years) and wide age range (18–75 years) in a large population of dizzy patients examined for suspected vestibular disorder. The long follow-up and inclusion of relatively young patients compared to previous studies, means that the study has potential for early detection and preventive measures related to long-term survival. The risk of attrition bias was considered by the authors and found to be low since <5 % of the cohort was lost to follow-up due to missing consent or unknown vital status at follow-up. The addition of standardized mortality ratios gives valuable information about the study sample in comparison to the general population.

Limitations include the fact that the patients were seen in a specialized clinic in an elective outpatient setting. The results are not necessarily applicable to patients seen for acute vestibular syndrome. Other studies indicate that people suffering from dizziness in the general population has a higher overall mortality (8). However, this does not invalidate the association between mortality and postural instability found in the present study, which agrees with other studies of less selected populations (10, 21). Since the causes of death were unknown, the direct causal link between postural instability and mortality cannot be ascertained. Future studies on disease specific mortality in patients with postural instability are needed. Until further research is available, dizzy patients with conspicuous unsteadiness should be evaluated for cerebrovascular risk factors. Preventive measures should focus on minimizing the risk of stroke and falls.

In conclusion, this study found that the Romberg sign in patients undergoing elective evaluation for vestibular symptoms was related to age and cerebrovascular risk factors including hypertension and diabetes as well as being an early predictor of mortality. It was not related to unilateral vestibulopathy as measured by the caloric test. This finding underscores the importance of differentiating objective unsteadiness from the subjective feeling of vertigo or dizziness. Patients with conspicuous unsteadiness with eyes closed require diagnostic evaluation for non-vestibular etiology and fall-risk.

Data availability statement

The original datasets presented in this article are not readily available due to Norwegian data protection legislation. Requests to access aggregated data should be directed to Frederik Kragerud Goplen (frederik.kragerud.goplen@helse-bergen.no).

Ethics statement

The study was approved in advance by the Regional Committee for Medical and Health Research Ethics of Western Norway (2012/1075/REK vest). Active consent was not required according to Norwegian legislation. Living participants were informed in writing about the study and given the opportunity to withdraw by phone, e-mail or by returning a prepaid envelope.

Author contributions

JB, FG, and TS: data collection. JB and FG: data analysis and drafting the manuscript. All authors contributed in concept

and design of the study, revision of the article for important intellectual content, and approval of the submitted version.

Conflict of interest

The authors declare that the research was conducted in the absence of any commercial or financial relationships that could be construed as a potential conflict of interest.

Publisher's note

References

1. Lanska DJ, Goetz CG. Romberg's sign: development, adoption, and adaptation in the 19th century. *Neurology.* (2000) 55:1201–6. doi: 10.1212/WNL.55.8.1201

2. Halmágyi GM, Curthoys IS. Vestibular contributions to the romberg test: testing semicircular canal and otolith function. *Eur J Neurol.* (2021) 28:3211–9. doi: 10.1111/ene.14942

3. Krishnan K, Bassilious K, Eriksen E, Bath PM, Sprigg N, Braekken SK, et al. Posterior circulation stroke diagnosis using HINTS in patients presenting with acute vestibular syndrome: a systematic review. *Eur stroke J.* (2019) 4:233–9. doi: 10.1177/2396987319843701

4. Carmona S, Martínez C, Zalazar G, Moro M, Bateucas-Caletrio A, Luis L, et al. The diagnostic accuracy of truncal ataxia and HINTS as cardinal signs for acute vestibular syndrome. *Front Neurol.* (2016) 7:125. doi: 10.3389/fneur.2016.00125

5. Kingma H, Gauchard GC, de Waele C, van Nechel C, Bisdorff A, Yelnik A, et al. Stocktaking on the development of posturography for clinical use. *J Vestib Res.* (2011) 21:117–25. doi: 10.3233/VES-2011-0397

6. Kroenke K, Hoffman RM, Einstadter D. How common are various causes of dizziness? A critical review. *South Med J.* (2000) 93:160–7. doi: 10.1097/00007611-200093020-00001

7. Berge JE, Nordahl SHG, Aarstad HJ, Goplen FK. Long-term survival in 1,931 patients with dizziness: disease- and symptom-specific mortality. *Laryngoscope.* (2021) 131:E2031–7. doi: 10.1002/lary.29465

8. Corrales CE, Bhattacharyya N. Dizziness and death: an imbalance in mortality. *Laryngoscope.* (2016) 126:2134–6. doi: 10.1002/lary.25902

9. Cesari M, Onder G, Zamboni V, Manini T, Shorr RI, Russo A, et al. Physical function and self-rated health status as predictors of mortality: results from longitudinal analysis in the ilSIRENTE study. *BMC Geriatr.* (2008) 8:34. doi: 10.1186/1471-2318-8-34

10. Cooper R, Strand BH, Hardy R, Patel KV, Kuh D. Physical capability in mid-life and survival over 13 years of follow-up: British birth cohort study. *BMJ.* (2014) 348:g2219. doi: 10.1136/bmj.g2219

11. Berge JE, Nordahl SHG, Aarstad HJ, Gilhus NE, Goplen FK. Evaluation of self-reported symptoms in 1,457 dizzy patients and associations with caloric testing and posturography. *Otol Neurotol.* (2020) 41:956–63. doi: 10.1097/MAO.0000000000002670

12. Statistics Norway. *07902: Life Tables, By Sex and Age 1966–2020.* Available online at: https://www.ssb.no/en/statbank/table/07902/ (accessed March 31, 2021).

13. Goplen FK, Grønning M, Irgens A, Sundal E, Nordahl SHG. Vestibular symptoms and otoneurological findings in retired offshore divers. *Aviat Space Environ Med.* (2007) 78:414–9.

14. Carstensen B, Plummer M, Laara E, Hills M. *Epi: A Package for Statistical Analysis in Epidemiology. R Package Version 2.43.* (2021). Available online at: https://cran.r-project.org/package=Epi (accessed February 15, 2021).

15. Miettinen J, Rantanen M. *popEpi: Functions for Epidemiological Analysis Using Population Data. R Package Version 0.4.8.* (2019). Available online at: https://cran.r-project.org/package=popEpi (accessed February 15, 2021).

16. Deuschl G, Beghi E, Fazekas F, Varga T, Christoforidi KA, Sipido E, et al. The burden of neurological diseases in Europe: an analysis for the global burden of disease study 2017. *Lancet Public Heal.* (2020) 5:e551–67. doi: 10.1016/S2468-2667(20)30190-0

17. Tehrani ASS, Kattah JC, Mantokoudis G, Pula JH, Nair D, Blitz A, et al. Small strokes causing severe vertigo: frequency of false-negative MRIs and non-lacunar mechanisms. *Neurology.* (2014) 83:169–73. doi: 10.1212/WNL.0000000000000573

18. Kim AS, Fullerton HJ, Johnston SC. Risk of vascular events in emergency department patients discharged home with diagnosis of dizziness or vertigo. *Ann Emerg Med.* (2011) 57:34–41. doi: 10.1016/j.annemergmed.2010.06.559

19. Choi JH, Park MG, Choi SY, Park KP, Baik SK, Kim JS, et al. Acute transient vestibular syndrome: prevalence of stroke and efficacy of bedside evaluation. *Stroke.* (2017) 48:556–62. doi: 10.1161/STROKEAHA.116.015507

20. van Vugt VA, Bas G, van der Wouden JC, Dros J, van Weert HCPM, Yardley L, et al. Prognosis and survival of older patients with dizziness in primary care: a 10-year prospective cohort study. *Ann Fam Med.* (2020) 18:100–9. doi: 10.1370/afm.2478

21. Blain H, Carriere I, Sourial N, Berard C, Favier F, Colvez A, et al. Balance and walking speed predict subsequent 8-year mortality independently of current and intermediate events in well-functioning women aged 75 years and older. *J Nutr Health Aging.* (2010) 14:595–600. doi: 10.1007/s12603-010-0111-0

22. Tabara Y, Okada Y, Ohara M, Uetani E, Kido T, Ochi N, et al. Association of postural instability with asymptomatic cerebrovascular damage and cognitive decline: the Japan Shimanami health promoting program study. *Stroke.* (2015) 46:16–22. doi: 10.1161/STROKEAHA.114.006704

23. Qazi SL, Sirola J, Kröger H, Honkanen R, Isanejad M, Airaksinen O, et al. High postural sway is an independent risk factor for osteoporotic fractures but not for mortality in elderly women. *J Bone Miner Res.* (2019) 34:817–24. doi: 10.1002/jbmr.3664

24. Tuunainen E, Rasku J, Jäntti P, Pyykkö I. Risk factors of falls in community dwelling active elderly. *Auris Nasus Larynx.* (2014) 41:10–6. doi: 10.1016/j.anl.2013.05.002

25. Agrawal Y, Carey JP, Della Santina CC, Schubert MC, Minor LB. Disorders of balance and vestibular function in US adults: data from the national health and nutrition examination survey, 2001–2004. *Arch Intern Med.* (2009) 169:938–44. doi: 10.1001/archinternmed.2009.66

26. Siracuse JJ, Odell DD, Gondek SP, Odom SR, Kasper EM, Hauser CJ, et al. Health care and socioeconomic impact of falls in the elderly. *Am J Surg.* (2012) 203:335–8. doi: 10.1016/j.amjsurg.2011.09.018

frontiers | Frontiers in Neurology

TYPE Original Research
PUBLISHED 11 August 2022
DOI 10.3389/fneur.2022.963968

OPEN ACCESS

EDITED BY
Diego Kaski,
University College London,
United Kingdom

REVIEWED BY
Terence Leung,
University College London,
United Kingdom
Stephen Cox,
University of East Anglia,
United Kingdom

*CORRESPONDENCE
Kemar E. Green
DO kgreen66@jhmi.edu

SPECIALTY SECTION
This article was submitted to Neuro-Otology, a section of the journal Frontiers in Neurology

RECEIVED 08 June 2022
ACCEPTED 20 July 2022
PUBLISHED 11 August 2022

CITATION
Wagle N, Morkos J, Liu J, Reith H, Greenstein J, Gong K, Gangan I, Pakhomov D, Hira S, Komogortsev OV, Newman-Toker DE, Winslow R, Zee DS, Otero-Millan J and Green KE (2022) aEYE: A deep learning system for video nystagmus detection. *Front. Neurol.* 13:963968. doi: 10.3389/fneur.2022.963968

aEYE: A deep learning system for video nystagmus detection

Narayani Wagle[1,2], John Morkos[3], Jingyan Liu[1], Henry Reith[1], Joseph Greenstein[4], Kirby Gong[1], Indranuj Gangan[1], Daniil Pakhomov[2], Sanchit Hira[1], Oleg V. Komogortsev[5], David E. Newman-Toker[4,6,7], Raimond Winslow[1,2,8], David S. Zee[4,8,9], Jorge Otero-Millan[10,11] and Kemar E. Green[1,4]*

[1]Department of Biomedical Engineering, The John Hopkins University, Baltimore, MD, United States, [2]Department of Computer Science, The Johns Hopkins University, Baltimore, MD, United States, [3]The John Hopkins University School of Medicine, Baltimore, MD, United States, [4]Institute for Computational Medicine, The Johns Hopkins University, Baltimore, MD, United States, [5]Department of Computer Science, Texas State University, San Marcos, TX, United States, [6]Departments of Ophthalmology and Otolaryngology, The John Hopkins University School of Medicine, Baltimore, MD, United States, [7]Department of Emergency Medicine, The John Hopkins University School of Medicine, Baltimore, MD, United States, [8]Departments of Electrical and Computer Engineering, The John Hopkins University, Baltimore, MD, United States, [9]Department of Neurosciences, The John Hopkins University School of Medicine, Baltimore, MD, United States, [10]Department of Neurosciences, The John Hopkins University School of Medicine, Baltimore, MD, United States, [11]School of Optometry University of California—Berkeley, Berkeley, CA, United States

Background: Nystagmus identification and interpretation is challenging for non-experts who lack specific training in neuro-ophthalmology or neuro-otology. This challenge is magnified when the task is performed *via* telemedicine. Deep learning models have not been heavily studied in video-based eye movement detection.

Methods: We developed, trained, and validated a deep-learning system (aEYE) to classify video recordings as normal or bearing at least two consecutive beats of nystagmus. The videos were retrospectively collected from a subset of the monocular (right eye) video-oculography (VOG) recording used in the Acute Video-oculography for Vertigo in Emergency Rooms for Rapid Triage (AVERT) clinical trial (#NCT02483429). Our model was derived from a preliminary dataset representing about 10% of the total AVERT videos ($n = 435$). The videos were trimmed into 10-sec clips sampled at 60 Hz with a resolution of 240 × 320 pixels. We then created 8 variations of the videos by altering the sampling rates (i.e., 30 Hz and 15 Hz) and image resolution (i.e., 60 × 80 pixels and 15 × 20 pixels). The dataset was labeled as "nystagmus" or "no nystagmus" by one expert provider. We then used a filtered image-based motion classification approach to develop aEYE. The model's performance at detecting nystagmus was calculated by using the area under the receiver-operating characteristic curve (AUROC), sensitivity, specificity, and accuracy.

Results: An ensemble between the ResNet-soft voting and the VGG-hard voting models had the best performing metrics. The AUROC, sensitivity, specificity, and accuracy were 0.86, 88.4, 74.2, and 82.7%, respectively. Our validated folds had an average AUROC, sensitivity, specificity, and accuracy of 0.86, 80.3, 80.9, and 80.4%, respectively. Models created from the compressed videos decreased in accuracy as image sampling rate decreased from 60 Hz to 15 Hz. There was only minimal change in

the accuracy of nystagmus detection when decreasing image resolution and keeping sampling rate constant.

Conclusion: Deep learning is useful in detecting nystagmus in 60 Hz video recordings as well as videos with lower image resolutions and sampling rates, making it a potentially useful tool to aid future automated eye-movement enabled neurologic diagnosis.

KEYWORDS

nystagmus, vertigo, artificial intelligence, dizziness, machine learning, telemedicine, deep learning, eye movements

Introduction

Nystagmus is an involuntary, rhythmic ocular instability that is initiated by an unwanted slow-phase drift in one direction followed by a corrective phase (fast or slow) in the opposite direction (1, 2). The waveforms can be divided into two morphologies: (1) pendular (sinusoid slow slow-phase drift and slow-phase correction) and (2) jerk (slow-phase drift and fast-phase correction). The "jerk" waveform can be further divided based on the velocity profile of the slow-phase into linear (or constant velocity slow-phase), velocity-decreasing and velocity-increasing (Figure 1). The pattern of nystagmus often localizes the underlying neural substrate that is damaged, and thus provides rapid diagnostic clues about changes in neurophysiology that occur in various lesions affecting these circuits. It has been shown that nystagmus and other subtle eye movement abnormalities are more sensitive and specific than early neuroimaging in distinguishing potentially devastating strokes from more benign inner ear problems (3, 4). These subtle findings are often missed by those on the frontlines in the emergency room and are often appreciated only by neurologists specializing in neuro-otology; there are < 50 of these providers practicing in the United States. Additionally, there are other "non-nystagmoid" movements such as square-wave jerks, ocular flutter, opsoclonus and other voluntary ocular oscillations that might pose a diagnostic challenge for both experts and non-experts alike.

The shift toward remote health assessment in the setting of the pandemic negatively impacted the quality of the physician's neurological assessment; the major limitation being the patient video capability. For nystagmus detection, simulated data of nystagmus waveforms showed that it is difficult to appreciate these subtle clinical findings on videos with lower frame rates (5). In the absence of an expert neuro-otologist/neuro-ophthalmologist, an automated model that could detect subtle degrees of nystagmus from video recordings, when video qualities poor, would be a boon to frontline practitioners facing a diagnostic challenge.

Others have successfully classified nystagmus from waveforms directly (6–9) and by generating waveforms from recorded videos (10, 11) using various machine/deep learning methods. Classification of nystagmus from video motion features independent of the calibration and calculation of eye movement velocity has only been rarely attempted (12). We developed, trained, and validated an artificial intelligence (AI)-based deep learning model (aEYE) directly from video recordings and investigated its utility as a potential screening tool for video nystagmus detection in various simulated video recording conditions.

Methods

Study design and dataset description

aEYE was developed using infrared monocular video-oculography recordings retrospectively obtained from the AVERT (13) research dataset. The AVERT trial is a multicenter, randomized clinical trial comparing the diagnostic accuracy of care guided by video oculography (VOG)-based eye movement recordings (supervised decision support) vs. standard care in diagnosing patients with acute dizziness and vertigo in the emergency department (ClinicalTrials.gov #NCT02483429). Both the AVERT trial and the current study were approved by the Johns Hopkins University School of Medicine's Institutional Review Board (IRB). Our dataset consisted of 435 monocular infrared VOG recordings of dizzy patients that represented about 10% of the total AVERT video dataset. All videos used were obtained from 30 patients. In the AVERT dataset, the videos were recorded in primary gaze, eccentric gaze, Dix-Hallpike, supine head roll, bow, lean and post-horizontal headshaking. Primary and eccentric gaze videos were recorded with and without visual fixation, while all others were recorded without visual fixation. In the videos that contained nystagmus ($n = 218$), 95% were linear jerk (vestibular nystagmus) and 5% velocity decreasing jerk (gaze-evoked nystagmus); there were

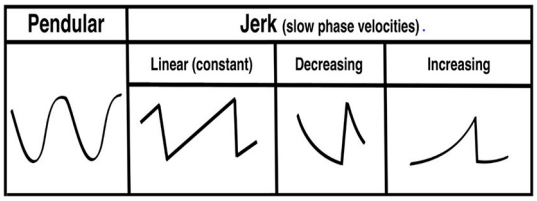

FIGURE 1
Pendular and jerk nystagmus waveform morphologies.

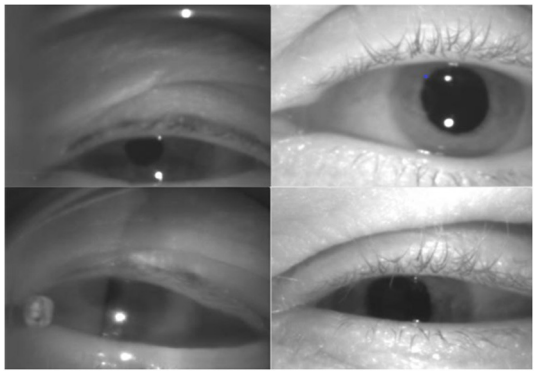

FIGURE 2
Variations in video quality of the dataset.

no pendular nystagmus videos in the dataset. Of the 95% of linear jerk nystagmus videos, 9.1% ($n = 20$) had nystagmus in primary gaze; the remainder were from positional testing. All videos were of the right eye; nystagmus in dizziness is almost always the same in both eyes. All videos were recorded using the Natus/Otometrics ICS Impulse infrared VOG googles (14). Recordings were all grayscale and sampled at 60 Hz and had a resolution of 240 × 320 pixels. We then simulated 8 variations of videos of varying sampling rates (i.e., 30 Hz and 15 Hz) and image resolution (i.e., 60 × 80 pixels and 15 × 20 pixels). Only the first 10 sec of each video (600 frames) were used. The quality of the recording (i.e., lighting and visualization of the eyes) varied as shown in Figure 2. Each video was labeled as "nystagmus" or "no nystagmus" by one expert Neuro-otologist (K.E.G.) based on the presence of two consecutive slow and fast phase alternations (beats). The "nystagmus" to "no nystagmus" in our dataset was approximately 1:1; the train to test split was about 3:1. There was equal representation of videos from both classes from each of the 30 patients in both the training and test sets to account for potential bias in the model. The best performing model was then validated using k-fold cross-validation with k = 3 folds.

Filtered image construction

We adopted and modified a previously described recursive filtering method (15, 16) used for detecting walking for the purposes of detecting ocular movements. A filtered image was created by applying recursive filtering to a 10-sec grayscale video clip (600 frames). This creates a representation of video motion based on the idea that a filtered image ($\boldsymbol{F_t}$) at time ($\boldsymbol{t}$) is defined as the absolute value of the difference between a raw video frame ($\boldsymbol{I_t}$) at time ($\boldsymbol{t}$) and an intermediate image ($\boldsymbol{M_t}$) at time ($\boldsymbol{t}$) that combines content of raw video frames prior to time point $\boldsymbol{t}$.

$$\begin{aligned} \boldsymbol{F_t} &= |\boldsymbol{I_t} - \boldsymbol{M_t}| \\ \boldsymbol{M_t} &= (\boldsymbol{1}-\beta)\,\boldsymbol{M_{t-1}} + \beta \boldsymbol{I_{t-1}} \\ \boldsymbol{M_0} &= \boldsymbol{I_1} \\ \textbf{where t} &= \mathbf{1, 2, \ldots, n} \end{aligned}$$

The appearance of the filtered image can be modified by changing the parameter ($\boldsymbol{\beta}$) that control the weights of the prior context of the intermediate image ($\boldsymbol{M}$) and the raw video frame ($\boldsymbol{I}$) as shown in Figure 3.

The result is a set of images containing at maximum 599 filtered images that depicts motion at points in time as shown in Figure 4. In addition to the "original" filtered image (non-sliding window), we also constructed sliding window filtered images [10 frames (150 ms), 20 frames (333 ms), 30 frames(500 ms), and 60 frames(1s)] to consider the temporal criteria for slow and fast phase combinations (i.e., beats) of nystagmus.

Video quality variations

We simulated 8 variations of videos from the original recordings (i.e., sampling rate = 60 Hz and resolution = 240 × 320 pixels) of varying sampling rates (i.e., 30 Hz and 15 Hz) and image resolution (i.e., 60 × 80 pixels and 15 × 20 pixels) as shown in Figure 5A. The compressed images were then converted into filtered images (Figure 5B) using the method illustrated in Figure 4.

Deep learning model (aEYE) architecture

The proposed motion classification algorithm is a filtered image-based (16) approach (Figure 6). The filtered image-based motion classification algorithm uses a set of filtered images as video motion data. Each filtered image is labeled according to the label from the video it was generated and used to train a classifier in a supervised fashion. We trained classifiers from the ImageNet dataset (ResNet) using transfer learning approaches to detect nystagmus from filtered images. The videos in each test set were equally balanced between "nystagmus" and "no nystagmus". aEYE was trained and tested to yield a

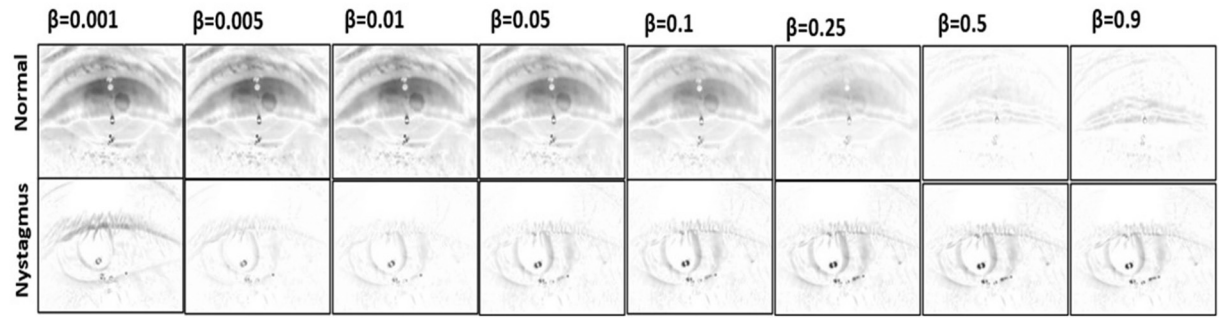

FIGURE 3
Filtered image appearance across different beta values.

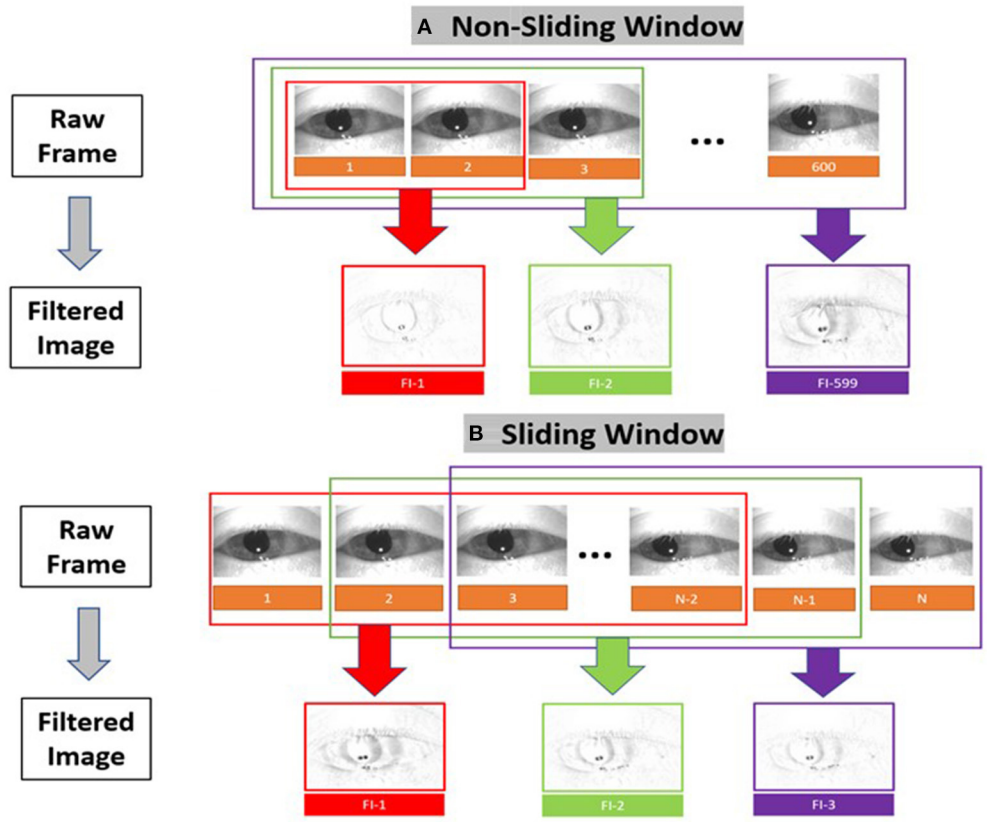

FIGURE 4
Filtered image construction for **(A)** the non-sliding window and **(B)** the sliding window variations.

binary class prediction of "nystagmus" or "no nystagmus" for each filtered image in the test set. Hard (majority) voting was performed to summate the filtered images from each video that were classified as nystagmus. In hard voting, only videos that have an average probability of nystagmus amongst all filtered images ($n = 599$) are classified as nystagmus (17). We also experimented with a form of soft voting where every individual filtered image provides a probability value that a specific video belongs to a particular target class (nystagmus or no nystagmus).

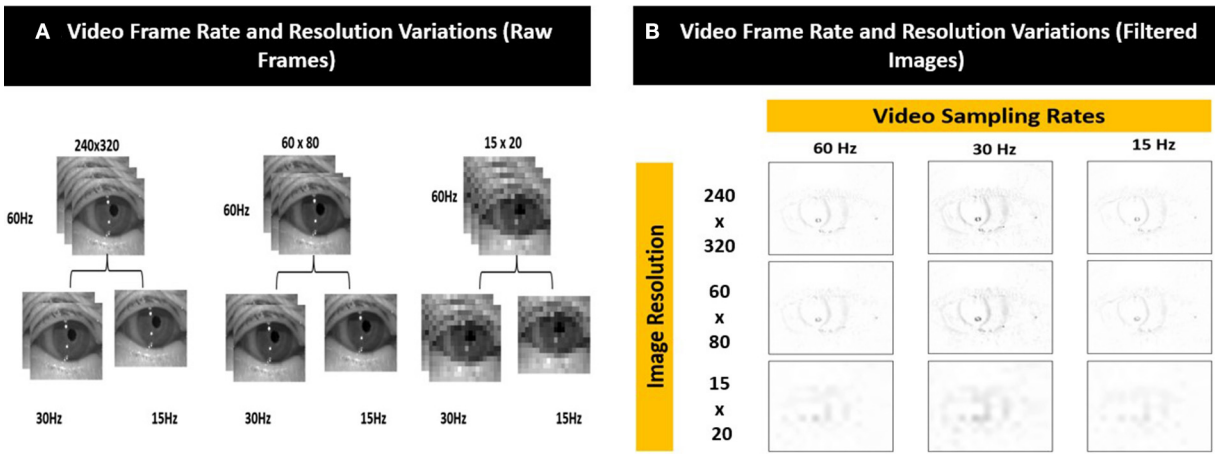

FIGURE 5
Examples of the different video frame rate and resolution variations for **(A)** raw frames and **(B)** corresponding filtered images.

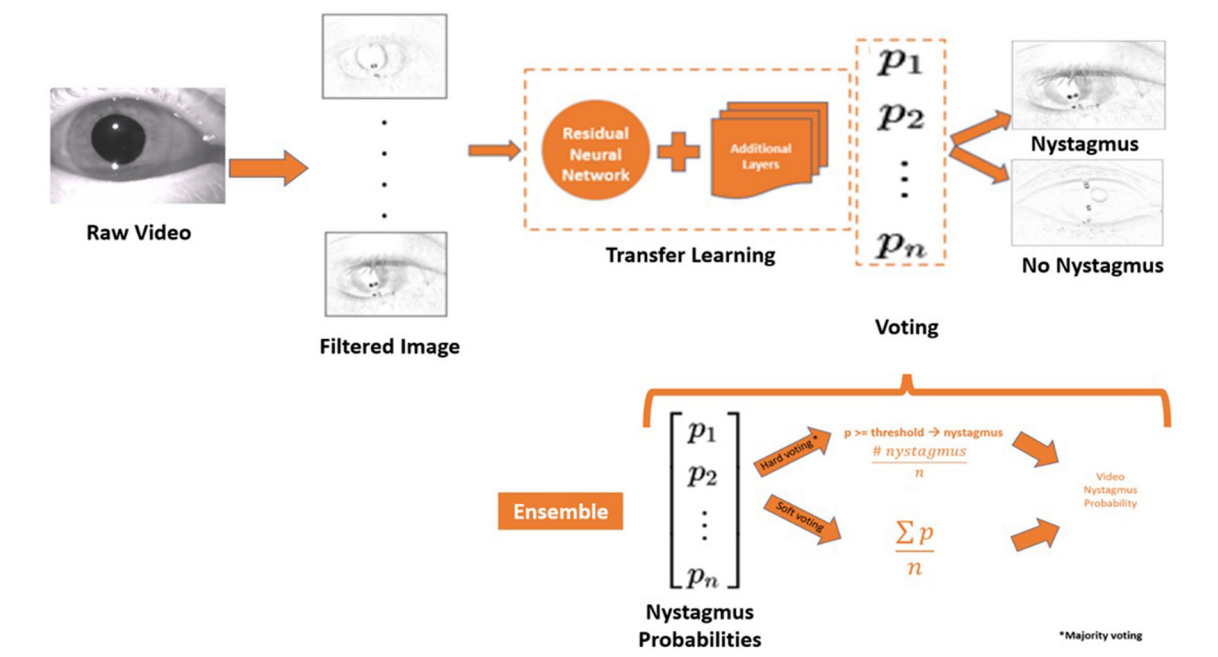

FIGURE 6
Model architecture and the framework of the ensemble model. *P*, probability; *n*, number of filtered images; ∑, the sum of; *n*, number of filtered images.

Voting based on the temporal criteria of nystagmus

Nystagmus as defined in our dataset is at least two contiguous cycles (beats) of alternating fast and slow phase combinations along any plane. The duration of a slow phase can vary from ∼150 msec (∼10 frames) to ∼350 msec (∼20 frames)—closely representing the duration of a beat. The aim of this experiment is to determine if aEYE's performance can be improved by changing the voting method to identify consecutive filtered images bearing a probability of nystagmus. We experimented with the following four temporal voting criteria: (1) ≥50 consecutive frames (∼750 ms), ≥100 consecutive frames (∼1,500 ms); ≥150 consecutive frames (∼2,250 ms), and ≥350 consecutive frames (∼5,250 ms).

Data split modifications

Based on the filtered image misclassifications (false positives and false negatives) videos where the eyes were eccentrically positioned (i.e., not looking straight ahead) ranked the highest. We evaluated how an equal split of eccentrically positioned videos in both the training and test sets impacted the model's performance.

ImageNet classifier comparison

Classifiers for the ImageNet dataset, such as ResNet, DenseNet, VGG and Inception which perform better on medical data, were trained to detect nystagmus from filtered images (16). Nystagmus detection was compared across all four ImageNet classifiers.

Ensemble model

Ensemble techniques involve model averaging that is aimed at reducing generalization errors. We applied an ensemble technique like bootstrap aggregating (or bagging) (19) where different models are trained separately (on the same dataset), and the output is determined by averaging different voting methods. Hard and soft voting methods were used to create an ensemble model (Figure 5) that averages both voting methods to decide on the final class designation (nystagmus or no nystagmus).

Comparison with existing video classification method

We adopted a simple long short-term memory (LSTM) and convolutional neural network (CNN) model (18) without any frame sampling that has been shown to produce state-of-the-art performance for other action recognition problems.

Statistical analysis

The performance was based on the model's detection of videos with or without nystagmus. The performance of the models was calculated using the area under the receiver operating characteristic curve (AUROC) at the operating point with accuracy sensitivity and specificity. It is important to note the differences between accuracy (the ratio between the number of correctly predicted samples to the total number of samples) and AUROC (the ratio of the false positive and true positive rates at different probability thresholds of the model's prediction) (19). We also compared the best AUROC for each model experiment to the best overall AUROC using two sample (unpaired) t-test. A p-value < 0.05 indicates evidence of statistical difference between two experiments.

Internal validation of our best performing model was done using stratified k-fold cross-validation (19) that partitions our data into $k = 3$ folds as demonstrated in Figure 7A. Each fold contains an evenly distributed sample of both class. In the validation experiments, we also ensured that there was equal representation of videos in both classes from an individual patient. To maintain these constraints, it was not feasible to balance video heterogeneity. The performance was measured in aggregate across each test set. Each subset was stratified, ensuring an even class split in each set.

Results

Filtered image optimization

The filtered image calculation described above includes a free parameter ($\boldsymbol{\beta}$) that controls their temporal dynamics. We tested the performance of the best performing ResNet model (non-sliding window and soft voting) with 7 different $\boldsymbol{\beta}$ values (0.001, 0.005, 0.01, 0.05, 0.1, 0.25, and 0.5—see Figure 2 and Table 1). Filtered images obtained with $\boldsymbol{\beta}$ of 0.25 resulted in the highest accuracy (79.3%) at detecting nystagmus; however, specificity was low (69.3%)—implying a high false positive rate.

Sliding windows comparison

Filtered images with a beta value of 0.25 were used to carry out the sliding window experiments. The filtered images were created based on the following sliding windows: 10 frames (150 ms), 20 frames (333 ms), 30 frames (500 ms), and 60 frames (1 s). None showed any improvement in the model's overall performance.

Voting

Our neural network classifies individual filtered images as containing or not containing nystagmus. However, to evaluate the results against our labeled data, we classified the entire video. We then compared different voting strategies where each image votes toward the result of the video classification. Hard (majority voting) and soft voting techniques were compared using the value of $\boldsymbol{\beta}$ previously determined to be best ($\boldsymbol{\beta} = 0.25$). While the soft voting model had a slightly higher AUROC (0.85), there was better overall sensitivity (72.4%) and specificity (83.8%) with majority voting (Table 1).

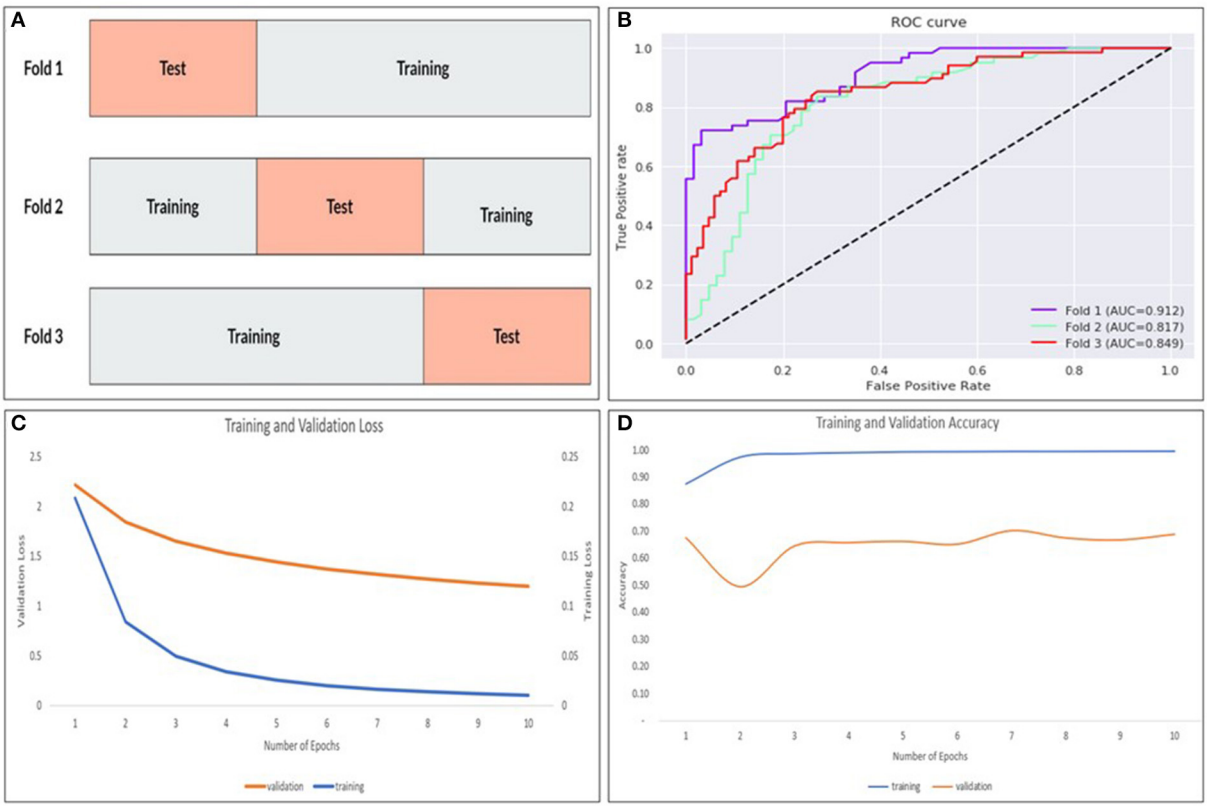

FIGURE 7
The k-fold cross validation architecture with the data partitioned into training and tests sets for k = 3–folds **(A)**, AUROC curves for each fold **(B)** as well as training/validation loss **(C)** and training/validation accuracy **(D)** for the model.

Sliding window-temporal voting criteria

The result of combining the sliding window models with different temporal voting criteria is shown in Table 1. As we increased the number of consecutive frames, the overall AUROC and sensitivity decreased while the specificity increased.

Data split modification

In our dataset (n = 435 videos), 44.3% (n = 193) of the videos had eccentric gaze positioning of the eye during the recording. As shown in Table 1, there were no improvement in any of the measured performance parameters in the model accounting for equal eccentric gaze splits.

ImageNet classifier comparison

We compared our best performing ResNet trained model (β = 0.25, non-sliding window and soft voting) to models trained on different ImageNet dataset (DenseNet, VGG and Inception) with the same β, sliding window and voting parameters. As shown in Table 1, the VGG model had a slightly higher AUROC (0.85); however overall sensitivity and specificity were better with the ResNet and Inception models.

Ensemble model

Bootstrap aggregating techniques (17) were applied to the best performing models from the ImageNet classifier comparison experiments with different hard and soft voting combinations. The ResNet-soft vote + VGG-hard vote ensemble model had the most ideal performance metrics (Sensitivity = 88.4%; Specificity = 74.1%) of all the models as shown in Table 1. When the same model was tested with reversed videos, it performed poorly (AUROC = 0.50).

Stratified k-fold cross validation

The ResNet-soft vote + VGG-hard vote ensemble model (best performing model) was cross validated using stratified k-fold cross validation. As shown in Figure 7B and Table 1,

TABLE 1 Performance metrics for model experiments.

	AUROC	Sensitivity	Specificity	Accuracy
Filtered image optimization				
$\beta = 0.001$	0.75	68.1%	77.4%	72.5%
$\beta = 0.005$	0.79	81.1%	62.9%	72.5%
$\beta = 0.01$	0.83	84.0%	69.3%	77.1%
$\beta = 0.05$	0.78	60.8%	80.6%	70.2%
$\beta = 0.1$	0.81	71.0%	80.6%	75.5%
$\beta = 0.25$	0.85	88.4%	69.3%	79.3%
$\beta = 0.5$	0.79	75.3%	74.1%	74.8%
Sliding window comparison				
150 msec	0.80	78.3%	75.8%	77.1%
333 msec	0.80	75.4%	77.4%	76.3%
500 msec	0.82	71.0%	83.9%	77.1%
1,000 msec	0.81	72.5%	82.3%	77.1%
2,000 msec	0.75	61.0%	75.8%	67.9%
Voting ($\beta = 0.25$)				
Hard voting	0.84	72.4%	83.8%	77.8%
Soft voting	0.85	88.4%	69.3%	79.3%
Sliding window-temporal voting criteria				
1,000 msec−50 frames	0.77	60.9%	88.7%	74.1%
500 msec−50 frames	0.78	75.4%	74.2%	74.8%
333 msec−50 frames	0.74	71.0%	71.0%	71.0%
150 msec−50 frames	0.74	71.0%	71.0%	71.0%
1,000 msec−100 frames	0.70	47.8%	90.3%	67.9%
500 msec−100 frames	0.71	52.2%	88.7%	69.5%
333 msec−100 frames	0.69	49.3%	87.1%	67.2%
150 msec−100 frames	0.71	59.4%	82.3%	70.2%
1,000 msec−150 frames	0.67	36.2%	96.8%	64.9%
500 msec−150 frames	0.68	46.4%	88.7%	66.4%
333 msec−150 frames	0.67	44.9%	87.1%	64.9%
150 msec−150 frames	0.69	49.3%	87.1%	67.2%
1,000 msec−350 frames	0.59	20.3%	96.8%	56.5%
500 msec−350 frames	0.62	27.5%	95.2%	59.5%
333 msec−350 frames	0.58	17.4%	98.4%	55.7%
150 msec−350 frames	0.61	27.5%	93.5%	58.8%
Data split modification				
Balanced eccentric gaze videos	0.83	83.1%	72.1%	77.8%
ImageNet classifier comparison				
ResNet	0.84	72.4%	83.8%	77.8%
DenseNet	0.81	75.3%	79.0%	77.1%
VGG	0.85	59.4%	96.7%	77.1%
Inception	0.82	84.0%	72.5%	78.6%
Ensemble				
ResNet-soft vote	0.85	88.4%	69.3%	79.3%
VGG-hard vote	0.85	59.4%	96.7%	77.1%
ResNet-soft vote + VGG-hard vote ensemble*	0.86	88.4%	74.2%	81.7%
ResNet-soft vote + VGG-hard vote ensemble model in reverse				
Reverse model	0.50	0.00%	100%	47.7%

(Continued)

TABLE 1 Continued

	AUROC	Sensitivity	Specificity	Accuracy
Stratified k-fold cross validation (k = 3–folds)				
Fold 1	0.91	72.1%	97.0%	84.7%
Fold 2	0.82	83.6%	73.0%	78.3%
Fold 3	0.85	85.3%	72.9%	78.4%
Average	0.86	80.3%	80.9%	80.4%
Comparison with existing video classification method				
LSTM + CNN	0.46	100%	2.00%	48.4%
Frame rate/resolution combinations				
60 Hz (240 × 320)	0.86	88.4%	74.2%	81.7%
60 Hz (60 × 80)	0.84	78.3%	83.9%	80.9%
60 Hz (15 × 20)	0.83	68.1%	85.5%	76.3%
30 Hz (240 × 320)	0.83	76.8%	77.4%	77.1%
30 Hz (60 × 80)	0.85	71.0%	87.1%	78.6%
30 Hz (15 × 20)	0.83	89.9%	66.1%	78.6%
15 Hz (240 × 320)	0.81	65.2%	83.9%	74.1%
15 Hz (60 × 80)	0.82	78.3%	74.2%	76.3%
15 Hz (15 × 20)	0.72	55.1%	82.3%	67.9%

AUROC, area under the receiver operating characteristic curve; CNN, convolutional neural network; LTSM, long-term short-term memory. (*)indicating the best performing model.

fold 1 returned the highest accuracy (84.7%), and there was a mean accuracy of (80.4%) across all 3–folds. Learning curves (Figures 7C,D) showed that our training loss follows a consistent trend and begins to converge early in training—indicating no overfitting.

Comparison with existing video classification method

As expected, the LSTM + CNN model performed poorly (AUROC = 0.46) compared to (AUROC = 0.86) in the best performing filtered image model as shown in Table 1.

Frame rate/resolution combinations

As shown in Table 1, the best performing model (AUROC = 0.86) was obtained from the videos with the original image specifications (i.e., sampling rate = 60 Hz and resolution = 240 × 320 pixels). Overall, there was a decrease in accuracy as image sampling rate decreased from 60 Hz to 15 Hz; however, there was only minimal change in the accuracy of nystagmus detection when image resolution was decreased while sampling rate was kept constant.

AUROC comparison

As shown in Table 1, the overall best performing model (ResNet-soft vote + VGG-hard vote ensemble) had an AUROC of 0.86. Of the $n = 131$ predictions from the test samples, the mean model prediction probability was 0.251 with a standard deviation (SD) of 0.159. As shown in Table 2, no statistical difference ($p = 0.837$) exists between the AUROC of the overall best performing model and the 500 msec-50 frames model from the sliding window-temporal voting criteria experiments. There were statistically significant differences ($p \leq 0.05$) between the AUROC of the ResNet-soft vote + VGG-hard vote ensemble model and the best AUROC for all the remaining experiments.

Discussion

We developed aEYE (a new deep learning method for nystagmus detection) from videos using non-traditional eye tracking techniques. Traditional nystagmus detection involves tracking the change in eye position over time using the pupil or other ocular features (e.g., the iris) (1, 20), which serves as surrogates for eye movements. With these methods, you can appreciate the quick and slow phases that define nystagmus—allowing for detection from characteristic nystagmus waveform morphologies. For the most robust nystagmus waveform detection, high frame rate video recordings are necessary for extraction of the precise ocular position data. The use of mobile devices (especially during the pandemic) has shifted the focus

TABLE 2 Comparing best overall AUROC (ResNet-soft vote + VGG-hard vote ensemble) with best AUROC from each model experiment shown in Table 1 using two sample (unpaired) *t*-test.

Experiment	Best AUROC	Mean MP	SD	*p*-value
AUROC Comparisons				
Filtered image optimization	0.85	0.529	0.369	<0.001
Sliding window comparison	0.82	0.518	0.379	<0.001
Voting ($\beta = 0.25$)	0.85	0.599	0.340	<0.001
Sliding window-temporal voting criteria	0.78	0.244	0.356	0.837
Data split modification	0.83	0.558	0.369	<0.001
ImageNet classifier comparison	0.85	0.439	0.328	<0.001
ResNet-soft vote + VGG-hard vote ensemble in reverse	0.50	0.000	0.000	<0.001
Comparison with existing video classification method	0.46	0.492	0.008	<0.001
Frame rate/resolution combinations (15 Hz)	0.82	0.604	0.292	<0.001
Frame rate/resolution combinations (30 Hz)	0.85	0.517	0.331	<0.001

AUROC, area under the receiver operating characteristic curve. MP, Model Predictions; SD, Standard Deviation.

of eye tracking toward mobile solutions. While current mobile VOG technology exists (21), we are still not clear on their accuracy in detecting nystagmus since most mobile devices have relatively lower video qualities compared to standard eye trackers. Furthermore, simulated data of nystagmus waveform at different video sampling rates demonstrated degradation in the nystagmus waveform morphology after ∼ 30Hz (5); other recording conditions such as recording distance may also play a role.

The result from our experiments suggests that the filtered image approach (15, 16) is well–suited for nystagmus detection from a relatively smaller dataset of low-quality videos. Reassuringly, the reproducibility of the model's performance in the stratified k-fold cross validation experiments suggests potential generalizability on external video datasets of similar size and quality. It is important to note that the video heterogeneity in our dataset (not accounted for in the validation experiments) implies that the model would likely perform better with less noise given fold 1's results (Table 1). In evaluating the performance of our model, the significance of the AUROC vs. the accuracy should be noted. For the AVERT patient population (all dizzy patients), the 1:1 split between nystagmus to "no nystagmus" is equivalent to what one would expect in that population, therefore the accuracy (81.7%) is a reliable measure of aEYE's performance; however, the AUROC (0.864) suggests a high probability of the model reproducing similar accuracies in "AVERT-like" patient population.

In the world of deep learning and image recognition, large datasets are often needed to ensure more accurate and reliable results (22, 23). In our study, we used a smaller video dataset ($n = 435$); however, since our input data was individual filtered images rather than the entire video clip, aEYE was trained on 179,700 (300 videos × 599 filtered images) data points. We believe this increased our model's performance tremendously, and probably explained why the non-sliding window model outperformed the sliding window models that created filtered images based on the temporal definition of a slow phase and contained fewer overall frames (see Table 1).

There are existing video classification methods (24) that uses forms of frame sampling for model input. Therefore, only a subset of the video frames is selected. Two consecutive beats of nystagmus can have a very short duration (as short as ∼500 msec or ∼30 frames) and is likely to be found in tiny chunks of the videos in our dataset (given the relative frequency of noise imparted by eye closure, blinks and other technical issues affecting video recording quality). As a result, implementing these methods risks eliminating the portions of our video that correspond to the class label (i.e., 2 consecutive beats of nystagmus). To counteract this, we used a simple LSTM and CNN model without any frame sampling (18). As suspected, the LSTM model performed poorly (AUROC = 0.46) as shown in Table 1. We believe the results seen may be due to one or both of the following factors. Since 600 frames per video was inputted, the complexity of the LSTM + CNN network was limited to handle the computational load. Additionally, video classification methods perform predictions at a video level while our proposed method performs predictions at an image level. With video classification, our dataset for training was ∼ 300 videos whereas with our method, our dataset for training was ∼ 180,000 filtered images.

The way the model makes its prediction remains a mystery. We attempted to decipher this problem by studying the characteristics of the misclassified videos. Our evaluation revealed that 8/11 (72.7%) and 7/10 (70%) of the false positive and false negative cases respectively were videos with eccentric eye positioning (i.e., not looking straight ahead). Additionally, while analyzing learning curves (Figures 7C,D), unusual behavior was observed in our validation loss curve in folds 2 and 3. We speculate that this is driven by the fact that our validation sets only represent a small proportion of training data. Therefore, understanding misclassified videos may provide insight to improve model learning and optimization in training.

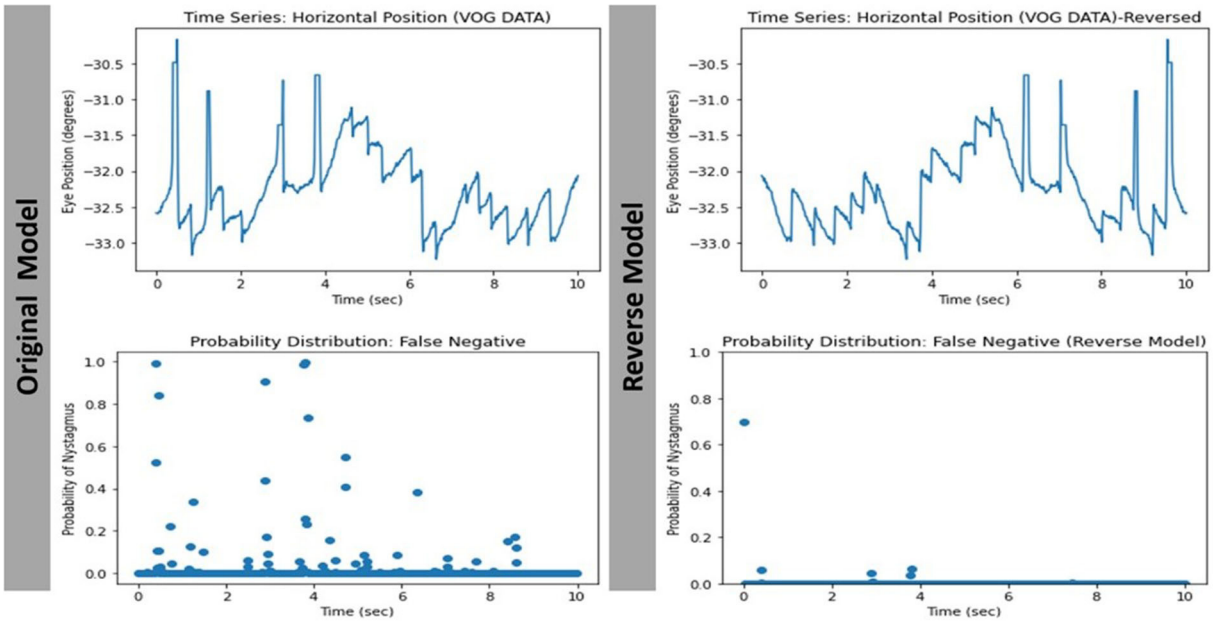

FIGURE 8
Comparing the filtered-image probability distribution of the same false negative video with nystagmus in eccentric eye position toward the end of video.

We then hypothesized that we may be able to improve the model's performance if we had an equal split of eccentrically positioned videos in both the training and test sets. As shown in Table 1 there was no improvement in any of the performance parameters measured in the new balanced split model. One possible explanation for these findings was that most of the eccentrically positioned videos only had nystagmus at the end of the video. Since each filtered image carries motion information from earlier frames, the last filtered image will contain the motion information of the entire video. In our dataset, the 10 sec recordings may contain a plethora of non-nystagmus eye motion features (e.g., blinks, eye closure, square-wave jerks, etc,). Therefore, as we move from filtered image 1 to 599 in a nystagmus video with other motion features, it is possible that the average number of images with nystagmus probability will be much lower in the second half of the video. To test the second hypothesis, we created a reversed version of the non-sliding window model to decrease both the false positive and false negative rates. As shown in Table 1, the overall model performance was significantly worse. A closer look at the filtered image probability distributions of a false negative video example (containing nystagmus in eccentric eye position toward the end of video) in both the original and reverse model revealed an over lower number of filtered images with nystagmus probabilities in the reverse model (Figure 8).

The lack of a clear clinically relevant explanation for aEYE's prediction brings into question the likelihood that there might be other "markers" of nystagmus recognizable by the machine, that may not yet be apparent to clinicians. Future studies to investigate our deep learning model's decision making using novel and existing explainable AI methods will be needed to better understand predictions and decipher the "Blackbox" (25, 26).

Conclusion

aEYE could be used for remote detection of nystagmus with potential future application in the detection of other eye movement types (square-wave jerks, ocular flutter, opsoclonus, etc). Further research into understanding the model's predictions using explainable AI (27) may be useful for improving the model's performance. Robust, international multicenter external cross validation will be needed to prove generalizability in different populations with various video recording capabilities.

Data availability statement

The datasets presented in this article are not readily available because of ethical and privacy restrictions. Requests to access the datasets should be directed to KG, kgreen66@jhmi.ed.

Ethics statement

The studies involving human participants were reviewed and approved by Johns Hopkins Medicine IBB. The patients/participants provided their written informed consent to participate in this study.

Author contributions

NW, JM, JL, HR, JG, KG, SH, OK, RW, and DZ: data analysis and drafting and revision of manuscript. DN-T: drafting and revision of manuscript. JO-M: study concept and design, data analysis, and drafting and revision of manuscript. KG: study concept and design, data analysis, and drafting and revision of manuscript. All authors contributed to the article and approved the submitted version.

Acknowledgments

We acknowledge the National Institute on Deafness and Other Communication Disorders [NIDCD U01 DC013778, AVERT Trial (ClinicalTrials.gov #NCT02483429)] for providing the dataset for this study. We also acknowledge the Johns Hopkins Department of Neurology (specifically Justin C. McArthur MBBS/MPH) and The Whiting School of Engineering for supporting the project.

Conflict of interest

Author DN-T conducts research related to diagnosis of dizziness and stroke, as well as diagnostic error. He serves as the principal investigator for multiple grants and contracts on these topics, including the NIH-sponsored AVERT clinical trial (NIDCD U01 DC013778, ClinicalTrials.gov #NCT02483429). Johns Hopkins has been loaned research equipment [video-oculography (VOG) systems] by two companies for use in DN-T's research; one of these companies has also provided funding for research on diagnostic algorithm development related to dizziness, inner ear diseases, and stroke. DN-T has no other financial interest in these or any other companies. DN-T is an inventor on a provisional patent (US No. 62/883,373) for smartphone-based stroke diagnosis in patients with dizziness. He gives frequent academic lectures on these topics and occasionally serves as a medico-legal consultant for both plaintiff and defense in cases related to dizziness, stroke, and diagnostic error.

The remaining authors declare that the research was conducted in the absence of any commercial or financial relationships that could be construed as a potential conflict of interest.

Publisher's note

References

1. Leigh RJ, Zee DS. *The Neurology of Eye Movements*. 5th edition Oxford New York: Oxford University Press (2015).

2. Green KE, Gold DR. Nystagmus and Superior Oblique Myokymia [Internet]. In: Henderson AD, Carey AR, editors. *Controversies in Neuro-Ophthalmic Management*. Cham: Springer International Publishing (2021). p. 157–68.

3. Kattah JC, Talkad AV, Wang DZ, Hsieh Y-H. Newman–Toker DE, et al. HINTS to diagnose stroke in the acute vestibular syndrome: three-step bedside oculomotor examination more sensitive than early MRI diffusion-weighted imaging. *Stroke*. (2009) 40:3504–10. doi: 10.1161/STROKEAHA.109.551234

4. Newman-Toker DE, Kerber KA, Hsieh Y-H, Pula JH, Omron R, Tehrani ASS, et al. HINTS outperforms ABCD2 to screen for stroke in acute continuous vertigo and dizziness. *Acad Emerg Med*. (2013) 20:986–96. doi: 10.1111/acem.12223

5. Green KE, Pogson JM, Otero-Millan J, Gold DR. Tevzadze, Tehrani ASS, et al. Opinion and special articles: remote evaluation of acute vertigo: strategies and technological considerations [Internet]. *Neurology*. (2021) 96:34–8. doi: 10.1212/WNL.0000000000010980

6. Punuganti SA, Tian J, Otero-Millan J. Automatic quick-phase detection in bedside recordings from patients with acute dizziness and nystagmus [Internet]. In: *Proceedings of the 11th ACM Symposium on Eye Tracking Research & Applications Denver Colorado: ACM*. (2019).

7. Phillips JS, Newman JL, Cox SJ. An investigation into the diagnostic accuracy, reliability, acceptability and safety of a novel device for continuous ambulatory vestibular assessment (CAVA). *Sci Rep*. (2019) 9:10452. doi: 10.1038/s41598-019-46970-7

8. Newman JL, Phillips JS, Cox SJ. 1D Convolutional neural networks for detecting nystagmus. *IEEE J Biomed Health Inform*. (2021) 25:1814–23. doi: 10.1109/JBHI.2020.3025381

9. Newman JL, Phillips JS, Cox SJ. Detecting positional vertigo using an ensemble of 2D convolutional neural networks [Internet]. *Biomed Signal Process Control*. (2021) 68:102708. doi: 10.1016/j.bspc.2021.102708

10. Reinhardt S, Schmidt J, Leuschel M, Schule C, Schipper J. VertiGo – a pilot project in nystagmus detection via webcam [Internet]. *Curr Dir Biomed Eng*. (2020) 6:20200043. doi: 10.1515/cdbme-2020-0043

11. Lim E-C, Park JH, Jeon HJ. Kim H–J, Lee H–J, Song C–G, et al. Developing a diagnostic decision support system for benign paroxysmal positional vertigo using a deep-learning model. *J Clin Med*. (2019) 8:E633. doi: 10.3390/jcm8050633

12. Zhang W, Wu H, Liu Y, Zheng S, Liu Z, Li Y, et al. Deep learning based torsional nystagmus detection for dizziness and vertigo diagnosis. *Biomed Signal Process Control*. (2021) 68:102616. doi: 10.1016/j.bspc.2021.102616

13. *AVERT Clinical Trial* [Internet]. Available online at: https://clinicaltrials.gov/ct2/show/NCT02483429 (accessed August 25, 2021).

14. *ICS Impulse* [Internet]. Available online at: https://hearing-balance.natus.com/en-us/products-services/ics-impulse (accessed August 25, 2021).

15. Masoud O, Papanikolopoulos N. A method for human action recognition [Internet]. *Image Vis Comput.* (2003) 21:729–43. doi: 10.1016/S0262-8856(03)00068-4

16. Dongwei Cao, Masoud OT, Boley D, Papanikolopoulos N. Online motion classification using support vector machines [Internet]. In: Meng M, editor. *IEEE International Conference on Robotics and Automation*. New Orleans, LA: IEEE (2004).

17. Goodfellow I, Bengio Y, Courville A. *Deep Learning*. Cambridge, MA: MIT Press (2017).

18. Hochreiter S, Schmidhuber J. Long short-term memory. *Neural Comput.* (1997) 9:1735–80. doi: 10.1162/neco.1997.9.8.1735

19. Hastie T, Tibshirani R, Friedman JH. *The Elements of Statistical Learning: Sata Mining, Inference, and Prediction*. 2nd ed. New York, NY: Springer (2009).

20. Otero-Millan J, Roberts DC, Lasker A, Zee DS, Kherdmand A. Knowing what the brain is seeing in three dimensions: a novel, noninvasive, sensitive, accurate, and low-noise technique for measuring ocular torsion. *J Vis.* (2015) 15:11. doi: 10.1167/15.14.11

21. Parker TM, Farrell N, Otero-Millan J, Kherdmand A, McClenney A, Newman–Toker DE, et al. Proof of Concept for an "eyePhone" App to Measure Video Head Impulses. *Digit Biomark.* (2020) 5:1–8. doi: 10.1159/000511287

22. Hey T, Butler K, Jackson S, Thiyagalingam J. Machine learning and big scientific data. *Philos Trans A Math Phys Eng Sci.* (2020) 378:20190054. doi: 10.1098/rsta.2019.0054

23. Fang Y, Wang J, Ou X, Ying H, Hu C, Zhang Z, et al. The impact of training sample size on deep learning-based organ auto-segmentation for head-and-neck patients. *Phys Med Biol.* (2021) 66:185012. doi: 10.1088/1361-6560/ac2206

24. Karpathy A, Toderici G, Shetty S, Leung T, Sukthankar R, Fei–Fei L. Large-scale video classification with convolutional neural networks [Internet]. In: Mortensen E, Fidler S, editors. *2014 IEEE Conference on Computer Vision and Pattern Recognition*. Columbus, OH: IEEE (2014). p. 1725–32.

25. Hiley L, Preece A, Hicks Y. *Explainable Deep Learning for Video Recognition Tasks: A Framework and; Recommendations* [Internet]. (2019). Available online at: https://arxiv.org/abs/1909.05667 (accessed April 16, 2022).

26. Selvaraju RR, Cogswell M, Das A, Vedantam R, Parikh D, Batra D, et al. Grad-CAM: visual explanations from deep networks via gradient-based localization. *Int J Comput Vis.* (2020) 128:336–59. doi: 10.1007/s11263-019-01228-7

27. Linardatos P, Papastefanopoulos V, Kotsiantis S. Explainable AI: a review of machine learning interpretability methods. *Entropy (Basel).* (2020) 23:E18. doi: 10.3390/e23010018

frontiers | Frontiers in Neurology

TYPE Brief Research Report
PUBLISHED 17 August 2022
DOI 10.3389/fneur.2022.921341

OPEN ACCESS

EDITED BY
Dominik Straumann,
University of Zurich, Switzerland

REVIEWED BY
James Phillips,
University of Washington,
United States
Liu Dave Liu,
Baylor College of Medicine,
United States

*CORRESPONDENCE
João Lemos
merrin72@hotmail.com

†These authors have contributed equally to this work and share first authorship

SPECIALTY SECTION
This article was submitted to Neuro-Otology, a section of the journal Frontiers in Neurology

RECEIVED 15 April 2022
ACCEPTED 25 July 2022
PUBLISHED 17 August 2022

CITATION
Martins AI, Soares-dos-Reis R, Jorge A, Duque C, Pereira DJ, Fontes Ribeiro C, Sargento-Freitas J, Matos A, Negrão L and Lemos J (2022) A 6-month trial of memantine for nystagmus and associated phenomena in oculopalatal tremor. *Front. Neurol.* 13:921341. doi: 10.3389/fneur.2022.921341

A 6-month trial of memantine for nystagmus and associated phenomena in oculopalatal tremor

Ana Inês Martins[1†], Ricardo Soares-dos-Reis[2,3†], André Jorge[1], Cristina Duque[4], Daniela Jardim Pereira[5], Carlos Fontes Ribeiro[6], João Sargento-Freitas[1,6], Anabela Matos[1], Luís Negrão[1] and João Lemos[1,6*]

[1]Department of Neurology, Coimbra University and Hospital Centre, Coimbra, Portugal, [2]Department of Neurology, Centro Hospitalar Universitário de São João, Porto, Portugal, [3]Department of Clinical Neurosciences and Mental Health, Faculty of Medicine, University of Porto, Porto, Portugal, [4]Department of Neurology, Pedro Hispano Hospital, Matosinhos, Portugal, [5]Department of Neuroradiology Unit/Imaging, Coimbra University and Hospital Centre, Coimbra, Portugal, [6]Faculty of Medicine, Coimbra University, Coimbra, Portugal

Introduction: Oculopalatal tremor (OPT) is a late manifestation of a Guillain-Mollaret triangle lesion. Memantine has been shown to improve nystagmus in OPT, but its long-term efficacy and putative distinct effects on each plane of nystagmus and on associated phenomena (e.g., gravity perception) are largely unknown.

Methods: We conducted a 6-month open-label study to evaluate the effect of memantine in OPT patients. Baseline (visit 1), 2 (visit 2), and 6 months (visit 3) assessments included video-oculography, best corrected visual acuity (BCVA), visual function questionnaire (VFQ25), palatal tremor frequency, and subjective visual vertical (SVV). Memantine was titrated to 20 mg per day and stopped after 6 months.

Results: We included six patients (5 females; mean age 68.5+/-9.7). At visit 2, nystagmus improved >50% only along the horizontal plane in two patients, while worsening >50% along the vertical and horizontal planes in 4 and 1 patients, respectively. At visit 3, previous improvement of nystagmus along the horizontal plane in two patients was not sustained, and it further worsened >50% along the vertical plane in 4. The mean vertical velocity and amplitude of nystagmus in the left eye significantly worsened from visit 2 to visit 3 ($p = 0.028$). Throughout the study, nystagmus frequency remained unchanged ($p = 0.074$), BCVA improved in both eyes ($p = 0.047$, $p = 0.017$), SVV progression was unpredictable ($p = 0.513$), and the mean VFQ-25 score ($p = 0.223$) and mean palatal frequency remained unchanged.

10.3389/fneur.2022.921341

Conclusion: The long-term use of memantine 20 mg per day in OPT produced a modest and only transient improvement in nystagmus, predominantly along the horizontal plane. Visual acuity improved, albeit without relevant changes in vision-related quality of life.

KEYWORDS

memantine, nystagmus, palatal tremor, oculopalatal tremor, Guillain-Mollaret triangle

Introduction

Oculopalatal tremor (OPT) is a rare and delayed complication of damage to the dentatorubro-olivary pathway—the Guillain and Mollaret's triangle (GMT). It is characterized by the presence of pendular nystagmus (PN), frequently synchronous with palate tremor (PT). Most patients exhibit predominantly vertical PN, accompanied by a variable degree of a horizontal and torsional nystagmus. PN is usually large, fast, irregular, and disconjugate between eyes (1). Jerk nystagmus might accompany PN, possibly due to damage to nearby structures (2). Importantly, patients with OPT-related PN complain of disturbing oscillopsia and decreased visual acuity, with deterioration of vision-specific health-related quality of life (1). PN in OPT has been attributed to an abnormal neuronal firing of the inferior olivary nucleus (ION), further amplified by the cerebellum, due to maladaptive cerebellar learning (2). Hypertrophy and T2 hyperintensity of the ION reflecting trans-synaptic degeneration is classically seen on MRI (3). Moreover, OPT patients also seem to show a deficit in estimating the direction of gravity (i.e., subjective visual vertical, SVV), possibly due to associated dentate nucleus (DN) dysfunction (4).

There is anecdotal data showing that memantine, an N-methyl-D-aspartate (NMDA) receptor antagonist, might reduce PN amplitude, velocity and frequency variability, and improve visual acuity and distance oscillopsia in some but not all patients with OPT-related PN (5–7). An additional increase in PN waveform randomness (i.e., waveform heterogeneity and visible differences in their shapes) may account for the idiosyncratic subjective visual response, often not correlating with an objective reduction of PN (6, 8). Jerk nystagmus has also been shown to improve with memantine (6). Importantly, all the above studies were small (4–6 OPT patients), with a short follow-up (15–21 days), frequently using memantine 40 mg per day, and usually only providing data from the dominant plane of PN (i.e., the plane [horizontal, vertical, or torsional] with the more regular and/or the largest amplitude of eye oscillation in each eye) as an outcome for therapeutic response (5–8). Almost all patients in the above series had at least one side effect while taking memantine 40 mg per day, including lethargy, drowsiness, maniac episode/confusional state, increased emotionality, irritability and anxiety, ataxia, and neuropathic pain (5–8). Therefore, lower doses have been recommended (5).

Given the previously reported disparity between amplitude reduction of the dominant plane of PN and the relatively mild or unpredictable subjective visual improvement in OPT patients, in this work, we asked if there are distinctive effects of memantine on horizontal and vertical components of nystagmus (including PN, and associated jerk nystagmus, if present) in individual patients, which could also help to explain the idiosyncratic subjective visual response seen in OPT (8). In addition, as data are sparse regarding long-term outcomes for memantine response in OPT, we evaluated the effect of memantine 20 mg per day in OPT patients during a 6-month period, focusing on several aspects of the outcome, including nystagmus intensity in each plane, visual acuity, SVV, PT and facial movements frequency, and quality of life measurements.

Methods

Study design and setting, protocol approvals, and patient consents

We conducted a single-center, open-label trial to test the effects of memantine in patients with OPT. The research followed the tenets of the Declaration of Helsinki. The study was approved by our local medical ethical committee, study number 41.2016. All patients were informed about the design and the purpose of the study. Patients provided informed, written consent to the protocol and study procedures.

Participants

We included patients diagnosed with symptomatic OPT at our tertiary referral center. Patients with other ophthalmological disorders that could impair vision, unable to perform video-oculographic assessment, or those with ongoing seizures, severe neurological disability, psychiatric disorder, or other contraindication to memantine therapy, were excluded. Memantine was titrated through a 21-day period to 20 mg/day

and stopped after 6 months. Patients under specific treatment for OPT before the study had to suspend it for at least 6 months before entering the study.

Patients were evaluated at baseline (visit 1, prior to memantine introduction), 2 months (visit 2), and 6 months (visit 3) post-treatment initiation. In each visit, patients underwent a complete neurologic, neuro-ophthalmologic and neuro-otologic exam (only visit 1), video-oculography (VOG), best corrected near visual acuity (BCVA) by using a Rosenbaum Eye Chart scale and then converted into a decimal scale, subjective visual vertical (SVV) assessment, visual function questionnaire (NEI-VFQ-25), and PT and facial movements assessment using video recordings and orbicularis oris/oculis and frontalis muscles electromyography (EMG). In visits 2 and 3, the assessment was performed at least 2 h after drug dosing. Side effects and subjective improvement of oscillopsia were ascertained by direct questioning of the participants. All patients underwent head MRI at the beginning of the study.

Video-oculography

Eye movements were recorded using binocular video-oculography (Interacoustics VO425, Assen, Denmark; 105 Hz). After 5-point calibration, spontaneous nystagmus was assessed while fixating a 1.5-m distance centered target, for 30 s. The patient's head was manually restrained throughout the eye movement recording.

Subjective visual vertical

SVV was assessed through the "bucket test". The examiner rotated a bucket placed near the subject's head, clockwise and anticlockwise for six trials, asking the subject to re-rotate it until he/she perceived that the radiant line displayed inside the bucket was vertical. The angle of deviation was measured by an oscillometer attached on the outside. A mean of the result of six trials was taken as an absolute value (9).

Vision-specific quality of life questionnaire

To evaluate the impact of nystagmus on quality of life, we used the 25-Item National Eye Institute Visual Functioning Questionnaire (NEI-VFQ-25) (10).

Palatal tremor and facial movements

A 30-s videotape of the palatal movements was obtained during each visit. Additionally, when facial muscles other than soft palate/pharynx were also involved, these were electrographically recorded through EMG for 30 s (Nicolet Viking Quest 21.1, Middletown, USA).

MRI

All patients were scanned using a 3T Magnetom Trio scanner (Siemens, Erlangen, Germany). The imaging protocol included at least: (1) high-resolution 3D T1 MPRAGE anatomical sequence; (2) 3 mm-thick axial FLAIR and DP/T2 for evaluation of IO hypertrophy and damage in other components of GMT; and (3) susceptibility-weighted imaging or T2* gradient echo (GRE), since all the patients included in this study had brainstem or cerebellar hemorrhage.

Analysis

VOG horizontal and vertical eye tracings from each eye were analyzed offline with custom software (*http://faculty.washington.edu/jokelly/voganalysis)*. After manual artifact rejection (i.e., blinks, drop-outs, saccades, and erroneous gaze shifts), mean amplitude, velocity, and frequency of nystagmus were computed in a stable baseline tracing (11, 12). The mean velocity was calculated using desaccaded tracings with an array size >2,000 points. The mean amplitude and frequency of nystagmus were calculated manually, by inspecting each cycle of nystagmus. In patients with a jerk form of nystagmus superimposed on the pendular form, amplitude and frequency were calculated separately for each form. As there were no differences when using either form, in the final results, only nystagmus amplitude and frequency data concerning pendular nystagmus are shown. PT frequency was calculated manually from each video. Facial movement frequency was analyzed with EMG built-in software.

For individual analysis of nystagmus, a significant change was defined as a 50% decrease (i.e., improvement) or increase (i.e., worsening) of velocity and/or amplitude between visits (5). For group analysis of nystagmus and other variables, related-samples Friedman test with x^2 test statistics was run to determine whether there were differences in measured scores between baseline, 2 and 6-month visits. *Post hoc* analysis was conducted using the Wilcoxon signed-rank test. Spearman rank correlation coefficient was used to assess the relationships between tested variables at each visit. Statistical analysis was performed using SPSS version 22.0.0 (IBM, Armonk, NY). Differences were considered significant at $p < 0.05$.

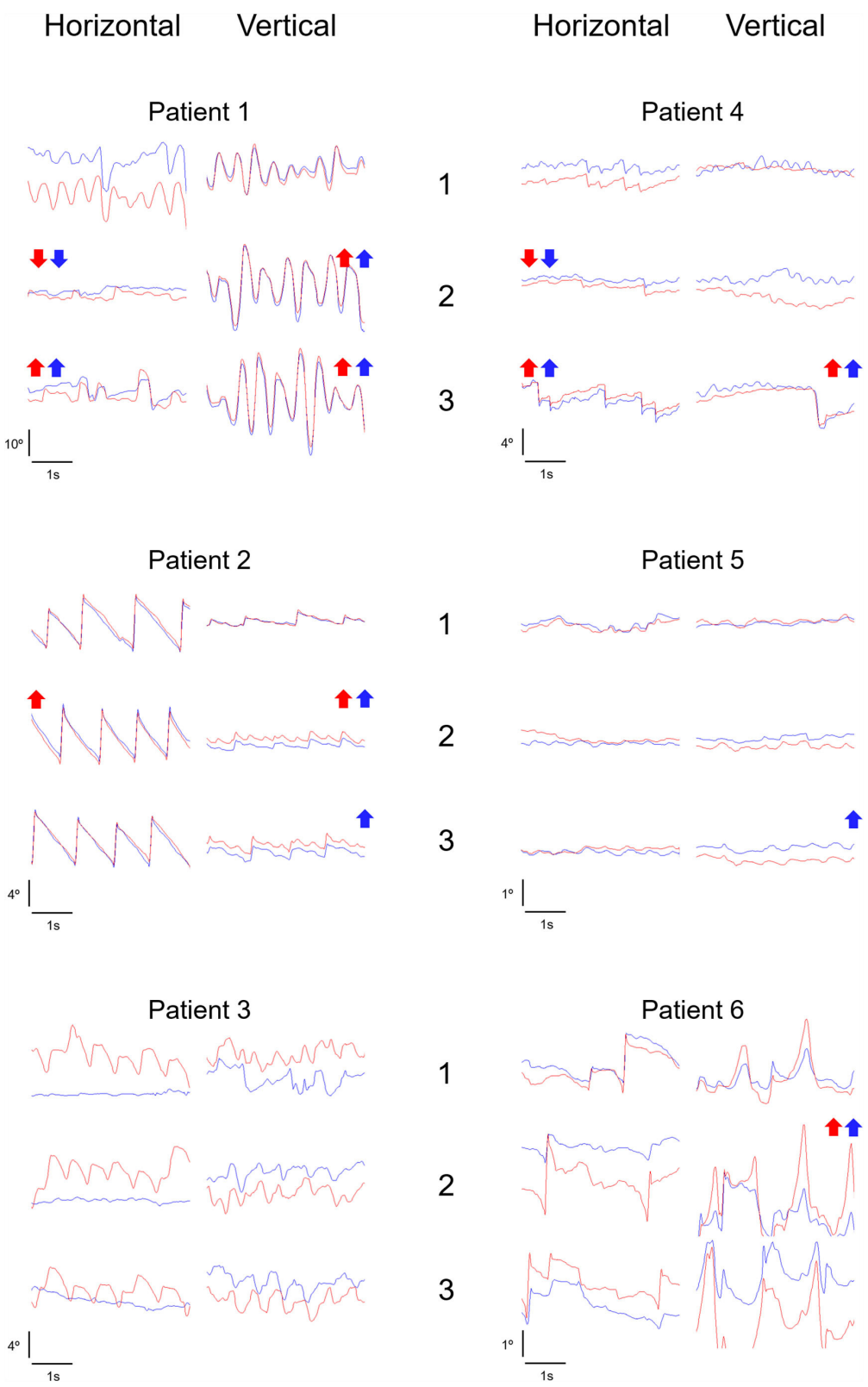

FIGURE 1
Ocular motor data. Nystagmus horizontal and vertical representative tracings in visits 1, 2, and 3 are depicted for each patient. Arrows up represent a >50% increase (i.e., worsening) in amplitude and/or velocity of nystagmus (red arrow, right eye; blue arrow, left eye), relative to the previous visit. Arrows down represent a >50% decrease (i.e., improvement) in amplitude and/or velocity of nystagmus (red arrow, right eye; blue arrow, left eye), relative to the previous visit. Red tracing, right eye. Blue tracing, left eye.

TABLE 1 Demographic and clinical data.

Patient number	Age (years)	Gender	MRI	Disease duration* (months)	Neurological findings	Ocular motor findings
1	66	F	Right pontine hemorrhage (C), right ION hypertrophy and hyperintensity	59	Dysarthria, dysphagia, left hemiparesis and hemiataxia, PT and associated facial movements	Pendular vertical and horizontal OD=OS nystagmus, bilateral INO
2	83	F	Right cerebellar hemorrhage (AVM), bilateral ION hypertrophy and hyperintensity	43	Dysarthria, generalized ataxia, PT and associated facial movements	Pendular vertical and torsional OD>OS nystagmus, jerk right beating nystagmus
3	59	F	Right pontine hemorrhage (C), right ION hypertrophy and hyperintensity	54	Dysarthria, left sensory loss, hemiparesis and hemiataxia, PT and associated facial movements	Pendular vertical OD>OS, torsional OD<OS, horizontal OD nystagmus
4	67	F	Right pontine hemorrhage (H), right ION hypertrophy and hyperintensity	78	Left hemiparesis and hemiataxia, PT	Pendular vertical and torsional OD<OS nystagmus, jerk left beating nystagmus, right one and half syndrome
5	77	M	Right pontine hemorrhage (C), no ION abnormality	36	Generalized ataxia, PT	Pendular vertical and torsional OD>OS nystagmus
6	59	F	Left pontine hemorrhage (C), left ION hypertrophy and hyperintensity	41	Right hemiparesis and hemitremor, PT	Pendular vertical and torsional OD>OS nystagmus, left one and half syndrome

F, Female; M, Male; MRI, Magnetic Resonance Imaging; ION, Inferior Olivary Nucleus; C, Cavernoma; AVM, Arterio-Venous Malformation; H, Hypertension; PT, Palatal Tremor; INO, Internuclear Ophthalmoplegia; OD, Right eye; OS, Left eye.
*Time from hemorrhage to study entrance.

Results

Demographic and clinical data

Six OPT patients reporting oscillopsia were included, mean age 68.5 ± 9.7, range 59–83 years, five females. Two additional patients declined to participate in the study. OPT's causative lesions were either pontine (5) or cerebellar (1) hemorrhages, which occurred with a mean time of 51.5 ± 15.4 months before study entry. All patients had additional ocular motor and/or neurological signs, apart from OPT. PT propagated to facial musculature in 3 patients. Nystagmus was mostly pendular vertical and torsional, and asymmetric between eyes. Associated jerk nystagmus was present in two patients. MRI showed ION hypertrophy and hyperintensity in five patients (unilateral, 4; bilateral, 1). Patients' demographic and clinical data are summarized in Table 1.

Ocular motor data

At baseline (visit 1), the mean vertical velocity and amplitude of nystagmus were 10.3–11.6°/s and 2.0–2.3°, mean horizontal velocity and amplitude of nystagmus were 9.4–13.8°/s and 2.8–3.7°, and mean frequency of nystagmus was 2.3 Hz. After 2 months of memantine intake (visit 2), for the horizontal plane, a 50% improvement of nystagmus velocity and/or amplitude in one or two eyes was seen in two patients, and a >50% worsening nystagmus velocity and/or amplitude in one or two eyes was seen in one patient. In contrast, for the vertical plane, 3 patients demonstrated a 50% worsening of nystagmus velocity and/or amplitude in one or two eyes, while the remaining patients showed no relevant change. After 6 months of memantine intake (visit 3), for the horizontal plane, two patients showed a 50% worsening of nystagmus velocity and/or amplitude in one or two eyes, while in the remaining patients, no relevant change was observed. For the vertical plane, four patients showed a 50% worsening of nystagmus velocity and/or amplitude in one or two eyes, while the remaining evidenced no relevant change. When performing group analysis, the mean vertical velocity and amplitude of the left eye significantly worsened from visit 2 to visit 3 ($p = 0.028$). Nystagmus frequency remained relatively unchanged throughout the study ($p = 0.074$). Ocular motor data is detailed in Figure 1, Table 2.

Visual data

At baseline, mean BCVA was 0.4 and 0.3 in the right and left eye respectively. During the study, there was a significant

TABLE 2 Ocular motor data.

	Plane	Eye	V1	V2	Change V1 vs. V2 (number of patients) (Worsening, improvement)	V3	Change V2 vs. V3 (number of patients) (Worsening, improvement)	*P*	*P* (V1 vs. V2)	*P* (V2 vs. V3)	*P* (V1 vs. V3)
Mean velocity+/-SD (Degrees per second)	Vertical	OS	10.3+/−14.7	14.8+/−24.6	(3,0)	23.1+/−42.7	(3,0)	***0.038***	*0.345*	***0.028***	*0.116*
		OD	11.6+/−17.7	15.0+/−22.0	(2,0)	23.7+/−43.8	(1,0)	*0.247*			
	Horizontal	OS	9.4+/−13.1	4.9+/−5.5	(0,2)	6.9+/−6.8	(2,0)	*0.438*			
		OD	13.8+/−18.2	7.4+/−6.9	(1,2)	8.9+/−8.1	(2,0)	*0.580*			
Mean amplitude+/-SD (Degrees)	Vertical	OS	2.0+/−3.0	3.1+/−5.8	(1,0)	5.4+/−10.7	(3,0)	***0.042***	*0.600*	***0.028***	*0.075*
		OD	2.3+/−3.7	3.2+/−5.3	(3,0)	4.4+/−8.0	(2,0)	*0.607*			
	Horizontal	OS	2.8+/−3.6	1.4+/−2.4	(0,1)	2.0+/−2.5	(2,0)	*0.337*			
		OD	3.7+/−4.1	2.3+/−2.2	(0,1)	5.0+/−7.2	(2,0)	*0.607*			
Frequency+/-SD (Hertz)	Frequency	OU	2.3+/−0.8	2.2+/−0.8	–	2.1+/−0.9	-	*0.074*			

SD, Standard deviation; OS, Left eye; OD, Right eye; V1, Visit 1; V2, Visit 2; V3, Visit 3.
Significant differences are marked in bold.

10.3389/fneur.2022.921341

improvement in BCVA in both eyes ($p = 0.047$, $p = 0.017$). In post analysis, this was most evident for the left eye, between visits 1 and 3 ($p = 0.028$), while a similar trend was observed for the right eye between visits 1 and 2, and 1 and 3. Throughout the study, SVV progression among patients was unpredictable, as reflected in group analysis ($p = 0.513$). Both SVV worsening, improvement, or no relevant change were observed. In two patients there was actually a relevant shift in SVV toward the opposite side (patients 2 and 3) (see Supplementary Table 1 for details). The mean NEI-VFQ-25 score at baseline was 63.8 and there was no significant change during the study ($p = 0.223$). Visual data is detailed in Table 3. Subjective improvement of oscillopsia was reported in three patients (patients 3, 4, and 6) and remained throughout the study.

Tremor data

Mean PT frequency ± SD remained unchanged during the study (Visit 1, 9.8 ± 2.7 Hz; visit 2, 10.3 ± 2.4 Hz; visit 3, 11.0 ± 3.8; $p = 0.568$). Three patients had PT propagation to facial muscles (patients 1, 2, and 3). At baseline, EMG-derived frequency was 2.5 Hz, 3.0 Hz, and 2.0 Hz, respectively, and did not significantly change between visits (data not shown).

Correlations

At baseline, BCVA in both eyes negatively correlated with nystagmus frequency ($r = -0.833$, $p = 0.039$; $r = -0.841$, $p = 0.036$), BCVA in the left eye negatively correlated with a horizontal velocity of nystagmus in the left eye ($r = -0.841$, $p = 0.036$), and NEI-VFQ-25 score negatively correlated with vertical and horizontal velocity ($r = -0.886$, $p = 0.019$; $r = -0.886$, $p = 0.019$) and horizontal amplitude of nystagmus in the right eye ($r = -0.829$, $p = 0.042$). In visit 2, BCVA in the right eye negatively correlated with a horizontal velocity and amplitude of nystagmus in the right eye ($r = -0.820$, $p = 0.046$; $r = -0.820$, $p = 0.046$), BCVA in the left eye negatively correlated with a horizontal velocity and amplitude of nystagmus in the left eye ($r = -0.899$, $p = 0.015$; $r = -0.812$, $p = 0.049$), and NEI-VFQ-25 score negatively correlated with a horizontal velocity of nystagmus in the left eye ($r = -0.886$, $p = 0.019$) and positively correlated with BCVA in both eyes ($r = 0.880$, $p = 0.021$; $r = 0.928$, $p = 0.008$). Finally, at visit 3, BCVA in the right eye negatively correlated with a horizontal velocity of nystagmus in the right eye ($r = -0.883$, $p = 0.020$), BCVA in the left eye negatively correlated with a horizontal velocity and amplitude of nystagmus in the left eye ($r = -0.928$, $p = 0.008$; $r = -0.899$, $p = 0.015$), and NEI-VFQ-25 score negatively correlated with a horizontal and vertical velocity of nystagmus in both eyes ($r = -0.943$, $p = 0.005$; $r = -0.829$, $p = 0.042$; $r = -0.829$, $p = 0.042$; $r = -0.829$, $p = 0.042$) and a horizontal amplitude of nystagmus in the right eye ($r = -0.886$, $p = 0.019$). The 3 patients who reported subjective improvement of oscillopsia showed disparate outcomes in terms of BCVA, nystagmus parameters, and NEI-VFQ-25 score.

Memantine 20 mg per day was generally well tolerated, with only one patient reporting transient drowsiness at the beginning of the treatment.

Discussion

We studied the effectiveness of memantine 20 mg per day for 6 months in OPT patients, focusing on the detection of putative distinctive effects on horizontal and vertical components of nystagmus, which could further help to explain the idiosyncratic subjective visual response previously seen in OPT patients. Importantly, we also aimed to ascertain if the effect of memantine on nystagmus and associated phenomena, including visual acuity, quality of life, estimation of gravity, and palatal/facial movements, was sustained over a period of 6 months.

Indeed, after 2 months, memantine improved the velocity and/or amplitude of nystagmus, but *only* along the horizontal plane, and just in two patients, while the vertical component worsened in four patients. At 6 months, improvement of nystagmus along the horizontal plane was not sustained in the two patients previously showing improvement, and there was an overall worsening of both horizontal and vertical amplitude and/or velocity of nystagmus at the group level. In contrast, visual acuity significantly improved throughout the study. Still, vision-targeted, health-related quality of life remained unchanged. Moreover, despite the apparent discrepancies in the long term between nystagmus intensity, visual acuity, and quality of life, the above parameters tended to correlate with each other at each visit. Oscillopsia improvement could not be consistently correlated with any of the above parameters. Finally, nystagmus frequency, gravity estimation, and palate tremor frequency did not seem to be influenced by memantine.

PN in OPT is thought to be due to a synchronized discharge of ION neurons. Further maladaptive learning by the cerebellar cortex is believed to amplify PN amplitude and frequency irregularity. The blockade of NMDA receptors by memantine seems to exert its major effect in the cerebellum, at the projections of the ION to the deep cerebellar nuclei, of the climbing fibers to the Purkinje neurons, and/or those of the parallel fibers onto the Purkinje neurons, ultimately leading to decreased Purkinje cells/cerebellar output (2, 13). This might explain why memantine in our and others' work was able to reduce PN amplitude and/or velocity but not its fundamental frequency (5–7). Specifically, PN amplitude seems to be a direct product of cerebellar output, while PN frequency is believed to be set by the intrinsic properties of the ION neurons the latter feature probably less amenable to memantine's effect (a similar

TABLE 3 Visual data.

	Eye	V1	V2	V3	*P*	P (V1 vs. V2)	P (V2 vs. V3)	P (V1 vs. V3)
Mean visual acuity +/−SD (Decimal scale)	OD	0.4+/−0.1	0.6+/−0.2	0.6+/−0.3	***0.047***	*0.067*	*0.593*	*0.065*
	OS	0.3+/−0.1	0.5+/−0.2	0.6+/−0.3	***0.017***	*0.109*	*0.225*	***0.028***
Mean subjective visual vertical+/−SD (Degrees*)	OU	6.6+/−5.3	5.2+/−2.8	5.4+/−4.0	*0.513*			
Mean NEI−VFQ−25 score+/−SD		63.8+/−22.7	66.7+/−18.2	71.4+/−19.1	*0.223*			

SD, Standard Deviation; OS, Left eye; OD, Right eye; NEI-VFQ-25, 25-Item National Eye Institute Visual Functioning Questionnaire; V1, Visit 1; V2, Visit 2; V3, Visit 3.
*Torsional degrees away from 0, regardless of the direction of deviation (i.e., clockwise or counter-clockwise).
Significant differences are marked in bold.

conclusion may be drawn for the pathogenesis of palatal tremor frequency, which was also unaffected by memantine) (7). However, in our study, the improvement in nystagmus velocity and/or amplitude seemed to be distinct for the horizontal and vertical planes of nystagmus since the improvement was only seen along the horizontal plane and never along the vertical. Albeit rarely the focus of analysis in OPT-related nystagmus, there has been anecdotal data showing that responses to memantine might in fact be distinct between the horizontal, vertical, and torsional planes of PN. Specifically, the frequency irregularity of PN seems to improve in general with the use of memantine, but not along the horizontal plane (7). We hypothesize that memantine in our and others' cases might have exerted its action predominantly on projections from ION to the deep cerebellar nuclei carrying signals from independent olivary generators, giving rise exclusively to horizontal eye movements while showing less or no influence on projections signaling vertical and torsional eye movements (2). Whether such selective effect of memantine on fibers carrying signals for horizontal eye movements could be dosage-dependent, i.e., particularly seen when using lower dosages of memantine is highly speculative and lacks clinical and experimental evidence. Another non-mutually exclusive explanation for distinct/opposite responses to memantine depending on nystagmus plane is an increase in the nystagmus waveform randomness (i.e., nystagmus waveform shape from trial to trial) after memantine use, which might influence final/mean nystagmus velocity/amplitude waveform in different planes (8). Importantly, one cannot exclude that, particularly in patients with mild nystagmus, the aforementioned changes in nystagmus over time might reflect natural fluctuations. Still, if any improvement can be associated with the use of memantine, this was only seen for the horizontal plane, and it was not sustained, only being observed transiently.

While near visual acuity subjectively improved throughout the study, vision-related quality of life remained unchanged. This is in agreement with previous data (5). This finding either suggests that the amount of amplitude reduction of nystagmus was not adequate to provide a benefit in the visual quality of life, or other factors, besides visual acuity, might influence the overall visual function of OPT patients. Such factors might include memantine's "unwanted" effect on the PN waveform randomness (i.e., increase in waveform shape heterogeneity), coexisting ocular motor deficits also impairing vision (e.g., internuclear ophthalmoplegia, gaze palsies, vestibular deficits, etc.), and/or the presence of distinct/opposite effects of memantine on OPT-related nystagmus planes (i.e., horizontal, vertical and/or torsional) as shown in the present study (5, 7, 8). In addition, it must also be stressed that while NEI-VFQ-25 has been used before to evaluate OPT patients, this tool has not been specifically designed to assess the functional consequences of nystagmus (5). Still, the NEI-VFQ-25 global score correlated with visual acuity in one or both eyes at specific timepoints in our study, suggesting a weak, but nevertheless real association between both. Indeed, our results are in agreement with previous work showing improvement of visual acuity in OPT patients after memantine. Distance visual acuity has been previously shown to modestly improve in 6 out of 11 eyes after 2 weeks of memantine 40 g per day (6, 8). In another study using a similar protocol, only near visual acuity improved on memantine (5). Importantly, in our study, near visual acuity correlated with nystagmus parameters at specific timepoints. This finding emphasizes that nystagmus intensity by itself seems to directly impair vision in OPT (5). Other factors which might also be influencing visual acuity outcomes in the current work include improvement of torsional

velocity/amplitude of nystagmus (which was not quantitatively measured), and patient's level of cooperation and/or learning effects throughout the study. Oscillopsia improved in half of our patients. Previously, oscillopsia was either unchanged or modestly improved in 4 OPT patients (6). Importantly, in another study, this effect was only observed for distance oscillopsia (5). As we did not perform a separate assessment for distance and near oscillopsia, further interpretation of our results is precluded.

Taking into account the side effects/tolerability profile of memantine 40 mg per day, the dosage of 20 mg per day was chosen for the current study (6). Indeed, memantine 40 mg per day has been discontinued in 18.8% of patients in one study, reduced to 20 mg per day in one patient in another study, and voluntarily stopped or reduced by all OPT patients once the above studies ended (5, 6). Rather expectedly, using half of the dosage, only one patient reported mild imbalance in our study, which was nevertheless tolerated. The use of a smaller dosage could eventually explain the lack of benefit in nystagmus parameters in some of our patients, but the memantine-related improvement on OPT-related nystagmus has nevertheless been demonstrated when using the dosage of 20 mg per day for 2 weeks (6). Still, our results are difficult to compare with those from previous studies, due to our particularly long study duration, i.e., 6 months, vs. <1 month in previous works (5–7). This is actually one of the main strengths of our study. Such a long duration allowed us to demonstrate that any potential benefit on nystagmus intensity seen early on in the study was not relevantly sustained over time, thus providing important data concerning the long-term management of OPT patients.

Finally, gravity perception has been seldomly investigated in OPT patients (4). In our work, SVV deviations were pathological in five patients and further evidenced significant shifts over time in two patients. The above findings seem to reflect the simultaneous contribution of co-existent lesions affecting the vestibular graviceptive pathways and an over-excitation of the dentate nucleus due to a lack of ION inhibition (4). Not surprisingly, memantine showed no relevant effect on SVV, since none of the aforementioned mechanisms seem to be strongly dependent on NMDA receptor-related modulation (4).

There are several limitations to the current study. Apart from the limited size of the sample reflecting the rarity of OPT, further analyses on nystagmus frequency irregularity, conjugacy, waveform randomness, and assessment of distance visual acuity were not performed and could have provided further insight. Similarly, while the torsional component of nystagmus did not seem to relevantly change before and after treatment in any patient (data not shown), quantitative analysis of the torsional plane of nystagmus was not performed. Additionally, the lack of a placebo treatment design in the current study did not allow us to control and evaluate the magnitude of a potential placebo effect and/or normal nystagmus fluctuation over time in our results (14). This issue becomes particularly relevant in patients whose nystagmus was mild, where minor changes might naturally occur over time.

We conclude that the use of memantine 20 mg per day for 6 months in our OPT patients showed a modest improvement in nystagmus horizontal amplitude and velocity, which was not sustained over time. Although there was a sustained improvement in visual acuity, vision-related quality of life remained unchanged. A long-term (e.g., 6 months) placebo-controlled trial using different dosages of memantine (e.g., 20 and 40 mg), including analyses of nystagmus in each plane and waveform randomness, and assessments of near and distance visual acuity, near and distance oscillopsia, and quality of life as main outcomes, in a larger sample of patients, is needed to further elucidate the role of memantine in OPT.

Data availability statement

The raw data supporting the conclusions of this article will be made available by the authors, without undue reservation.

Ethics statement

The studies involving human participants were reviewed and approved by Comissão de Ética para a Saúde. The patients/participants provided their written informed consent to participate in this study. Written informed consent was obtained from the individual(s) for the publication of any potentially identifiable images or data included in this article.

Author contributions

AIM and RS contributed to the acquisition, analysis and interpretation of the data, and drafting of the manuscript. AJ, CD, CF, and JS-F contributed to the acquisition, analysis, and interpretation of the data. DP, LN, and AM contributed to the acquisition, analysis, interpretation of the data, and study concept and design. JL contributed to the acquisition, analysis, interpretation of the data, study supervision, concept, design, and critical revision of manuscript for intellectual content. All authors contributed to the article and approved the submitted version.

Conflict of interest

The authors declare that the research was conducted in the absence of any commercial or financial relationships that could be construed as a potential conflict of interest.

Publisher's note

All claims expressed in this article are solely those of the authors and do not necessarily represent those of their affiliated organizations, or those of the publisher, the editors and the reviewers. Any product that may be evaluated in this article, or claim that may be made by its manufacturer, is not guaranteed or endorsed by the publisher.

Supplementary material

The Supplementary Material for this article can be found online at: https://www.frontiersin.org/articles/10.3389/fneur.2022.921341/full#supplementary-material

References

1. Tilikete C, Desestret V. Hypertrophic olivary degeneration and palatal or oculopalatal tremor. *Front Neurol.* (2017) 8:302. doi: 10.3389/fneur.2017.00302

2. Shaikh AG, Hong S, Liao K, Tian J, Solomon D, Zee DS, et al. Oculopalatal tremor explained by a model of inferior olivary hypertrophy and cerebellar plasticity. *Brain.* (2010) 133:923–40. doi: 10.1093/brain/awp323

3. Goyal M, Versnick E, Tuite P, Cyr JS, Kucharczyk W, Montanera W, et al. Hypertrophic olivary degeneration: metaanalysis of the temporal evolution of MR findings. *Am J Neuroradiol.* (2000). 21:1073–7.

4. Tarnutzer AA, Palla A, Marti S, Schuknecht B, Straumann D. Hypertrophy of the inferior olivary nucleus impacts perception of gravity. *Front Neurol.* (2012). 3:79. doi: 10.3389/fneur.2012.00079

5. Nerrant E, Abouaf L, Pollet-Villard F, Vie A, Vukusic S, Berthiller J, et al. Gabapentin and memantine for treatment of acquired pendular nystagmus: effects on visual outcomes. *J Neuroophthalmol.* (2020) 40:198–206. doi: 10.1097/WNO.0000000000000807

6. Thurtell MJ., Joshi AC, Leone AC, Tomsak RL, Kosmorsky GS, Stahl JS, et al. Crossover trial of gabapentin and memantine as treatment for acquired nystagmus. *Ann Neurol.* (2010) 67:676–80. doi: 10.1002/ana.21991

7. Shaikh AG, Thurtell MJ, Optican LM, Leigh RJ. Pharmacological tests of hypotheses for acquired pendular nystagmus. (2011) 1233:320–6. doi: 10.1111/j.1749-6632.2011.06118.x

8. Theeranaew W, Thurtell MJ, Loparo K, Shaikh AG. Gabapentin and memantine increases randomness of oscillatory waveform in ocular palatal tremor. *J Comput Neurosci.* (2020) 49:319–31. doi: 10.1007/s10827-020-00753-6

9. Zwergal A, Rettinger N, Frenzel C, Dieterich M, Brandt T, Strupp M. A bucket of static vestibular function. *Neurology.* (2009) 72:1689–92. doi: 10.1212/WNL.0b013e3181a55ecf

10. Das A, Quartilho A, Xing W, Bunce C, Rubin G, MacKenzie K, et al. Visual functioning in adults with Idiopathic Infantile Nystagmus Syndrome (IINS). *Strabismus.* (2018) 26:203–9. doi: 10.1080/09273972.2018.1526958

11. Kelly JP, Phillips JO, Weiss AH. Does eye velocity due to infantile nystagmus deprive visual acuity development? *J AAPOS.* (2018) 22:50–55.e1. doi: 10.1016/j.jaapos.2017.10.008

12. Kori AA, Robin NH, Jacobs JB, Erchul DM, Zaidat OO, Remler BF, et al. Pendular nystagmus in patients with peroxisomal assembly disorder. *Arch Neurol.* (1998) 55:554–8. doi: 10.1001/archneur.55.4.554

13. Strupp M, Thurtell MJ, Shaikh AG, Brandt T, Zee DS, Leigh RJ, et al. Pharmacotherapy of vestibular and ocular motor disorders, including nystagmus. *J Neurol.* (2011) 258:1207–22. doi: 10.1007/s00415-011-5999-8

14. Theeranaew W, Kim HJ, Loparo K, Kim JS, Shaikh AG. Hyperventilation Increases the Randomness of Ocular Palatal Tremor Waveforms. *Cerebellum.* (2021) 20:780–7. doi: 10.1007/s12311-020-01171-1

frontiers | Frontiers in Neurology

TYPE Original Research
PUBLISHED 01 September 2022
DOI 10.3389/fneur.2022.857133

OPEN ACCESS

EDITED BY
Ji Soo Kim,
Seoul National University, South Korea

REVIEWED BY
Bernardo Faria Ramos,
Universidade Federal do Espírito Santo, Brazil
Seong-Joon Lee,
Ajou University, South Korea

*CORRESPONDENCE
Ke-Hang Xie
kehan826@126.com

†These authors have contributed equally to this work

SPECIALTY SECTION
This article was submitted to Neuro-Otology, a section of the journal Frontiers in Neurology

RECEIVED 18 January 2022
ACCEPTED 30 May 2022
PUBLISHED 01 September 2022

CITATION
Xie K-H, Chen L-C, Liu L-L, Su C-Y, Li H, Liu R-N, Chen Q-Q, He J-S, Ruan Y-K and He W-K (2022) Elevated red cell distribution width predicts residual dizziness in patients with benign paroxysmal positional vertigo. *Front. Neurol.* 13:857133. doi: 10.3389/fneur.2022.857133

Elevated red cell distribution width predicts residual dizziness in patients with benign paroxysmal positional vertigo

Ke-Hang Xie[1*†], Li-Chun Chen[2†], Ling-Ling Liu[3†], Chu-Yin Su[4], Hua Li[4], Run-Ni Liu[4], Qing-Qing Chen[4], Jia-Sheng He[4], Yong-Kun Ruan[4] and Wang-Kai He[4]

[1]Department of Neurology, Zhuhai Hospital of Integrated Traditional Chinese and Western Medicine, Zhuhai, China, [2]Department of Encephalopathy, Shantou Hospital of Traditional Chinese Medicine, Shantou, China, [3]Department of Nephrology, The Fifth Affiliated Hospital of Sun Yat-sen University, Zhuhai, China, [4]Department of Neurology, Zhuhai Hospital of Integrated Traditional Chinese and Western Medicine, Zhuhai, China

Objective: The present study aimed to determine whether residual dizziness (RD) after successful repositioning treatment in benign paroxysmal positional vertigo (BPPV) patients could be predicted by red blood cell distribution width (RDW).

Materials and methods: In this study, a total of 303 BBPV patients hospitalized at the neurology department were investigated. The enrolled patients were divided into two groups after successful repositioning treatment: non-RD group included patients who were completely cured, and RD group included patients with RD. We collected data on all subjects, including general information, blood routine examination, blood biochemical examination, and magnetic resonance imaging tests.

Results: The mean RDW values of patients in the RD group were significantly higher than that in the non-RD group (13.63 ± 1.8 vs. 12.5 ± 0.8; $p < 0.001$). In subsequent multivariate analysis, elevated RDW levels were a statistically significant risk factor associated with the occurrence of RD [odds ratio = 2.62, 95% confidence interval (CI) 1.88–3.64, $p < 0.001$]. The area under the ROC curve was 0.723 in terms of its predictive ability to distinguish patients with RD. A cut-off point of 12.95% of RDW predicted RD with a sensitivity of 75.6% and a specificity of 69.5%. Moreover, the AUC for the ability of the RDW to predict recurrence were 0.692 (95% CI = 0.561–0.831; $p < 0.014$).

Conclusions: Elevated RDW level was related to increased risk of RD among BPPV patients, requiring further efforts to clarify the actual underlying pathophysiology.

KEYWORDS

residual dizziness, benign paroxysmal positional vertigo, red cell distribution width, oxidative stress, inflammation

Introduction

Up to 31%∼61% of benign paroxysmal positional vertigo (BPPV) patients suffered from residual dizziness (RD) in the first few days or weeks after successful canalith repositioning procedures (CRPs) (1, 2). Characterized by dizziness, balance disorders, or unsteadiness, RD could seriously affect older adults' gait and balance and increase their risk of falling and consequent injuries (3).

The exact pathophysiology of RD remains controversial (4–7). Oxidative stress (OS) is known to play an important role in several inner ear diseases (8–10). Previous studies have shown that BPPV patients suffered from higher levels of OS than healthy groups (11). In addition, after complete recovery of BPPV symptoms, the index of the OS status decreased significantly (12). Therefore, it can be inferred that the reduction of OS in patients with BPPV after treatment is parallel to symptomatic relief. Whether there is a difference in OS status between RD and non-RD after treatment in BPPV patients has rarely been studied.

The red cell distribution width (RDW) is a biochemical parameter representing the variability in size of circulating red blood cells, which is considered as an informative clinical marker outside of anemia assessment in routine practice (13). Elevated RDW is associated with the occurrence, development, and prognosis of central nervous system diseases (14–16). OS and subsequent subclinical inflammation may be important pathophysiological mechanisms of this clinical phenomenon as increased RDW comprehensively represents a higher level of OS damage (17, 18). Recent experimental evidence has shown that the vestibular system is very sensitive to oxidative damage (12, 19). Therefore, it is compelling to speculate that the alteration of RDW level may be a predictive indicator of RD in BPPV patients. As far as we know, no study has focused on the relationship between RDW and RD.

In this study, we aimed to investigate whether RDW value was helpful in the prediction of RD after successful CRPs in patients with BPPV.

Materials and methods

Participants

Thorough history, neurological, and magnetic resonance imaging (MRI) examinations were performed on all BPPV patients at the neurology department of Zhuhai Hospital of Integrated Traditional Chinese and Western Medicine between December 2014 and December 2020. In this study, only patients with posterior semicircular canal lithiasis (PSC-BPPV) were included and treated with the Epley maneuver. For patients with severe cervical spondylosis or obesity, which could not be coordinated with Epley's maneuver, Semont maneuver was used for reduction.

All patients underwent a bedside neurological assessment, including examination of a mixed torsional and upward beating nystagmus during the Dix-Hallpike position, vestibulo-ocular reflex, and optokinetic and balance tests (20). During the evaluation period, the patients also underwent diagnostic location testing for BPPV assessment. On the second week following successful CRPs, the enrolled patients were subsequently divided into two groups (based on the results of the second Dix-Hallpike test): non-RD group included 509 patients without any dizziness, and RD group included 186 patients with persistent and non-positional atypical dizziness (absence of true positional vertigo and nystagmus). The characteristics of nystagmus in the enrolled patients were observed and recorded by Danish Vestibular nystagmus view analyzer VN415/VO425. In addition, the observation of nystagmus was performed with the patient wearing a blindfold and in a dark room to eliminate the effects of fixation suppression.

Participants also had to meet the following inclusion criteria: (1) no central diseases (including central vertigo), cranial traumas, or stroke; (2) no anemia, immunologic diseases erythrocytosis, cancer, infection, severe cardiovascular disease, and hepatic or renal impairment.

In total, 101 RD subjects (RD group) and 202 age- and sex-matched BPPV patients (non-RD group) were enrolled in the study (Figure 1). We followed the recurrence rate of the enrolled patients at 1, 3, and 6 months. We determined whether there was a recurrence by examining the patient's medical record and confirming the patient's symptoms over the phone.

Measures

All patients presented to the emergency room with fasting blood collection within 48 h of vertigo. Complete blood counts were determined using the ethylenediaminetetraacetic acid blood sample method on a Toshiba analyzer (Hitachi High Technologies Corporation, Tokyo, Japan). RDW-CV value was calculated as follows: RDW – CV = [red blood cell (RBC) volume standard deviation/average RBC volume] × 100 (13). The normal reference range for RDW in this study was between 11 and 14%. This study reported RDW-CV and denoted RDW.

Meanwhile, serum C-reactive protein (CRP), homocysteine (HCY), albumin (ALB), total bilirubin (TB) levels, alanine aminotransferase (ALT), fasting blood glucose (FBG), uric acid (UA), and creatinine (CRE) were measured by a Hitachi LST008 Analyzer (Hitachi High-Tech, Tokyo, Japan). The values of total cholesterol (TC), triglycerides (TG), high-density lipoprotein cholesterol (HDL), and low-density lipoprotein cholesterol (LDL) were measured with the same analyzer. In addition, fibrinogen (FIB) was measured using an automated coagulation analyzer (ACL-TOP-700, Wolfen, Spain).

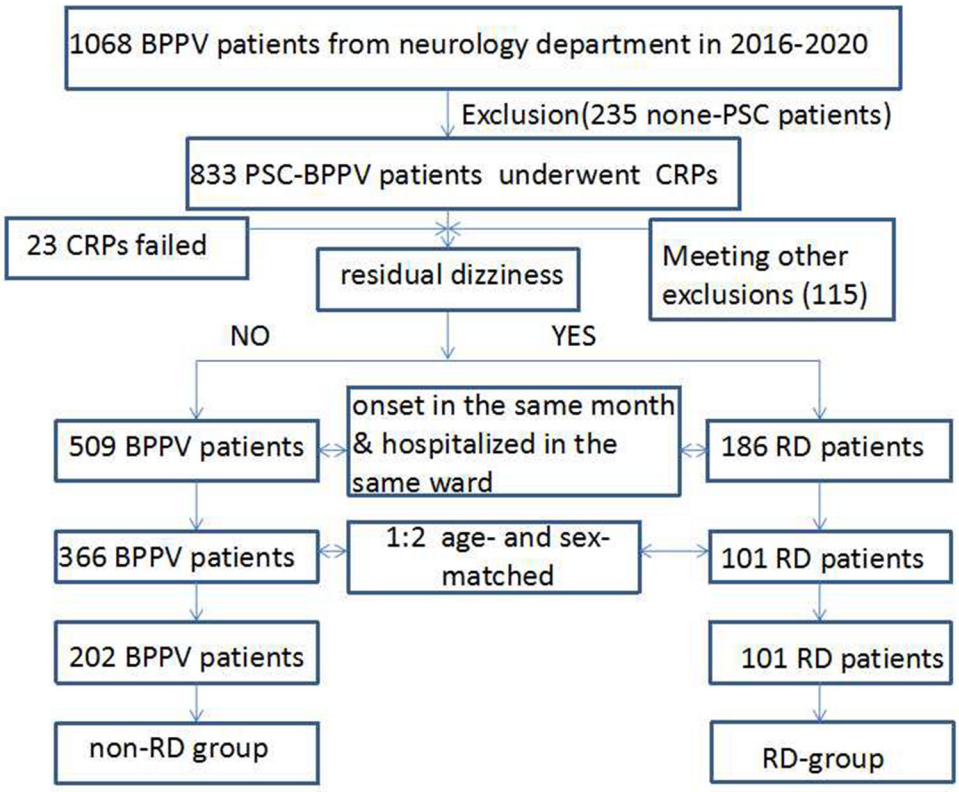

FIGURE 1
Flow chart for patient enrollment of the retrospective cohort study.

Statistical analysis

Statistical Package for the Social Sciences (SPSS) for Windows (version 24.0. Chicago, IL) was used to describe the enumeration data by the number of cases (constituent ratio); the measurement data was described by the mean ± standard deviation ($x \pm s$). Count data were analyzed by chi-square test or Fisher exact test; normally distributed measurement data were analyzed by variance analysis; non-normally distributed data of multiple independent samples were analyzed by Kruskal–Wallis test, and non-normally distributed data of two independent samples were analyzed by Mann–Whitney test. Pearson method was used for correlation analysis of normal distribution materials, and the Spearman method was used for correlation analysis of non-normal distribution materials. Variables with $p < 0.05$ in Table 1 were entered into a forward logistic regression model to identify risk factors for developing RD after BPPV. Results were shown as adjusted ORs (odds ratios) and corresponding 95% confidence intervals (CIs). Receiver operating characteristic (ROC) curve analysis was used to evaluate the ability of RDW to predict RD. The optimal diagnostic cutoff point for RDW was recorded when the Youden index was maximal, and the sensitivity and specificity were calculated separately. Statistical significance was set at $p < 0.05$.

Ethical considerations

The data and samples analyzed in this study were obtained according to the standards and approval of the Ethics Committee of Zhuhai Hospital of Integrated Traditional Chinese and Western Medicine. Because this study was retrospective and all patient data were analyzed anonymously, the Ethics Committee waived the informed consent of the participants.

Results

General statistics

Comparative analysis of clinical characteristics of RD and non-RD patients is shown in Table 1. In terms of personal medical history, there were no differences between

the two groups in alcohol consumption, smoking habit, and hypertension ($p = 0.912$, 0.236, and 0.226, respectively). No differences were observed with respect to BMI, blood pressure, RBC, HGB, PLT, ALT, TG, TC, LDL, HDL, or FIB (all $p > 0.05$). RD group had more diabetes and higher fasting blood glucose (FBG) than the non-RD group ($p = 0.002$ and $p < 0.001$, respectively). Regarding the duration of symptoms, the RD group had a longer time from onset to treatment (20.04 $\pm$ 22.33 vs. 21.00 $\pm$ 21.15, p =0.116). There was a significant difference in the recurrence between RD and non-RD groups ($p < 0.001$). Compared with the non-RD group, the number of CRPs was significantly higher ($p < 0.001$) in the RD group.

OS and inflammatory markers

Higher levels of OS and inflammatory markers in RD patients compared to non-RD patients ($p < 0.001$). Serum levels of UA, TB, ALB, and CRE in patients with RD were lower than those in the non-RD group (all $p < 0.05$), indicating a lower antioxidant status at hospital admission (11). In terms of non-specific inflammatory markers, RD patients had higher levels of N/L and CRP ($p = 0.006$ and 0.003, respectively).

Spearman's correlation analysis about OS and inflammatory markers

Figure 2 shows the results of Spearman's correlation between OS and inflammatory markers and RD in BPPV patients. RDW was positively correlated with CRP and negatively correlated with CRE (both $p < 0.05$). However, RDW had no correlation with ALB, TB, UA, or N/L (all $p > 0.05$).

The relationship between RDW value and the number of CRPs

The effects of RDW on the number of CRPs between the non-RD and RD group were determined. The results showed significant differences in serum RDW levels between the number of CRPs in both inter-group and intra-group comparisons (all $p < 0.05$). In all, our results showed the number of CRPs in both groups increased with RDW values (Table 2, Figure 3A).

The relationship between RDW value and recurrence of BPPV in 6 months of follow-up

By categorizing the time of recurrence, it can be concluded that the higher the baseline RDW, the earlier the recurrence onset (although not all $p < 0.05$; Table 2, Figure 3B).

TABLE 1 The clinical characteristics of the study samples.

Characteristics	None-RD ($n = 202$)	RD ($n = 101$)	p-Value
Age (years), mean (SD)	58.34 (10.06)	58.34 (10.06)	—
Male, *n* (%)	116 (58)	58 (58)	—
Alcohol consumption, *n* (%)	33 (17)	16 (16)	0.912
Current smoking, *n* (%)	76 (38)	33 (33)	0.236
Hypertension, *n* (%)	64 (32)	27 (27)	0.226
Diabetes mellitus, *n* (%)	42 (21)	38 (38)	0.002*
BMI, mean (SD)	24.29 (3.42)	24.27 (3.14)	0.862
SBP (mm Hg), mean (SD)	136.56 (21.99)	134.80 (22.33)	0.360
DBP (mm Hg), mean (SD)	83.60 (12.66)	85.21 (13.52)	0.533
WBC (10^9/Ul), mean (SD)	7.16 (2.05)	7.50 (1.98)	0.088
N/L, median (IQR)	2.59 (2.43)	2.71 (1.48)	0.006**
HGB (10^9/L), mean (SD)	140.90 (13.49)	142.26 (15.63)	0.464
RBC(10^9/L), mean (SD)	4.68 (0.56)	4.74 (0.47)	0.073
RDW (%) median (IQR)	12.51 (0.78)	13.63 (1.75)	0.000 ***
PLT (10^9 /L), mean (SD)	233.37 (54.72)	236.17 (61.27)	0.615
ALT (U/L), median (IQR)	20.55 (9.88)	20.51 (9.63)	0.877
TB (μmol/L), median (IQR)	13.74 (5.97)	12.19 (4.76)	0.028*
CR (μmol/L), median (IQR)	71.93 (16.60)	67.31 (16.26)	0.016
CRP (mg/L) median (IQR)	4.63 (3.80)	5.96 (3.62)	0.003**
FIB (g/L), median (IQR)	2.64 (0.72)	2.79 (0.79)	0.126
ALB (g/L), median (IQR)	42.11 (3.06)	40.85 (3.08)	0.001 ***
UA (μmol/L), median (IQR)	375.03 (100.88)	351.69 (92.90)	0.043
TG (mmol/L), mean (SD)	1.54 (0.76)	1.66 (0.87)	0.212
TC (mmol/L), mean (SD)	4.99 (1.06)	5.08 (1.18)	0.741
LDL (mmol/L), mean (SD)	3.06 (0.90)	3.20 (1.04)	0.379
HDL (mmol/L), mean (SD)	1.28 (0.27)	1.25 (0.27)	0.190
FBG (mmol/L), mean (SD)	7.27 (3.00)	8 (1.79)	0.000***
Time from onset to hospital (h), median (IQR)	20.04 (22.33)	21.00 (21.15)	0.116
6-month recurrence rate, *n* (%) mean (SD)	32 (16)	38 (38)	0.000***
Number of CRPs, median (IQR)	1 (1–5)	2 (1–5)	0.000***
Medication history			
Antihypertensive therapy, *n* (%)	52 (81)	23 (85)	0.452
Antiglycemic therapy, *n* (%)	26 (62)	15 (40)	0.037*

BMI, body mass index, defined as weight in kilograms divided by the square of height in meters; SBP, systolic blood pressure; DBP, diastolic blood pressure; WBC, white blood cells; N/L :Neutrophilic /lymphocytes; HGB, hemoglobin; RBC, red blood cell; RDW, red blood cell distribution width; PLT, blood platelet; ALT, alanine transaminase; TB, total bilirubin; CR, creatinine; CRP, c reactive protein; FIB, fibrinogen; ALB, albumin; UA, uric acid; TG, triglyceride; TC, total cholesterol; LDL, low-density lipoprotein cholesterol; HDL, high-density lipoprotein cholesterol; FBG, fasting blood-glucose.
The differences were considered significant if p-value < 0.05.
***p-value < 0.001.
**p-value < 0.01.
*p-value < 0.05.

Multivariate analysis

In the multivariate analysis (Table 3), elevated RDW levels was demonstrated as an independent risk factor which may

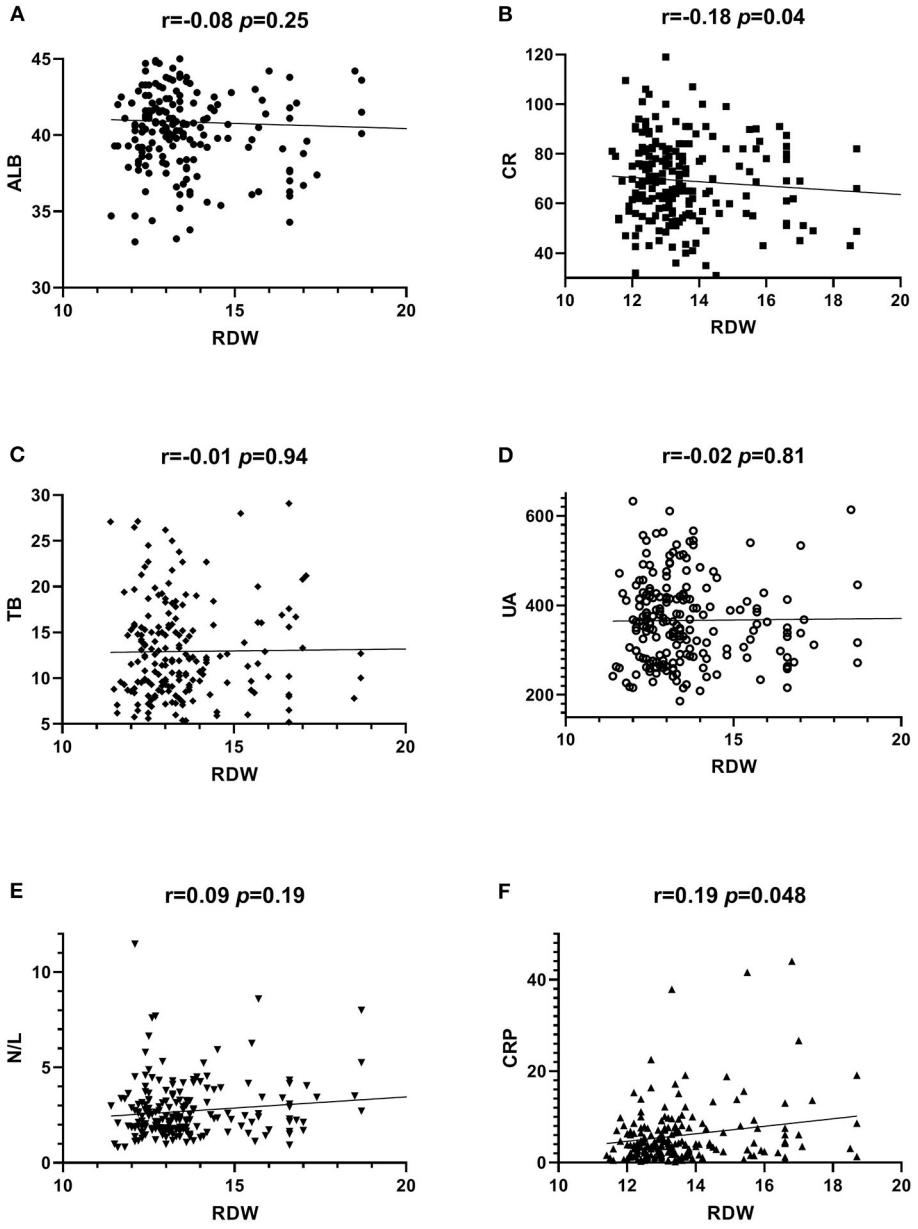

FIGURE 2
Correlation between serum RDW level and ALB, CR, TB, UA, CRP and N/L in RD patients.

predict prognosis for patients with RD (OR = 2.62; 95% CI, 1.88–3.64; $p < 0.001$).

ROC analyses

According to the ROC curve analysis, the optimal cutoff value of the RDW that best distinguished the presence of RD was 12.95%. The area under the curve (AUCs) for the ability of the RDW to predict RD was 0.723 with 75.6% sensitivity and 69.5% specificity, respectively. The AUC for the ability of the RDW to predict recurrence was 0.692 (95% CI = 0.561–0.831; $p < 0.014$), and the optimal cutoff value was 13.45% (Figure 4)

Discussion

Our results suggested that (1) RDW was significantly higher in the RD group than in non-RD group, (2) RDW was independently associated with RD-causing 2.62-fold risk increase for every one unit increase in RDW value, (3) a cutoff

TABLE 2 The relationship between RDW value and number of CRPs, and recurrence of BPPV in 6 months of follow-up.

	Non-RD group	RD group	*p*-Value
The number of CRPs			
1 median (SD)	12.79 (0.69)	13.18 (1.17)	0.045*
>1–≤3 median (SD)	13.25 (0.62)	13.82 (1.94)	0.031*
>3–≤5 median (SD)	14.63 (0.77)	15.37 (1.43)	0.028*
Recurrence rate			
1-month median (SD)	14.74 (1.57)	16.01 (0.73)	0.004**
3-month median (SD)	13.60 (1.31)	15.61 (1.22)	0.000***
6-month median (SD)	13.49 (1.11)	14.90 (1.90)	0.005**

The differences were considered significant if p-value < 0.05.
***p-value < 0.001.
**p-value < 0.01.
*p-value <0.05.

value of 12.95 for RDW with a sensitivity of 75.6% and a specificity of 69.5% was obtained in the ROC analyses. To our knowledge, this was the first study to investigate the association of RD with RDW, and the first report on RDW as indicators to evaluate the OS status of RD.

Otolithic organ disorder (OOD) is considered the most studied and persuasive among the hypotheses of RD's occurrence and recurrence (21). Emerging literature has shown that patients with BPPV had higher levels of OS and subsequent elevated inflammatory responses, which may contribute to the development of OOD (22, 23). Other studies concluded that OS caused damage to vestibular hair cells and neurons in the inner ear, impairing vestibular function (19). Sequentially, we hypothesized that patients with BPPV were more prone to RD after recovery of CRPs if accompanied by higher OS.

RDW and OS

Cumulative evidence indicated that serum levels of oxidants increased with RDW (18, 24). In this study, the RDW in RD patients was significantly higher than that in non-RD subjects, indicating that RD incidence in BPPV patients may be caused by higher OS. The antioxidant and oxidant systems were imbalanced. Theoretically, low serum antioxidant concentrations may be inversely associated with RDW. Some scholars have found that UA, TB, ALB, and CR can comprehensively reflect the antioxidant status of patients with BPPV (11). Our study found that these four indicators were lower in the RD group than in non-RD group, suggesting that RD patients have lower antioxidant capacity. Moreover, RDW values were inversely correlated with the levels of these four markers (although not all findings were statistically significant), which also indicated that RD patients had weaker antioxidant capacity.

The imbalance between antioxidant and oxidant causes oxidative damage, which can lead to OOD. OS occurs under conditions of increased reactive oxygen species or depletion of antioxidants. Scholars investigated the relationship between antioxidants (serum selenium) and RDW and found that patients with higher RDW had lower serum selenium levels (25). Activation of OS and reduction or depletion of endogenous antioxidant activity promote the increase of RDW.

As we all know, OS plays an important role in several inner ear diseases and normal aging (26). Many studies have shown that the incidence of RD was higher with increasing age, which also proves from another perspective that the etiology of RD may be the result of long-term OS accumulation (27, 28). It is well known that RDW levels increase with age (29), which proves that RDW is an indicator of OS in terms of physiological degradation. In our study, higher OS was a risk factor for the development of RD, suggesting an important role of OS in the pathogenesis. The reasons behind this interesting result deserve further investigation.

RDW and OS-related inflammation

Researchers have found that serum levels of inflammation increased with RDW (25). OS can decrease the lifespan of erythrocytes, while subsequent inflammation is strongly associated with inhibited erythropoiesis, both of which may increase RDW level (24). Scholars investigated the relationship between inflammation markers and RDW and found that patients with higher RDW had higher levels of N/L and IL-6 (25, 30). Similarly, in our study, we found higher levels of RDW, N/L, and CRP in the RD group, which were statistically different from the non-RD group. We excluded infectious diseases and compared WBCs between the two groups to make sure the data were accurate. Given this premise, RDW was positively correlated with CRP in this study, suggesting that RD patients suffered a more severe inflammatory response.

The inflammation cascade reactions may be involved in the pathogenesis of the otolith organ (31). The inner ear has a blood-labyrinth barrier, is connected to the cervical lymph nodes, and produces cytokines through the spiral ligament to participate in the inflammatory response (32). Based on the above mechanisms, the link between inflammation and RD will become more apparent as the disease progresses.

Taken together, our study showed that patients with RD had upregulated inflammation, and the OS-related inflammation was a possible mechanism in the pathogenesis of RD.

RDW and microcirculation

Oxidative stress is a critical factor that causes microcirculation disturbance (33). OS induces erythrocyte

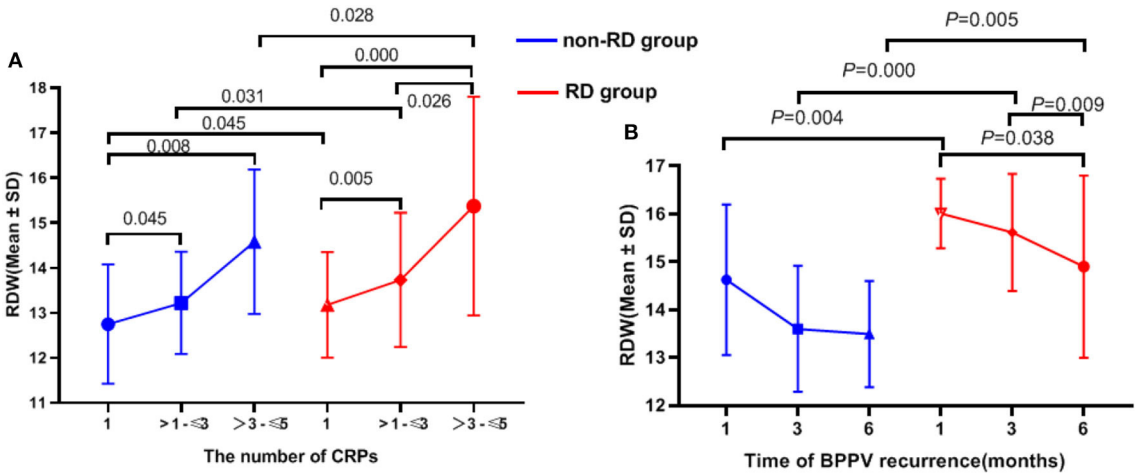

FIGURE 3
The relationship between RDW value and number of CRPs **(A)**, recurrence of BPPV in 6 months of follow-up **(B)**.

TABLE 3 Risk factors for RD using multiple logistic regression.

Risk factors	OR	95% CI	*p*-Value
RDW	2.615	1.875–3.648	0.000***
CR	1.048	1.018–1.079	0.002**
ALB	0.847	0.770–0.931	0.001**
TB	1.082	1.022–1.145	0.007**
GLU	1.327	1.143–1.542	0.000***

The differences were considered significant if p-value < 0.05.
***p-value < 0.001.
**p-value < 0.01.
*p-value < 0.05.

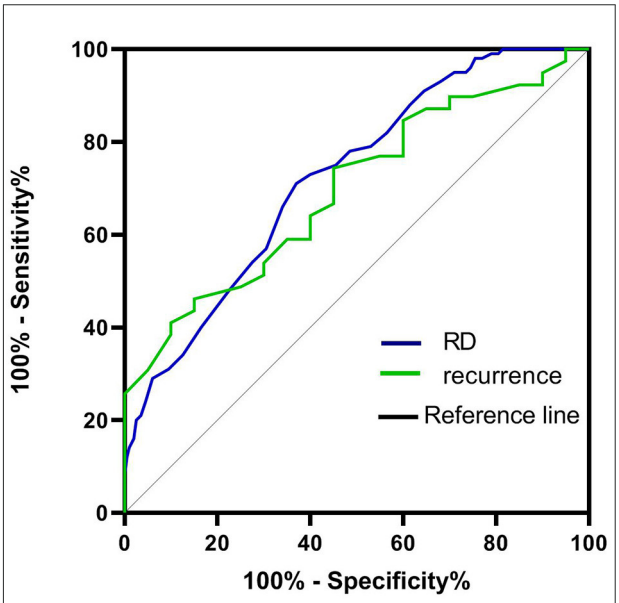

FIGURE 4
ROC curve to establish the sensitivity and specificity of RDW levels to predict the risk of RD and recurrence after BPPV.

adhesion to the vascular endothelium and reduces erythrocyte deformability (34). Moreover, the elevated RDW promotes platelet activation and aggregation, which serves as a marker of the procoagulant status of RBCs (35). The two interact with each other and play a role in the elevation of vessel resistance, which would deform worse and impair blood flow through microcirculation. Increased baseline RDW has been shown to be associated with poor collateral flow in large artery atherosclerosis stroke patients (36). The labyrinthine artery, as the only artery supplying the vestibular system, has less collateral circulation. Therefore, it is reasonable to believe that when RDW increases, its microcirculation becomes poorer and OS is more severe.

The present study revealed that FIB levels were elevated in RD group, indicating higher procoagulant status and worse microcirculation. This is in agreement with a previous study focused on microcirculation, which found that elevated RDW led to slow coronary flow (37). Apart from continuous degradation of the vestibule caused by OS, the deterioration of microcirculation caused by OS may be another reason for the high incidence of RD in older adults. Deng et al. found that Danhong injection significantly improved RD through antioxidant activity and microcirculation improvement (38). However, their results were speculative theories that were supported mostly by pathophysiologic reasoning.

RDW value and the recurrence rate of BPPV and number of CRPs

OS is related to OOD, and it could also be related to its recurrence rate and not only with RD. In this study, the recurrence rate of BPPV was higher in the RD group as compared to the non-RD group, suggesting an association between RDW and recurrence (Table 1). As shown in Figure 3, it can be concluded that the higher the baseline RDW, the earlier the recurrence onset (although not all $p < 0.05$; Table 2, Figure 3B). Moreover, the AUC for the ability of the RDW to predict recurrence was 0.692. In terms of the number of CRPs, our results showed that RDW values in the two groups increased with CRPs (all $p < 0.05$; Table 2, Figure 3A). The number of CRPs was proportional to the RDW value. The reasons behind the interesting results deserve further investigation.

As mentioned above, the results of this study showed a higher RDW in the RD group, indicating a higher level of OS in RD patients. In addition, we corroborated the lower antioxidant levels of RD patients by their serum levels of UA, TB, ALB, and CR. In conclusion, our study shows that BPPV patients with a higher OS are more prone to develop RD, which may help to evaluate the prognosis of BPPV patients.

Limitation

Our study has the following limitations. First, the one-time measurement of the RDW value was prone to lead to analytical errors. Second, this was a retrospective study, and the sample was relatively small, which may bias the findings. Third, several OS markers (such as MDA and SOD) and vestibular function test (VEMP and SVV) were not adequately evaluated.

Conclusions

To sum up, our result suggested that RDW could be considered as potential biomarkers of RD. As it is a rapid, inexpensive, and easily available laboratory marker, it can be used in clinical practice for prediction of RD. Also, we put forward a hypothesis that OS plays a role in RD, which needs further investigations.

Data availability statement

The raw data supporting the conclusions of this article will be made available by the authors, without undue reservation.

Ethics statement

The studies involving human participants were reviewed and approved by Zhuhai Hospital of Integrated Traditional Chinese and Western Medicine. Written informed consent for participation was not required for this study in accordance with the national legislation and the institutional requirements.

Author contributions

Conceptualization, data curation, and writing review and editing: K-HX. Formal analysis: L-LL. Investigation and writing original draft: L-CC. Project administration: C-YS and HL. Resources: Q-QC. Software: R-NL. Supervision: W-KH. Validation: L-CC. Visualization: J-SH. All authors contributed to the article and approved the submitted version.

Conflict of interest

The authors declare that the research was conducted in the absence of any commercial or financial relationships that could be construed as a potential conflict of interest.

Publisher's note

All claims expressed in this article are solely those of the authors and do not necessarily represent those of their affiliated organizations, or those of the publisher, the editors and the reviewers. Any product that may be evaluated in this article, or claim that may be made by its manufacturer, is not guaranteed or endorsed by the publisher.

References

1. Teggi R, Giordano L, Bondi S, Fabiano B, Bussi M. Residual dizziness after successful repositioning maneuvers for idiopathic benign paroxysmal positional vertigo in the elderly. *Eur Arch Otorhinolaryngol.* (2011) 268:507–11. doi: 10.1007/s00405-010-1422-9

2. Seok JI, Lee HM, Yoo JH, Lee DK. Residual dizziness after successful repositioning treatment in patients with benign paroxysmal positional vertigo. *J Clin Neurol.* (2008) 4:107–10. doi: 10.3988/jcn.2008.4.3.107

3. Oghalai JS, Manolidis S, Barth JL, Stewart MG, Jenkins HA. Unrecognized benign paroxysmal positional vertigo in elderly patients. *Otolaryngol Head Neck Surg.* (2000) 122:630–4. doi: 10.1067/mhn.2000.105415

4. Kim HA, Lee H. Autonomic dysfunction as a possible cause of residual dizziness after successful treatment in benign paroxysmal positional vertigo. *Clin Neurophysiol.* (2014) 125:608–14. doi: 10.1016/j.clinph.2013.08.008

5. Mulavara AP, Cohen HS, Peters BT, Sangi-Haghpeykar H, Bloomberg JJ. New analyses of the sensory organization test compared to the clinical test of sensory integration and balance in patients with benign paroxysmal positional vertigo. *Laryngoscope.* (2013) 123:2276–80. doi: 10.1002/lary.24075

6. Jung HJ, Koo JW, Kim CS, Kim JS, Song JJ. Anxiolytics reduce residual dizziness after successful canalith repositioning maneuvers in benign paroxysmal positional vertigo. *Acta Otolaryngol.* (2012) 132:277–84. doi: 10.3109/00016489.2011.637179

7. Hegemann SCA, Weisstanner C, Ernst A, Basta D, Bockisch CJ. Constant severe imbalance following traumatic otoconial loss: a new explanation of residual dizziness. *Eur Arch Otorhinolaryngol.* (2020) 277:2427–35. doi: 10.1007/s00405-020-05926-8

8. Poirrier AL, Pincemail J, Van Den Ackerveken P, Lefebvre PP, Malgrange B. Oxidative stress in the cochlea: an update. *Curr Med Chem.* (2010) 17:3591–604. doi: 10.2174/092986710792927895

9. Tan WJT, Song L, Graham M, Schettino A, Navaratnam D. Yarbrough WG, et al. Novel role of the mitochondrial protein Fus1 in protection from premature hearing loss *via* regulation of oxidative stress and nutrient and energy sensing pathways in the inner ear. *Antioxid Redox Signal.* (2017) 27:489–509. doi: 10.1089/ars.2016.6851

10. Scuto M, Di Mauro P, Ontario ML, Amato C, Modafferi S, Ciavardelli D, et al. Nutritional mushroom treatment in Meniere's disease with coriolus versicolor: a rationale for therapeutic intervention in neuroinflammation and antineurodegeneration. *Int J Mol Sci.* (2019) 21. doi: 10.3390/ijms21010284

11. Xie KH, Liu LL, Su CY, Huang XF, Wu BX. Liu RN, et al. Low antioxidant status of serum uric acid, bilirubin, albumin, and creatinine in patients with benign paroxysmal positional vertigo. *Front Neurol.* (2020) 11:601695. doi: 10.3389/fneur.2020.601695

12. Tsai KL, Cheng YY, Leu HB, Lee YY, Chen TJ. Liu DH, et al. Investigating the role of Sirt1-modulated oxidative stress in relation to benign paroxysmal positional vertigo and Parkinson's disease. *Neurobiol Aging.* (2015) 36:2607–16. doi: 10.1016/j.neurobiolaging.2015.05.012

13. Parizadeh SM, Jafarzadeh-Esfehani R, Bahreyni A, Ghandehari M, Shafiee M. Rahmani F, et al. The diagnostic and prognostic value of red cell distribution width in cardiovascular disease; current status and prospective. *Biofactors.* (2019) 45:507–16. doi: 10.1002/biof.1518

14. Celikbilek A, Zararsiz G, Atalay T, Tanik N. Red cell distribution width in migraine. *Int J Lab Hematol.* (2013) 35:620–8. doi: 10.1111/ijlh.12100

15. Wang C, Wang L, Zhong D, Deng L, Qiu S, Li Y, et al. Association between red blood cell distribution width and hemorrhagic transformation in acute ischemic stroke patients. *Cerebrovasc Dis.* (2019) 48:193–9. doi: 10.1159/000504742

16. Kim J, Kim YD, Song TJ, Park JH, Lee HS. Nam CM, et al. Red blood cell distribution width is associated with poor clinical outcome in acute cerebral infarction. *Thromb Haemost.* (2012) 108:349–56. doi: 10.1160/TH12-03-0165

17. Peng YF, Pan GG. Red blood cell distribution width predicts homocysteine levels in adult population without vitamin B12 and folate deficiencies. *Int J Cardiol.* (2017) 227:8–10. doi: 10.1016/j.ijcard.2016.11.012

18. Zhao Z, Liu T, Li J, Yang W, Liu E, Li G. Elevated red cell distribution width level is associated with oxidative stress and inflammation in a canine model of rapid atrial pacing. *Int J Cardiol.* (2014) 174:174–6. doi: 10.1016/j.ijcard.2014.03.189

19. Tanigawa T, Tanaka H, Hayashi K, Nakayama M, Iwasaki S. Banno S, et al. Effects of hydrogen peroxide on vestibular hair cells in the guinea pig: importance of cell membrane impairment preceding cell death. *Acta Otolaryngol.* (2008) 128:1196–202. doi: 10.1080/00016480801918539

20. Fetter M. Assessing vestibular function: which tests, when? *J Neurol.* (2000) 247:335–42. doi: 10.1007/s004150050599

21. Seo T, Shiraishi K, Kobayashi T, Mutsukazu K, Fujita T. Saito K, et al. Residual dizziness after successful treatment of idiopathic benign paroxysmal positional vertigo originates from persistent utricular dysfunction. *Acta Otolaryngol.* (2017) 137:1149–52. doi: 10.1080/00016489.2017.1347824

22. Ozbay I, Topuz MF, Oghan F, Kocak H, Kucur C. Serum prolidase, malondialdehyde and catalase levels for the evaluation of oxidative stress in patients with peripheral vertigo. *Eur Arch Otorhinolaryngol.* (2021) 278:3773–6. doi: 10.1007/s00405-020-06466-x

23. Labbe D, Teranishi MA, Hess A, Bloch W, Michel O. Activation of caspase-3 is associated with oxidative stress in the hydropic guinea pig cochlea. *Hear Res.* (2005) 202:21–7. doi: 10.1016/j.heares.2004.10.002

24. Patel KV, Semba RD, Ferrucci L, Newman AB, Fried LP. Wallace RB, et al. Red cell distribution width and mortality in older adults: a meta-analysis. *J Gerontol A Biol Sci Med Sci.* (2010) 65:258–65. doi: 10.1093/gerona/glp163

25. Semba RD, Patel KV, Ferrucci L, Sun K, Roy CN. Guralnik JM, et al. Serum antioxidants and inflammation predict red cell distribution width in older women: the Women's Health and Aging Study I. *Clin Nutr.* (2010) 29:600–4. doi: 10.1016/j.clnu.2010.03.001

26. Iwasaki S, Yamasoba T. Dizziness and imbalance in the elderly: age-related decline in the vestibular system. *Aging Dis.* (2015) 6:38–47. doi: 10.14336/AD.2014.0128

27. Kim JS, Zee DS. Clinical practice. Benign paroxysmal positional vertigo. *N Engl J Med.* (2014) 370:1138–47. doi: 10.1056/NEJMcp1309481

28. de Moraes SA, Soares WJ, Rodrigues RA, Fett WC, Ferriolli E, Perracini MR. Dizziness in community-dwelling older adults: a population-based study. *Braz J Otorhinolaryngol.* (2011) 77:691–9. doi: 10.1590/S1808-86942011000600003

29. Patel KV, Ferrucci L, Ershler WB, Longo DL, Guralnik JM. Red blood cell distribution width and the risk of death in middle-aged and older adults. *Arch Intern Med.* (2009) 169:515–23. doi: 10.1001/archinternmed.2009.11

30. Tekesin A, Tunc A. Inflammatory biomarkers in benign paroxysmal positional vertigo: a Turkey case-control study. *Ideggyogy Sz.* (2018) 71:411–6. doi: 10.18071/isz.71.0411

31. Kinar A, Bucak A, Ulu S, Duman N, Bastug NB. Vestibular function in psoriasis patients. *Ear Nose Throat J.* (2020) 145561320970683. doi: 10.1177/0145561320970683

32. Ishiyama G, Wester J, Lopez IA, Beltran-Parrazal L, Ishiyama A. Oxidative stress in the blood labyrinthine barrier in the macula utricle of Meniere's disease patients. *Front Physiol.* (2018) 9:1068. doi: 10.3389/fphys.2018.01068

33. Crimi E, Ignarro LJ, Napoli C. Microcirculation and oxidative stress. *Free Radic Res.* (2007) 41:1364–75. doi: 10.1080/10715760701732830

34. Besedina NA, Skverchinskaya EA, Ivanov AS, Kotlyar KP, Morozov IA, Filatov NA, et al. Microfluidic characterization of red blood cells microcirculation under oxidative stress. *Cells.* (2021) 10. doi: 10.3390/cells10123552

35. Turcato G, Cappellari M, Follador L, Dilda A, Bonora A. Zannoni M, et al. Red blood cell distribution width is an independent predictor of outcome in patients undergoing thrombolysis for ischemic stroke. *Semin Thromb Hemost.* (2017) 43:30–5. doi: 10.1055/s-0036-1592165

36. Hong L, Fang K, Ling Y, Yang L, Cao W, Liu F, et al. Red blood cell distribution width is associated with collateral flow and final infarct volume in acute stroke with large artery atherosclerosis. *Semin Thromb Hemost.* (2020) 46:502–6. doi: 10.1055/s-0039-3400257

37. Akpinar I, Sayin MR, Gursoy YC, Aktop Z, Karabag T. Kucuk E, et al. Plateletcrit and red cell distribution width are independent predictors of the slow coronary flow phenomenon. *J Cardiol.* (2014) 63:112–8. doi: 10.1016/j.jjcc.2013.07.010

38. Deng W, Yang C, Xiong M, Fu X, Lai H, Huang W. Danhong enhances recovery from residual dizziness after successful repositioning treatment in patients with benign paroxysmal positional vertigo. *Am J Otolaryngol.* (2014) 35:753–7. doi: 10.1016/j.amjoto.2014.07.001

frontiers | Frontiers in Neurology

TYPE Original Research
PUBLISHED 08 September 2022
DOI 10.3389/fneur.2022.957283

OPEN ACCESS

EDITED BY
Miriam Welgampola,
The University of Sydney, Australia

REVIEWED BY
Ali S. Saber Tehrani,
Johns Hopkins Medicine, United States
Jorge Hernandez-Vara,
Hospital Universitari Vall
D'Hebron, Spain

*CORRESPONDENCE
Andreas Zwergal
Andreas.Zwergal@med.uni-muenchen.de

SPECIALTY SECTION
This article was submitted to
Neuro-Otology,
a section of the journal
Frontiers in Neurology

RECEIVED 30 May 2022
ACCEPTED 16 August 2022
PUBLISHED 08 September 2022

CITATION
Schuhbeck F, Strobl R, Conrad J, Möhwald K, Jaufenthaler P, Jahn K, Dieterich M, Grill E and Zwergal A (2022) Determinants of functioning and health-related quality of life after vestibular stroke.
Front. Neurol. 13:957283.
doi: 10.3389/fneur.2022.957283

Determinants of functioning and health-related quality of life after vestibular stroke

Franziska Schuhbeck[1,2], Ralf Strobl[1,3], Julian Conrad[1,2], Ken Möhwald[1,2], Patricia Jaufenthaler[1,2], Klaus Jahn[1,4], Marianne Dieterich[1,2,5], Eva Grill[1,3,6] and Andreas Zwergal[1,2]*

[1]German Center for Vertigo and Balance Disorders, DSGZ, LMU Hospital, Ludwig-Maximilians Universität Munich, Munich, Germany, [2]Department of Neurology, LMU Hospital, Ludwig-Maximilians Universität Munich, Munich, Germany, [3]Institute for Medical Information Processing, Biometry, and Epidemiology, Ludwig-Maximilians Universität Munich, Munich, Germany, [4]Schön Clinic Bad Aibling, Department of Neurology, Bad Aibling, Germany, [5]Munich Cluster for Systems Neurology, SyNergy, Munich, Germany, [6]Munich Center for Health Sciences, Ludwig-Maximilians Universität Munich, Munich, Germany

Background: Stroke accounts for 5–10% of all presentations with acute vertigo and dizziness. The objective of the current study was to examine determinants of long-term functioning and health-related quality of life (HRQoL) in a patient cohort with vestibular stroke.

Methods: Thirty-six patients (mean age: 66.1 years, 39% female) with an MRI-proven vestibular stroke were followed prospectively (mean time: 30.2 months) in the context of the EMVERT (EMergency VERTigo) cohort study at the Ludwig-Maximilians Universität, Munich. The following scores were obtained once in the acute stage (<24 h of symptom onset) and once during long-term follow-up (preferably >1 year after stroke): European Quality of Life Scale-five dimensions-five levels questionnaire (EQ-5D-5L) and Visual Analog Scale (EQ-VAS) for HRQoL, Dizziness Handicap Inventory (DHI) for symptom severity, and modified Rankin Scale (mRS) for general functioning and disability. Anxiety state and trait were evaluated by STAI-S/STAI-T, and depression was evaluated by the Patient Health Questionnaire-9 (PHQ-9). Voxel-based lesion mapping was applied in normalized MRIs to analyze stroke volume and localization. Multiple linear regression models were calculated to determine predictors of functional outcome (DHI, EQ-VAS at follow-up).

Results: Mean DHI scores improved significantly from 45.0 in the acute stage to 18.1 at follow-up ($p < 0.001$), and mean mRS improved from 2.1 to 1.1 ($p < 0.001$). Mean HRQoL (EQ-5D-5L index/EQ-VAS) changed from 0.69/58.8 to 0.83/65.2 ($p = 0.01$/$p = 0.11$). Multiple linear regression models identified higher scores of STAI-T and DHI at the time of acute vestibular stroke and larger stroke volume as significant predictors for higher DHI at follow-up assessment. The effect of STAI-T was additionally enhanced in women. There was a significant effect of patient age on EQ-VAS, but not DHI during follow-up.

Conclusion: The average functional outcome of strokes with the chief complaint of vertigo and dizziness is favorable. The most relevant predictors for individual outcomes are the personal anxiety trait (especially in combination

with the female sex), the initial symptom intensity, and lesion volume. These factors should be considered for therapeutic decisions both in the acute stage of stroke and during subsequent rehabilitation.

KEYWORDS

vertigo, vestibular disorders, stroke, quality of life, outcome prediction

Introduction

Acute stroke is responsible for 5% of all disability-adjusted life years (1). However, data on functional outcomes are almost exclusively available for patients with anterior circulation stroke, while prognostic markers for disability and functioning are largely missing for posterior circulation strokes (2). Frequently observed chief complaints associated with posterior circulation stroke, such as acute vertigo, dizziness, double vision, or gait instability, are underrepresented in clinical tools for stroke assessment, such as the National Institutes of Health Stroke Scale (NIHSS) (3). In consequence, there is no consensus, which symptoms should prompt a more extensive therapy during the acute stage (e.g., intravenous thrombolysis) and which patients should receive more intense rehabilitation on the course (4).

In vestibular disorders, several factors contribute to symptom severity, health-related quality of life (HRQoL), and psychological comorbidity (5–7). Generally, subjective symptoms and HRQoL tend to correlate with objective tests of semicircular canal function in acute peripheral and central vestibular disorders only (8), while there is no direct relationship between labyrinthine function and symptom intensity in their chronic stage (9). Long-term adaptation to deficits in vestibular processing seems to depend rather on the time course of vestibular symptoms (recurrent vs. chronic), the character traits of the patient (e.g., anxiety), as well as coping and resiliance mechanisms (10). Episodic vestibular syndromes such as vestibular migraine or Menière's disease are most frequently associated with anxiety and depression (11, 12), while patients with chronic unilateral or bilateral peripheral vestibulopathies do not have more psychiatric comorbidities than healthy controls (13). Signs of vestibular imbalance in central vestibular lesions (such as deviation of the subjective visual vertical) recover with a similar time course than in unilateral peripheral vestibulopathies (14), but it remains unclear, if this translates to an improvement of HRQoL and functioning.

In this study, we aimed to evaluate the trajectories and determinants of long-term functioning and HRQoL in a well-characterized cohort of patients with acute posterior circulation stroke, presenting with the chief complaints of acute vertigo, dizziness, double vision, or imbalance, based on a follow-up assessment. We hypothesized that the most relevant factors for the outcome will be the symptom intensity during the acute stroke stage, age, sex, localization, and volume of the lesion, as well as indicators of accompanying anxiety and depression.

Methods

Patient characteristics and study protocol

This prospective long-term follow-up study included a cohort of 36 patients (age: 66.1 years, sd: 12.0 years, 38.9% women), who initially presented to the Emergency Department (ED) of the LMU Hospital, Munich, with the chief complaints of acute vertigo, dizziness, double vision, or postural imbalance (symptom onset <24 h, symptom duration >10 min), and were subsequently diagnosed to have an acute brain stem-cerebellar stroke in MRI. Patients were recruited prospectively in the scope of the EMERT (EMergency VERTigo) trial (15). All patients received a *standardized and comprehensive investigation in the ED* including history taking, clinical neurological and neuro-otological examination, video-oculographic assessment (EyeSeeCam, Fürstenfeldbruck, Germany) of vestibular and ocular motor functions (e.g., video head impulse test, spontaneous nystagmus, smooth pursuit, gaze holding, and saccades), mobile posturography, bucket test for subjective visual vertical (SVV, normal range $0 \pm 2.5^{\circ}$) (16), as well as scales and scores for symptom severity (Dizziness Handicap Inventory, DHI), disability and functioning (modified Ranking Scale, mRS), and HRQoL (European Quality of Life Scale-five dimensions-five levels, EQ-5D-5L; European Quality of Life Scale—Visual Analog Scale, EQ-VAS). *A follow-up assessment* was done once after a mean time of 30.2 months (sd: 11.9 months) by standardized patient interviews including DHI, mRS, EQ-5D-5L, EQ-VAS, scales for anxiety (State-Trait-Anxiety Inventory—State and Trait: STAI-T, STAI-S), and depression (Patient-Health-Questionaire-9, PHQ-9). Furthermore, clinical neurological and neuro-otological assessments of vestibular, ocular motor, and postural functions were added. The long timespan for follow-up of preferably >1 year after stroke was chosen based on the assumption that a stable functional status of recovery should have been reached.

Protocol approval and patient consent

The study was approved by the Ethics Committee of the University of Munich on 02/23/2015 (57-15) and was conducted according to the Guideline for Good Clinical Practice, the Federal Data Protecting Act, and the Helsinki Declaration of the World Medical Association. All subjects gave their informed, written consent to participate in the study. The study was listed in the German Clinical Trial Registry under the ID DRKS00008992 and the Universal Trial Number ID U1111-1172-8719.

Scores and scales

We collected, standardized, and established scores and scales to assess HRQoL, functioning, symptom severity, and psychiatric comorbidity following vestibular stroke.

The *EQ-5D-5L questionnaire* consists of five questions, called dimensions (i.e., mobility, self-care, usual activities, pain/discomfort, and anxiety/depression), each with five answer choices (1–5), called levels. The result is reported as a five-digit number. In the present study, the EQ-5D-5L index was calculated from these figures using the German value set as a reference (−0.661 worst health status, 1 best health status) (17).

The EQ-5D-5L questionnaire also includes a visual analog scale, the *EQ-VAS*, which is used to determine the patients' current perceived health status. The EQ-VAS is a vertical scale with values ranging from 0 to 100, where 0 represents the worst and 100 represents the best state of health that the patient can imagine.

Patients' functionality and disability was evaluated using the *mRS*. The mRS ranges from 0 (no symptoms) to 6 (death) and describes the degree of patients' impairment and disability after stroke. The mRS can also be used to assess the outcome. In some studies, a favorable course is usually defined for values from 0 to 2 (18, 19).

The *DHI* was applied to rate the patients' subjective symptom severity due to vertigo and dizziness. The DHI is composed of 25 questions that assess the functional, emotional, and physical impact of vertigo and dizziness on the patient. Scores ranging from 0 (no impairment due to dizziness) to 100 (significant subjective impairment) are possible (20).

In the follow-up interview, anxiety and depression as frequent psychiatric comorbidities were specifically assessed. The STAI questionnaire, consisting of the *STAI-S* and *STAI-T*, each with 20 statements, was used to quantify anxiety. The STAI-S evaluates the patients' current level of anxiety, while the STAI-T indicates the extent to which anxiety is part of the patients' personality traits and is therefore thought to be a stable condition (21). Scores between 20 and 80 are possible in each case, with higher scores indicating increased anxiety. The *PHQ-9* was applied to identify depression in patients. The PHQ-9 contains nine questions based on the Diagnostic and Statistical Manual of Mental Disorders (DSM-IV) criteria for depressive disorders. The patient indicates how often various symptoms have occurred in the past 2 weeks (from 0: "not at all" to 3: "nearly every day"). A depressive disorder is considered, if at least two questions were answered with "more than half of the days" (=2), and depression or anhedonia is one of the symptoms mentioned. In general, a total score between 0 and 27 points is possible and provides information about the severity of a depressive disorder (22, 23). A *specially customized questionnaire* was developed to further evaluate the persistence of vertigo and dizziness, symptomatic days, as well as further strokes during the time to follow-up.

Magnetic resonance imaging and lesion mapping

A standardized MRI was performed within the first 7 days after stroke (mean 2.2 days, sd: 2.5 days), including whole brain and brain stem diffusion-weighted images (DWI), fine-slice 3 mm fluid-attenuated inversion recovery (FLAIR), T2, T2*, and 3D-T1, time-of-flight (TOF) angiography. Statistical parametric mapping (SPM) was used to determine lesion volume in voxels. Lesions were delineated on acute phase brain stem T2-weighted or brain stem DWI sequences using MRIcron. All lesion maps were then normalized into $1 \times 1 \times 1$ mm^3 MNI space using the Clinical Toolbox in SPM for visualization (24). In addition, stroke lesions were assigned to vascular territories by two expert neuro-radiologists. Furthermore, the Fazekas score for micro-vascular lesions was assessed on FLAIR sequences. The Fazekas score consists of 4 levels (range 0–3), describing the extent of hyperintensity in the periventricular and deep white matter (25).

Statistical analysis

All data were collected and organized by a REDCap (Research Electronic Data Capture) database. This software platform enabled error-free data entry and export to SPSS, as well as validation, quality control, and secure storage of the data (26).

Statistical analysis was carried out with SPSS (IBM SPSS Statistics, version 27.0.1.0). In the descriptive analysis, means, standard deviations (sd), variance, and sum scores of the questionnaires and variables were calculated. Additionally, absolute and relative frequencies of different variables were determined. Depending on the scale level, linear correlations were computed using the Bravais-Pearson, Spearman or Eta coefficient, or the Chi^2 test. *T*-tests for dependent samples were performed to analyze whether the progression parameters (DHI, mRS, EQ5D-5L, EQ-VAS) had changed over time. Independent sample *t*-tests were used to investigate whether

TABLE 1 Health-related quality of life (HRQoL), functioning, and symptom severity at acute stage and follow-up.

	Acute stage	Follow-up	*t*-test
DHI	45.0 ± 25.2	18.1 ± 24.8	$p < 0.001$, $t = -5.4$
mRS	2.1 ± 1.2	1.1 ± 1.3	$p < 0.001$, $t = -4.2$
EQ-5D-5L index	0.69 ± 0.3	0.83 ± 0.2	$p = 0.014$, $t = 2.6$
EQ-VAS	58.8 ± 19.1	65.2 ± 18.0	$p = 0.112$, $t = 1.6$

DHI, Dizziness Handicap Inventory; EQ-5D-5L, European Quality of Life-5 Dimensions-5 Levels questionnaire; EQ-VAS, European Quality of Life Scale—Visual Analog Scale; mRS, modified Rankin Scale.

distinct subgroups of the study population differed in their progression parameters.

Multiple linear regression models were calculated to analyze the factors predicting the long-term outcome of vestibular stroke patients. Two variables were selected to describe the outcome: Symptom-related outcome was represented by the DHI at follow-up and general health outcome by the EQ-VAS at follow-up. For both variables, a separate model was calculated. Patient-specific and lesion-specific variables were selected as predictors to comprehensively investigate possible factors influencing outcome: patient age at the time of stroke, gender, STAI-T, and DHI in the acute stage as patient-specific variables, and lesion volume measured in voxels as a lesion-specific variable.

Results

Clinical and imaging characteristics of the study cohort

Patients of the study cohort most frequently reported vertigo, dizziness, and double vision as their chief complaints during the acute stage of symptoms (Supplementary Table 1). Upon clinical neurological and neuro-otological exam, 21 patients had central ocular motor signs (such as saccadic smooth pursuit, direction-changing gaze-evoked nystagmus, and cross-coupling during head shaking), 19 patients had signs of vestibular asymmetry (such as spontaneous nystagmus, SVV tilt, and skew deviation), 16 patients had gait imbalance, and 5 patients had mild limb ataxia. Most patients had an extensive cardiovascular risk profile, with the most common factors being arterial hypertension, hypercholesterolemia, nicotin abuse, and a positive family history of cardiovascular disease. In the acute stage of symptoms, DHI was 45.0 ± 24.2, mRS was 2.1 ± 1.2, EQ-5D-5L index was 0.69 ± 0.3, and EQ-VAS was 58.8 ± 19.1 (Table 1).

Stroke lesions were mapped to the medial cerebellum and brain stem (Figure 1). The mean lesion volume in 1 mm isovoxels was 5,298 (sd: 9,244). In the cerebellum, most lesions were localized in the territories of the posterior inferior cerebellar artery (PICA) (30.6%) and the superior cerebellar artery (SCA) (8.3%). The lobules VIIIA/B (biventer lobule: 27.8%), lobules VII (inferior semilunar lobule: 19.4%; superior semilunar lobule: 11.1%), vermal lobules IX and X (uvula/nodulus: 8.3%), and lobules IV and V (anterior and posterior quandrangular lobule: 8.3%) were affected predominantly (Figure 1). Brain stem lesions affected the midbrain (27.8%), pons (19.4%), and medulla (5.6%) most frequently. The most prevalent etiologies for posterior circulation stroke were arterio-arterial embolism (44.4%) and cardiac embolism (30.6%). Fazekas score for cerebral microangiopathy was 1.1 ± 1.0.

Outcome parameters during follow-up

Compared to the acute stage, during follow-up (after a mean time of 30.2 months), DHI had significantly improved to 18.1 ± 24.8 ($p < 0.001$), mRS had improved to 1.1 ± 1.3 ($p < 0.001$), and EQ-5D-5L had improved to 0.83 ± 0.2 ($p = 0.014$), while EQ-VAS remained low ($p = 0.112$) (Table 1). The scales for anxiety at follow-up were 36.4 ± 11.2 (STAI-T) and 34.2 ± 12.1 (STAI-S). The depression score PHQ-9 was 3.2 ± 3.9. Two of the 36 enrolled patients had died, seven patients had another stroke (after a mean time of 10.7 ± 11.4 months), and nine patients had persistent dizziness or imbalance. These patients reported to have 13.9 ± 13.8 days per month, where they perceived balance-related symptoms.

Clinical follow-up assessment indicated mild central ocular motor signs in 8 patients, some degree of gait or limb ataxia in 6 patients, and signs of enduring vestibular asymmetry (deviation of SVV, provocation nystagmus) in only 4 of 34 patients.

Influencing factors on functional outcome

A multiple linear regression model with the dependent variable DHI at follow-up showed an independent and significant effect of an anxiety trait measured by STAI-T ($p < 0.001$), especially in combination with female gender ($p = 0.01$), of lesion volume ($p = 0.04$), and symptom severity (represented by DHI) in the acute stroke stage ($p = 0.01$), while age was irrelevant for the outcome (Table 2). When EQ-VAS at follow-up was chosen as an outcome variable for overall health status, only STAI-T ($p = 0.01$) and DHI during the acute stage ($p = 0.02$) persisted to be significant influencing factors, while lesion volume was not relevant ($p = 0.18$). In this model, age was an independent factor for outcome prediction ($p = 0.03$) (Table 3).

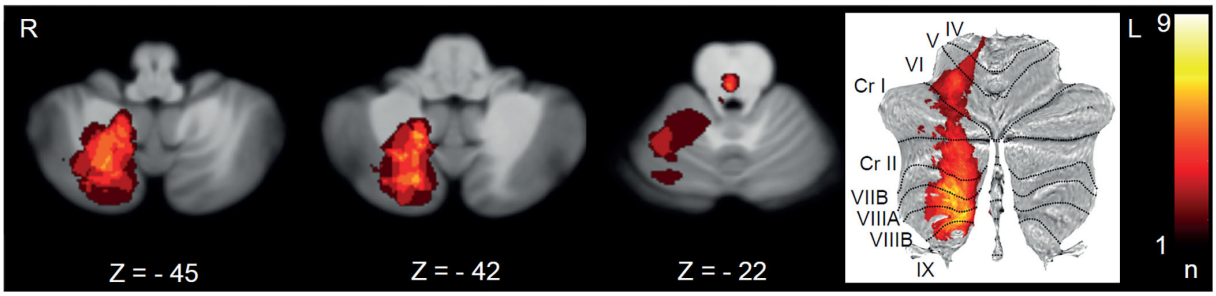

FIGURE 1
Lesion mapping of all strokes with the chief complaint of vertigo, dizziness, or double vision depicted on transverse sections (*Z*-scores in MNI space) and as a surface plot. L, left; R, right.

TABLE 2 Multiple linear regression model with DHI at follow-up as dependent variable and outcome parameter.

Model variables	Unstandardized coefficients		Standardized coefficients	Significance level
	B	Standard. error	Beta	
(Constant)	−97.45	31.98		0.01
Sex	−5.59	8.37	−0.11	0.51
Age	0.64	0.33	0.36	0.06
STAI-T	1.31	0.38	0.61	0.00
Lesion volume	0.92	0.42	0.33	0.04
DHI acute stage	0.49	0.18	0.52	0.01
STAI-T_Sex	2.31	0.75	0.54	0.01

Lesion volume: in voxels divided by factor 1,000; STAI-T_Sex: interaction variable of STAI-T and female sex. $R^2 = 0.60$; Adjusted $R^2 = 0.48$; Significance level <0.05.

TABLE 3 Multiple linear regression model with EQ-VAS at follow-up as dependent variable and outcome parameter.

Model variables	Unstandardized coefficients		Standardized coefficients	Significance level
	B	Standard. error	Beta	
(Constant)	153.07	26.13		0.00
Sex	5.85	6.84	0.15	0.40
Age	−0.64	0.27	−0.47	0.03
STAI-T	−0.87	0.31	−0.53	0.01
Lesion volume	0.48	0.35	0.22	0.18
DHI acute stage	−0.38	0.14	−0.51	0.02
STAI-T_Sex	0.11	0.61	0.03	0.87

Lesion volume: in voxels divided by factor 1,000; STAI-T_Sex: interaction variable of STAI-T and female sex. $R^2 = 0.56$; Adjusted $R^2 = 0.43$; Significance level < 0.05.

Discussion

The major findings of this longitudinal cohort study in patients with vestibular stroke were the following: (1) The overall prognosis of vestibular stroke was favorable. Scores for HRQoL, functioning and symptom intensity indicated a relevant long-term improvement on a group level. (2) The most important prognostic markers for enduring symptoms were patient-related factors, such as a higher degree of individual anxiety trait, especially combined with female gender, lesion-related factors, namely, stroke volume, and symptom-related factors, i.e., symptom severity in the acute stroke stage. (3) Worse subjective overall health status after vestibular stroke was related to older age, more trait anxiety, and more severe acute vertigo/dizziness symptoms. These findings emphasize the need for a multifaceted evaluation of patients with posterior circulation stroke (including psychological traits), in order to better estimate their functional outcome, and tailor therapeutic decisions (in the acute stage and during rehabilitation) to individual risk. In the following discussion, we will specifically address the importance of symptom-, patient-, and lesion-related features for functional outcomes in vestibular stroke.

Relevance of acute vestibular symptoms for functional outcome

The extent of acute symptoms of a vestibular stroke may greatly vary across patients (27). A recent study showed that patients with acute central vestibular disorders on average tend to have less vertigo-related symptoms than patients with acute peripheral vestibulopathies (8). However, until now it remained unclear, if the acute symptom load may also predict the long-term functional outcome in vestibular stroke. In this study, regression models (for DHI and EQ-VAS at follow-up) clearly indicate that the degree of vertigo, dizziness, and imbalance in the acute stage of vestibular stroke has a significant impact on the long-term functional outcome and perceived health status (see

Tables 2, 3). This finding is in accordance with a previous study, which indicated a worse outcome for patients with isolated cerebellar stroke, if they had more severe initial symptoms measured by the modified International Cooperative Ataxia Rating Scale (MICARS) (28). A relation between acute stroke symptoms and outcome is also well established for anterior circulation stroke (29–31). However, functional impairment and disability in posterior circulation stroke are not well represented in widely used stroke scales (such as the National Institutes of Health Stroke Scale—NIHSS), which may lead to some neglect for symptom severity in cerebellar and brain stem stroke. There is a need to establish and validate scales adapted to the posterior circulation to allow for a better assessment of HRQoL in patients with the chief complaints of vertigo, dizziness, imbalance, and double vision. Generally, the functional recovery after cerebellar and brain stem stroke is good in most cases both in our study and in literature (28, 32–35).

Outcome prediction cannot be based on quantitative testing of vestibular, ocular motor, or postural function only. While in acute vestibular stroke a moderate correlation is observed between the extent of spontaneous nystagmus and the severity of symptoms (8), many studies have failed to indicate a relationship between vestibular function tests (such as head impulse test and caloric irrigation) and subjective symptom severity in chronic vestibulopathies (9, 36). Similarly, in this study, vestibular test results assessed during the acute stroke stage (e.g., horizontal or vertical spontaneous nystagmus, and tilt of SVV) did not correlate with long-term functional outcome markers (data not shown). Given that vestibular signs in brain stem-cerebellar stroke tend to compensate rapidly (14) and completely (in 87% of patients in this study), it seems likely that the perceived symptoms and impairments are not related to vestibular processing only.

Patient characteristics and traits as risk factors for worse outcome

In this study, anxiety trait, especially in combination with the female gender, was the most important patient-related predictor for functional outcome after vestibular stroke, while the effect of age was ambiguous (Tables 2, 3). Anxiety scores (STAI-T/STAI-S), depression scores (PHQ-9), vertigo-related symptom scores (DHI), and HRQoL scores (EQ-VAS) on follow-up showed a moderate to strong correlation in our study cohort. It is well established for various peripheral vestibular disorders that anxiety and depression have a significant impact on the symptom course and are associated with higher total DHI scores (6, 7, 37, 38). Anxiety and depression are closely related to secondary functional dizziness in vestibular disorders (7, 11, 12, 39, 40). On the contrary, anxiety and depression are negative predictors of functional recovery after stroke (41, 42). There are different potential explanation models for why anxiety may cause persistent dizziness following acute vestibular lesions: anxious patients tend to perceive vestibular symptoms and balance-related body sensations more intensely, which in turn leads to an unfavorable closed loop and voluntary motor control (including muscle co-contractions) (43). Anxiety-related avoidance behavior may result in reduced physical activity and consequently less sensorimotor adaptation to balance problems (5). This study is to our best knowledge the first to establish the impact of anxiety on functional outcomes also for patients with acute vestibular stroke.

Regression models in this study suggest a gender-sensitive impact of anxiety on the course of symptoms, i.e., anxiety and female gender had an additive effect on symptom persistence. On the contrary, gender as a single feature had no significant impact on outcome after vestibular stroke. The effect of gender in our study cohort seems to be mediated rather by accompanying anxiety traits. Epidemiological studies have shown that the prevalence of anxiety and depression in women is higher both in the general population and in patients with vestibular symptoms (44–46). Female patients seem to be more severely impaired by vestibular symptoms (36, 38, 47). Furthermore, women more often develop post-stroke depression. Therefore, female patients seem to be more vulnerable to enduring symptoms and perceived impairment mediated by anxiety and avoidance behavior following brain stem-cerebellar stroke, which is reflected by higher mean DHI scores as compared to men in our study (data not shown).

Patient age was not relevant for symptom severity at follow-up. This observation is in accordance with a study on isolated cerebellar strokes, which also found no age effect on the outcome (28). On the contrary, several studies on patients with anterior circulation stroke have shown worse outcomes (loss of independent living and mortality) with older age (29, 48). This seems reasonable at first sight, as older patients have more comorbidities, which may impair their recovery. The question remains if there is a basic difference in the compensation and recovery of vestibular symptoms (e.g., vertigo) and non-vestibular symptoms (e.g., hemiparesis). Previous studies suggested that older patients with vestibular disorders might recover to a similar extent as younger patients with a comparable vestibular lesion (49). However, other groups have documented some age-dependency of central vestibular compensation and plasticity (50, 51). One factor, which needs to be considered for this study cohort, is the mean age of 66 years. For supratentorial strokes, patients above the age of 70 years had persistent disability and worse outcome (52). Therefore, it remains an open question for further investigations, i.e., if very old patients will have an age-dependent decline in functional outcomes.

Does stroke volume and localization predict outcome in vestibular stroke?

This study indicated stroke volume as a significant predictor of symptoms severity (Table 2). Previous studies were reporting controversial results about the impact of lesion size in posterior circulation strokes. Two previous studies also found stroke volume in cerebellar infarcts to be associated with outcome (34, 53). However, other studies failed to demonstrate a correlation between lesion size and persistent symptoms, but emphasized the importance of lesion localization and affected vascular territories for the latter (28, 33, 35). Ischemia in the SCA territory seems to cause more severe long-term impairment compared to PICA strokes, which is commonly explained by a higher degree of leg and gait ataxia in SCA strokes (28, 33, 54, 55). In the PICA territory, lesions in the posterior cerebellar lobe and around the dentate nucleus are associated with more persistent symptoms (35, 56). Furthermore, Baier and colleagues showed a clustering of impaired vestibular compensation of an SVV tilt with lesions of the lateral cerebellar hemispheres (lobule V, VI, VIIa) (57). For this study, we did neither find a difference of SCA vs. PICA strokes, nor of cerebellar vs. brain stem strokes, which most likely can be explained by the relatively small cohorts. For determination of the impact of lesion localization on functional outcome, more dedicated lesion-symptom mapping studies in larger cohorts of patients are needed.

Strengths and limitations of the study

This prospective study included patient-related, symptom-related, and lesion-related factors to describe long-term disability and functional outcome of patients with vestibular stroke, instead of only evaluating quantitative neurophysiological parameters (such as SVV or spontaneous nystagmus). We think that this approach accounts more appropriately for the determinants involved in functional compensation and recovery after vestibular stroke. A limitation of this study is the variable timespan to follow-up. While all but two patients were followed >1 year after stroke, the exact timespan was not standardized. However, adjusting the regression models to the time of follow-up or excluding the two patients with a follow-up of <1 year after stroke did not change the results and relevant factors for the outcome (Supplementary Table 2). The main findings of this study remain stable, even though follow-up times varied within patients.

Conclusion

The individual functional outcome in vestibular stroke mostly depends on the experience of acute symptom severity, unfavorable coping strategies for impairment by anxiety trait (especially in women), more extensive network damage by larger lesion volume, and older age. For the acute assessment of patients with vestibular stroke, commonly used stroke scales (such as the NIHSS or mRS) do not properly account for these factors. More meaningful scores and scales for the quantification of impairment and prediction of functional outcomes should be established in the future. Treatment plans should adapt the intensity of rehabilitation after vestibular stroke to the patients' risk factors. Psychological therapy elements should be considered in case of high anxiety traits.

Data availability statement

The raw data supporting the conclusions of this article will be made available by the authors, without undue reservation.

Ethics statement

The studies involving human participants were reviewed and approved by Ethics Committee of the University of Munich. The patients/participants provided their written informed consent to participate in this study.

Author contributions

FS: study concept, collection of data, statistical analysis, data interpretation, and drafting of the manuscript. RS and EG: statistical analysis, data interpretation, and review of the manuscript. JC: imaging analysis, data interpretation, and review of the manuscript. KM and PJ: collection of data, data interpretation, and review of the manuscript. KJ: study concept, data interpretation, and review of the manuscript. MD: data interpretation and review of the manuscript. AZ: study planning, funding, data interpretation, drafting, and reviewing of the manuscript. All authors contributed to the article and approved the submitted version.

Funding

This study was funded by the German Federal Ministry of Education and Research (BMBF) (Grant Number 01 EO 1401).

Conflict of interest

The authors declare that the research was conducted in the absence of any commercial or financial relationships

that could be construed as a potential conflict of interest.

Publisher's note

All claims expressed in this article are solely those of the authors and do not necessarily represent those of their affiliated organizations, or those of the publisher, the editors and the reviewers. Any product that may be evaluated in this article, or claim that may be made by its manufacturer, is not guaranteed or endorsed by the publisher.

Supplementary material

The Supplementary Material for this article can be found online at: https://www.frontiersin.org/articles/10.3389/fneur.2022.957283/full#supplementary-material

References

1. Feigin VL, Nguyen G, Cercy K, Johnson CO, Alam T, Parmar PG, et al. Global, regional, and country-specific lifetime risks of stroke, 1990 and 2016. *N Engl J Med.* (2018) 379:2429–37. doi: 10.1056/NEJMoa1804492

2. Schonewille WJ, Wijman CA, Michel P, Rueckert CM, Weimar C, Mattle HP, et al. Treatment and outcomes of acute basilar artery occlusion in the Basilar Artery International Cooperation Study (BASICS): a prospective registry study. *Lancet Neurol.* (2009) 8:724–30. doi: 10.1016/S1474-4422(09)70173-5

3. Kasner SE. Clinical interpretation and use of stroke scales. *Lancet Neurol.* (2006) 5:603–12. doi: 10.1016/S1474-4422(06)70495-1

4. Zwergal A, Dieterich M. Vertigo and dizziness in the emergency room. *Curr Opin Neurol.* (2020) 33:117–25. doi: 10.1097/WCO.0000000000000769

5. Yardley L, Redfern MS. Psychological factors influencing recovery from balance disorders. *J Anxiety Disord.* (2001) 15:107–19. doi: 10.1016/S0887-6185(00)00045-1

6. Dros J, Maarsingh OR, Beem L, van der Horst HE, ter Riet G, Schellevis FG, et al. Functional prognosis of dizziness in older adults in primary care: a prospective cohort study. *J Am Geriatr Soc.* (2012) 60:2263–9. doi: 10.1111/jgs.12031

7. Cousins S, Kaski D, Cutfield N, Arshad Q, Ahmad H, Gresty MA, et al. Predictors of clinical recovery from vestibular neuritis: a prospective study. *Ann Clin Transl Neurol.* (2017) 4:340–6. doi: 10.1002/acn3.386

8. Möhwald K, Hadzhikolev H, Bardins S, Becker-Bense S, Brandt T, Grill E, et al. Health-related quality of life and functional impairment in acute vestibular disorders. *Eur J Neurol.* (2020) 27:2089–98. doi: 10.1111/ene.14318

9. Yip CW, Strupp M. The Dizziness Handicap Inventory does not correlate with vestibular function tests: a prospective study. *J Neurol.* (2018) 265:1210–8. doi: 10.1007/s00415-018-8834-7

10. Tschan R, Best C, Beutel ME, Knebel A, Wiltink J, Dieterich M, et al. Patients' psychological well-being and resilient coping protect from secondary somatoform vertigo and dizziness (SVD) 1 year after vestibular disease. *J Neurol.* (2011) 258:104–12. doi: 10.1007/s00415-010-5697-y

11. Eckhardt-Henn A, Best C, Bense S, Breuer P, Diener G, Tschan R, et al. Psychiatric comorbidity in different organic vertigo syndromes. *J Neurol.* (2008) 255:420–8. doi: 10.1007/s00415-008-0697-x

12. Lahmann C, Henningsen P, Brandt T, Strupp M, Jahn K, Dieterich M, et al. Psychiatric comorbidity and psychosocial impairment among patients with vertigo and dizziness. *J Neurol Neurosurg Psychiatry.* (2015) 86:302–8. doi: 10.1136/jnnp-2014-307601

13. Decker J, Limburg K, Henningsen P, Lahmann C, Brandt T, Dieterich M, et al. Intact vestibular function is relevant for anxiety related to vertigo. *J Neurol.* (2019) 266:89–92. doi: 10.1007/s00415-019-09351-8

14. Cnyrim CD, Rettinger N, Mansmann U, Brandt T, Strupp M. Central compensation of deviated subjective visual vertical in Wallenberg's syndrome. *J Neurol Neurosurg Psychiatry.* (2007) 78:527–8. doi: 10.1136/jnnp.2006.100727

15. Möhwald K, Bardins S, Muller HH, Jahn K, Zwergal A. Protocol for a prospective interventional trial to develop a diagnostic index test for stroke as a cause of vertigo, dizziness and imbalance in the emergency room (EMVERT study). *BMJ Open.* (2017) 7:e019073. doi: 10.1136/bmjopen-2017-019073

16. Zwergal A, Rettinger N, Frenzel C, Dieterich M, Brandt T, Strupp MA, et al. bucket of static vestibular function. *Neurology.* (2009) 72:1689–92. doi: 10.1212/WNL.0b013e3181a55ecf

17. Ludwig K, Graf von der Schulenburg JM, Greiner W. German value set for the EQ-5D-5L. *Pharmacoeconomics.* (2018) 36:663–74. doi: 10.1007/s40273-018-0615-8

18. Uyttenboogaart M, Stewart RE, Vroomen PCAJ, De Keyser J, Luijckx GJ. Optimizing cutoff scores for the barthel index and the modified rankin scale for defining outcome in acute stroke trials. *Stroke.* (2005) 36:1984–7. doi: 10.1161/01.STR.0000177872.87960.61

19. Harrison JK, McArthur KS, Quinn TJ. Assessment scales in stroke: clinimetric and clinical considerations. *Clin Interv Aging.* (2013) 8:201–11. doi: 10.2147/CIA.S32405

20. Jacobson GP, Newman CW. The development of the Dizziness Handicap Inventory. *Arch Otolaryngol Head Neck Surg.* (1990) 116:424–7. doi: 10.1001/archotol.1990.01870040046011

21. Spielberger CD. *State-Trait Anxiety Inventory for Adults*. Palo Alto, CA: Consulting Psychologists Press, Inc; published by Mind Garden, Inc. (1983).

22. Spitzer RL, Kroenke K, Williams JB. Validation and utility of a self-report version of PRIME-MD: the PHQ primary care study. Primary care evaluation of mental disorders patient health questionnaire. *JAMA.* (1999) 282:1737–44. doi: 10.1001/jama.282.18.1737

23. Kroenke K, Spitzer RL, Williams JB. The PHQ-9: validity of a brief depression severity measure. *J Gen Intern Med.* (2001) 16:606–13. doi: 10.1046/j.1525-1497.2001.016009606.x

24. Rorden C, Bonilha L, Fridriksson J, Bender B, Karnath HO. Age-specific CT and MRI templates for spatial normalization. *Neuroimage.* (2012) 61:957–65. doi: 10.1016/j.neuroimage.2012.03.020

25. Fazekas F, Kleinert R, Offenbacher H, Schmidt R, Kleinert G, Payer F, et al. Pathologic correlates of incidental MRI white matter signal hyperintensities. *Neurology.* (1993) 43:1683–9. doi: 10.1212/WNL.43.9.1683

26. Harris PA, Taylor R, Thielke R, Payne J, Gonzalez N, Conde JG, et al. Research electronic data capture (REDCap)—A metadata-driven methodology and workflow process for providing translational research informatics support. *J Biomed Inform.* (2009) 42:377–81. doi: 10.1016/j.jbi.2008.08.010

27. Zwergal A, Möhwald K, Salazar López E, Hadzhikolev H, Brandt T, Jahn K, et al. A prospective analysis of lesion-symptom relationships in acute vestibular and ocular motor stroke. *Front Neurol.* (2020) 11:822. doi: 10.3389/fneur.2020.00822

28. Nickel A, Cheng B, Pinnschmidt H, Arpa E, Ganos C, Gerloff C, et al. Clinical outcome of isolated cerebellar stroke—A prospective observational study. *Front Neurol.* (2018) 9:580. doi: 10.3389/fneur.2018.00580

29. Hénon H, Godefroy O, Leys D, Mounier-Vehier F, Lucas C, Rondepierre P, et al. Early predictors of death and disability after acute cerebral ischemic event. *Stroke.* (1995) 26:392–8. doi: 10.1161/01.STR.26.3.392

30. Macciocchi SN, Diamond PT, Alves WM, Mertz T. Ischemic stroke: relation of age, lesion location, and initial neurologic deficit to functional outcome. *Arch Phys Med Rehabil.* (1998) 79:1255–7. doi: 10.1016/S0003-9993(98)90271-4

31. Adams HP, Davis PH, Leira EC, Chang KC, Bendixen BH, Clarke WR, et al. Baseline NIH Stroke Scale score strongly predicts outcome after stroke: a report of the Trial of Org 10172 in Acute Stroke Treatment (TOAST). *Neurology.* (1999) 53:126–31. doi: 10.1212/WNL.53.1.126

32. Malm J, Kristensen B, Carlberg B, Fagerlund M, Olsson T. Clinical features and prognosis in young adults with infratentorial infarcts. *Cerebrovasc Dis.* (1999) 9:282–9. doi: 10.1159/000015979

33. Konczak J, Pierscianek D, Hirsiger S, Bultmann U, Schoch B, Gizewski ER, et al. Recovery of upper limb function after cerebellar stroke: lesion symptom mapping and arm kinematics. *Stroke.* (2010) 41:2191–200. doi: 10.1161/STROKEAHA.110.583641

34. Bultmann U, Pierscianek D, Gizewski ER, Schoch B, Fritsche N, Timmann D, et al. Functional recovery and rehabilitation of postural impairment and gait ataxia in patients with acute cerebellar stroke. *Gait Posture.* (2014) 39:563–9. doi: 10.1016/j.gaitpost.2013.09.011

35. Picelli A, Zuccher P, Tomelleri G, Bovi P, Moretto G, Waldner A, et al. Prognostic importance of lesion location on functional outcome in patients with cerebellar ischemic stroke: a prospective pilot study. *Cerebellum.* (2017) 16:257–61. doi: 10.1007/s12311-015-0757-6

36. Robertson DD, Ireland DJ. Dizziness Handicap Inventory correlates of computerized dynamic posturography. *J Otolaryngol.* (1995) 24:118–24.

37. Yardley L, Luxon LM, Haacke NPA. longitudinal study of symptoms, anxiety and subjective well-being in patients with vertigo. *Clin Otolaryngol Allied Sci.* (1994) 19:109–16. doi: 10.1111/j.1365-2273.1994.tb01192.x

38. Ten Voorde M, van der Zaag-Loonen HJ, van Leeuwen RB. Dizziness impairs health-related quality of life. *Qual Life Res.* (2012) 21:961–6. doi: 10.1007/s11136-011-0001-x

39. Godemann F, Siefert K, Hantschke-Brüggemann M, Neu P, Seidl R, Ströhle A, et al. What accounts for vertigo one year after neuritis vestibularis—anxiety or a dysfunctional vestibular organ? *J Psychiatr Res.* (2005) 39:529–34. doi: 10.1016/j.jpsychires.2004.12.006

40. Dieterich M, Staab JP. Functional dizziness: from phobic postural vertigo and chronic subjective dizziness to persistent postural-perceptual dizziness. *Curr Opin Neurol.* (2017) 30:107–13. doi: 10.1097/WCO.0000000000000417

41. van de Weg FB, Kuik DJ, Lankhorst GJ. Post-stroke depression and functional outcome: a cohort study investigating the influence of depression on functional recovery from stroke. *Clin Rehabil.* (1999) 13:268–72. doi: 10.1191/026921599672495022

42. Chun HY, Whiteley WN, Dennis MS, Mead GE, Carson AJ. Anxiety After Stroke: The Importance of Subtyping. *S troke.* (2018) 49:556–64. doi: 10.1161/STROKEAHA.117.020078

43. Wuehr M, Pradhan C, Novozhilov S, Krafczyk S, Brandt T, Jahn K, et al. Inadequate interaction between open- and closed-loop postural control in phobic postural vertigo. *J Neurol.* (2013) 260:1314–23. doi: 10.1007/s00415-012-6797-7

44. Yardley L, Owen N, Nazareth I, Luxon L. Prevalence and presentation of dizziness in a general practice community sample of working age people. *Br J Gen Pract.* (1998) 48:1131–5.

45. Piker EG, Jacobson GP, McCaslin DL, Grantham SL. Psychological comorbidities and their relationship to self-reported handicap in samples of dizzy patients. *J Am Acad Audiol.* (2008) 19:337–47. doi: 10.3766/jaaa.19.4.6

46. Gazzola JM, Aratani MC, Doná F, Macedo C, Fukujima MM, Ganança MM, et al. Factors relating to depressive symptoms among elderly people with chronic vestibular dysfunction. *Arq Neuropsiquiatr.* (2009) 67:416–22. doi: 10.1590/S0004-282X2009000300009

47. Vanspauwen R, Knoop A, Camp S, van Dinther J, Erwin Offeciers F, Somers T, et al. Outcome evaluation of the dizziness handicap inventory in an outpatient vestibular clinic. *J Vestib Res.* (2016) 26:479–86. doi: 10.3233/VES-160600

48. Brown RD, Ransom J, Hass S, Petty GW, O'Fallon WM, Whisnant JP, et al. Use of nursing home after stroke and dependence on stroke severity: a population-based analysis. *Stroke.* (1999) 30:924–9. doi: 10.1161/01.STR.30.5.924

49. Cohen HS, Kimball KT. Increased independence and decreased vertigo after vestibular rehabilitation. *Otolaryngol Head Neck Surg.* (2003) 128:60–70. doi: 10.1067/mhn.2003.23

50. Cassel R, Wiener-Vacher S, El Ahmadi A, Tighilet B, Chabbert C. Reduced balance restoration capacities following unilateral vestibular insult in elderly mice. *Front Neurol.* (2018) 9:462. doi: 10.3389/fneur.2018.00462

51. Yan T, Zong F, Han X, Wang X, Li Q, Qiao R, et al. Vestibular neuritis in patients among different age groups: clinical features and outcomes. *J Am Acad Audiol.* (2020) 31:629–35. doi: 10.1055/s-0040-1717067

52. Fiorelli M, Alpérovitch A, Argentino C, Sacchetti ML, Toni D, Sette G, et al. Prediction of long-term outcome in the early hours following acute ischemic stroke. Italian acute stroke study group. *Arch Neurol.* (1995) 52:250–5. doi: 10.1001/archneur.1995.00540270038017

53. Calic Z, Cappelen-Smith C, Cuganesan R, Anderson CS, Welgampola M, Cordato DJ, et al. Frequency, aetiology, and outcome of small cerebellar infarction. *Cerebrovasc Dis Extra.* (2017) 7:173–80. doi: 10.1159/000481459

54. Tohgi H, Takahashi S, Chiba K, Hirata Y. Cerebellar infarction. Clinical and neuroimaging analysis in 293 patients The Tohoku Cerebellar Infarction Study Group. *Stroke.* (1993) 24:1697–701. doi: 10.1161/01.STR.24.11.1697

55. Kelly PJ, Stein J, Shafqat S, Eskey C, Doherty D, Chang Y, et al. Functional recovery after rehabilitation for cerebellar stroke. *Stroke.* (2001) 32:530–4. doi: 10.1161/01.STR.32.2.530

56. Schoch B, Dimitrova A, Gizewski ER, Timmann D. Functional localization in the human cerebellum based on voxelwise statistical analysis: a study of 90 patients. *Neuroimage.* (2006) 30:36–51. doi: 10.1016/j.neuroimage.2005.09.018

57. Baier B, Müller N, Rhode F, Dieterich M. Vestibular compensation in cerebellar stroke patients. *Eur J Neurol.* (2015) 22:416–408. doi: 10.1111/ene.12475

frontiers | Frontiers in Neurology

TYPE Original Research
PUBLISHED 08 September 2022
DOI 10.3389/fneur.2022.919777

OPEN ACCESS

EDITED BY
Dominik Straumann,
University of Zurich, Switzerland

REVIEWED BY
Leonel Luis,
Hospital de Santa Maria, Portugal
Luke Chen,
Monash University, Australia
Sun-Uk Lee,
Korea University Medical Center, South Korea

*CORRESPONDENCE
Georgios Mantokoudis
georgios.mantokoudis@insel.ch

SPECIALTY SECTION
This article was submitted to Neuro-Otology, a section of the journal Frontiers in Neurology

RECEIVED 13 April 2022
ACCEPTED 15 August 2022
PUBLISHED 08 September 2022

CITATION
Korda A, Wimmer W, Wyss T, Michailidou E, Zamaro E, Wagner F, Caversaccio MD and Mantokoudis G (2022) Artificial intelligence for early stroke diagnosis in acute vestibular syndrome. *Front. Neurol.* 13:919777. doi: 10.3389/fneur.2022.919777

Artificial intelligence for early stroke diagnosis in acute vestibular syndrome

Athanasia Korda[1], Wilhelm Wimmer[1,2], Thomas Wyss[1], Efterpi Michailidou[1], Ewa Zamaro[1], Franca Wagner[3], Marco D. Caversaccio[1] and Georgios Mantokoudis[1]*

[1]Department of Otorhinolaryngology, Head and Neck Surgery, Inselspital, University Hospital Bern and University of Bern, Bern, Switzerland, [2]Hearing Research Laboratory, ARTORG Center, University of Bern, Bern, Switzerland, [3]University Institute of Diagnostic and Interventional Neuroradiology, Inselspital, University Hospital Bern and University of Bern, Bern, Switzerland

Objective: Measuring the Vestibular-Ocular-Reflex (VOR) gains with the video head impulse test (vHIT) allows for accurate discrimination between peripheral and central causes of acute vestibular syndrome (AVS). In this study, we sought to investigate whether the accuracy of artificial intelligence (AI) based vestibular stroke classification applied in unprocessed vHIT data is comparable to VOR gain classification.

Methods: We performed a prospective study from July 2015 until April 2020 on all patients presenting at the emergency department (ED) with signs of an AVS. The patients underwent vHIT followed by a delayed MRI, which served as a gold standard for stroke confirmation. The MRI ground truth labels were then applied to train a recurrent neural network (long short-term memory architecture) that used eye- and head velocity time series extracted from the vHIT examinations.

Results: We assessed 57 AVS patients, 39 acute unilateral vestibulopathy patients (AUVP) and 18 stroke patients. The overall sensitivity, specificity and accuracy for detecting stroke with a VOR gain cut-off of 0.57 was 88.8, 92.3, and 91.2%, respectively. The trained neural network was able to classify strokes with a sensitivity of 87.7%, a specificity of 88.4%, and an accuracy of 87.9% based on the unprocessed vHIT data. The accuracy of these two methods was not significantly different ($p = 0.09$).

Conclusion: AI can accurately diagnose a vestibular stroke by using unprocessed vHIT time series. The quantification of eye- and head movements with the use of machine learning and AI can serve in the future for an automated diagnosis in ED patients with acute dizziness. The application of different neural network architectures can potentially further improve performance and enable direct inference from raw video recordings.

KEYWORDS

vertigo, artificial intelligence, video head impulse test, stroke diagnosis, emergency department

Introduction

Strokes presenting with symptoms of dizziness or vertigo often mimic benign inner ear diseases, which can lead to misdiagnosis by physicians (1). Failure to rapidly diagnose and promptly treat such strokes often results in disability or death (2). Strokes occur in up to 8% of dizzy patients presenting in the emergency department (ED) (3) and any support tool reducing stroke misdiagnosis is very important.

Currently, the most widely accepted triage tool for stroke detection in dizzy patients in the ED is the "HINTS" eye movement examination (4). "HINTS" is used as an acronym for the head impulse test, nystagmus test and test of skew. Such a clinical test can be applied in a timely and efficient manner at the bedside. However, the correct application and test assessment needs expertise, which is not always readily available. Even experts struggle with the assessment of head impulses when hidden (covert) corrective saccades and spontaneous nystagmus occur (5). In comparison to a clinical assessment, videooculography (VOG) devices enables a quantification of eye- and head movements at the bedside, which can improve the accuracy of HINTS (6, 7). The Vestibular-Ocular-Reflex (VOR) gain by video head impulse (vHIT), especially, has already been successfully used to differentiate between central and peripheral causes in patients with an acute vestibular syndrome (AVS) (6, 8).

These VOG devices are easy to use (9) and they can serve in the near future with telemedicine (10) and machine intelligence in a remoted setting such as smaller community hospitals lacking onsite experts, or in pandemic times as a diagnostic tool for acute dizziness (11, 12). VOG could potentially support physicians in the ED analog to an Eye ECG (13). Artificial intelligence (AI) has been suggested to improve stroke diagnosis in EDs, by implementing machine learning-enabled clinical decision support systems (14, 15). A concrete application of deep learning to vestibular disorder classification using videonystagmography was presented by Ben Slama et al. (16). The advantage of AI applied on raw VOG data for its assessment is the holistic approach on unprocessed head impulse test data compared to partial assessments such as VOR gain at one single time point or saccade latencies. Current analysis of vHIT data depend on the parameters assessed and the associated calculation methods (17).

In this study, we tried to test automated AI stroke classification based on vHIT time series and to compare whether the accuracy of the AI-based method is comparable to VOR gain based stroke classification.

Abbreviations: AVS, acute vestibular syndrome; AUVP, acute unilateral vestibulopathy; HINTS, Head-Impulse-Nystagmus-Test-of-Skew; ED, emergency department.

Materials and methods

Study design and patient characteristics

In this prospective, cross-sectional study, data were collected in the ED during office hours between 07/2015 and 04/2020, which was part of a larger study (DETECT–Dizziness Evaluation Tool for Emergent Clinical Triage). The local ethics committee (Kant. Ethikkommission Bern) approved this study (KEK # 047/14). We included patients with AVS who had a continuous dizziness, associated with nausea or vomiting, head-motion intolerance, new gait or balance disturbance, and nystagmus. We excluded patients younger than 18 years, if symptoms abated after 24 h, or if the index ED visit was >72 h after symptom onset. Patients with previous eye movement or vestibular disorders were also excluded. All enrolled patients gave written consent.

VHIT measurements

A subset of VOR gain data presented here have been published elsewhere (6, 18–21). A neurootologist with 2 years' experience in the field, performed physical examination, Caloric Testing, and vHIT testing in all enrolled patients. vHIT was performed using the EyeSeeCam (EyeSeeTec GmbH) (22) and by applying fast passive horizontal head movements (high frequency, 10–20° head excursion in 100–300 milliseconds corresponding to a 1,000–6,000°/sec^2 acceleration) in room light during visual target fixation at more than 1m distance. We assessed only data from valid vHIT marked by the device following data quality criteria such as peak head velocity exceeding 70°/s within the first 150 milliseconds with a head exceeding 1,000°/sec^2. Head impulses were excluded if the eyes or head were moving (>20°/s) before the onset of the head impulse or if the direction of the head impulse was not in the horizontal plane (i.e., within ±45°). Outliers regarding peak head velocity (1.5-fold interquartile range) were rejected (23). Two neurootologists (GM, AK) in a consensus meeting reviewed all vHITs for data quality and artifacts. Only clean data with non-disruptive artifacts were included based on a predefined classification (24).

Patient labeling and stroke diagnosis

All patients received an acute MR brain scan either within 48 h in the ED or a second, delayed MRI (3–10 days after symptoms onset), if there was no acute MRI indicated based on clinical grounds or if the first acute MRI was non-diagnostic. The delayed MRI served as a gold standard for stroke detection. A blinded experienced board-certified senior consultant in neuroradiology re-assessed all MRIs.

Patients with a negative MRI and a pathological caloric test were classified as acute unilateral vestibulopathy (AUVP) / vestibular neuritis.

VOR gain based stroke classification

VOR gain values were derived from eye velocity divided by head velocity at 60 ms after HIT onset. We calculated a best discrimination cut-off for stroke by applying a receiver operating characteristics curve (ROC). We did not use saccade analysis, since the currently used VOG software did not offer an automated feature for saccade analysis.

AI-based stroke classification of VOG

All data were evaluated in a time course between "start of head impulse" (which was defined as the point 250 ms before the maximal head velocity) and 700 ms after head movement stopped. Then all head impulses for both horizontal directions (right, left) of a single patient were concatenated into time series with two channels (channel 1: head velocity, channel 2: eye velocity). For classification, a neural network using a long short-term memory architecture with 64 hidden layers was trained with a batch size of 512 samples for 256 epochs (Figure 1). The neural net was implemented using MATLAB (Version R2020b, Mathworks, Inc., Natick, US). The data was split in a 70% training set ($N = 40$ patients) and a 30% test data set ($N = 17$ patients). The assignment of patients for the training and validation data set were randomly shuffled before each training epoch of the neural network to avoid overfitting to the training data set. To account for different time series lengths for individual patients, all input data were segmented into data-streams of 512 samples, typically covering 3 consecutive vHITs. One of our goals was to reduce the preprocessing of the data to a minimum. Therefore, we wanted the neural network to be able to process vHIT time sequences with different lengths (depending on the number of tests performed and the recording duration). Since our neural network requires input streams with constant length, we needed to find a suitable length for the data streams to avoid extensive padding and truncating. In our data, most sequences had about 4,100 samples, the shortest had 1,200 samples, and the longest consisted of 9,266 samples. To cover this range, we chose a stream length of 512 samples (practical sample size as a power of 2), which approximately corresponds to 3 vHITs. We also tried other sequence lengths, but found that a data stream length of 512 samples and a mini-batch size of 512 samples worked well. Data balancing was performed to avoid a biased training outcome of the network toward the more frequent "no stroke" cases (AUVP) by duplicating sequences (over-sampling) of the stroke data set to result in an equal amount of AUVP and stroke sequences. In total, this resulted in 535 data-streams for training and 233 data-streams for testing. No filtering of the time series was performed. All data streams were standardized by subtracting the overall mean value of the head and eye velocities and dividing by the standard deviation.

Statistical analysis

Descriptive statistics were reported using SPSS statistical software (IBM SPSS Statistics for Windows, Version 25.0. Armonk, NY: IBM Corp.). We used a binary logistic regression to evaluate stroke predictors derived from VOR gains and AI-Scores. We calculated a receiver characteristics curve (ROC) with its corresponding sensitivity, specificity, and accuracy for each test. Best cut-off points based on Youden's J. The two ROC curves were compared using the method of DeLong et al. (25).

Results

We analyzed data from 57 patients aged between 30 and 78 years (average 55 years) with a diagnosis of stroke or AUVP and valid vHIT measurements. Gold standard classification assigned (39 with AUVP and 18 with stroke).

VOR-gain based stroke classification of VHIT

We found odds ratio of 3.3 with a significant increase of stroke probability for each VOR gain increment of 1.194 ($p < 0.001$, CI 1.785–6.106) (see Table 1). The overall sensitivity and specificity for detecting a stroke with a VOR gain cut-off of 0.57 was 88.8 and 92.3% respectively and thus the accuracy was 91.2% (Table 2 and Figure 3).

AI-based stroke classification of VHIT

Table 1 shows the odds ratio of 1.52 with a significant increase of stroke probability for each AI score increment of 0.422 ($p < 0.001$, CI 1.394–1.669). The obtained network was able to classify strokes with an accuracy of 87.9% with a sensitivity of 87.7% and specificity of 88.4% (Table 2 and Figure 3). Example of the neural network activation patterns for a data-stream of an AUVP and a stroke patient are shown in Figure 2. Artifacts such as goggles slippage or head overshoot at the HIT end

FIGURE 1
Diagram of the recurrent neural network architecture used for the classification of VOG times series. A bidirectional long short-term memory (BiLSTM) model was used to enable context awareness between past and following sequences in a given time series of a patient.

TABLE 1 Logistic regression and predictive variables.

Test variable	Regression coefficient	Standard error	Wald	df	*p*-Value	Odds ratio	95% CI	
							Lower limit	Upper limit
VOR gain	1.194	0.314	14.500	1	<0.001	3.302	1.785	6.106
AI-score	0.422	0.046	84.698	1	<0.001	1.525	1.394	1.669

CI 95% confidence intervals, df degree of freedom.

TABLE 2 ROC curve.

	VOR gain	AI-score
Area under the curve	0.95	0.88
Std-error	0.03	0.23
p-Value	0.00	0.00
95% Lower limit	0.89	0.83
95% Upper limit	1.00	0.93
Positive, if smaller or equal*	0.57	0.46
Sensitivity	0.88	0.87
Specificity	0.92	0.88
Accuracy	0.91	0.87
Negative predictive value	0.95	0.80
Positive predictive value	0.84	0.92
Positive likelihood ratio	11	7.25
Negative likelihood ratio	0.13	0.14

*cut-off.

(Figure 2) were occurring randomly (random noise/variation) (17) with no systematic bias. There was no statistical difference between the two ROC curves ($p = 0.92$) and thus, there was no inferiority regarding AI classification (Figure 3).

Discussion

Our study showed that AI-based classification of unprocessed vHIT time series has a high accuracy und is as accurate as the VOR gain classification for differentiation between vestibular strokes and peripheral AVS.

Machine learning and the head impulse test

Our analysis showed encouraging results using a recurrent neural network architecture (long short-term memory) for the binary classification task ("stroke" vs. "no-stroke") of VOG time series as exported by the diagnostic software. The input time series were eye (from one eye only) and head velocities, taken from head impulses.

VOR gain using a vHIT device can be calculated by various methods (17). We used the velocity gain at 60 ms in order to avoid any bias from covered saccades or spontaneous nystagmus. Gain calculation might be more susceptible to artifacts and wrong eye calibrations resulting in wrong gain estimations compared to AI, which considers the whole velocity profile data. Therefore, it is mandatory to inspect visually the velocity profile of slow phase VOR which needs to be bell-shaped and not contaminated with artifacts. Such manual assessment needs expertise by the examiner.

With the advent of machine learning, these steps can be combined into a single machine-learning instance that is trained to directly classify eye movement video recordings (26). However, there are two steps that need to occur prior to trying to classify any new recording. First, a large dataset must be collected and labeled by a set of experts. This labeling must correspond with the indented classification to be performed by the machine. For example, a recording in a dataset could be labeled as stroke or no stroke according to neuroimaging results. Then, the machine is trained with this dataset and becomes ready to classify new recordings. Machine learning may increase its diagnostic accuracy by combining results and features obtained from multiple tests like nystagmus test and test of skew (14), or can also be used to only replace an individual step or group of steps in the classical analysis pipeline.

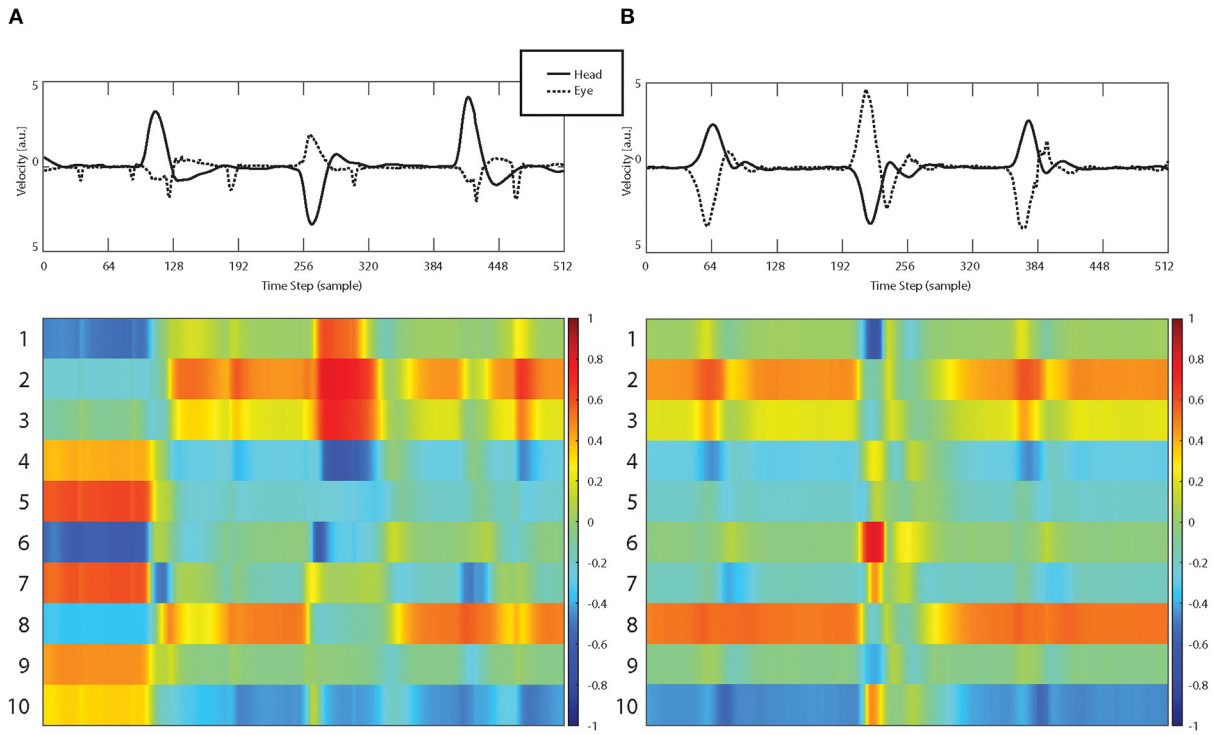

FIGURE 2
Examples of vHIT input streams (top row, raw data including artifacts) consisting of eye velocity (dashed curve) and head velocity (continuous curve) time series and corresponding activation patterns of the first 10 hidden LSTM layers for a patient with AUVP **(A)** and a stroke patient **(B)**.

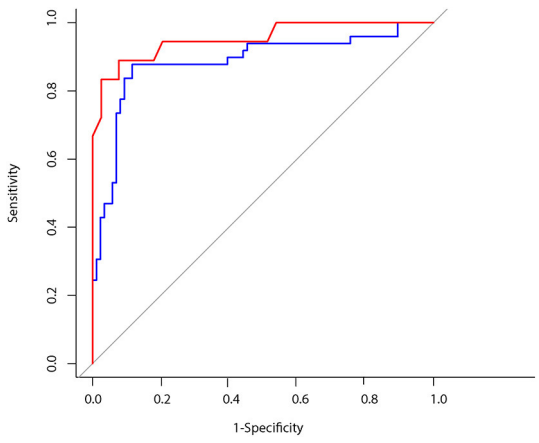

FIGURE 3
Blue line: ROC CURVE using artificial intelligence for head impulse test interpretation AUC: 0.88. Red line: ROC CURVE using VOR gain to predict a vestibular stroke AUC: 0.95.

While other studies used different data sets to apply AI on vestibular disorders (14, 27, 28), we chose to try AI in vHIT data because HIT has been previously considered the most important component of HINTS with a 18-fold stroke probability in AVS patients with a bilateral normal HIT (29). Accuracy of AI in stroke detection depends not only on the quality of disease labeling but also on the quality of the collected data. An expert can improve data quality of each performed impulse by encouraging subjects to keep their eyes open and by avoiding any physical contact between the examiners hand and the goggles. Applying specific recording techniques and avoiding some known pitfalls during eye- and head tracking minimize the risk of artifacts (9, 24, 30). Moreover, data from all impulses are averaged, further reducing the effect of noise or artifacts in single impulse (24).

Our results of VOR gain accuracy are similar to older studies (8). The known dissociation between caloric test results and vHIT might affect the overall specificity of this test (6). A recent study showed a slight worsening of accuracy of AI for stroke classification based on HINTS data (14). This discrepancy may be explained by the fact that we used different data forms. We used unprocessed raw data (including artifacts), whereas they used only pre-processed/calculated VOR gain values for AI. A single VOR gain number does not reflect the whole dynamic of a head impulse and informative data such as corrective saccades are completely ignored. Our approach, however, included the whole vHIT trace including the complete slow phase VOR

(ascending, peak and descending velocity profile) and the fast phase responses (compensatory saccades) for a period of 700 ms. This more holistic approach explains the improved accuracy of AI for stroke classification.

Strength and limitations

To our knowledge, this is the first study, which used AI in raw vHIT time series for stroke classification in AVS. The biggest limitation of our study is the small sample size used to train the neural net. For this reason, although we obtained promising results, our study should be considered as exploratory. More training data from multicenter prospective studies may improve the performance, as data set size is usually a limiting factor in machine-learning studies (31). The long short-time memory architecture is a commonly used model for the classification of time series. We can envision the use of other network architectures, e.g., used for image segmentation and classification tasks to directly utilize raw video recordings as predictive variables. Moreover, additional data, such as gyroscope recordings can be included for improved robustness. In addition, we did not analyze other tests such as nystagmus and test of skew. We expect that the combination of several tests (which is reflected in the three steps "HINTS" exam), would further improve AI sensitivity (32). AVS patients suffer from imbalance and gait disturbance. Additional tests, such the assessment of stance and gait, can already be assessed automatically by the application of machine learning (14, 33) and might be added in future triage protocols.

The application of head impulse data for stroke classification is restricted only for AVS patients and should not be applied to every acute vertigo patient (30). This fact means that AI based ED triage with the head impulse test can only be applied on selected patients with true AVS and is not generalizable to all dizzy ED patients. Patients with other causes of vertigo such as benign paroxysmal positional vertigo (BPPV) should be evaluated by positional tests either on site or remotely by the application of telehealth programs (34). Other modern machine learning methods can be successfully applied on patients with recurrent vertigo (spontaneous episodic vertigo syndromes) such as Menière's disease and vestibular migraine (35). It might also be used for the triage of common vestibular disorders however, (36) current classification accuracy is still low.

Clinical implications

The prospective collection of big data is the prerequisite for a future successful implementation of AI in clinical decision support systems (37–39).

An application of AI on big dizziness data repositories in the future can lead to a development of an automated interpretation of VOG results or automated early stroke detection in at risk dizzy patients. Clinical decision support systems are highly recommended for the assessment of the vHIT or "HINTS," since computer algorithms assess more than single VOR gain values or catch-up saccade frequency. Bedside clinical HIT tests, however, rely exclusively on the presence of catch-up saccades and need further expertise, which is not readily available in the ED. We recommend, therefore, future multicentric observational studies with systematic quantitative recordings of eye- and head movements combined with telemedicine services on every dizzy patient. Such big data approach has the potential for an automated VOG triage as a point-of-care decision support tool. We, therefore, believe that a more holistic approach offered by AI could not only pave the way for a widespread use of vHIT in EDs but could also substantially improve the objective assessment of vHIT at the bedside.

Conclusion

AI can accurately diagnose a vestibular stroke by using only vHIT unprocessed data in patients with AVS. Automated vHIT assessment for stroke prediction was not inferior to the current approach assessing a single VOR gain value. However, the algorithm might be further improved by larger training data sets and the implementation of additional tests collected with VOG at the bedside. The quantification of eye- and head movements with the use of machine learning and AI is a promising future tool for an automated diagnosis in ED patients with acute dizziness.

Data availability statement

The original contributions presented in the study are included in the article/supplementary material, further inquiries can be directed to the corresponding author.

Ethics statement

The study was approved by the Local Ethics Committee (KEK # 047/14). The patients/participants provided their written informed consent to participate in this study.

Author contributions

AK: investigation, data curation, and writing—original draft. WW: conceptualization, methodology, formal analysis, and writing—review and editing. TW and EM: data curation. EZ and FW: investigation. MC: supervision and project

administration. GM: conceptualization, formal analysis, writing—review and editing, project administration, and funding acquisition. All authors contributed to the article and approved the submitted version.

Funding

This study was supported by the Swiss National Science Foundation #320030_173081.

Acknowledgments

EyeSeeTec GmbH loaned the VOG goggles.

Conflict of interest

The authors declare that the research was conducted in the absence of any commercial or financial relationships that could be construed as a potential conflict of interest.

Publisher's note

References

1. Newman-Toker DE, Moy E, Valente E, Coffey R, Hines AL. Missed diagnosis of stroke in the emergency department: a cross-sectional analysis of a large population-based sample. *Diagnosis.* (2014) 1:155–66. doi: 10.1515/dx-2013-0038

2. Saber Tehrani AS, Kattah JC, Mantokoudis G, Pula JH, Nair D, Blitz A, et al. Small strokes causing severe vertigo: frequency of false-negative MRIs and nonlacunar mechanisms. *Neurology.* (2014) 83:169–73. doi: 10.1212/WNL.0000000000000573

3. Goeldlin M, Gaschen J, Kammer C, Comolli L, Bernasconi CA, Spiegel R, et al. Frequency, aetiology, and impact of vestibular symptoms in the emergency department: a neglected red flag. *J Neurol.* (2019) 266:3076–86. doi: 10.1007/s00415-019-09525-4

4. Newman-Toker DE, Kerber KA, Hsieh YH, Pula JH, Omron R, Saber Tehrani AS, et al. HINTS outperforms ABCD2 to screen for stroke in acute continuous vertigo and dizziness. *Acad Emerg Med.* (2013) 20:986–96. doi: 10.1111/acem.12223

5. Korda A, Carey JP, Zamaro E, Caversaccio MD, Mantokoudis G. How good are we in evaluating a bedside head impulse test? *Ear Hear.* (2020) 41:1747–51. doi: 10.1097/AUD.0000000000000894

6. Morrison M, Korda A, Zamaro E, Wagner F, Caversaccio MD, Sauter TC, et al. Paradigm shift in acute dizziness: is caloric testing obsolete? *J Neurol.* (2022) 269:853–60. doi: 10.1007/s00415-021-10667-7

7. Newman-Toker DE, Saber Tehrani AS, Mantokoudis G, Pula JH, Guede CI, Kerber KA, et al. Quantitative video-oculography to help diagnose stroke in acute vertigo and dizziness: toward an ECG for the eyes. *Stroke.* (2013) 44:1158–61. doi: 10.1161/STROKEAHA.111.000033

8. Mantokoudis G, Tehrani AS, Wozniak A, Eibenberger K, Kattah JC, Guede CI, et al. VOR gain by head impulse video-oculography differentiates acute vestibular neuritis from stroke. *Otol Neurotol.* (2015) 36:457–65. doi: 10.1097/MAO.0000000000000638

9. Korda A, Sauter TC, Caversaccio MD, Mantokoudis G. Quantifying a learning curve for video head impulse test: pitfalls and pearls. *Front Neurol.* (2020) 11:615651. doi: 10.3389/fneur.2020.615651

10. Müller-Barna P, Hubert ND, Bergner C, Schütt-Becker N, Rambold H, Haberl RL, et al. Televertigo: diagnosing stroke in acute dizziness: a telemedicine-supported approach. *Stroke.* (2019) 50:3293–8. doi: 10.1161/STROKEAHA.119.026505

11. Chari DA, Wu MJ, Crowson MG, Kozin ED, Rauch SD. Telemedicine algorithm for the management of dizzy patients. *Otolaryngol Head Neck Surg.* (2020) 163:857–9. doi: 10.1177/0194599820935859

12. Murdin L, Saman Y, Rea P. The remote neuro-otology assessment - managing dizziness in the coronavirus disease 2019 era. *J Laryngol Otol.* (2020) 134:1120–2. doi: 10.1017/S0022215120002273

13. Newman-Toker DE, Curthoys IS, Halmagyi GM. Diagnosing stroke in acute vertigo: the HINTS family of eye movement tests and the future of the "eye ECG". *Semin Neurol.* (2015) 35:506–21. doi: 10.1055/s-0035-1564298

14. Ahmadi SA, Vivar G, Navab N, Möhwald K, Maier A, Hadzhikolev H, et al. Modern machine-learning can support diagnostic differentiation of central and peripheral acute vestibular disorders. *J Neurol.* (2020) 267:143–52. doi: 10.1007/s00415-020-09931-z

15. Abedi V, Khan A, Chaudhary D, Misra D, Avula V, Mathrawala D, et al. Using artificial intelligence for improving stroke diagnosis in emergency departments: a practical framework. *Ther Adv Neurol Disord.* (2020) 13:1756286420938962. doi: 10.1177/17562864209 38962

16. Ben Slama A, Mouelhi A, Sahli H, Zeraii A, Marrakchi J, Trabelsi H, et al. deep convolutional neural network for automated vestibular disorder classification using VNG analysis. *Comput Method Biomech Biomed Eng Imaging Vis.* (2020) 8:334–42. doi: 10.1080/21681163.2019.1699165

17. Zamaro E, Saber Tehrani AS, Kattah JC, Eibenberger K, Guede CI, Armando L, et al. VOR gain calculation methods in video head impulse recordings. *J Vestib Res.* (2020) 30:225–34. doi: 10.3233/VES-200708

18. Mantokoudis G, Korda A, Zee DS, Zamaro E, Sauter TC, Wagner F, et al. Bruns' nystagmus revisited: A sign of stroke in patients with the acute vestibular syndrome. *Eur J Neurol.* (2021) 28:2971–9. doi: 10.1111/ene. 14997

19. Mantokoudis G, Wyss T, Zamaro E, Korda A, Wagner F, Sauter TC, et al. Stroke prediction based on the spontaneous nystagmus suppression test in dizzy patients: a diagnostic accuracy study. *Neurology.* (2021) 97:e42–51. doi: 10.1212/WNL.0000000000012176

20. Korda A, Zamaro E, Wagner F, Morrison M, Caversaccio MD, Sauter TC, et al. Acute vestibular syndrome: is skew deviation a central sign? *J Neurol.* (2022) 269:1396–403. doi: 10.1007/s00415-021-10692-6

21. Korda A, Zee DS, Wyss T, Zamaro E, Caversaccio MD, Wagner F, et al. Impaired fixation suppression of horizontal vestibular nystagmus during smooth pursuit: pathophysiology and clinical implications. *Eur J Neurol.* (2021) 28:2614–21. doi: 10.1111/ene.14909

22. Schneider E, Villgrattner T, Vockeroth J, Bartl K, Kohlbecher S, Bardins S, et al. EyeSeeCam: an eye movement-driven head camera for the examination of natural visual exploration. *Ann N Y Acad Sci.* (2009) 1164:461–7. doi: 10.1111/j.1749-6632.2009.03858.x

23. Glasauer S, von Lindeiner H, Siebold C, Büttner U. Vertical vestibular responses to head impulses are symmetric in downbeat nystagmus. *Neurology.* (2004) 63:621–5. doi: 10.1212/01.WNL.0000135022.14937.A9

24. Mantokoudis G, Saber Tehrani AS, Wozniak A, Eibenberger K, Kattah JC, Guede CI, et al. Impact of artifacts on VOR gain measures by video-oculography in the acute vestibular syndrome. *J Vestib Res.* (2016) 26:375–85. doi: 10.3233/VES-160587

25. DeLong ER, DeLong DM, Clarke-Pearson DL. Comparing the areas under two or more correlated receiver operating characteristic curves: a nonparametric approach. *Biometrics.* (1988) 44:837–45. doi: 10.2307/2531595

26. Newman JL, Phillips JS, Cox SJ. 1D convolutional neural networks for detecting nystagmus. *IEEE J Biomed Health Inform.* (2021) 25:1814–23. doi: 10.1109/JBHI.2020.3025381

27. Juhola M. On machine learning classification of otoneurological data. *Stud Health Technol Inform.* (2008) 136:211–6.

28. Kabade V, Hooda R, Raj C, Awan Z, Young AS, Welgampola MS, et al. Machine learning techniques for differential diagnosis of vertigo and dizziness: a review. *Sensors*. (2021) 21:7565. doi: 10.3390/s21227565

29. Tarnutzer AA, Berkowitz AL, Robinson KA, Hsieh YH, Newman-Toker DE. Does my dizzy patient have a stroke? A systematic review of bedside diagnosis in acute vestibular syndrome. *CMAJ*. (2011) 183:E571–92. doi: 10.1503/cmaj.100174

30. Mantokoudis G, Otero-Millan J, Gold DR. Current concepts in acute vestibular syndrome and video-oculography. *Curr Opin Neurol.* (2021) 35:75–83. doi: 10.1097/WCO.0000000000001017

31. Vabalas A, Gowen E, Poliakoff E, Casson AJ. Machine learning algorithm validation with a limited sample size. *PLoS ONE.* (2019) 14:e0224365. doi: 10.1371/journal.pone.0224365

32. Korda A, Wimmer W, Zamaro E, Wagner F, Sauter TC, Caversaccio MD, et al. Video-oculography 'HINTS' in acute vestibular syndrome: a prospective study. *Front Neurol*. (2022) 13:920357. doi: 10.3389/fneur.2022.920357

33. Pradhan C, Wuehr M, Akrami F, Neuhaeusser M, Huth S, Brandt T, et al. Automated classification of neurological disorders of gait using spatio-temporal gait parameters. *J Electromyogr Kinesiol.* (2015) 25:413–22. doi: 10.1016/j.jelekin.2015.01.004

34. Barreto RG, Yacovino DA, Teixeira LJ, Freitas MM. Teleconsultation and teletreatment protocol to diagnose and manage patients with benign paroxysmal positional vertigo (BPPV) during the COVID-19 Pandemic. *Int Arch Otorhinolaryngol.* (2021) 25:e141–e9. doi: 10.1055/s-0040-1722252

35. Groezinger M, Huppert D, Strobl R, Grill E. Development and validation of a classification algorithm to diagnose and differentiate spontaneous episodic vertigo syndromes: results from the DizzyReg patient registry. *J Neurol.* (2020) 267:160–7. doi: 10.1007/s00415-020-10061-9

36. Vivar G, Strobl R, Grill E, Navab N, Zwergal A, Ahmadi SA. Using Base-ml to learn classification of common vestibular disorders on DizzyReg registry data. *Front Neurol.* (2021) 12:681140. doi: 10.3389/fneur.2021.681140

37. Gamache R, Kharrazi H, Weiner JP. Public and population health informatics: the bridging of big data to benefit communities. *Yearb Med Inform.* (2018) 27:199–206. doi: 10.1055/s-0038-1667081

38. Dash S, Shakyawar SK, Sharma M, Kaushik S. Big data in healthcare: management, analysis and future prospects. *J Big Data.* (2019) 6:54. doi: 10.1186/s40537-019-0217-0

39. Dagliati A, Tibollo V, Sacchi L, Malovini A, Limongelli I, Gabetta M, et al. Big data as a driver for clinical decision support systems: a learning health systems perspective. *Front Digit Humanit*. (2018) 5. doi: 10.3389/fdigh.2018.00008

frontiers | Frontiers in Neurology

TYPE Original Research
PUBLISHED 20 September 2022
DOI 10.3389/fneur.2022.883213

OPEN ACCESS

EDITED BY
Ji Soo Kim,
Seoul National University, South Korea

REVIEWED BY
Laurent Goffart,
Centre National de la Recherche Scientifique (CNRS), France
Thomas Eggert,
Ludwig Maximilian University of Munich, Germany
Ziad M. Hafed,
University of Tübingen, Germany

*CORRESPONDENCE
Christoph Helmchen
christoph.helmchen@neuro.uni-luebeck.de

SPECIALTY SECTION
This article was submitted to Neuro-Otology, a section of the journal Frontiers in Neurology

RECEIVED 24 February 2022
ACCEPTED 23 August 2022
PUBLISHED 20 September 2022

CITATION
Helmchen C, Machner B, Schwenke H and Sprenger A (2022) Bilateral lesion of the cerebellar fastigial nucleus: Effects on smooth pursuit acceleration and non-reflexive visually-guided saccades. *Front. Neurol.* 13:883213. doi: 10.3389/fneur.2022.883213

Bilateral lesion of the cerebellar fastigial nucleus: Effects on smooth pursuit acceleration and non-reflexive visually-guided saccades

Christoph Helmchen[1,2]*, Björn Machner[1,2], Hannes Schwenke[2,3] and Andreas Sprenger[1,2,4]

[1]Department of Neurology, University Hospitals Schleswig-Holstein, Campus Lübeck, Lübeck, Germany, [2]Center of Brain, Behavior and Metabolism (CBBM), University of Lübeck, Lübeck, Germany, [3]Department of Neuroradiology, University Hospitals Schleswig-Holstein, Lübeck, Germany, [4]Institute of Psychology II, University of Lübeck, Lübeck, Germany

Background: "Central dizziness" due to acute bilateral midline cerebellar disease sparing the posterior vermis has specific oculomotor signs. The oculomotor region of the cerebellar fastigial nucleus (FOR) crucially controls the accuracy of horizontal visually-guided saccades and smooth pursuit eye movements. Bilateral FOR lesions elicit bilateral saccade hypermetria with preserved pursuit. It is unknown whether the initial acceleration of smooth pursuit is impaired in patients with bilateral FOR lesions.

Objective: We studied the effect of a cerebellar lesion affecting the deep cerebellar nuclei on the initial horizontal pursuit acceleration and investigated whether saccade dysmetria also affects other types of volitional saccades, i.e., memory-guided saccades and anti-saccades, which are not performed in immediate response to the visual target.

Methods: We recorded eye movements during a sinusoidal and step-ramp target motion paradigm as well as visually-guided saccades, memory-guided saccades, and anti-saccades in one patient with a circumscribed cerebellar hemorrhage and 18 healthy control subjects using a video-based eye tracker.

Results: The lesion comprised the FOR bilaterally but spared the posterior vermis. The initial pursuit acceleration was low but not significantly different from the healthy control subjects and sinusoidal pursuit was normal. Bilateral saccade hypermetria was not only seen with visually-guided saccades but also with anti-saccades and memory-guided saccades. The final eye position remained accurate.

Conclusion: We provide new insights into the contribution of the bilateral deep cerebellar nuclei on the initial acceleration of human smooth pursuit in midline cerebellar lesions. In line with experimental bilateral FOR lesion data in non-human primates, the initial pursuit acceleration in our patient was not significantly reduced, in contrast to the effects of unilateral experimental FOR lesions. Working memory and neural representation of target locations seem to remain unimpaired. Our data argue against an impaired common

command feeding the circuits controlling saccadic and pursuit eye movements and support the hypothesis of independent influences on the neural processes generating both types of eye movements in the deep cerebellar nuclei.

KEYWORDS

initial smooth pursuit, fastigial nucleus, cerebellum, saccade hypermetria, bilateral

Introduction

"Central dizziness" can be caused by cerebellar disease. In the absence of vestibular abnormalities (e.g., spontaneous nystagmus, gaze-evoked nystagmus) or limb ataxia, oculomotor abnormalities can be the only signs indicative of a cerebellar disease in a very specific way. Here, we present a rare case history of a bilateral fastigial nucleus lesion that reveals new insights into the functional role of the patient's initial pursuit generation, i.e., pursuit acceleration. To our knowledge, this has not been examined in previous patient studies.

Role of the cerebellum on saccades and smooth pursuit eye movements

As the cerebellar neural control of both smooth pursuit eye movements and saccades rest upon bilateral fastigial nuclei activity (1–3), unilateral lesions of the oculomotor parts of the cerebellar vermis (OMV) and the underlying deep cerebellar nuclei, specifically the fastigial nuclei (FOR), elicit unilaterally impaired smooth pursuit and direction-specific saccade dysmetria, which can be clinically recognized. Even inexperienced clinicians recognize saccade dysmetria as the saccade hypometria in one direction is contrasted by hypermetria on the other side.

In bilateral cerebellar lesions, however, clinical signs become more difficult to be identified as the balance of the abnormal driving forces counterbalance each other and may even elicit normal appearing signs (normal smooth pursuit) (4), bilateral saccade hypermetria in bilateral fastigial lesions (5) or bilateral hypometria in OMV lesions (6). On clinical examination, saccade dysmetria, in this case, is usually missed because the pathological dysmetria, in particular in saccade hypermetria, does not appear different from the dysmetric saccade toward the contralateral side, pretending a normal saccade behavior. While the latter effects have been elicited by posterior vermis (7) and FOR (4, 5) inactivation studies in non-human primates, they have been replicated in single patient studies with vermal and FOR lesions (8–11). The opposite effects of lesions in both structures, the oculomotor vermis (OMV) and the FOR, are possibly related to the inhibitory control of the Purkinje cells of the OMV on the FOR (12).

Role of the fastigial nucleus on smooth pursuit eye movements

The activity of smooth pursuit neurons in the FOR is direction-specific and encodes eye acceleration: as their discharge precedes the time of peak eye velocity during contralateral movements, these neurons have been functionally linked to eye acceleration. Neurons with preferred modulation of their discharge rates during ipsilateral smooth pursuit lag peak velocity and discharge during eye deceleration (13). Assuming a role of the FOR in accelerating contralateral and decelerating ipsilateral smooth pursuit, it remained unclear in the few related studies whether eye acceleration during the initial period of pursuit (i.e., after a target has started moving or has changed its speed) is impaired in patients with FOR lesions, as bilateral FOR lesions would suppress the imbalance between the sustained activity emitted by both FOR.

The pursuit acceleration in the initial, open-loop phase of pursuit tracking behavior seems to be selectively vulnerable in some patients with cerebellar lesions (14) but the lesion site remained unraveled and has not been examined in patients with circumscribed FOR lesions yet (8–10). In non-human primates, bilateral experimental FOR lesions do not or only mildly reduce the initial acceleration of smooth pursuit (4). However, an impairment has been shown in lesions of the oculomotor vermis, possibly related to asymmetrical lesions (7).

Noticeably, as pursuit and saccade fibers cross the midline at the rostral level and project to the contralateral side, unilateral FOR lesions may have bidirectional effects. A recent anatomical study has shown inter-fastigial projections along the roof of the fourth ventricle in mice (15) but these projections have neither been identified in the non-human primate yet nor been functionally characterized as related to the control of eye movements.

Based on these animal studies, we tested the hypothesis that unpredictive initial acceleration of smooth pursuit is not impaired in a patient with a circumscribed bilateral lesion of the deep cerebellar nuclei, specifically involving the FOR. For better comparison with previous studies, we also tested predictive sinusoidal pursuit behavior. Importantly, this patient's lesion spared the oculomotor vermis and the flocculus. The patient's eye movements were compared with 18 healthy control

subjects to investigate the role of this patient's FOR in the initial pursuit acceleration.

Role of the fastigial nucleus on saccadic eye movements

Both structures, the OMV (6, 16) and the FOR (17), crucially control the accuracy of visually-guided saccades (18). Purkinje cells of the OMV (lobules VI and VII) contain saccade-related neurons (19, 20) and lesions elicit uni- (6) or bilateral saccade hypometria and increased trial-to-trial variability of saccade amplitude (21). Unilateral FOR lesions in animals cause direction-specific saccade deficits: contralesional hypometria and ipsilesional hypermetria in the head restrained (2, 5, 22) and unrestrained (23, 24) conditions. Dysmetria affected the horizontal components of saccades in all directions. These direction-specific oculomotor signs can be clinically recognized in patients with direct or indirect FOR lesions (25). In contrast, bilateral FOR lesions elicit severe bilateral saccade hypermetria during visually-guided saccades, in non-human primates (5) and patients (9, 11, 26).

Dysmetria is not only seen during visually-guided saccades to stationary but also to moving targets and interceptive saccades follow the same directional dependence (2, 3), with hypometric contralesional and hypermetric ipsilesional saccades. Moreover, saccade-related burst neurons in the FOR are not only active during visually-guided and memory-guided saccades but also during spontaneous saccades in light and darkness (27), although not always (28). Volitional saccades may be initiated during visual scanning as part of a visual recognition or natural orientation behavior to remembered or estimated target locations (29). Saccade dysmetria was not found during internally triggered saccades of a patient scanning a set of targets (9). In order to look at targets of interest that one recognizes during visual scanning, the subject must encode and remember the location of the (peripheral) target. Like in other visually-guided saccades, potential changes in eye position must be taken into account for accurate orientation of gaze before the saccade to the remembered target location is executed (10). This function engages control functions of disengaging from the fixated target, maintaining gaze direction during fixation, suppressing looking at distracting targets, and looking as precisely as possible at the remembered location. These functions crucially involve the frontal cortex with the supplementary (SEF) and frontal eye field (FEF), dorsolateral prefrontal cortex (DLPFC)(30, 31), and the cerebellum, particularly the OMV and the underlying deep cerebellar nuclei, specifically the FOR (32, 33). Up to now, only a few studies investigated memory-guided saccades in cerebellar disease (10, 26, 34). Memory-guided saccades were found to be as dysmetric as visually-guided saccades (10, 26) or even more dysmetric (34). However, these studies did not show lesions constrained to the deep cerebellar nuclei. A recent study examined saccade hypermetria of a patient with bilateral FOR lesion sparing the vermis but did not examine saccades toward remembered visual targets (memory saccades) or anti-saccades (11).

Anti-saccades are directed to the opposite side of the presented stationary target (35, 36) which are usually examined in patients with frontal lobe and basal ganglia disease (37, 38) or schizophrenic patients (39) but not in cerebellar disease.

In memory-guided saccades, an efference copy signal is usually not needed toward a memorized visual target since no motor command is generated when the target is presented. It is a matter of debate whether non-visual, extra-retinal signals (e.g., efference copy) could influence the programming of the direction and accuracy of memory-guided saccades (10). Cerebellar patients have been suggested to lack an efference copy of the eye position after the first saccade due to the lack of corrective saccades in the dark (34). In line with this notion, dysmetria of memory-guided saccades increase once the eyes move during the memory period (10). The authors suggested that an efference copy could come into play not as a precise record of the motor command but as a cue to re-evaluate the visual consequences of the saccade.

Both types of saccades are endogenously driven voluntary saccades and engage different mechanisms and neural networks (29). Subjects have to look at an imagined target position during the anti-saccade paradigm without having seen a visual target at this location. In a memory-guided paradigm, they have to keep the target position in mind within a variable interval, challenging working memory. Thus, the execution follows a mental representation of a target that is no longer visible. If non-visual signals influence saccade execution under these circumstances, the magnitude of dysmetria may differ between on the one hand pro-saccades, on the other hand, memory-guided and anti-saccades.

We hypothesized that saccade dysmetria in our patient with a bilateral FOR lesion differs between memory-guided, anti-saccades, and visually-guided saccades.

Methods and participants

Participants

Oculomotor data of a 43-year-old man were compared with 18 healthy subjects (age: 38 ± 8 years, mean ± standard deviation). The study was approved by the Ethics Committee of the University of Lübeck (AZ12-219), and all participants gave written informed consent.

History of present illness

The formerly healthy patient complained about sudden headache, dizziness, blurred vision, and pronounced

unsteadiness of stance and gait with some short-lasting slurring of speech. He did not notice oscillopsia or lateropulsion. On examination, there was severe saccade hypermetria bilaterally to foveopetal and foveofugal visual targets. Horizontal and vertical smooth pursuit appeared normal. Slow di- and convergence was slightly cogwheel. Transient horizontal nystagmus was reported in the emergency room that could not be identified any longer a few hours later. Horizontal and vertical head-impulse testing was normal. There was no head-shaking, gaze-evoked, positional, or rebound nystagmus. Past medical history was otherwise unremarkable. There was postural unsteadiness with a slightly broad-based stance in the light, which increased on eye closure, but there was no ataxia of the extremities.

Clinical MRI (Siemens Vida 3 T MRI, Erlangen, Germany) was performed with a hospital-specific cerebral hemorrhage detection protocol. On high-resolution FLAIR images (voxel size 1 mm, TR 6,500 ms, and TE 393 ms), the deep cerebellar nuclei were localized by means of triplanar reconstruction, with the strict matching of the hypointense deep cerebellar nuclei regions by means of clinical atlases (40). Furthermore, in the same manner, anatomical localization of the cerebellar lobules was performed (41).

Experimental setup and oculomotor paradigms

Eye movements were recorded with a video-based eye-tracker (Eyelink II, SR Research Ltd., Ontario, Canada). We recorded both eyes but only movements of the left eye were analyzed. The fixation target was placed straight ahead of the nose. During experiments, subjects sat in a comfortable chair; the head was immobilized by a chin rest and a forehead-holding device. The visual stimulus consisted of a red laser dot (diameter of 0.1°), rear-projected onto a translucent screen at a viewing distance of 1.4 m. The laser dot was moved by two galvanometer scanners (GSI Lumonics, Munich, Germany), driven by an analog output card in the stimulus PC (AT-AO6/10, National Instruments). Except when otherwise mentioned, subjects were asked to look at the laser dot as fast and accurately as possible. For calibration, we first presented a sequence of stimuli in central, horizontal, and vertical deflected positions. Recordings were performed in darkness. Visual acuity was >0.8, including the patient (inclusion criteria).

We investigated all participants (patient and healthy subjects) under head-stationary conditions in the dark using the following paradigms which are described in detail elsewhere (37): fixation at gaze straight ahead and on vertical and horizontal eccentric gaze positions (10°, 20°), reflexive horizontal and vertical visually guided saccades (10°, 15°) to a small laser target (VGS = pro-saccades), volitional saccades, i.e., anti-saccades (10°, 15°), and saccades to memorized ("imagined") target locations (memory-guided saccades; 10°, 15°), as well as smooth pursuit paradigms.

The data analysis was performed in MATLAB® (R2021b, The Mathworks, Natick/MA).

Sinusoidal smooth pursuit paradigms The predictive, closed-loop smooth pursuit was tested in a sinusoidal smooth pursuit paradigm composed of horizontal oscillations of 0.2 Hz (amplitudes of 15.9°; i.e., maximum stimulus velocity of 20°/s; 4 cycles). After the elimination of saccades, the phase and amplitude of a sinusoid were adjusted to match the slow phase velocity of the eye. The fitting was performed with the least-squares method. The gain was calculated by the ratio of eye velocity to target velocity.

The step-ramp paradigm (42, 43) was used as described before (37, 44). This paradigm was used to quantify the initial response of unpredictive smooth pursuit without visual feedback (open loop) and the closed-loop period. During each trial, the target stepped away horizontally from the gaze straight ahead position and then moved with a constant velocity in the opposite direction. Because we used step amplitudes of 2.4° and ramp velocities of 16°/s, the stimulus passed the center after 150 ms, thus allowing smooth pursuit initiation without an initial saccade. Each sequence consisted of 20 ramps to either side in random order. Foveofugal ramps (4 to the left and 4 to the right) with horizontal target steps away from the center position and consecutive constant velocity stimuli in the same direction were interspersed to keep the level of attention high. The duration of the fixation interval before each trial was varied from 1,600 to 1,900 ms randomly (44).

Analysis of pursuit acceleration

The onset of pursuit acceleration (pursuit latency) was defined as the time when eye velocity exceeded 3.2 times the standard deviation of the baseline velocity signal (measured over a 200-ms interval before the target started to move). Subsequent data in a 60 ms time window were used to calculate the slope of a least square fit (robust fit function within Matlab®) of eye velocity (43), as described in detail by one of us (AS) before (45). The intersection (green dot in Figure 3) between the regression line (orange line) and mean eye velocity before target motion onset (blue line) indicates the start of the pursuit eye movement. The slope (of the orange line) indicates pursuit acceleration.

Pro-saccades

Gain, latency, and velocity of pro-saccades to visual targets at different locations and displacements (10°, 15°) were examined for the horizontal and vertical directions (30 saccades per direction). Direction and amplitude were randomized, the preceding fixation phase was varied from 1,000 to 1,400 ms followed by a gap of 200 ms. Saccade amplitude gain was

calculated as the ratio between the amplitudes of the primary saccade and the target displacement.

As the subjects had to fixate the target for some 1,000–1,400 ms (and a gap of 200 ms) before the next target displacement, eye position was usually on target. However, target retinal eccentricity became important for correction saccades, as the correction saccades of the patient started from an eye position several degrees off the target position (offset). We calculated the amplitude gain of the secondary saccade, i.e., the first correction saccade toward the visual target position (e.g., 10° right or left) as the ratio of the eye amplitude to the distance between the eye position at the start of the secondary saccade and the actual target position. The patient's hypermetria of the correction saccades is better reflected by the mean amplitude of the correction saccades than by the mean amplitude gain. We, therefore, report both values. Furthermore, we prefer to use the term "correction saccade" instead of "corrective saccade" since the patient's saccades following the primary saccade do not always correct the position error.

Latency was the interval from stimulus to saccade onset. Eye velocity was calculated by [difference of median eye position of five data points before and after the actual data point] * sampling rate (1,000 Hz).

The main sequence of all visually guided saccades was fitted as in previous studies (44, 46) by the common equation: Peak velocity = vmax * (1- $e^{-amplitude/c}$) using the *fminsearch* function within Matlab®. Using the parameters derived from the fit, we calculated saccade peak velocity for a 15° saccade amplitude. The rationale for this procedure was to compare the peak velocities between the patient and the healthy controls who differed in saccade amplitude: the peak velocity of the patients' saccades was transformed into those expected for saccades with the amplitudes of the healthy controls, i.e., we used transformed eye velocities.

Anti-saccade paradigm

While fixating the gaze-straight ahead target, participants were asked not to look as it jumps sideways at 10° and 15° horizontally to the right or left side (direction at random order) but to look in the opposite direction with the same amplitude after a gap (200 ms). We presented 20 steps in each direction. The percentage of errors (error rate, i.e., misdirected saccades toward the target) and latencies of correct saccades were calculated. Anticipatory saccades (*latency < 70 ms)* were excluded (44).

Memory-guided saccade paradigm

In the memory-guided saccade paradigm (30 trials), subjects not only had to suppress reflexive saccades toward the presented lateral target but also had to keep the location in mind for the consecutive task. While they fixated the laser in its initial position at gaze straight ahead, an additional target was flashed for 200 ms at a 10° or 15° peripheral position left or right from the center of the visual display (random direction and unpredictable). The subjects were instructed not to look at the peripheral target but to keep its position in mind within a variable interval (1,500, 2,500, and 3,500 ms). When the central fixation point was switched off, they had to look at the remembered, previously shown target position. After an additional 2 s, the peripheral target showed up again at the previously flashed location and subjects had to fixate this visible target. The number and amplitude of correction saccades toward the remembered target position and the difference between the final eye position and the correct position of the memorized target were analyzed. Fifteen trials in each direction were performed. The percentage of reflexive misdirected saccades toward the flashed target (error rate), the latency, and the amplitude of the first memory-guided saccade were analyzed. To evaluate the accuracy of spatial memory, we calculated the final eye position error, defined as the distance between the eye position at target reappearance and the target position. Accordingly, the final eye position gain is the final eye position error divided by the target amplitude.

Statistical analysis

Horizontal and vertical eye positions were analyzed using Matlab® (R2021b, The Mathworks Inc., Natick, MA, USA). We used statistical comparisons by the Revised Standardized Difference Test developed for suspected impairments and dissociations in single-case studies (47). If not stated otherwise, subsequently reported values are means (±1 standard deviation).

Results

Lesion pattern

MRI identified a hemorrhage with surrounding edema at the level of the deep cerebellar nuclei, involving bilateral fastigial nuclei, extending laterally to the globose and emboliform nuclei on both sides and the medial aspects of the dentate nuclei (Figure 1). The bleeding extended into the anterior vermis (lobules IV and V) but spared the oculomotor vermis (lobules VI, VII) (40, 41). There was no brainstem lesion.

A summary of the important eye movement data is listed in Table 1.

Smooth pursuit

Pursuit maintenance

The sustained smooth pursuit was analyzed both in the step-ramp and in the sinusoidal pursuit paradigm.

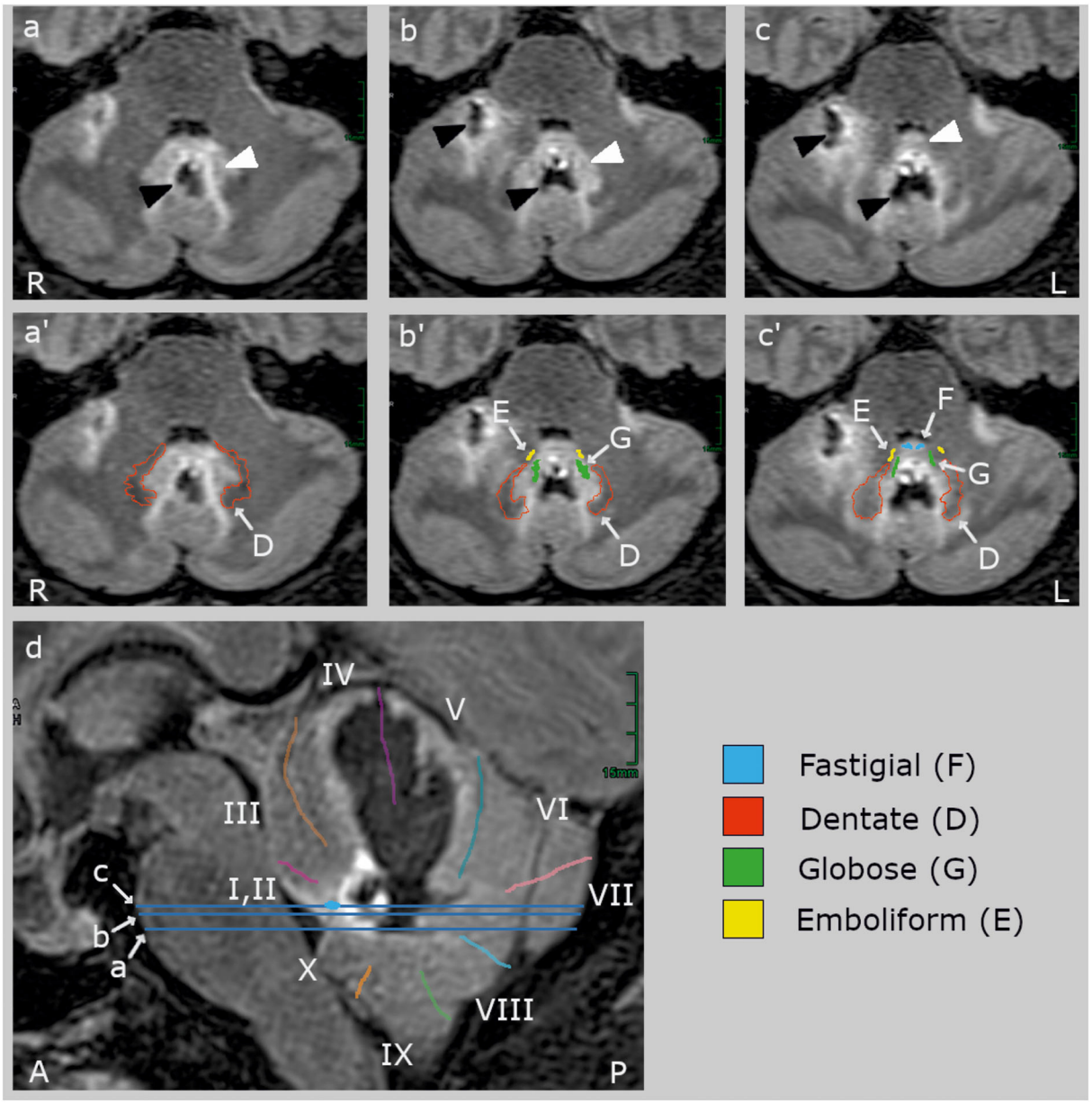

FIGURE 1
Clinical high-resolution FLAIR images (Siemens Vida 3 T MRI, Erlangen, Germany) with axial **(a–c)** and sagittal slices **(d)**. The blue lines on the sagittal slice indicate the location of the axial slices. The upper row **(a–c)** shows the lesion (black arrowheads) and its edema (white arrowheads) without cerebellar landmarks which are labeled in the middle **(a'–c')** and lower row **(d)**. The hemorrhage (hypointense, black) centered in the midline between the deep cerebellar nuclei and extended rostrally into the vermal lobules IV and V and the right hemispheric lobules V and VI (40, 41). The edema (hyperintense, light gray) involved bilaterally the fastigial nucleus (F, blue) anteriorly to the hemorrhage at the roof of the fourth ventricle, most likely impairing inter-fastigial projections (15), and laterally the interpositus composed of the globose (G) and emboliform (E) nuclei, and the medial part of the dentate nucleus (D). The lesion did not comprise (oculomotor) hemispheric lobule VI (simple lobule), the posterior oculomotor vermal lobules VI and VI (OMV), flocculus, paraflocculus, and caudal vermal uvula and nodulus. There was no brainstem lesion.

Smooth pursuit maintenance was normal in the patient during slow predictive sinusoidal pursuit (0.2 Hz) with a horizontal velocity gain of 0.8 [0.1 Hz: 0.9, 0.3 Hz: 0.68] and 0.7 for the vertical direction [0.1 Hz: 0.96, 0.3 Hz: 0.68], respectively (Figure 2). There was no significant difference to the healthy subjects [$n = 18$, 0.2 Hz: horizontal velocity gain 0.88 ± 0.07; $t_{(17)} = -1.143$, $p = 0.14$, vertical 0.69 ± 0.14; $t_{(17)} = 0.278$, $p = 0.39$]. The patient showed a slightly reduced horizontal steady-state velocity gain (0.69, Figure 3A) during the horizontal step-ramp stimulus, which was not significantly different from

TABLE 1 Horizontal eye movementparameters of the patient and the healthy subjects, with the mean (patient) and the mean (±standard deviation) of the median of the healthy subjects, the number of measurements (N), and the level of statistically significant differences.

Oculomotor paradigms	Patient	N	Healthy subjects ($n = 18$)	N	Level of significance
Initial smooth pursuit (step ramp)		40		40	
Latency (ms)	192		245 ± 62		n.s.
Initial acceleration (°/s^2)	36		91 ± 43		n.s.
Catch-up saccade (°) during pursuit	3.29 ± 2.1		1.56 ± 1.2		n.s.
Pro-saccades		30		30	
Gain	1.59 ± 0.08		0.96 ± 0.06		$p = 0.001$
Gain (correction saccade)	1.1 ± 0.3		0.89 ± 1.22		n.s.
Amplitude (°) of correction saccade	−6.4 ± 7.0		2.4 ± 1.5		$p = 0.001$
Velocity (°/s)	398 ± 57		377 ± 48		n.s.
Latency (ms)	214 ± 68		182 ± 33		n.s.
Anti-saccades		40		40	
Error rate (%)	20		24.07		n.s.
Gain	1.47 ± 0.45		0.83 ± 0.22		$p = 0.007$
Gain (correction saccade)	0.64 ± 0.36		0.48 ± 0.21		n.s.
Amplitude (°) of correction saccade	−2.92 ± 5.8		0.84 ± 1.68		$p = 0.023$
Latency	400 ± 73		328 ± 53 ms		n.s.
Memory-guided saccades		30		30	
Reflexive saccade (%)	16.6		16 ± 11.5		n.s.
Gain	1.14 ± 0.34		0.84 ± 0.68		$p = 0.001$
Gain (correction saccade)	0.71 ± 0.44		0.65 ± 0.26		n.s.
Amplitude (°) of correction saccade	−2.3 ± 1.9		0.8 ± 0.9		n.s. ($p = 0.06$)
Final eye position error (°)	0.98 ± 0.26		0.93 ± 0.05		n.s.
Variability (final eye position)	0.26		0.19 ± 0.11		n.s.
Latency (ms)	322 ± 100		452 ± 110		n.s.

the healthy subjects [0.79 ± 0.15; $t_{(17)} = -0.649$, $p = 0.263$]. As pursuit velocity was within normal limits, there were only a few catch-up saccades in the patient, and even less in the healthy subjects. Mean amplitude of catch-up saccades was not different between the patient (3.29 ± 2.08) and the healthy subjects [1.56 ± 1.18; $t_{(17)} = 1.43$, $p = 0.08$].

Smooth pursuit initiation in the step-ramp paradigm

The mean latency of horizontal smooth pursuit onset in the foveopetal step-ramp paradigm of the patient (on average 192 ms) was not different from the healthy subjects [horizontal: 245 ± 62 ms, $t_{(17)} = 0.211$, $p = 0.422$] (Figure 2D). The initial pursuit acceleration was low (36°/s^2) but not significantly different from the healthy control subjects [91 ± 43°/s^2; $t_{(17)} = 0.117$, $p = 0.234$] (Figures 2B–D, 3). Note the variability of initial acceleration in the healthy subjects (Figures 2C,D, 3).

Saccades

Pro-saccades

Horizontal saccade amplitude gain (30 saccades) was significantly larger (hypermetria) in the patient (gain: 1.59 ± 0.08) than in the healthy subjects [gain 0.96 ± 0.06; $t_{(18)} = 11.04$; $p < 0.001$; Figure 4]. Vertical saccade gain (30 saccades) was also larger (0.98 ± 0.22) compared to the healthy subjects (0.91 ± 0.11) but this difference failed to reach statistical significance ($p > 0.05$). There was often a vertical (usually downward) deflection of the saccade trajectory during horizontal saccades (Figure 5). The majority (93.3%) of all horizontal saccades of the patient were followed by correction saccades (with a median normalized gain of 0.78).

The amplitude of the patient's secondary saccade, i.e., the first correction saccade after the primary saccade, was significantly larger than in the healthy subjects (Table 1, the negative values in the patient reflect a correction in the direction opposite to the hypermetric primary saccade). This larger amplitude of the correction saccade not only results from the different starting point after the primary saccade and its long distance to the target but the correction saccades were considerably larger than required to reach the target, reflecting hypermetria (Figures 4, 5). The gain of the patient's secondary saccade did not differ from the healthy controls (Table 1). The variability of the gain of the first correction saccade was −0.118 ± 0.04.

Horizontal peak velocity of 15° saccades looked normal and did not differ between the patient (398 ± 57°/s) and the

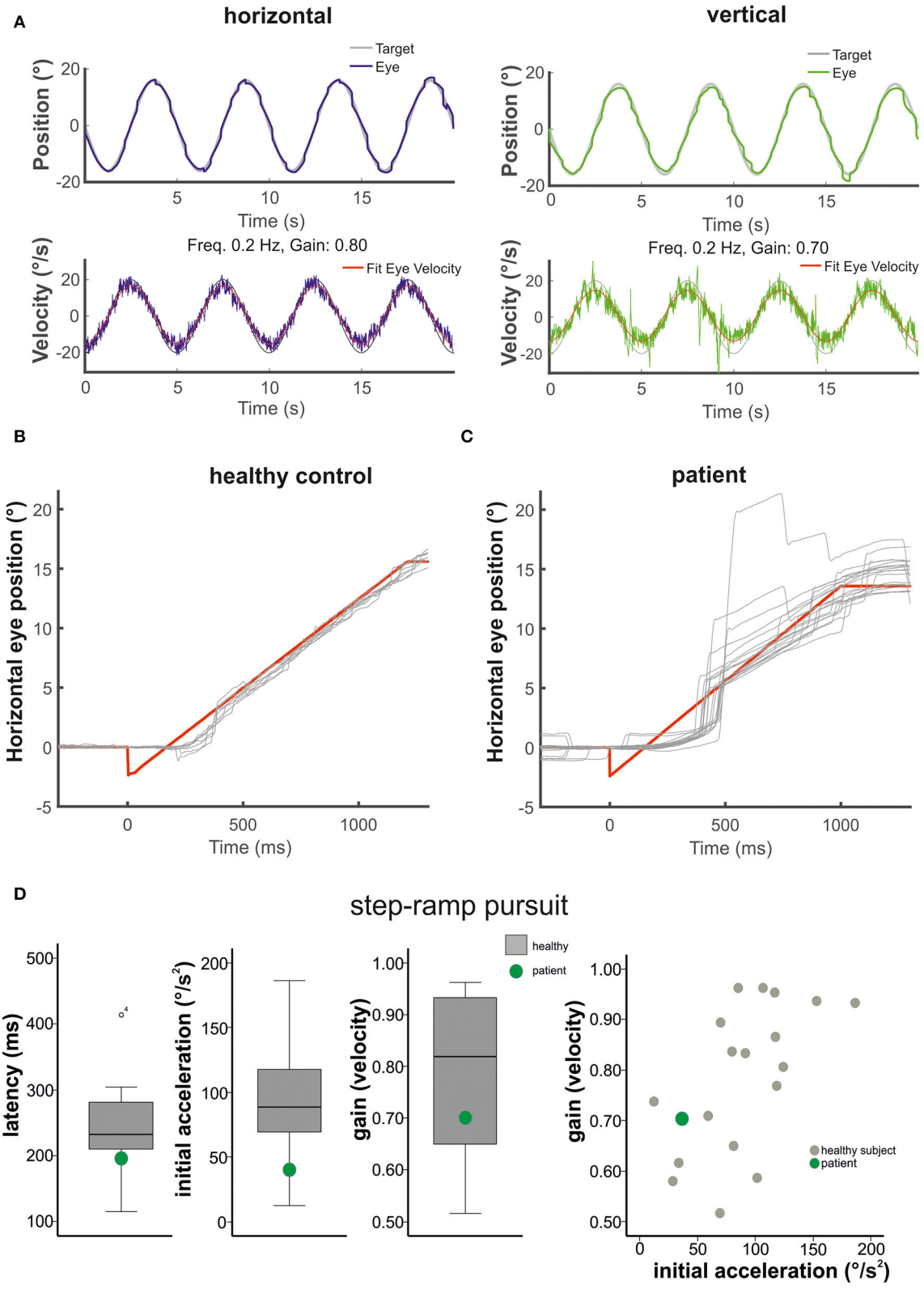

FIGURE 2
The figure shows in **(A)** the horizontal (left) and vertical (right) sinusoidal smooth pursuit of the patient. Upper traces indicate horizontal (blue) and vertical (green) eye position (target in gray), and lower traces indicate horizontal (blue) and vertical (green) eye velocity (°/s). The responses to the step-ramp stimuli (target = red) are shown in **(B)** for a healthy control subject and the patient **(C)**. Note the low initial acceleration in the

(Continued)

FIGURE 2 (Continued)
patient with subsequent catch-up saccades while he pursued the target. **(D)** (from left to right): Mean values (40 ramps) for the latency (ms), the initial acceleration (°/s^2), and the pursuit maintenance velocity gain are indicated in box plots (with median, upper and lower quartiles, e.g., 75 and 25% percentiles, and outliers) for the healthy subjects (gray) and the patient (green). The distribution of the initial acceleration values (plotting initial acceleration vs. maintenance pursuit velocity) on the right side shows that the low initial acceleration of the patient (green circle) is within the data distribution of the healthy subjects (see also Figure 3).

healthy subjects (377 ± 48°/s; $p > 0.05$). As the patient made larger (hypermetric) saccades we calculated saccade velocity of a defined amplitude derived from the main sequence, e.g., the patient's peak velocity of a 15° amplitude saccade.

Latency of 30 horizontal pro-saccades of the patient (mean: 214 ± 68 ms) was not different from the healthy control subjects [mean: 182 ± 33 ms; $t_{(18)} = 0.959$; $p < 0.176$].

Anti-saccades

The patient had an error rate of 20%, i.e., 8 of 40 saccades were directed to the visual target instead of the opposite direction. The patient's rate of misdirected saccades did not differ from the error rate of healthy subjects [24%; $t_{(16)} = 0.321$; $p > 0.05$]. The amplitude gain of horizontal anti-saccades ($n = 32$) was significantly larger in the patient (1.47 ± 0.45) than in the healthy subjects ($n = 30$) [0.83 ± 0.223; $t_{(16)} = -2.815$, $p = 0.007$; Figures 4, 6]. Almost half (45%) of all horizontal anti-saccades of the patient were followed by correction saccades. The number of anti-saccades with correction saccades was not different from the healthy subjects [54 ± 2%, $t_{(16)} = -0.42$; $p > 0.05$]. The gain of the patient's first correction saccade did not differ from the healthy controls (Table 1). The mean amplitude of the patient's first correction saccade was also significantly larger than in the healthy subjects (Table 1), with correction saccades in the direction opposite to the primary saccade.

Latency of anti-saccades of the patient (mean: 400 ± 72 ms) was not different from the healthy control subjects [mean: 328 ± 53 ms; $t_{(16)} = 1.29$; $p = 0.109$].

Memory-guided saccades

The frequency of reflexive saccades (toward the memorized target at 10 or 15°) was not different between the patient (16.6%) and the healthy subjects [16% ± 11.5; $t_{(15)} = 0.049$, $p = 0.481$]. The gain of the patient's primary memory-guided saccades was significantly larger than in the healthy participants (Figure 6). The gain of the patient's first correction saccade toward the memorized target was not different from the healthy subjects (Table 1). The proportion of correction saccades was not different between the patient (in 16/30 of saccades; i.e., 53% of all saccades) and the healthy subjects [66 ± 17.7%, $t_{(16)} = 0.726$; $p = 0.24$]. Apart from square wave jerks during fixation (0.5–2°, 200 ms duration; only found in the patient's records), there were neither macrosaccadic oscillations nor irrepressible saccades.

The final eye position gain did not differ between the patient (0.98 ± 0.26) and the healthy subjects [0.93 ± 0.05, $t_{(16)} = 1.008$; $p = 0.165$]. The variability of the final eye position (standard deviation of the gain of each single subject) was not different between the patient (0.26) and the healthy subjects [0.19 ± 0.11; $t_{(16)} = 0.626$, $p = 0.27$]. The latency of the first saccade of the patient (452 ± 110 ms) was not different from the healthy participants [322 ± 100 ms, $t_{(15)} = 1.257$, $p = 0.115$].

Unfortunately, a statistical within-subject comparison for pro-saccades with memory-guided saccades is technically limited due to the case nature of this study. As a 2 × 3, ANOVA [two groups, three saccade tasks (pro/anti/memory-guided saccades)] is technically not valid, we can only state trends. They are based on an ANOVA analysis of each group (patients and healthy subjects) separately comparing the three different saccade conditions (Figure 6). For the patient, the ANOVA of the primary saccade gain showed a significant main effect for the saccade tasks [$F_{(2,87)} = 8.955$, $p < 0.001$]: saccade amplitude of memory-guided saccades was smaller compared to anti-saccades ($p = 0.008$) and pro-saccades ($p < 0.001$).

Fixation and gaze holding

During fixation, there were numerous square wave jerks. We neither found irrepressible saccades nor macrosaccadic oscillations. There was no spontaneous nystagmus and or gaze-evoked nystagmus during sustained eccentric vertical and horizontal fixation for at least 20 s in the light and darkness. After eccentric fixation (20 s), there was no rebound nystagmus.

Discussion

Our main goal was to investigate the effects of bilateral lesions of the deep cerebellar nuclei on the initial smooth pursuit acceleration.

As a main result, initial pursuit acceleration was low but not statistically different from the healthy control subjects, as was the predictive (sinusoidal) pursuit velocity. Bilateral saccade hypermetria was not only seen in visually-guided saccades but also in anti-saccades and memory-guided saccades. The final eye position remained accurate. We will first describe the lesioned cerebellar structures of our patient, relate them to mechanisms causing the pursuit and saccade abnormalities, and

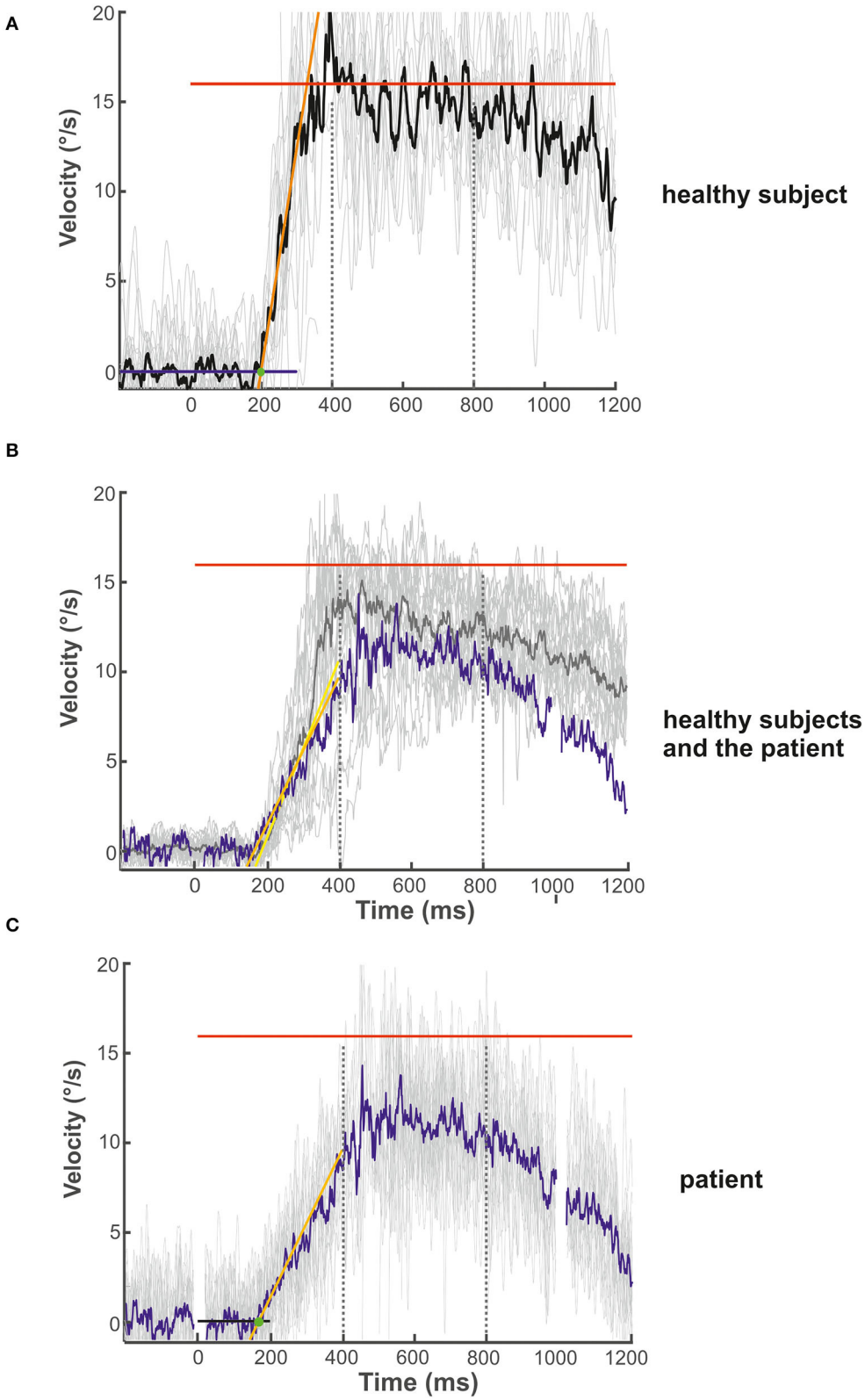

FIGURE 3
Examples of the initial and maintenance pursuit velocity in a healthy control subject [**(A)**: gain: 0.89, latency: 199 ms, acc.: 123.35 °/s²] and the patient [**(C)**: gain: 0.69, latency: 192 ms, acc.: 35.94 °/s²] responding to the step-ramp stimulus paradigm. For each subject, the bold trace shows the median of all individual (thin gray lines) ramp velocities. Figure **(B)** shows the mean (thick gray trace) of the individual median eye velocity of
(Continued)

FIGURE 3 (Continued)
all healthy subjects to illustrate the variability of initial acceleration values. For comparison, the blue trace in **(B)** shows the median of the patient's pursuit velocity values, as shown in **(C)**. While there is no difference in pursuit latency, the initial acceleration and velocity gain is low in the patient compared to this healthy control **(C)** but within the data range of the healthy subject group **(B)**. This difference was not significant for the group comparison (see Figure 2D). The target velocity (16°/s) is indicated by the red line. The blue **(A)** and black **(C)** line at the bottom reflects the baseline velocity prior to the ramp, the orange line the regression line of the average pursuit velocity (60 ms after pursuit onset), and the green dot the intersection of the regression line and the baseline before target motion onset. The slope of the orange line indicates pursuit acceleration for both individuals [yellow regression line = mean slope of all healthy subjects in **(B)**]; the time between trial start and the intersection indicates pursuit latency. The interval between both dotted vertical lines was taken for the maintenance pursuit velocity analysis.

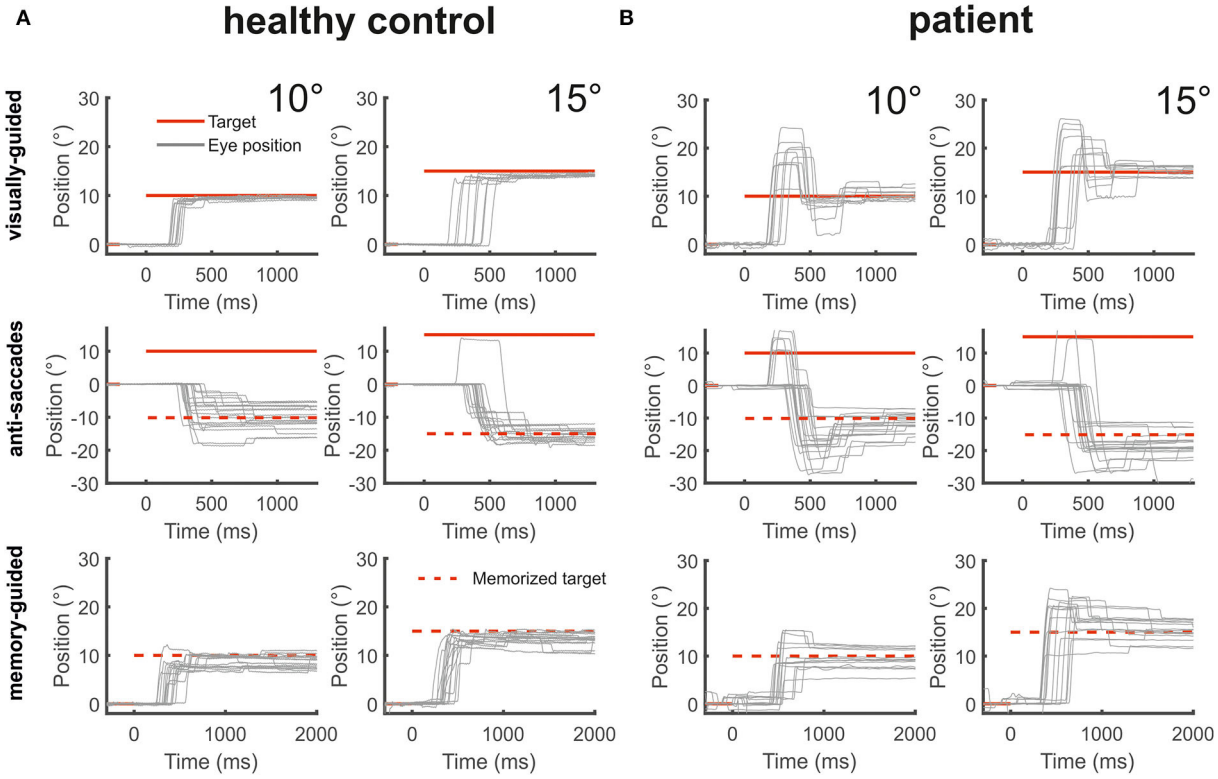

FIGURE 4
The figure shows from top to bottom horizontal eye position data (gray) during visually-guided saccades (pro-saccades), anti-saccades, and memory-guided saccades for two amplitudes (10 and 15°) for a healthy control [**(A)**, left side] and the patient [**(B)**, right side]. The target at gaze straight ahead or at the defined peripheral location is shown in red lines. The dashed red lines indicate the mirrored target position in the anti-saccade task and the previously presented target position that is to be remembered during the memory-guided saccade task. The patient's saccades during all three saccade tasks were severely hypermetric.

finally elaborate on the dysmetria of his volitional saccades, i.e., antisaccades and memory-guided saccades.

The patient's hemorrhage was centered in the midline between the deep cerebellar nuclei and extended rostrally into the vermal lobules IV and V and the right hemispheric lobules V and VI (40, 41). The edema bilaterally involved the fastigial nuclei anteriorly to the hemorrhage at the roof of the fourth ventricle, most likely impairing inter-fastigial projections (15), and laterally the interpositus nuclei (globose and emboliform nuclei) and the medial part of the dentate nuclei (Figure 1). The lesion did not comprise hemispheric lobule VI (simple lobule), the posterior oculomotor vermal lobules VI and VI (OMV), flocculus, paraflocculus, and caudal vermal uvula and nodulus. Functionally, the only lesion site in the whole brain known to elicit such a striking bilateral saccade hypermetria is a bilateral impairment of the FOR.

Smooth pursuit eye movements

Experimental unilateral FOR lesions in non-human primates elicit severe contralesional smooth pursuit impairment comparable in magnitude to the deficit observed during floccular lesions (48). Unilateral FOR lesions in the non-human

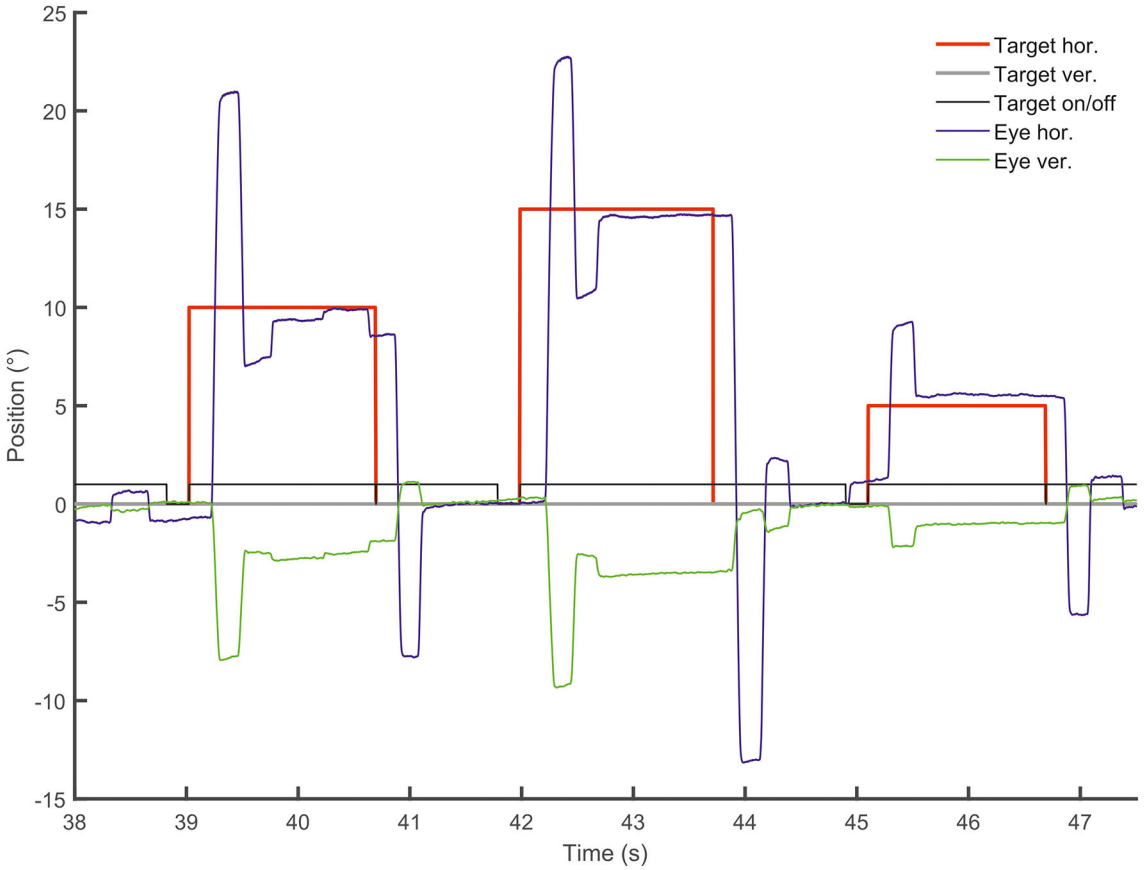

FIGURE 5
Vertical deflection during horizontal visually-guided pro-saccades. Vertical (green) and horizontal (blue) eye position is shown over time (sec) following horizontal target displacements (red). Note the large vertical deflection during hypermetric horizontal saccades.

primates not only impair contralateral but also increase ipsilesional pursuit acceleration (4) as the FOR neurons burst throughout the initial third of the eye acceleration with a subsequent steady firing (13). Moreover, it has been proposed that unilateral FOR lesions change the bilateral balance of pursuit-related activity in the recipients from the FOR (49), either directly in the pontine or indirectly in the ventral posterolateral thalamic nuclei (50, 51). Accordingly, the bilateral equilibrium is impaired by the asymmetrical FOR input (1, 49). According to this equilibrium hypothesis, the contralesional (e.g., right) pursuit impairment after unilateral (i.e., left-sided) FOR lesions is functionally related to the unilateral suppression of the pursuit-related activity in the pontine and thalamic nuclei (1).

In bilateral FOR lesions, however, the impaired contralesional pursuit acceleration is counterbalanced by the impaired ipsilesional pursuit deceleration making the pursuit maintenance phase appear normal (4). Thus, both fastigial nuclei would dynamically adjust the balance (symmetry) of directional smooth pursuit premotor commands (1, 49, 52). In bilateral lesions, the pontine and thalamic pursuit-related structures do not receive any or very little symmetrical action potentials from the FOR.

Bilateral FOR lesions in non-human primates (4) showed normal pursuit latency and sinusoidal pursuit gain was normal toward the ipsilesional direction and only slightly reduced toward the contralesional direction. In unilateral FOR lesions, pursuit acceleration was found to be increased to the ipsilesional side or decreased to the contralesional side. Subsequent inactivation of the contralateral FOR, functionally resulting in bilateral FOR lesions, normalized pursuit acceleration as FOR activity that aids contralateral and reduces ipsilateral acceleration, was abolished. Accordingly, bilateral FOR lesions restore the imbalance of opposing driving pursuit forces that are impressively seen in unilateral FOR lesions. Thus, a deficient pursuit acceleration due to a unilateral FOR lesion can be normalized by an additional contralateral FOR lesion (bilateral FOR lesion).

It has therefore been proposed that the pursuit acceleration is generated outside the FOR (4). A study on a cohort

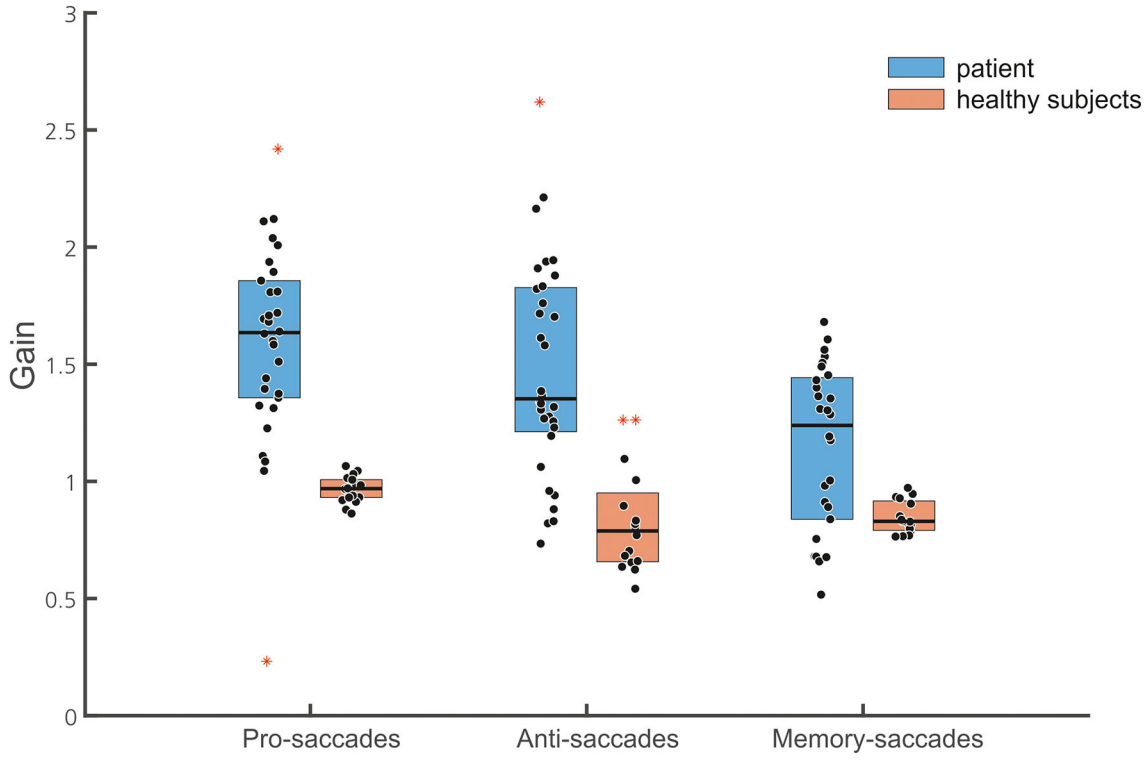

FIGURE 6
Box plots of the normalized gain of the different saccade tasks are shown (30 pro-saccades, 32 antisaccades, and 28 memory-guided saccades, with marked median; upper and lower quartiles, i.e., 75th and 25th percentiles). Outliers are marked in red. Note that data points of the patient (blue boxes) indicate gain values of single saccades while they represent the mean of the normalized gain of individual subjects in the healthy subject group (brown box). The median gain of all three saccade tasks is larger in the patient than in the healthy subjects.

of stroke patients with unilateral cerebellar lesions revealed impaired pursuit acceleration to the ipsilesional side but only some (5 of 10) patients had lesions spreading into the FOR (14). Noticeably, pursuit acceleration to the ipsilateral side was impaired while experimental unilateral FOR inactivations impaired contralateral pursuit acceleration (4). In contrast, bilateral FOR inactivation in non-human primates did not impair the initial acceleration of smooth pursuit, i.e., the open-loop period of smooth tracking behavior (first 100 ms) (4). In line with these animal data, the initial acceleration of smooth pursuit of our patient was at the lower level of the normal reference range in related studies, e.g., 42 ± 6°/s² (53), 40–100°/s² (54) or 44–124°/s² (55). The difference with our control group did not reach statistical significance. Therefore, this result should be confirmed in a larger cohort of patients with confined FOR lesions. As they are very rare, we felt compelled to report this first recording of the initial pursuit acceleration in this patient.

Instead, reduced initial acceleration is found in posterior vermal lesions in non-human primates (7) with moderately impaired sustained pursuit (56) suggesting that the oculomotor vermis plays a critical role in the online control of pursuit (7, 57).

Clinically, vermal lesions cause a decrease of ipsilateral smooth pursuit gain (56), which was not found in our patient. The lesion of our patient affected the FOR bilaterally but clearly did not involve the OMV (vermal lobules VI, VII). We cannot, however, rule out that the hemorrhage or its edema damaged the inhibitory control of the Purkinje cell fibers from the OMV (lobules VIIA and VIc) to the smooth pursuit neurons in the FOR. This functional impairment could have contributed to the low initial pursuit acceleration. Other cerebellar structures controlling smooth pursuit were not lesioned, even by edema, in particular the flocculus and paraflocculus (48, 58, 59).

Lesions of bilateral interpositus (globose and emboliform) nuclei, which were involved in our patient's edema, slightly affect vertical smooth pursuit and vertical saccades but not horizontal pursuit and saccades (60). The hemispheric oculomotor region (HOR) is a relatively large region that extends from the OMV into the simple lobules of the cerebellar hemispheres (12) which were spared in our patient's lesion. Up to now, there is no evidence that lesions of the dentate or vermal lobules IV and V (being affected by the patient's hemorrhage) control visually-guided goal-directed eye movements.

Visually-guided pro-saccades

Dysmetria of visually-guided saccades (VGS) in cerebellar disease is caused by midline lesions affecting the OMV or the FOR. While vermal lesions elicit hypometric saccades (6, 21), FOR lesion causes contralesional saccade hypometria and ipsilesional hypermetria when it is unilateral, bilateral hypermetria when it is bilateral (1, 2, 5, 22). In line with previous clinical reports (11, 34) our patient showed severe bilateral saccade hypermetria when visual information about the target was provided. Evidence for some visual influence on saccade dysmetria comes from the following observations in patients: (i) saccade dysmetria is heavily dependent on visual signals as it may disappear in darkness (61); (ii) correction saccades are dysmetric (62), in line with our patient, i.e., his consecutive correction saccades (in contrast to the non-visually guided saccades) remained hypermetric until he reached the visible target; and (iii) dysmetria increases once the target jumps from one to another target in brief succession (double-step paradigm) (63) suggesting impaired neural parallel processing of saccadic signals in cerebellar disease (64). Noticeably, saccades of non-human primates toward flashed peripheral visual targets in complete darkness were still dysmetric (22, 23).

It has been proposed that bilateral saccade hypermetria results from a faulty feedback control of saccades in the brain stem, manifesting with an impairment to accelerate contralateral and decelerate ipsilateral saccades (5). Accordingly, bilateral hypermetria in bilateral FOR lesions results from both impaired saccade acceleration and deceleration. In line with experimental FOR lesions hypermetria of vertical saccades and vertical deflection during horizontal saccades were smaller in our patient (Figure 5). The latency and saccade velocity of our patient's visually-guided saccades were normal, in accord with experimental FOR lesions (5). The patient's final eye position was on target, i.e., there was no increased end-point variability as seen in cerebellar disease which has been attributed to an increase of accumulating signal noise (65) or a feedforward rather than feedback saccade control, respectively (66, 67).

The mechanisms for the saccade and pursuit disorders in experimental FOR lesions seem to be unrelated as they were not correlated to each other (1) suggesting that caudal FOR processes saccade and pursuit signals independently.

This visual influence implies that saccade hypermetria may decrease or disappear in the absence of a visual target. But even visual objects may not necessarily elicit saccade dysmetria as it is not found during visual scanning (8). Therefore, we examined memory-guided saccades and antisaccades (29). Although initiated by a visual cue, the neural drive of these volitional saccades is based on a calculated but not a visible target position. Subjects had to look at an imagined target position during the anti-saccade paradigm without having seen a visual target at this location. In the memory-guided paradigm, they had to keep the visible target position in mind within a variable interval challenging working memory. Thus, the execution follows a neural representation of a previously shown visible target that is no longer visible anymore.

Memory-guided saccade and anti-saccades

Up to now, three studies investigated memory-guided saccades in cerebellar disease but only a few patients had lesions involving the FOR (10, 26, 34). As memory-guided saccades (MGS) were equally hypermetric compared to VGS, the authors proposed that these cerebellar patients were unable to use feedforward internal signals (e.g., efference copy signals) to estimate final eye position (34). In our patient, there was a trend toward a lesser hypermetria in MGS and anti-saccades compared to VGS. Correction saccades following the first MGS were hypometric while those directed toward the reilluminated target in the gaze straight ahead position were always hypermetric. Accordingly, the gain of the correction saccades was also smaller in MGS and anti-saccades compared to VGS. Noticeably, the proportion of correction saccades in the MGS task did not differ from healthy subjects but its direction differed: while correction saccades of the patient were directed backward toward the memorized target (due to hypermetria), it was directed toward it in the healthy participants due to physiological hypometria (62). However, the final eye position after correction saccades was normal indicating preserved internal spatial representation of the target. This is in contrast to FOR patients who maintained their gaze toward the erroneous eye position until the target was switched on again (34). Our patient seems to be able to use internal (e.g., efferent copy) signals to control saccade accuracy which is in line with previous data (63). Both cerebellar midline structures (the FOR and the OMV) contain not only saccade-related neurons that are more active in the light compared to darkness (19, 27) but also a type of neurons whose discharge is unrelated to eye movements but to the memory of a previously seen smooth pursuit target as they discharge in the "no-go instruction" period (33). The authors suggested that this pathway contributes specifically to motor planning engaging the working memory of no-go instructions and the preparation of tracking eye movements. It is supposed to be part of the cerebro-cerebellar loops (involving the supplementary eye field and the pontine nuclei) for no-go instruction working memories and is engaged in the decision of whether or not to, and what to pursue. Unfortunately, it is unknown how these cells respond to MGS. Recently, new projections from the deep cerebellar nuclei to the hippocampus *via* the thalamic nuclei have been identified in mice that may subserve memory-related cognitive functions (68). In the posterolateral region of the thalamus, pursuit-related neurons discharge before and during the initiation of ipsiversive

pursuit and may receive projections from the contralateral FOR (1, 50, 51).

Anti-saccades have not been studied in FOR lesions before. Similar to MGS, our patient's anti-saccades were also hypermetric, with a trend to larger amplitudes compared to MGS and smaller compared to VGS. The execution of anti-saccades not only requires suppression of reflexive involuntary saccades to the target but to mirror and memorize the visual target position which clearly engages working memory as well. Correction saccades were hypometric compared to those of hypermetric VGS and larger compared to those of healthy control subjects. As the final eye position did not differ from controls, the working memory of the target location and of its mirrored position was intact. Along with the normal latency and error rate of anti-saccades disease-related cognitive (e.g., attention) deficits are unlikely to contribute to saccade dysmetria.

In conclusion, we provide some clinical evidence that a bilateral lesion of the deep cerebellar nuclei does not impair the initial acceleration of smooth pursuit, as it is found in unilateral FOR lesions. This result is in line with experimental FOR lesions in non-human primates. At the same time, the lesion caused severe saccade hypermetria. The neural correlate of peripheral target locations seems to remain unimpaired in our patient and in fact, contributes to the pronounced hypermetria of MGS and antisaccades. In light of the dissociation of moderately preserved initial and maintenance smooth pursuit but severe saccade hypermetria, our data argue against an impaired common command feeding the circuits controlling saccadic and pursuit eye movements. Instead, they are consistent with independent influences on the neural processes generating both eye movements (1).

Data availability statement

The raw data supporting the conclusions of this article will be made available by the authors on request.

Ethics statement

The studies involving human participants were reviewed and approved by the Ethics Committee of the University of Lübeck. Written informed consent for participation was not required for this study in accordance with the national legislation and the institutional requirements.

Author contributions

CH: design or conceptualization of the study, analysis and interpretation of the data, and drafting the manuscript. BM: interpretation of the data and revising the manuscript for intellectual content. HS: analysis or interpretation of the data and revising the manuscript for intellectual content. AS: acquisition, analysis, and interpretation of the data, and revising the manuscript for intellectual content. All authors contributed to the article and approved the submitted version.

Conflict of interest

The authors declare that the research was conducted in the absence of any commercial or financial relationships that could be construed as a potential conflict of interest.

Publisher's note

References

1. Bourrelly C, Quinet J, Goffart L. Pursuit disorder and saccade dysmetria after caudal fastigial inactivation in the monkey. *J Neurophysiol.* (2018) 120:1640–54. doi: 10.1152/jn.00278.2018

2. Bourrelly C, Quinet J, Goffart L. The caudal fastigial nucleus and the steering of saccades toward a moving visual target. *J Neurophysiol.* (2018) 120:421–38. doi: 10.1152/jn.00141.2018

3. Bourrelly C, Quinet J, Goffart L. Bilateral control of interceptive saccades: evidence from the ipsipulsion of vertical saccades after caudal fastigial inactivation. *J Neurophysiol.* (2021) 125:2068–83. doi: 10.1152/jn.00037.2021

4. Robinson FR, Straube A, Fuchs AF. Participation of caudal fastigial nucleus in smooth pursuit eye movements. II. Effects of muscimol inactivation. *J Neurophysiol.* (1997) 78:848–59. doi: 10.1152/jn.1997.78.2.848

5. Robinson FR, Straube A, Fuchs AF. Role of the caudal fastigial nucleus in saccade generation. II. Effects of muscimol inactivation. *J Neurophysiol.* (1993) 70:1741–58. doi: 10.1152/jn.1993.70.5.1741

6. Takagi M, Zee DS, Tamargo RJ. Effects of lesions of the oculomotor vermis on eye movements in primate: saccades. *J Neurophysiol.* (1998) 80:1911–31. doi: 10.1152/jn.1998.80.4.1911

7. Takagi M, Zee DS, Tamargo RJ. Effects of lesions of the oculomotor cerebellar vermis on eye movements in primate: smooth pursuit. *J Neurophysiol.* (2000) 83:2047–62. doi: 10.1152/jn.2000.83.4.2047

8. Büttner U, Straube A. The effect of cerebellar midline lesions on eye movements. *Neuroophthalmology.* (1995) 15:75–82. doi: 10.3109/01658109509009646

9. Büttner U, Straube A, Spuler A. Saccadic dysmetria and "intact" smooth pursuit eye movements after bilateral deep cerebellar nuclei lesions. *Neuroophthalmology.* (1995) 15:67–74. doi: 10.3109/01658109509009645

10. Kori AA, Das VE, Zivotofsky AZ, Leigh RJ. Memory-guided saccadic eye movements: effects of cerebellar disease. *Vision Res.* (1998) 38:3181–92. doi: 10.1016/S0042-6989(98)00026-1

11. Milenkovic I, Kasprian G, Wiest G. Saccadic hypermetria from a selective lesion of the fastigial oculomotor region. *Neurology.* (2021) 96:449–51. doi: 10.1212/WNL.0000000000011462

12. Thier P, Markanday A. Role of the vermal cerebellum in visually guided eye movements and visual motion perception. *Annu Rev Vis Sci.* (2019) 5:247–68. doi: 10.1146/annurev-vision-091718-015000

13. Fuchs AF, Robinson FR, Straube A. Participation of the caudal fastigial nucleus in smooth-pursuit eye movements. I. Neuronal activity. *J Neurophysiol.* (1994) 72:2714–28. doi: 10.1152/jn.1994.72.6.2714

14. Straube A, Scheuerer W, Eggert T. Unilateral cerebellar lesions affect initiation of ipsilateral smooth pursuit eye movements in humans. *Ann Neurol.* (1997) 42:891–8. doi: 10.1002/ana.410420611

15. Gomez-Gonzalez GB, Martinez-Torres A. Inter-fastigial projections along the roof of the fourth ventricle. *Brain Struct Funct.* (2021) 226:901–17. doi: 10.1007/s00429-021-02217-8

16. Thier P, Dicke PW, Haas R, Thielert CD, Catz N. The role of the oculomotor vermis in the control of saccadic eye movements. *Ann N Y Acad Sci.* (2002) 978:50–62. doi: 10.1111/j.1749-6632.2002.tb07555.x

17. Fuchs AF, Robinson FR, Straube A. Role of the caudal fastigial nucleus in saccade generation. i. neuronal discharge pattern. *J Neurophysiol.* (1993) 70:1723–40. doi: 10.1152/jn.1993.70.5.1723

18. Shemesh AA, Zee DS. Eye movement disorders and the cerebellum. *J Clin Neurophysiol.* (2019) 36:405–14. doi: 10.1097/WNP.0000000000000579

19. Helmchen C, Buttner U. Saccade-related purkinje cell activity in the oculomotor vermis during spontaneous eye movements in light and darkness. *Exp Brain Res.* (1995) 103:198–208. doi: 10.1007/BF00231706

20. Ohtsuka K, Noda H. Burst discharges of mossy fibers in the oculomotor vermis of macaque monkeys during saccadic eye movements. *Neurosci Res.* (1992) 15:102–14. doi: 10.1016/0168-0102(92)90023-6

21. Sato H, Noda H. Saccadic dysmetria induced by transient functional decortication of the cerebellar vermis [corrected]. *Exp Brain Res.* (1992) 88:455–8. doi: 10.1007/BF02259122

22. Goffart L, Chen LL, Sparks DL. Deficits in saccades and fixation during muscimol inactivation of the caudal fastigial nucleus in the rhesus monkey. *J Neurophysiol.* (2004) 92:3351–67. doi: 10.1152/jn.01199.2003

23. Quinet J, Goffart L. Head-unrestrained gaze shifts after muscimol injection in the caudal fastigial nucleus of the monkey. *J Neurophysiol.* (2007) 98:3269–83. doi: 10.1152/jn.00741.2007

24. Pelisson D, Goffart L, Guillaume A. Contribution of the rostral fastigial nucleus to the control of orienting gaze shifts in the head-unrestrained cat. *J Neurophysiol.* (1998) 80:1180–96. doi: 10.1152/jn.1998.80.3.1180

25. Helmchen C, Straube A, Buttner U. Saccadic lateropulsion in wallenberg's syndrome may be caused by a functional lesion of the fastigial nucleus. *J Neurol.* (1994) 241:421–6. doi: 10.1007/BF00900959

26. Kanayama R, Bronstein AM, Shallo-Hoffmann J, Rudge P, Husain M. Visually and memory guided saccades in a case of cerebellar saccadic dysmetria. *J Neurol Neurosurg Psychiatry.* (1994) 57:1081–4. doi: 10.1136/jnnp.57.9.1081

27. Helmchen C, Straube A, Buttner U. Saccade-related activity in the fastigial oculomotor region of the macaque monkey during spontaneous eye movements in light and darkness. *Exp Brain Res.* (1994) 98:474–82. doi: 10.1007/BF00233984

28. Ohtsuka K, Noda H. Burst discharges of fastigial neurons in macaque monkeys are driven by vision- and memory-guided saccades but not by spontaneous saccades. *Neurosci Res.* (1992) 15:224–8. doi: 10.1016/0168-0102(92)90009-2

29. McDowell JE, Dyckman KA, Austin BP, Clementz BA. Neurophysiology and neuroanatomy of reflexive and volitional saccades: evidence from studies of humans. *Brain Cogn.* (2008) 68:255–70. doi: 10.1016/j.bandc.2008.08.016

30. Nyffeler T, Muri RM, Bucher-Ottiger Y, Pierrot-Deseilligny C, Gaymard B, Rivaud-Pechoux S. Inhibitory control of the human dorsolateral prefrontal cortex during the anti-saccade paradigm–a transcranial magnetic stimulation study. *Eur J Neurosci.* (2007) 26:1381–5. doi: 10.1111/j.1460-9568.2007.05758.x

31. Ploner CJ, Gaymard BM, Rivaud-Pechoux S, Pierrot-Deseilligny C. The prefrontal substrate of reflexive saccade inhibition in humans. *Biol Psychiatry.* (2005) 57:1159–65. doi: 10.1016/j.biopsych.2005.02.017

32. Guerrasio L, Quinet J, Buttner U, Goffart L. Fastigial oculomotor region and the control of foveation during fixation. *J Neurophysiol.* (2010) 103:1988–2001. doi: 10.1152/jn.00771.2009

33. Kurkin S, Akao T, Fukushima J, Shichinohe N, Kaneko CR, Belton T, et al. No-Go neurons in the cerebellar oculomotor vermis and caudal fastigial nuclei: planning tracking eye movements. *Exp Brain Res.* (2014) 232:191–210. doi: 10.1007/s00221-013-3731-x

34. Gaymard B, Rivaud S, Amarenco P, Pierrot-Deseilligny C. Influence of visual information on cerebellar saccadic dysmetria. *Ann Neurol.* (1994) 35:108–12. doi: 10.1002/ana.410350117

35. Crawford TJ, Higham S, Renvoize T, Patel J, Dale M, Suriya A, et al. Inhibitory control of saccadic eye movements and cognitive impairment in Alzheimer's disease. *Biol Psychiatry.* (2005) 57:1052–60. doi: 10.1016/j.biopsych.2005.01.017

36. Antoniades C, Ettinger U, Gaymard B, Gilchrist I, Kristjansson A, Kennard C, et al. An internationally standardised antisaccade protocol. *Vision Res.* (2013) 84:1–5. doi: 10.1016/j.visres.2013.02.007

37. Sprenger A, Hanssen H, Hagedorn I, Prasuhn J, Rosales RL, Jamora RDG, et al. Eye movement deficits in x-linked dystonia-parkinsonism are related to striatal degeneration. *Parkinsonism Relat Disord.* (2019) 61:170–8. doi: 10.1016/j.parkreldis.2018.10.016

38. Antoniades CA, Demeyere N, Kennard C, Humphreys GW, Hu MT. antisaccades and executive dysfunction in early drug-naive Parkinson's disease: the discovery study. *Mov Disord.* (2015) 30:843–7. doi: 10.1002/mds.26134

39. Crawford TJ, Bennett D, Lekwuwa G, Shaunak S, Deakin JF. Cognition and the inhibitory control of saccades in Schizophrenia and Parkinson's disease. *Prog Brain Res.* (2002) 140:449–66. doi: 10.1016/S0079-6123(02)40068-4

40. Diedrichsen J, Maderwald S, Kuper M, Thurling M, Rabe K, Gizewski ER, et al. Imaging the deep cerebellar nuclei: a probabilistic atlas and normalization procedure. *Neuroimage.* (2011) 54:1786–94. doi: 10.1016/j.neuroimage.2010.10.035

41. Schmahmann JD, Doyon J, Toga A, Petrides M, Evans A. *Mri Atlas of the Human Cerebellum.* New York, NY: Academic Press (2000).

42. Rashbass C. The relationship between saccadic and smooth pursuit tracking eye movements. *J Physiol.* (1961) 159:326–38. doi: 10.1113/jphysiol.1961.sp006811

43. Carl JR, Gellman RS. Human smooth pursuit: stimulus-dependent responses. *J Neurophysiol.* (1987) 57:1446–63. doi: 10.1152/jn.1987.57.5.1446

44. Hubner J, Sprenger A, Klein C, Hagenah J, Rambold H, Zuhlke C, et al. Eye movement abnormalities in spinocerebellar ataxia type 17 (Sca17). *Neurology.* (2007) 69:1160–8. doi: 10.1212/01.wnl.0000276958.91986.89

45. Lencer R, Sprenger A, Trillenberg P. Smooth eye movements in humans: smooth pursuit, optokinetic nystagmus and vestibular ocular reflex. In: Klein C, Ettinger U, editors. *Eye Movement Research an Introduction to Its Scientific Foundations and Applications*. Springer Nature Switzerland AG (2019). p. 120–54. doi: 10.1007/978-3-030-20085-5_4

46. Sprenger A, Weber FD, Machner B, Talamo S, Scheffelmeier S, Bethke J, et al. Deprivation and recovery of sleep in succession enhances reflexive motor behavior. *Cereb Cortex.* (2015) 25:4610–8. doi: 10.1093/cercor/bhv115

47. Crawford JR, Garthwaite PH. Testing for suspected impairments and dissociations in single-case studies in neuropsychology: evaluation of alternatives using monte carlo simulations and revised tests for dissociations. *Neuropsychology.* (2005) 19:318–31. doi: 10.1037/0894-4105.19.3.318

48. Zee DS, Yamazaki A, Butler PH, Gucer G. Effects of ablation of flocculus and paraflocculus of eye movements in primate. *J Neurophysiol.* (1981) 46:878–99. doi: 10.1152/jn.1981.46.4.878

49. Goffart L. Kinematics and the neurophysiological study of visually-guided eye movements. *Prog Brain Res.* (2019) 249:375–84. doi: 10.1016/bs.pbr.2019.03.027

50. Noda H, Sugita S, Ikeda Y. Afferent and efferent connections of the oculomotor region of the fastigial nucleus in the macaque monkey. *J Comp Neurol.* (1990) 302:330–48. doi: 10.1002/cne.903020211

51. Tanaka M. Involvement of the central thalamus in the control of smooth pursuit eye movements. *J Neurosci.* (2005) 25:5866–76. doi: 10.1523/JNEUROSCI.0676-05.2005

52. Goffart L, Bourrelly C, Quinton JC. Neurophysiology of visually guided eye movements: critical review and alternative viewpoint. *J Neurophysiol.* (2018) 120:3234–45. doi: 10.1152/jn.00402.2018

53. Helmchen C, Hagenow A, Miesner J, Sprenger A, Rambold H, Wenzelburger R, et al. Eye movement abnormalities in essential tremor may indicate cerebellar dysfunction. *Brain.* (2003) 126(Pt 6):1319–32. doi: 10.1093/brain/awg132

54. Leigh RJ, Zee DS. *The Neurology of Eye Movements.* 5th ed. New York, Y: Oxford University Press (2015). doi: 10.1093/med/9780199969289.001.0001

55. Moschner C, Crawford TJ, Heide W, Trillenberg P, Kompf D, Kennard C. Deficits of smooth pursuit initiation in patients with degenerative cerebellar lesions. *Brain.* (1999) 122 (Pt 11):2147–58. doi: 10.1093/brain/122.11.2147

56. Vahedi K, Rivaud S, Amarenco P, Pierrot-Deseilligny C. Horizontal eye movement disorders after posterior vermis infarctions. *J Neurol Neurosurg Psychiatry.* (1995) 58:91–4. doi: 10.1136/jnnp.58.1.91

57. Dash S, Catz N, Dicke PW, Thier P. Encoding of Smooth-Pursuit Eye Movement Initiation by a Population of Vermal Purkinje cells. *Cereb Cortex.* (2012) 22:877–91. doi: 10.1093/cercor/bhr153

58. Rambold H, Churchland A, Selig Y, Jasmin L, Lisberger SG. Partial ablations of the flocculus and ventral paraflocculus in monkeys cause linked deficits in smooth pursuit eye movements and adaptive modification of the vor. *J Neurophysiol.* (2002) 87:912–24. doi: 10.1152/jn.00768.2000

59. Suzuki DA, Keller EL. The role of the posterior vermis of monkey cerebellum in smooth-pursuit eye movement control. II. Target velocity-related purkinje cell activity. *J Neurophysiol.* (1988) 59:19–40. doi: 10.1152/jn.1988.59.1.19

60. Robinson FR. Role of the cerebellar posterior interpositus nucleus in saccades. I. Effect of temporary lesions. *J Neurophysiol.* (2000) 84:1289–302. doi: 10.1152/jn.2000.84.3.1289

61. Selhorst JB, Stark L, Ochs AL, Hoyt WF. Disorders in cerebellar ocular motor control. I. Saccadic overshoot dysmetria. An oculographic, control system and clinico-anatomical analysis. *Brain.* (1976) 99:497–508. doi: 10.1093/brain/99.3.497

62. Botzel K, Rottach K, Buttner U. Normal and pathological saccadic dysmetria. *Brain.* (1993) 116 (Pt 2):337–53. doi: 10.1093/brain/116.2.337

63. King S, Chen AL, Joshi A, Serra A, Leigh RJ. Effects of cerebellar disease on sequences of rapid eye movements. *Vision Res.* (2011) 51:1064–74. doi: 10.1016/j.visres.2011.02.019

64. King SA, Schneider RM, Serra A, Leigh RJ. Critical role of cerebellar fastigial nucleus in programming sequences of saccades. *Ann N Y Acad Sci.* (2011) 1233:155–61. doi: 10.1111/j.1749-6632.2011.06119.x

65. Eggert T, Robinson FR, Straube A. Modeling inter-trial variability of saccade trajectories: effects of lesions of the oculomotor part of the fastigial nucleus. *PLoS Comput Biol.* (2016) 12:e1004866. doi: 10.1371/journal.pcbi.1004866

66. Glasauer S. Cerebellar contribution to saccades and gaze holding: a modeling approach. *Ann N Y Acad Sci.* (2003) 1004:206–19 doi: 10.1196/annals.1303.018

67. Eggert T, Straube A. Saccade variability in healthy subjects and cerebellar patients. *Prog Brain Res.* (2019) 249:141–52. doi: 10.1016/bs.pbr.2019.03.021

68. Bohne P, Schwarz MK, Herlitze S, Mark MD. A new projection from the deep cerebellar nuclei to the hippocampus via the ventrolateral and laterodorsal thalamus in mice. *Front Neural Circuits.* (2019) 13:51. doi: 10.3389/fncir.2019.00051

frontiers | Frontiers in Neurology

TYPE Brief Research Report
PUBLISHED 26 September 2022
DOI 10.3389/fneur.2022.941909

OPEN ACCESS

EDITED BY
Dominik Straumann,
University of Zurich, Switzerland

REVIEWED BY
Sun-Uk Lee,
Korea University Medical Center, South Korea
Diego Kaski,
University College London, United Kingdom
Maurizio Versino,
Humanitas Mater Domini, Italy

*CORRESPONDENCE
Tzu-Pu Chang
neurochang0617@gmail.com

SPECIALTY SECTION
This article was submitted to Neuro-Otology, a section of the journal Frontiers in Neurology

RECEIVED 12 May 2022
ACCEPTED 06 September 2022
PUBLISHED 26 September 2022

CITATION
Bery AK and Chang TP (2022) Positive horizontal-canal head impulse test is not a benign sign for acute vestibular syndrome with hearing loss. *Front. Neurol.* 13:941909. doi: 10.3389/fneur.2022.941909

Positive horizontal-canal head impulse test is not a benign sign for acute vestibular syndrome with hearing loss

Anand K. Bery[1] and Tzu-Pu Chang [2,3]*

[1]Division of Neurology, Department of Medicine, University of Ottawa, Ottawa, ON, Canada, [2]Department of Neurology/Neuro-Medical Scientific Center, Taichung Tzu Chi Hospital, Buddhist Tzu Chi Medical Foundation, Taichung, Taiwan, [3]Department of Neurology, School of Medicine, Tzu Chi University, Hualien, Taiwan

Background: Diagnosis of acute vestibular syndrome (AVS) with hearing loss is challenging because the leading vascular cause—AICA territory stroke—can appear benign on head impulse testing. We evaluated the diagnostic utility of various bedside oculomotor tests to discriminate imaging-positive and imaging-negative cases of AVS plus hearing loss.

Method: We reviewed 13 consecutive inpatients with AVS and acute unilateral hearing loss. We compared neurologic findings, bedside and video head impulse testing (bHIT, vHIT), and other vestibular signs (including nystagmus, skew deviation, and positional testing) between MRI+ and MRI− cases.

Results: Five of thirteen patients had a lateral pontine lesion (i.e., MRI+); eight did not (i.e., MRI−). Horizontal-canal head impulse test showed ipsilateral vestibular loss in all five MRI+ patients but only in three MRI− patients. The ipsilesional VOR gains of horizontal-canal vHIT were significantly lower in the MRI+ than the MRI− group (0.56 ± 0.11 vs. 0.87 ± 0.24, $p = 0.03$). All 5 MRI+ patients had horizontal spontaneous nystagmus beating away from the lesion (5/5). One patient (1/5) had direction-changing nystagmus with gaze. Two had skew deviation (2/5). Among the 8 MRI− patients, one (1/8) presented as unilateral vestibulopathy, four (4/8) had positional nystagmus and three (3/8) had isolated posterior canal hypofunction.

Conclusion: The horizontal-canal head impulse test poorly discriminates central and peripheral lesions when hearing loss accompanies AVS. Paradoxically, a lateral pontine lesion usually mimics unilateral peripheral vestibulopathy. By contrast, patients with peripheral lesions usually present with positional nystagmus or isolated posterior canal impairment, risking misdiagnosis as central vestibulopathy.

KEYWORDS

vertigo, dizziness, acute vestibular syndrome, hearing loss, central vestibulopathy, stroke, head impulse test, nystagmus

Introduction

Acute vestibular syndrome (AVS) is defined as prolonged vertigo, vomiting, or unsteadiness more than 24 h (1, 2). The most common cause of AVS is vestibular neuritis (representing ∼75% of AVS), followed by posterior fossa stroke (∼25% of AVS) (3, 4). Differentiating central from peripheral causes of AVS remains a diagnostic challenge. The bedside oculomotor exam battery known as HINTS (i.e., Head Impulse test, Nystagmus, and Test of Skew deviation), is an accurate method for clinically distinguishing stroke from AVS (5). HINTS is designed to maximize sensitivity for detecting stroke; thus, to conclude a peripheral cause for vertigo, each of the three bedside maneuvers must point to a peripheral etiology. In other words, one requires positive head impulse test (HIT) AND unidirectional horizontal nystagmus AND negative test of skew to conclude a peripheral etiology. Any ONE of the following: negative HIT, direction-changing nystagmus, positive test of skew suggests that a central lesion is possible. Among the three tests, a positive HIT (6) (where an ocular refixation is seen) suggests a peripheral etiology since it usually indicates vestibular neuritis while normal HIT could portend a stroke (3, 5).

Stroke in the territory of AICA (the anterior inferior cerebellar artery) presents particular challenge because it is a central event (stroke) but can present with a positive HIT, which may be incorrectly interpreted as a benign finding. Because the blood supply of the inner ear originates from AICA, AICA infarction is often accompanied by labyrinthine ischemia and presents as acute audio-vestibular loss (7, 8). Therefore, these patients experience acute unilateral hearing loss with a positive HIT on the side of hearing loss, and are hard to differentiate from those with pure peripheral audio-vestibular loss. In order not to miss this type of stroke, the addition of acute hearing loss to the HINTS battery has previously been proposed (a strategy previously termed "HINTS Plus" for "HINTS Plus hearing loss") (9). Under HINTS Plus, acute hearing loss is a red flag feature supporting a stroke survey including brain MRI, even if all other signs point to a peripheral disorder.

HINTS Plus remains controversial, in part because infarction is historically felt to be an uncommon cause of sudden sensorineural hearing loss (SSNHL) *without* vertigo. Most cases of SSNHL are believed to be inflammatory rather than vascular in origin, and SSNHL with vertigo has sometimes been termed "labyrinthitis," which implies viral infection of the labyrinth (10). Some experts feel AICA stroke is a rare cause of SSNHL when compared to viral labyrinthitis (11–13). However, prior epidemiological studies have shown patients with SSNHL have a higher risk of stroke than the general population (14), and SSNHL with vertigo portends greater risk of stroke than either SSNHL or vertigo alone (15).

In this study, we systematically classified a series of patients with AVS plus acute hearing loss into central vs. peripheral etiologies by neuroimaging. We then compared clinical, oculomotor, and vestibular signs among groups to determine which features provide diagnostic value in this challenging clinical presentation.

Methods

We reviewed consecutive inpatients hospitalized for acute vertigo at our institution's neurology ward (Taichung Tzu Chi Hospital) between July 2017 and March 2022. We retained only those patients who had acute unilateral hearing loss accompanying their vertigo (in other words, the AVS plus acute unilateral hearing loss). AVS was defined as persistent vertigo and/or unsteadiness $\geq$24 h. Unilateral hearing loss was defined here as patient complaint of newly developing hearing loss that was confirmed by calibrated finger rub auditory screening test (CALFRAST) in the acute stage of vertigo (16). As per standard of care at our institution, all patients with this presentation are hospitalized for stroke workup and MRI study. We excluded patients who had a history of Ménière's disease, vestibular migraine, or other episodic vestibular syndromes.

Patients underwent bedside oculomotor testing by a single vestibular neurologist (TPC) in the ED before admission. This included the bedside head impulse test (bHIT), assessment of spontaneous and gaze-evoked nystagmus (GEN) with unaided eyes, and test of skew deviation. They also underwent positional testing in the ED, including the bow-and-lean test, Dix-Hallpike test, and supine-roll test, all *via* videonystagmoscopy with fixation block (i.e., without fixation). In addition, all patients underwent general neurological examinations in the emergency department, including comprehensive examination of cranial nerve function, muscle strength, myotatic reflexes and Babinski sign, sensory testing, finger-to-nose test, heel-to-shin test, rapid alternating movement, and assessment of gait.

Once hospitalized, patients underwent video-oculography (VOG) with video head impulse testing (vHIT). Patients routinely underwent horizontal-canal vHIT (H-vHIT), and those with normal H-vHIT results further underwent vertical-canal vHIT. A positive result was defined as vestibulo-ocular reflex (VOR) gain $<$0.8 in H-vHIT or VOR gain $<$0.75 in vertical-canal vHIT. The patients also underwent the bucket test for subjective visual vertical (SVV) with four trials (17). The mean SVV deviation of four trials $>$2.3 degrees was defined as abnormal. All patients underwent brain MRI and pure-tone audiometry during hospitalization. The sequences of brain MRI included DWI, T1WI, T2WI, FLAIR, SWAN, and MRA. For audiometry, pure-tone average (PTA) was defined as the average of hearing thresholds at 500, 1,000, and 2,000 Hz. Normal hearing was defined as thresholds $\leq$25 dB at all frequencies of the audiogram. All the exams were completed within 1 week of vertigo onset.

Patients were classified by MRI findings into two groups; those with posterior fossa lesions were classified as "MRI+," and

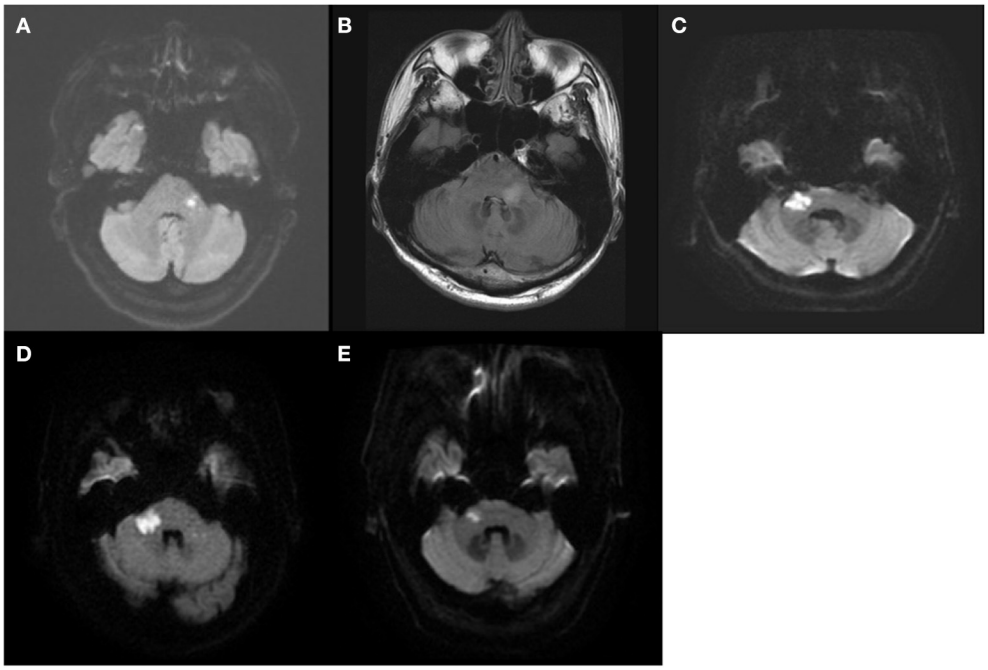

FIGURE 1
The MRI findings of the five patients with posterior fossa lesion (MRI+ group). Four had acute lateral pontine infarction **(A,C–E)** and one had acute demyelinating lesion in left lateral pons **(B)**.

those without posterior fossa lesions were classified as "MRI–." We compared demographic, bedside oculomotor, VOG, and other neurologic findings between groups. This included bHIT, vHIT, spontaneous nystagmus, GEN, positional nystagmus, skew deviation, SVV, PTA, and presence of vascular risk factors. Analysis was done in SPSS (IBM, v23). Continuous variables were compared *via* Mann-Whitney *U*-test. p-value < 0.05 was considered statistically significant.

Results

Thirteen patients with AVS plus acute hearing loss were included. All thirteen patients were hospitalized within 2 days of vertigo onset, and underwent brain MRI between 2 and 5 days (48–120 h) after vertigo onset. Among them, five patients had a posterior fossa lesion on MRI (and thus comprise the "MRI+" group). This includes four patients with acute lateral pontine infarction belonging to AICA territory and one patient with an acute demyelinating lesion in left lateral pons, who was ultimately diagnosed with multiple sclerosis (Figure 1). The other eight patients did not have posterior fossa lesion (and thus comprise the "MRI–" group).

Full clinical and neuro-otologic details of the included patients are available in Table 1. Four patients were female. The mean age was 59.4 years (56.2 in MRI+ and 61.4 in MRI–). Seven patients had diabetes mellitus (2/5 in MRI+ and 5/8 in MRI–), nine had hypertension (4/5 in MRI+ and 5/8 in MRI–), and six had dyslipidemia (4/5 in MRI+ and 2/8 in MRI–). The ABCD2 was not significantly different between groups (mean ABCD2 score 3.6 in MRI+ vs 3.9 in MRI–, $p = 0.72$). Three patients (3/5) in the MRI+ group had focal neurological signs, including one with diplopia and two with a lower motor neuron facial palsy. None of the patients in the MRI– group had focal neurological signs, and none developed focal signs or worsening in gait during hospitalization or follow-up clinic visits at 2 and 4 weeks, respectively, after vertigo onset.

Bedside head impulse test and vestibular exams

Patients underwent bedside vestibular testing within 2 days of vertigo onset. Horizontal canal bedside head impulse testing (H-bHIT) showed unilateral vestibular loss on the side of hearing loss (i.e., ipsilateral to the lesion side) in all MRI+ patients (5/5). Among MRI+ patients, all (5/5) had horizontal spontaneous nystagmus beating away from lesion side, never changing direction during positional testing (5/5). One MRI+ patient (1/5) had direction-changing gaze-evoked nystagmus (GEN), and two (2/5) had skew deviation.

Among the eight MRI– patients, only three patients (3/8) had unilateral vestibular loss on H-bHIT. One patient (1/8)

TABLE 1 Clinical and neuro-otologic findings in the patients with acute vestibular syndrome plus hearing loss.

Pt	Age/Sex	HL	PTA (dB)	H-bHIT	H-vHIT		Fixation		Fixation block		Skew	SVV (°)	Other signs	MRI
					Ipsi-lesional	Contra-lesional	SN	GEN	SN	PN				
1	68/F	L	29	L	0.45	1.26	RBN	–	RBN	RBN	–	L, 6	–	–
2	48/M	L	65	L	0.64	1.11	RBN	+	RBN	RBN	+	L, 5	Diplopia	Left lateral pontine infarction
3	41/M	L	25	L	0.56	0.61	RBN	–	RBN	RBN	+	L, 5	Left facial palsy	Left lateral pontine demyelinating lesion
4	46/M	R	49	R	0.49	0.78	LBN	–	LBN	LBN	–	R, 10	–	Right lateral pontine infarction
5	77/M	R	90	R	0.68	0.68	LBN	–	LBN	LBN	–	R, 15	–	Right lateral pontine infarction
6	69/M	R	24	R	0.42	1.17	LBN	–	LBN	LBN	–	R, 1	Right facial palsy	Right lateral pontine infarction
7	62/M	R	90	Normal	1.14	0.92	–	–	–	RBN in right lying	–	L, 1	Right PC impaired at bHIT and vHIT (0.57)*	–
8	69/M	R	104	Normal	ND	ND	–	–	LBN	LBN	–	0	Right PC impaired at bHIT	–
9	60/F	R	79	Normal	1.14	1.15	–	–	LBN	LBN	–	R, 2	Right PC impaired at bHIT and vHIT (0.29)*	–
10	58/F	R	113	Normal	0.77	0.69	RBN	–	RBN	Geotropic	–	L, 3	–	–
11	62/M	L	115	Normal	0.88	0.88	LBN	–	LBN	Geotropic	–	ND	–	–
12	53/M	R	109	R	0.87	0.86	LBN	–	LBN	Apogeotropic	–	R, 3	–	–
13	59/F	L	79	L	0.82	0.98	RBN	–	RBN	Geotropic	–	L, 1	–	–

HL, hearing loss; PTA, pure-tone average (the average of pure tone thresholds at 500, 1,000, and 2,000 Hz in the lesion ear); H-bHIT, horizontal-canal bedside head impulse test; H-vHIT, horizontal-canal video head impulse test; SN, spontaneous nystagmus; GEN, gaze-evoked nystagmus; PN, positional nystagmus; SVV, subjective visual vertical; F, female; M, male; L, left; R, right; B, bilateral; RBN, right-beating nystagmus; LBN, left-beating nystagmus; PC, posterior semicircular canal; ND, not documented.

*The numbers in the parentheses are the VOR gains of vertical-canal vHIT.

10.3389/fneur.2022.941909

with positive H-bHIT presented with spontaneous nystagmus beating away from the lesion side which did not change direction during positional testing. Four other patients (4/8, including 2/8 with positive H-bHIT and 2/8 with negative H-bHIT) also had horizontal spontaneous nystagmus *via* unaided eyes, but presented with persistent geotropic (3/8) or apogeotropic nystagmus (1/8) on the supine-roll test. In the other three (3/8) patients with negative H-bHIT, no spontaneous nystagmus could be seen *via* unaided eyes; when observed by video-nystagmoscopy with fixation block, two had weak horizontal nystagmus and one had weak positional nystagmus in right side-lying position. All the directions of nystagmus were mainly horizontal. None of the patients in the MRI– group had GEN or skew deviation (Table 1).

Video head impulse test

Two to three days after vertigo onset, all but one patient (one MRI– patient with normal H-bHIT refused vHIT) underwent vHIT. Among the MRI+ patients presenting with unilateral vestibular loss in bHIT, two (2/5) had ipsilesional vestibular loss on H-vHIT, and the other three (3/5) had bilateral vestibular loss on vHIT (ipsilesional/contralesional VOR gains were 0.56/0.61 in Pt #3, 0.49/0.78 in Pt #4, and 0.68/0.68 in Pt #5).

On the other hand, only one MRI– patient (1/7) had ipsilesional vestibular loss and one (1/7) had bilateral vestibular loss in H-vHIT. We selectively performed the vertical canal-vHIT for the other five patients having normal H-vHIT to check the function of vertical semicircular canals, and found two patients (2/7) had hypofunction of the posterior canal (PC) in the lesion side. The patient who refused vHIT received vertical-canal bHIT, which also showed PC hypofunction on the lesion side. All three patients with isolated PC hypofunction were those patients whose nystagmus was weak and could only be seen in fixation block.

We compared the VOR gains of H-vHIT between the two groups. The MRI+ group had significantly lower ipsilesional VOR gain than the MRI– group (0.56 ± 0.11 vs 0.87 ± 0.24, $p = 0.03$) (Figure 2A). The contralesional VOR gains did not show significant difference between MRI+ and MRI– groups (0.87 ± 0.25 vs 0.96 ± 0.19, $p = 0.43$) (Figure 2B).

Subjective visual vertical

All but one (in MRI– group) patients underwent testing for shift of the subjective visual vertical (using the bucket test) 2–3 days after vertigo onset. Six patients (4/5 in MRI+ and 2/7 in MRI–) has SVV deviations toward the ipsilesional side while one MRI– patient (1/7) deviated toward the contralesional side. When comparing the absolute values of SVV, the MRI+ group tended to have greater SVV deviation than MRI– though the difference did not reach statistical significance (mean deviation 7.2° in MRI+ vs 2.3° in MRI–, $p = 0.11$) (Figure 2C).

Pure-tone audiometry

All patients underwent pure-tone audiometry 3–7 days after symptom onset. Patients in the MRI+ group had lesser degree of sensorineural hearing loss than those in the MRI– group (PTA 50.6 ± 28.0 in MRI+ vs 89.8 ± 28.5 in MRI–, $p = 0.03$) (Figure 2D). Seven MRI– patients (7/8) met the formal definition of SSNHL while only two MRI+ patients (2/5) met SSNHL. Moreover, two MRI+ patients had regained normal hearing when undergoing audiometry 5–7 days after onset.

Discussion

In this study, we consecutively reviewed inpatients with AVS associated with acute unilateral hearing loss, to determine whether bedside neuro-otologic testing could differentiate central from peripheral lesions.

The study has two important findings. First, unlike in AVS without hearing loss, in AVS with hearing loss positive H-HIT is not a benign sign predicting a peripheral lesion. In fact, in the present study, positive H-HIT is more strongly associated with lateral pontine lesions (e.g., AICA infarction) than is negative H-HIT. Second, contrary to traditional teaching, the vestibular signs of the MRI+ group commonly mimics peripheral vestibulopathy while the presentation of MRI– group can be confused with central vestibulopathy given some combination of negative H-HIT, atypical positional nystagmus, or paucity of nystagmus in many MRI negative cases.

The MRI+ group in our study presented with the vestibular signs of unilateral peripheral vestibulopathy: ipsilesional vestibular loss on H-HIT, spontaneous nystagmus beating to contralesional side, and fixed-direction positional nystagmus. Clinical signs suggesting a central lesion, such as direction-changing GEN and skew deviation (18, 19), occurred in fewer than half of MRI+ patients. In other words, more than half of patients with central lesions have HINTS exam findings that point to a peripheral etiology (Table 2). As such, this group is at high risk of misdiagnosis. Our study therefore supports the use of acute hearing loss as a red flag feature in AVS to ensure that an acute lateral pontine lesion, such as an AICA stroke, is not missed. In other words, our study supports the use of HINTS Plus (where the finding of acute hearing loss prompts neuroimaging to search for a central cause).

Understanding the test characteristics of the three items of HINTS may partially explain our findings. Among the three items, direction-changing nystagmus and skew deviation are highly specific to central lesions (92 & 98%) but their sensitivities are low (38 & 30%). The high sensitivity for HINTS to identify

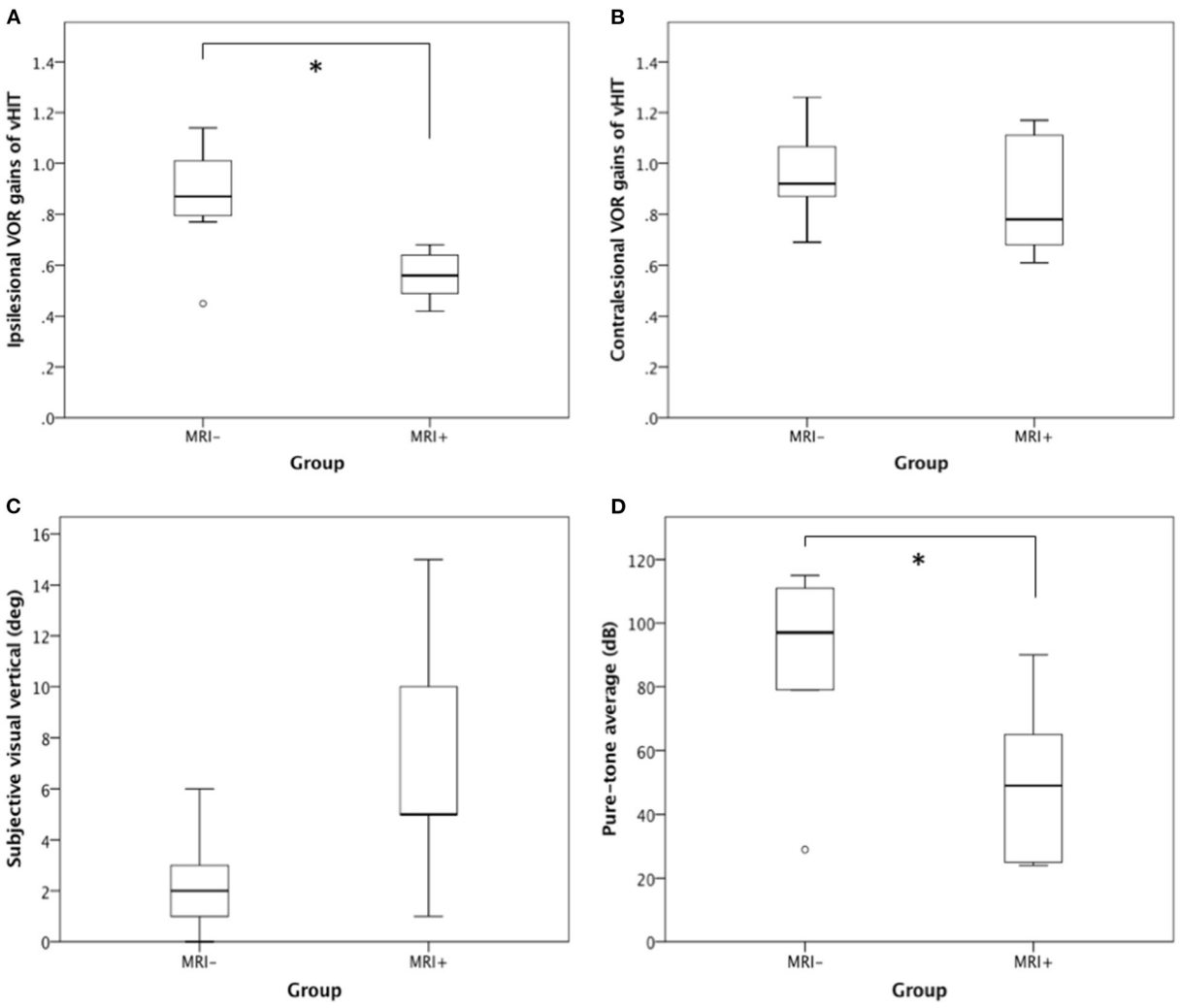

FIGURE 2
H-vHIT, SVV, and PTA between MRI+ and MRI− group. When compared with the MRI− group, the MRI+ group had **(A)** lower ipsilesional VOR gain in H-vHIT (0.56 ± 0.11 vs. 0.87 ± 0.24, $p = 0.03$), **(B)** similar contralesional VOR gain in H-vHIT (0.87 ± 0.25 vs. 0.96 ± 0.19, $p = 0.43$), **(C)** suggestion of greater SVV deviation (7.2 ± 5.4° vs. 2.3 ± 2.0°, $p = 0.11$), and **(D)** lesser degree of hearing loss on PTA (50.6 ± 28.0 dB vs. 89.8 ± 28.5 dB, $p = 0.03$). *Signifies statistically significant difference.

central lesions mainly comes from the contribution of H-HIT (sensitivity 85%) (20). However, when applied in our specific condition—AVS plus hearing loss—the positive H-HIT no longer indicates a pure peripheral lesion. In fact, it may even suggest proximal AICA infarction. Thus, the sensitivity of H-HIT decreases in this situation and cannot be well-compensated by the other two tests, which in turns limits the applicability of HINTS for AVS plus hearing loss, and necessitates the more conservative approach (HINTS Plus).

Although positive H-HIT is usually a peripheral sign, the literature has shown several exceptions. Lesions in multiple brain structures can cause positive HIT, including in CN VIII fascicles in the brainstem, the vestibular nucleus, the cerebellar flocculus, and the nucleus prepositus hypoglossi (21–23). Most notably, a positive H-HIT is often seen in AICA stroke because the labyrinthine artery originates from AICA (24). The presence of lateral pontine infarction with AVS and hearing loss implies the vessel occlusion occurs at a proximal site of AICA, which in turns results in whole labyrinthine infarction and typical presentation of unilateral vestibular loss. Interestingly, in a previous study some patients with AICA stroke have bilateral vestibular hypofunction in vHIT (24). In our study, this finding was also seen in two cases of AICA stroke (Patients #4 & #5) and one with a lateral pontine demyelinating lesion (patient #3) (25). It cannot be explained by labyrinthine infarction. On the other hand, the cerebellar flocculus has been shown to inhibit low-frequency VOR but facilitate high-frequency VOR (23). Impairment of bilateral high-frequency VOR gains in unilateral

TABLE 2 The distribution of the 13 patients in HINTS battery and MRI findings.

	MRI+	MRI−
Central HINTS	Pt #2, #3 ($n = 2$)	Pt #7, #8, #9, #10, #11 ($n = 5$)
Peripheral HINTS	Pt #4, #5, #6 ($n = 3$)	Pt #1, #12, #13 ($n = 3$)
Total, *n*	5	8

Central HINTS: negative head impulse test OR direction-changing nystagmus OR positive test of skew.
Peripheral HINTS: positive head impulse test AND unidirectional horizontal nystagmus AND negative test of skew.
MRI+: with posterior fossa lesions on MRI.
MRI−: without posterior fossa lesions on MRI.

floccular infarction has been proven not only by vHIT but also by the HIT using scleral search coils (23, 26). Since the flocculus belongs to AICA territory, in some cases of AICA stroke, the bilateral hypofunction in vHIT testing may be caused by floccular ischemia. Neural substrates in the lateral pons such as the vestibular commissure may equally be responsible for this phenomenon.

The peripheral AVS with hearing loss, usually termed "labyrinthitis," is expected to have typical signs of unilateral vestibular loss. Surprisingly, in our study, fewer than half of the MRI− patients had positive H-HIT. Furthermore, three patients with normal H-HIT and weak nystagmus presented with isolated PC hypofunction. This subgroup is against the rule of HINTS and may be misdiagnosed with central vestibulopathy. Indeed, this phenomenon has been reported in other studies (27–29). In one study with 29 SSNHL patients 45% had vestibular dysfunction, in which 53% showed isolated PC impairment (28). Another study showed the same finding in 30% of 27 patients with acute vertigo and SSNHL (27). The most likely reason behind this phenomenon is infarction of the common cochlea artery, which supplies the cochlea and PC (27, 28, 30). In other words, this finding supports the vascular etiology of SSNHL (i.e., occlusion of AICA terminal branch). Clinicians should be aware of the possibility of distal vascular occlusion in patients with AVS plus hearing loss even if MRI brain fails to show a stroke. Critical control of vascular risk factors and even antithrombotic agents should be considered to prevent future stroke even in cases where the MRI is negative.

In our study, there were four other MRI− patients presenting with persistent geotropic or apogeotropic nystagmus during supine-roll test. Of course, the most common etiology of geotropic or apogeotropic nystagmus is H-BPPV. In our cases, however, the persistence of geotropic nystagmus did not match H-BPPV, and the apogeotropic nystagmus was not eliminated by the repositioning maneuver for H-cupulolithiasis (31). Instead, they corresponded to the previously reported "light cupula" and "heavy cupula," which is probably due to change of specific gravity in the cupula or endolymph, resulting in cupula deviation to one side during head position change (32–34). The mechanism of so-called light/heavy cupula syndrome is thought to be either vascular (33–35) or inflammatory (33) in origin, and is sometimes associated with unilateral hearing loss (34). Our study supports previous findings, and further confirms that light/heavy cupula syndrome can be associated with SSNHL. More importantly, the H-HIT findings in these patients were not consistent, in which two patients had positive H-bHIT but negative H-vHIT, one had negative H-bHIT and positive H-vHIT, and one had both negative H-bHIT and H-vHIT. To our knowledge, apogeotropic or geotropic nystagmus can result from central lesions involving nodulus, uvula, or middle or inferior cerebellar peduncle (36–38). Accordingly, the vestibular signs in this subgroup are also inconsistent with those typical signs in unilateral peripheral vestibulopathy, and easily confused with central positional nystagmus.

In our study, audiograms showed the degree of hearing loss was less severe in the MRI+ group than the MRI− group, and two MRI+ patients with initial hearing loss had recovered during audiometry testing. This is a counterintuitive finding because hearing loss caused by vascular occlusion is theoretically more profound and irreversible than other causes (39).

In our study, the MRI+ group showed a tendency toward greater SVV deviation, which may hint at a role of SVV in identifying central lesions. Though three MRI+ patients had other focal neurological signs, two presented with peripheral-type facial palsy and one was initially misdiagnosed with Ramsay Hunt syndrome.

Our study has several limitations. First, our study is retrospective and sample size is small. A prospective study with larger sample size is warranted in the future to validate our findings. Second, we did not routinely perform vertical-canal vHIT, but only performed it when H-vHIT was normal. Third, we did not perform vestibular evoked myogenic potentials. Last, due to logistical factors at our center, our cases underwent audiometry 3–7 days after symptom onset so quantitative results of hearing loss in the first 2 days was not available.

In conclusion, in this study of 13 patients with AVS plus hearing loss, five patients (38.5%) had an acute lateral pontine lesion. All five of these patients had H-HIT that pointed incorrectly toward a peripheral etiology. While the other two items in the HINTS battery (direction-changing nystagmus and skew deviation) would correctly have identified two additional cases of stroke, and one patient had other focal findings (facial palsy), two of the five patients had no central findings (Table 2). This put them at risk of misdiagnosis. These findings suggest that every patient with AVS plus hearing loss should undergo brain MRI, and clinicians should be aware of the possibility of a lateral pontine lesion when a positive H-HIT is seen in patients with AVS with hearing loss.

Data availability statement

The raw data supporting the conclusions of this article will be made available by the authors, without undue reservation.

Ethics statement

The studies involving human participants were reviewed and approved by Research Ethics Committee of Taichung Tzu Chi Hospital. Written informed consent for participation was not required for this retrospective study.

Author contributions

AB is responsible for interpretation of the data and drafting of the manuscript. TPC is responsible for collection, analysis, interpretation of the data, and drafting of the manuscript. All authors contributed to the article and approved the submitted version.

Conflict of interest

The authors declare that the research was conducted in the absence of any commercial or financial relationships that could be construed as a potential conflict of interest.

Publisher's note

All claims expressed in this article are solely those of the authors and do not necessarily represent those of their affiliated organizations, or those of the publisher, the editors and the reviewers. Any product that may be evaluated in this article, or claim that may be made by its manufacturer, is not guaranteed or endorsed by the publisher.

References

1. Kerber KA. Acute vestibular syndrome. *Semin Neurol.* (2020) 40:59–66. doi: 10.1055/s-0039-3402739

2. Venhovens J, Meulstee J, Verhagen WI. Acute vestibular syndrome: a critical review and diagnostic algorithm concerning the clinical differentiation of peripheral versus central etiologies in the emergency department. *J Neurol.* (2016) 263:2151–7. doi: 10.1007/s00415-016-8081-8

3. Newman-Toker DE, Kattah JC, Alvernia JE, Wang DZ. Normal head impulse test differentiates acute cerebellar strokes from vestibular neuritis. *Neurology.* (2008) 70:2378–85. doi: 10.1212/01.wnl.0000314685.01433.0d

4. Norrving B, Magnusson M, Holtas S. Isolated acute vertigo in the elderly; vestibular or vascular disease? *Acta Neurol Scand.* (1995) 91:43–8. doi: 10.1111/j.1600-0404.1995.tb05841.x

5. Kattah JC, Talkad AV, Wang DZ, Hsieh YH, Newman-Toker DE. Hints to diagnose stroke in the acute vestibular syndrome: three-step bedside oculomotor examination more sensitive than early MRI diffusion-weighted imaging. *Stroke.* (2009) 40:3504–10. doi: 10.1161/STROKEAHA.109.551234

6. Halmagyi GM, Curthoys IS. A clinical sign of canal paresis. *Arch Neurol.* (1988) 45:737–9. doi: 10.1001/archneur.1988.00520310043015

7. Lee H, Kim JS, Chung EJ, Yi HA, Chung IS, Lee SR, et al. Infarction in the territory of anterior inferior cerebellar artery: spectrum of audiovestibular loss. *Stroke.* (2009) 40:3745–51. doi: 10.1161/STROKEAHA.109.564682

8. Lee H. Audiovestibular loss in anterior inferior cerebellar artery territory infarction: a window to early detection? *J Neurol Sci.* (2012) 313:153–9. doi: 10.1016/j.jns.2011.08.039

9. Newman-Toker DE, Kerber KA, Hsieh YH, Pula JH, Omron R, Saber Tehrani AS, et al. Hints outperforms Abcd2 to screen for stroke in acute continuous vertigo and dizziness. *Acad Emerg Med.* (2013) 20:986–96. doi: 10.1111/acem.12223

10. Linthicum FH Jr, Doherty J, Berliner KI. Idiopathic sudden sensorineural hearing loss: vascular or viral? *Otolaryngol Head Neck Surg.* (2013) 149:914–7. doi: 10.1177/0194599813506546

11. Singh A, Kumar Irugu DV. Sudden sensorineural hearing loss—a contemporary review of management issues. *J Otol.* (2020) 15:67–73. doi: 10.1016/j.joto.2019.07.001

12. Chau JK, Lin JR, Atashband S, Irvine RA, Westerberg BD. Systematic review of the evidence for the etiology of adult sudden sensorineural hearing loss. *Laryngoscope.* (2010) 120:1011–21. doi: 10.1002/lary.20873

13. Schuknecht HF, Donovan ED. The pathology of idiopathic sudden sensorineural hearing loss. *Arch Otorhinolaryngol.* (1986) 243:1–15. doi: 10.1007/BF00457899

14. Kuo CL, Shiao AS, Wang SJ, Chang WP, Lin YY. Risk of sudden sensorineural hearing loss in stroke patients: a 5-year nationwide investigation of 44,460 patients. *Medicine.* (2016) 95:e4841. doi: 10.1097/MD.0000000000004841

15. Chang TP, Wang Z, Winnick AA, Chuang HY, Urrutia VC, Carey JP, et al. Sudden hearing loss with vertigo portends greater stroke risk than sudden hearing loss or vertigo alone. *J Stroke Cerebrovasc Dis.* (2018) 27:472–8. doi: 10.1016/j.jstrokecerebrovasdis.2017.09.033

16. Torres-Russotto D, Landau WM, Harding GW, Bohne BA, Sun K, Sinatra PM. Calibrated finger rub auditory screening test (Calfrast). *Neurology.* (2009) 72:1595–600. doi: 10.1212/WNL.0b013e3181a41280

17. Zwergal A, Rettinger N, Frenzel C, Dieterich M, Brandt T, Strupp M, et al. Bucket of static vestibular function. *Neurology.* (2009) 72:1689–92. doi: 10.1212/WNL.0b013e3181a55ecf

18. Korda A, Zamaro E, Wagner F, Morrison M, Caversaccio MD, Sauter TC, et al. Acute vestibular syndrome: is skew deviation a central sign? *J Neurol.* (2022) 269:1396–403. doi: 10.1007/s00415-021-10692-6

19. Mantokoudis G, Korda A, Zee DS, Zamaro E, Sauter TC, Wagner F, et al. Bruns' nystagmus revisited: a sign of stroke in patients with the acute vestibular syndrome. *Eur J Neurol.* (2021) 28:2971–9. doi: 10.1111/ene.14997

20. Tarnutzer AA, Berkowitz AL, Robinson KA, Hsieh YH, Newman-Toker DE. Does my dizzy patient have a stroke? A systematic review of bedside diagnosis in acute vestibular syndrome. *CMAJ.* (2011) 183:E571–92. doi: 10.1503/cmaj.100174

21. Kim SH, Zee DS, du Lac S, Kim HJ, Kim JS. Nucleus prepositus hypoglossi lesions produce a unique ocular motor syndrome. *Neurology.* (2016) 87:2026–33. doi: 10.1212/WNL.0000000000003316

22. Lee SU, Park SH, Park JJ, Kim HJ, Han MK, Bae HJ, et al. Dorsal medullary infarction: distinct syndrome of isolated central vestibulopathy. *Stroke.* (2015) 46:3081–7. doi: 10.1161/STROKEAHA.115.010972

23. Park HK, Kim JS, Strupp M, Zee DS. Isolated floccular infarction: impaired vestibular responses to horizontal head impulse. *J Neurol.* (2013) 260:1576–82. doi: 10.1007/s00415-013-6837-y

24. Mantokoudis G, Tehrani AS, Wozniak A, Eibenberger K, Kattah JC, Guede CI, et al. Vor gain by head impulse video-oculography differentiates acute vestibular neuritis from stroke. *Otol Neurotol.* (2015) 36:457–65. doi: 10.1097/MAO.0000000000000638

25. Valente P, Pinto I, Aguiar C, Castro E, Conde A, Larangeiro J. Acute vestibular syndrome and hearing loss mimicking labyrinthitis as initial presentation of multiple sclerosis. *Int J Pediatr Otorhinolaryngol.* (2020) 134:110048. doi: 10.1016/j.ijporl.2020.110048

26. Yacovino DA, Akly MP, Luis L, Zee DS. The floccular syndrome: dynamic changes in eye movements and vestibulo-ocular reflex in isolated infarction of the cerebellar flocculus. *Cerebellum.* (2018) 17:122–31. doi: 10.1007/s12311-017-0878-1

27. Pogson JM, Taylor RL, Young AS, McGarvie LA, Flanagan S, Halmagyi GM, et al. Vertigo with sudden hearing loss: audio-vestibular characteristics. *J Neurol.* (2016) 263:2086–96. doi: 10.1007/s00415-016-8214-0

28. Rambold H, Boenki J, Stritzke G, Wisst F, Neppert B, Helmchen C. Differential vestibular dysfunction in sudden unilateral hearing loss. *Neurology.* (2005) 64:148–51. doi: 10.1212/01.WNL.0000148599.18397.D2

29. Yao Q, Xu C, Wang H, Shi H, Yu D. Video head impulse test results suggest that different pathomechanisms underlie sudden sensorineural hearing loss with vertigo and vestibular neuritis: our experience in fifty-two patients. *Clin Otolaryngol.* (2018) 43:1621–4. doi: 10.1111/coa.13196

30. Kim JS, Kim HJ. Inferior vestibular neuritis. *J Neurol.* (2012) 259:1553–60. doi: 10.1007/s00415-011-6375-4

31. Kim SH, Jo SW, Chung WK, Byeon HK, Lee WS. A cupulolith repositioning maneuver in the treatment of horizontal canal cupulolithiasis. *Auris Nasus Larynx.* (2012) 39:163–8. doi: 10.1016/j.anl.2011.03.008

32. Tomanovic T, Bergenius J. Vestibular findings in patients with persistent geotropic positional nystagmus: the 'light cupula' phenomenon. *Acta Otolaryngol.* (2014) 134:904–14. doi: 10.3109/00016489.2014.928421

33. Kim CH, Kim MB, Ban JH. Persistent geotropic direction-changing positional nystagmus with a null plane: the light cupula. *Laryngoscope.* (2014) 124:E15–9. doi: 10.1002/lary.24048

34. Hiruma K, Numata T, Mitsuhashi T, Tomemori T, Watanabe R, Okamoto Y. Two types of direction-changing positional nystagmus with neutral points. *Auris Nasus Larynx.* (2011) 38:46–51. doi: 10.1016/j.anl.2010.07.004

35. Ando M, Takeuchi S, Kakigi A, Raicu V, Yagyu K, Sato T. Acute ischemia causes 'dark cell' change of strial marginal cells in gerbil cochlea. *Cell Tissue Res.* (2002) 309:229–35. doi: 10.1007/s00441-002-0597-9

36. Lee SU, Kim HJ, Lee ES, Choi JH, Choi JY, Kim JS. Central positional nystagmus in inferior cerebellar peduncle lesions: a case series. *J Neurol.* (2021) 268:2851–7. doi: 10.1007/s00415-021-10435-7

37. Lemos J, Martins AI, Duque C, Pimentel S, Nunes C, Goncalves AF. Positional testing in acute vestibular syndrome: a transversal and longitudinal study. *Otol Neurotol.* (2019) 40:e119–29. doi: 10.1097/MAO.0000000000002067

38. De Schutter E, Adham ZO, Kattah JC. Central positional vertigo: a clinical-imaging study. *Prog Brain Res.* (2019) 249:345–60. doi: 10.1016/bs.pbr.2019.04.022

39. Hirano K, Ikeda K, Kawase T, Oshima T, Kekehata S, Takahashi S, et al. Prognosis of sudden deafness with special reference to risk factors of microvascular pathology. *Auris Nasus Larynx.* (1999) 26:111–5. doi: 10.1016/S0385-8146(98)00072-8

frontiers | Frontiers in Neurology

TYPE Brief Research Report
PUBLISHED 30 September 2022
DOI 10.3389/fneur.2022.967521

OPEN ACCESS

EDITED BY
Dominik Straumann,
University of Zurich, Switzerland

REVIEWED BY
Andrés Soto-Varela,
Complejo Hospitalario Universitario de Santiago, Spain
Ludimila Labanca,
Universidade Federal de Minas Gerais, Brazil

*CORRESPONDENCE
Diego Kaski
d.kaski@ucl.ac.uk

SPECIALTY SECTION
This article was submitted to Neuro-Otology, a section of the journal Frontiers in Neurology

RECEIVED 13 June 2022
ACCEPTED 08 August 2022
PUBLISHED 30 September 2022

CITATION
Patel P, Castro P, Koohi N, Arshad Q, Gargallo L, Carmona S and Kaski D (2022) Head shaking does not alter vestibulo ocular reflex gain in vestibular migraine.
Front. Neurol. 13:967521.
doi: 10.3389/fneur.2022.967521

Head shaking does not alter vestibulo ocular reflex gain in vestibular migraine

Priyani Patel[1,2], Patricia Castro[1,3,4], Nehzat Koohi[2,5], Qadeer Arshad[5,6], Lucia Gargallo[7,8], Sergio Carmona[7,8] and Diego Kaski[2,5]*

[1]Adult Diagnostic Audiology Department, University College London Hospitals, London, United Kingdom, [2]The Ear Institute, Faculty of Brain Sciences, University College London, London, United Kingdom, [3]Department of Brain Sciences, Imperial College London, London, United Kingdom, [4]Universidad del Desarrollo, Escuela de Fonoaudiologia, Facultad de Medicina Clinica Alemana, Santiago, Chile, [5]Department of Clinical and Movement Neurosciences, Centre for Vestibular and Behavioural Neuroscience, Institute of Neurology, University College London, London, United Kingdom, [6]inAmind Laboratory, Department of Neuroscience, Psychology and Behaviour, University of Leicester, Leicester, United Kingdom, [7]Fundación San Lucas para la Neurociencia, Rosario, Argentina, [8]Cátedra Neurofisiología de la Universidad Nacional de Rosario, Rosario, Argentina

Vestibular Migraine (VM) is the most common cause of non-positional episodic vestibular symptoms. Patients with VM commonly report increased motion sensitivity, suggesting that vestibular responses to head movement may identify changes specific to VM patients. Here we explore whether the vestibulo-ocular reflex (VOR) gain alters in response to a clinical "headshake" maneuver in patients with VM. Thirty patients with VM in the inter-ictal phase, 16 patients with Benign Positional Paroxysmal Vertigo (BPPV) and 15 healthy controls were recruited. Patients responded to the question "Do you feel sick reading in the passenger seat of a car?" and completed a validated motion sickness questionnaire as a measure of motion sensitivity. Lateral canal vHIT testing was performed before and after headshaking; the change in VOR gain was calculated as the primary outcome. Baseline VOR gain was within normal limits across all participants. There was no significant change in VOR gain after headshaking in any group ($p = 0.264$). Patients were 4.3 times more likely to be in the VM group than in the BPPV group if they reported nausea when reading in the passenger seat of a car. We postulate that a headshake stimulus may be insufficient to disrupt cortical interactions and induce a change in VOR gain. Alternatively, changes in VOR gain may only be apparent in the acute phase of VM. Reading in the passenger seat of a car was considered uncomfortable in all VM patients suggesting that this specific question may be useful for the diagnosis of VM.

KEYWORDS

vestibular migraine, vestibulo ocular reflex, head shake, motion sensitivity, vHIT

Introduction

Vestibular Migraine (VM) is the most common cause of non-positional episodic vestibular symptoms, affecting 1.4% of the general population (1). The migrainous symptoms of VM include recurrent headaches with heightened sensitivity to sensory stimulus, nausea and/or vomiting (2) with recurrent episodic vertigo attacks lasting minutes to several hours (3). The pathophysiology of VM is incompletely understood and the diagnosis is based on clinical features as there are no objective biomarkers to provide a definitive diagnosis (4).

From a clinical perspective, there is a need for an objective marker for VM that can be applied in the clinical setting. A sensitive test for VM would enable clinicians to differentiate between VM and other vestibular disorders with overlapping symptoms (e.g., Meniere's disease). Moreover, a clinical biomarker would facilitate an earlier diagnosis of VM, a major limitation of the current diagnostic criteria that require at least five episodes for diagnosis (3); thus, patients may be underdiagnosed and consequently inappropriately treated when presenting with the first few attacks.

The development of clinical biomarkers may be informed by the nature of patient-reported symptoms in VM. Thus, patients with VM commonly describe excessive motion sensitivity (5, 6), suggesting a role for impaired visuo-vestibular interactions as an underlying mechanism of VM symptoms (7). Other hypotheses to account for vestibular symptoms experienced by VM patients include abnormalities in the integration of inner ear semi-circular canals (SCC) and otolith afferents, and between these and other sensory modalities (e.g., vision) (8), a mechanism that may account for increased head movement induced dizziness and disorientation in VM (9).

A clinical test involving head movement is head-shaking nystagmus (HSN) (10, 11). Here, the head is tilted forward 30 degrees and rotated to the left and right in the yaw plane in order to elicit subclinical vestibular abnormalities by activation of the velocity storage mechamsim that prolongs the time constant of the rotational vestibulo-ocular reflex (VOR) (10–12). This test is abnormal mostly in peripheral disorders, however, abnormalities have been described in central disorders, including "perverted" HSN (13–16) and in patients with recurrent spontaneous vertigo with interictal HSN—where horizntal HSN nystagmus can be found in the absence of peripheral dysfunction (17). Central HSN may arise from an assymetry in the velocity storage mechanism, central gain or the central adaptation, or from an abnormal cross-coupling of velocity storage pathways (18).

It is a recognized finding that patients with VM may have abnormally elevated VOR (nystagmic) responses to water caloric irrigation (19, 20). This is thought to be due to a hyper-excitable vestibular network leading to increased motion sensitivity. To our knowledge changes in vestibular excitability that can be induced by head shaking has not been previously explored. Here we explore the change in VOR gain using the video head impulse test (vHIT) following a clinical "headshake" maneuver in patients with VM. We also explore the frequency of motion sensitivity in VM and BPPV as measured using questionnaires.

Methods

Patients with VM and healthy controls (HC) were invited to participate. Participants were recruited from neuro-otology clinics in the United Kingdom and Argentina from 1st November 2020 to 30th June 2021. All patients were diagnosed by a Neurologist with expertise in VM (DK and SC) and met the criteria for VM by Bárány (3) or the third edition of the International Classification of Headache Disorders (21). Patients with benign paroxysmal positional vertigo (BPPV) were recruited as a disease control, following first diagnosis, prior to treatment repositioning maneuvers, and in accordance with established diagnostic criteria (22). VM participants were on various prophylaxis medications. All participants had an attack within the last year and were tested in the inter-ictal phase.

Participants with eye movement abnormalities, ocular pathologies affecting detection of pupils, or neck problems that could interfere with the headshake were excluded. In addition, patients with an overlap of two or more diagnoses were not included in this study.

Sample size calculation was performed using the outcomes and effect sizes from Bednarczuk et al. (7). The authors found a significant increase in rotation thresholds in VM patients following prolonged optokinetic stimulation. When using the effect size found in this study, for a power of 80% and a significance of 0.05, the required sample size was 4. Given the small estimated sample size required in view of the expected variability in neurophysiological outcomes in patients with VM, 30 patients with VM were recruited.

Before being tested, we evaluated patients' motion sickness susceptibility by asking: "Do you feel sick reading in the passenger seat of a car?" and asked them to complete the Motion Sickness Susceptibility Questionnaire (MSSQ).

vHIT testing, prior to head shaking (PRE-HS) was performed for the right and left lateral semicircular canal in each ear independently. A minimum of 20 head thrusts with a head displacement of 10–20 degrees, and a range of peak head velocities (150–200 deg/s) and peak head acceleration (1,200–2,500 deg/s) were obtained for each lateral semicircular canal. The VOR gain was defined as the sum of eye movement velocity divided by the sum of head movement velocity during head turn. The normal VOR gain value is 1.0 which means there is compensatory eye velocity which is equal to head velocity in the opposite direction (23).

Immediately following vHIT testing, a standard clinical headshake was carried out. Participants were asked to close their eyes and tilt their head downward by 30 degrees to ensure their

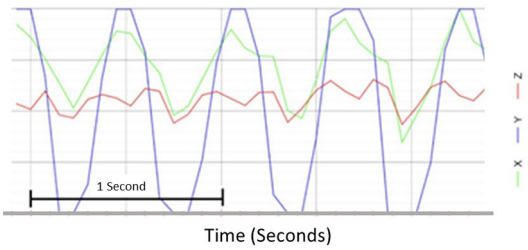

FIGURE 1
Representative trace of a 2 Hz head shaking using the accelerometer in a graph format. Headshake stimulus using an accelerometer was measured in the y-axis.

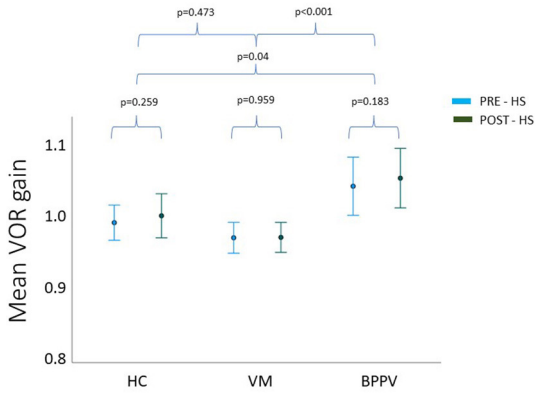

FIGURE 2
Mean pre and post headshake VOR gain for each group. HC, healthy controls; BPPV, benign paroxysmal positional vertigo; VM, vestibular migraine.

lateral canals were on its horizontal axis; the participant's head was then passively oscillated from side to side at a frequency of 2 Hz for a total of 30 s. To ensure there was no variability in headshake between participants, an accelerometer was used to control and measure each headshake (Figure 1) secured over the participant's occiput using a tight velcro strap that did not interfere with the vHIT setup. Immediately following headshake, a second vHIT (post head shaking, POST-HS) to test lateral SCCs was performed. Participant instructions, test set-up and vHIT testing parameters remained the same as for the PRE-HS vHIT.

Data analysis

Data was analyzed using Shapiro-Wilk test to identify the distribution. A normal distribution was observed so parametric testing was used. Change in VOR gain was calculated as POST-HS VOR gain subtracted from PRE-HS VOR gain. Bonferroni correction *post hoc* analysis was used. Significance was considered when $p < 0.05$. All statistical analysis was performed using Statistical Package for Social Sciences (SPSS, Version 27, IBM Corporation, NY). Paired sample *t*-test was used to compare pre- and post-VOR gain. Two-way mixed model analysis of variance (ANOVA) was used to compare the means of VOR gain pre vs. post headshake between VM, BPPV group, and HC group. To compare the change in VOR gain between pre- and post- between groups a one-way ANOVA was performed.

Results

Thirty patients with VM (mean age 48.3, age range 28–67, 22 female/8 male), 16 participants with BPPV (mean age 52.1, age range 31–66, 10 female/6 male), and 15 healthy controls (mean age 43.0, age range 27–65, 10 female/5 male) were recruited for this research study, following informed written consent. All participants in the three groups (VM, BPPV, and HC) had baseline VOR gain within normal limits. Nevertheless, BPPV patients had significantly higher mean VOR gain compared to the VM patients ($p < 0.01$ for PRE-HS, and $p < 0.001$ for POST-HS) that also trended toward significance with the HC ($p = 0.067$ for PRE-HS, and $p = 0.068$ for POST-HS), in keeping with previous reports (7).

Repeated measures ANOVA showed no statistically significant interaction between time*group on VOR gain PRE- and POST-HS ($p = 0.711$). The main effect of time was not statistically different for mean VOR gain at the different time points (PRE- and POST-HS) ($p = 0.264$) (Figure 2). As there was no effect of headshake within groups (VM, BPPV, HC), the PRE- and POST-HS VOR gains were grouped to provide a total mean vHIT VOR gain value per group.

One way ANOVA revealed a statistically significant difference in the total mean VOR gain between the three groups ($F = 9.725$, $p < 0.001$). *Post hoc* analysis showed this was driven by a difference between the BPPV and VM group ($p < 0.001$), and this time the difference between BPPV and HC was also significant ($p = 0.04$). Again, there was no statistical significance between the VM and HC groups ($p = 0.473$).

The change in VOR gain was calculated by subtracting the VOR gain POST-HS from VOR gain PRE-HS. In all three groups, this value showed an increase in mean VOR gain POST-HS compared to PRE-HS. The VM group had the widest range of VOR gain change, while the other two groups showed similar dispersion. One-way ANOVA however found no significant differences between groups in the VOR gain change ($F = 0.343$, $p = 0.711$).

Regarding the subjective measures, all patients with VM referred feeling sick when reading in the passenger seat of a car, while none of the HC and only 9 patients with BPPV replied positively to this question. We calculated the odds ratio of a

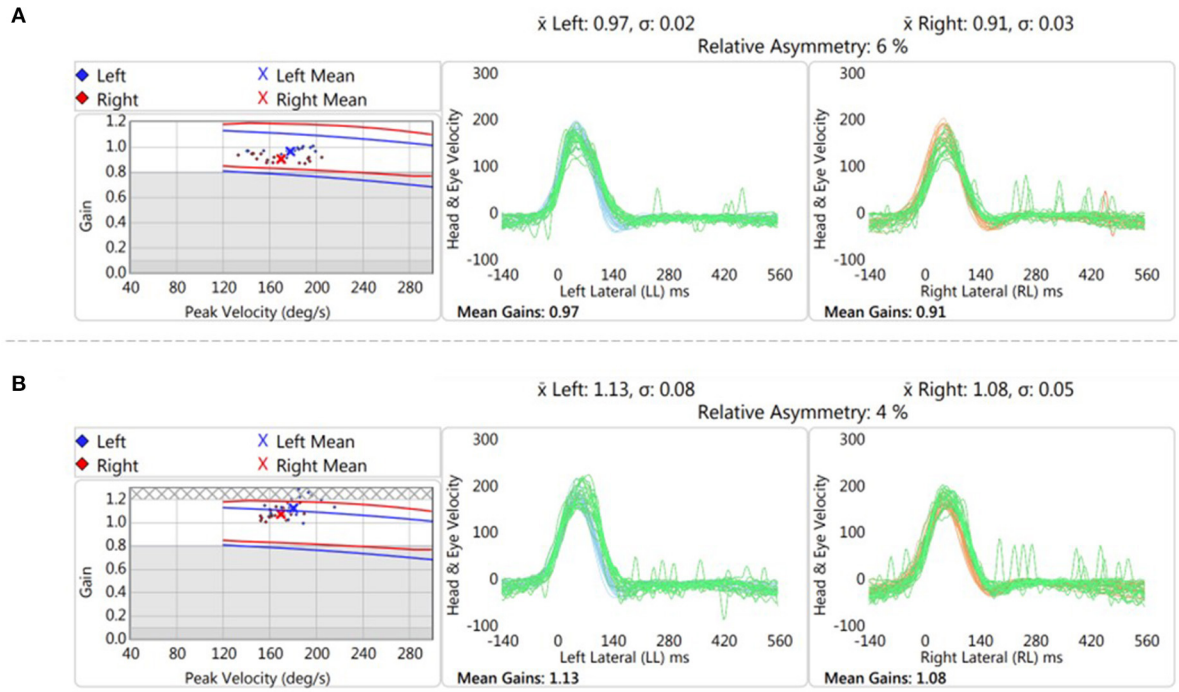

FIGURE 3
Representative trace of vHIT testing pre **(A)** and post **(B)** headshake in an VM patient in the acute phase. There was an increase of 0.165 in the gain after the head oscillation ("headshaking").

patient being in the VM group when replying "yes" to this question with a result of patients being 4.3 times more likely to be in the VM group than in the BPPV group. However, patients with VM did not have significantly higher scores in the MSSQ compared to BPPV patients ($p = 0.92$). Additionally, the MSSQ score did not correlate with the change in VOR gain after headshake ($r = 0.17$, $p = 0.91$).

Discussion

We show that patients with VM do not have heightened VOR gain immediately following headshake compared to patients with BPPV or healthy controls. Our data confirms previous reports of heightened VOR gain in patients with BPPV who have elevated VOR gain (here both PRE- and POST-HS) compared to VM and healthy controls (7).

Headshaking was used in our paradigm to generate a change in vestibular network excitability which could be non-invasively measured using a simple bedside test. We postulate that a clinical headshake stimulus may be insufficient to disrupt cortical interactions and induce a change in VOR gain. This study delivered a stimulus of 2 Hz for 30 s, following clinical headshaking nystagmus test protocols (10, 11). Although this stimulus seems the most appropriate as it is already clinically applicable, it would be of interest to discern whether changing the frequency, duration, or amplitude of the headshake could induce greater changes to the VOR gain. However, VM patients are sensitive to head movements so performing a faster headshake may not be tolerable for patients, thus limiting its use clinically (24). Alternative stimuli, such as moving visual stimuli may alter vestibular excitability thresholds via modulation of visuo-vestibular interactions, without necessitating head movements. Visual-vestibular interactions in patients with a pre-existing peripheral vestibular disorder has been investigated previously (7), where VOR thresholds were significantly increased following visual motion exposure of 5 min in VM patients compared to migraine patients (without vestibular symptoms) and BPPV patients. These findings support the concept that visual stimulation alters normal visual-vestibular network function in patients with VM and lend further support to the notion that assessing vHIT pre and post prolonged visual motion may be a suitable candidate as a possible biomarker, although of lesser practicality, than the headshake employed in this study.

Another explanation for the lack of change in VOR gain following headshaking is that the VM patients included in the study were in an inter-ictal phase. Whilst both perceptual and cognitive deficits have been reported in the inter-ictal phase in VM, and also patients with episodic vertigo from inner ear pathologies, changes in VOR gain may be more pronounced in the acute, ictal, phase (25). Indeed, in a single patient

that was tested acutely (Figure 3), we observed an increase in VOR gain POST-HS that was >2.5 standard deviations of the mean POST-HS VOR gain of chronic VM patients in our cohort.

In this study, we measured VOR gain using vHIT as a simple method of recording VOR gain and a surrogate measure of vestibular excitability. Other studies may explore canal-otolith interactions, as dizziness in VM patients is provoked typically when the superior semicircular canals and otolith organs are stimulated simultaneously (9). Accordingly, the use of cervical or ocular vestibular evoked myogenic potentials (VEMP) instead of vHIT could give information on saccule and utricle vestibular function (26).

It is possible that a significant change in VOR gain between PRE- and POST-HS was not seen because the vHIT is a supra-threshold stimulus at high frequencies (above 5 Hz), so increases in gain are less likely when the VOR is already functioning at its optimal level (23), thus representing a physiological ceiling effect on the VOR. The fact that all VM patients but roughly half of the BPPV patients and none of the HC in our study referred feeling sick when reading in the passenger seat of a car and a heightened motion susceptibility supports the idea that head motion could be a variable of interest in the diagnosis of VM patients. Perhaps the use of a low frequency test of VOR function may be a more suitable stimulus, but not without its own limitations. Whilst patients with VM report nausea or motion sickness symptoms when reading in the passenger seat of a car, the MSSQ was not significantly different for the VM group compared to disease and healthy controls. That this specific compliant is more than four times more likely to be a factor in VM relative to BPPV suggests that a question specifically addressing concurrent visual and motion stimuli in the context of motion sickness (i.e., reading in a moving vehicle) may be more sensitive than a motion susceptibility questionnaire for VM.

Given that this study was sufficiently powered to detect an effect on VOR gain thresholds (7), physiological changes to the high-frequency VOR gain may be less likely to occur where the VOR may be functioning at ceiling. Future studies may need to explore the use of lower-frequency VOR stimuli to overcome this potential limitation.

Conclusion

Patients with VM do not have heightened VOR gain immediately following headshake in the inter-ictal phase. Other studies may wish to apply this protocol in patients with acute VM or use visual motion stimuli instead of headshaking to alter visuo-vestibular interactions. Understanding the pathophysiological mechanisms of VM and development of simple clinical biomarkers are urgently needed to ensure timely and accurate diagnosis of one of the most common episodic vestibular disorders.

Data availability statement

The raw data supporting the conclusions of this article will be made available by the authors, without undue reservation.

Ethics statement

The studies involving human participants were reviewed and approved by Northwest - Greater Manchester South Research Ethics Committee. The patients/participants provided their written informed consent to participate in this study.

Author contributions

PC, NK, QA, and DK: conceptualization. PP, SC, and LG: data collection. PP and PC: analysis and first draft. PC, QA, and DK: manuscript preparation and revision. All authors contributed to the article and approved the submitted version.

Conflict of interest

The authors declare that the research was conducted in the absence of any commercial or financial relationships that could be construed as a potential conflict of interest.

Publisher's note

All claims expressed in this article are solely those of the authors and do not necessarily represent those of their affiliated organizations, or those of the publisher, the editors and the reviewers. Any product that may be evaluated in this article, or claim that may be made by its manufacturer, is not guaranteed or endorsed by the publisher.

References

1. Qi XK, Zhao XQ. Multidisciplinary experts consensus for assessment and management of vestibular migraine. *Chin Med J.* (2019) 132:183–9. doi: 10.1097/CM9.0000000000000064

2. Li V, McArdle H, Trip SA. Vestibular migraine. *BMJ.* (2019) 366:l4213. doi: 10.1136/bmj.l4213

3. Lempert T, Olesen J, Furman J, Waterston J, Seemungal B, Carey J, et al. Vestibular migraine: diagnostic criteria. *J Vestib Res.* (2012) 22:167–72. doi: 10.3233/VES-2012-0453

4. Colombo B, Teggi R. Vestibular migraine: who is the patient? *Neurol Sci.* (2017) 38:107–10. doi: 10.1007/s10072-017-2882-0

5. Marcus DA, Furman JM, Balaban CD. Motion sickness in migraine sufferers. *Expert Opin Pharmacother.* (2005) 6:2691–7. doi: 10.1517/14656566.6.15.2691

6. Jeong SH, Oh SY, Kim HJ, Koo JW, Kim JS. Vestibular dysfunction in migraine: effects of associated vertigo and motion sickness. *J Neurol.* (2010) 257:905–12. doi: 10.1007/s00415-009-5435-5

7. Bednarczuk NF, Bonsu A, Ortega MC, Fluri AS, Chan J, Rust H, et al. Abnormal visuo-vestibular interactions in vestibular migraine: a cross sectional study. *Brain.* (2019) 142:606–16. doi: 10.1093/brain/awy355

8. Wang J, Lewis RF. Contribution of intravestibular sensory conflict to motion sickness and dizziness in migraine disorders. *J Neurophysiol.* (2016) 116:1586–91. doi: 10.1152/jn.00345.2016

9. King S, Wang J, Priesol AJ, Lewis RF. Central integration of canal and otolith signals is abnormal in vestibular migraine. *Front Neurol.* (2014) 5:233. doi: 10.3389/fneur.2014.00233

10. Tseng H-Z, Chao W-Y. Head-shaking nystagmus: a sensitive indicator of vestibular dysfunction. *Clin Otolaryngol Allied Sci.* (1997) 22:549–52.

11. Hain TC, Fetter M, Zee DS. Head-shaking nystagmus in patients with unilateral peripheral vestibular lesions. *Am J Otolaryngol.* (1987) 8:36–47. doi: 10.1016/S0196-0709(87)80017-0

12. Kim MB, Huh SH, Ban JH. Diversity of head shaking nystagmus in peripheral vestibular disease. *Otol Neurotol.* (2012) 33:634–9. doi: 10.1097/MAO.0b013e31824950c7

13. Choi JY, Jung I, Jung JM, Kwon DY, Park MH, Kim HJ, et al. Characteristics and mechanism of perverted head-shaking nystagmus in central lesions: video-oculography analysis. *Clin Neurophysiol.* (2016) 127:2973–8. doi: 10.1016/j.clinph.2016.07.003

14. Choi KD, Kim JS. Head-shaking nystagmus in central vestibulopathies. *Ann N Y Acad Sci.* (2009) 1164:338–43. doi: 10.1111/j.1749-6632.2008.03737.x

15. Yang TH, Lee JH, Oh SY, Kang JJ, Kim JS, Dieterich M. Clinical implications of head-shaking nystagmus in central and peripheral vestibular disorders: is perverted head-shaking nystagmus specific for central vestibular pathology? *Eur J Neurol.* (2020) 27:1296–303. doi: 10.1111/ene.14161

16. Lee SU, Kim HJ, Choi JY, Kim JK, Kim JS. Acute vestibular syndrome associated with anti-GQ1b antibody. *Neurology.* (2019) 93:e1085–92. doi: 10.1212/WNL.0000000000008107

17. Lee SU, Choi JY, Kim HJ, Kim JS. Recurrent spontaneous vertigo with interictal headshaking nystagmus. *Neurology.* (2018) 90:e2127–34. doi: 10.1212/WNL.0000000000005689

18. Minagar A, Sheremata WA, Tusa RJ. Perverted head-shaking nystagmus: a possible mechanism. *Neurology.* (2001) 57:887–9. doi: 10.1212/WNL.57.5.887

19. Lidvall HF. Mechanisms of motion sickness as reflected in the vertigo and nystagmus responses to repeated caloric stimuli. *Acta Otolaryngol.* (1962) 55:527–36. doi: 10.3109/00016486209127388

20. Mallinson AI, Longridge NS. Motion sickness and vestibular hypersensitivity. *J Otolaryngol.* (2002) 31:381–5. doi: 10.2310/7070.2002.34575

21. Olesen J. Headache Classification Committee of the International Headache Society (IHS) the international classification of headache disorders, 3rd edition. *Cephalalgia.* (2018) 38:1–211. doi: 10.1177/0333102417738202

22. Von Brevern M, Bertholon P, Brandt T, Fife T, Imai T, Nuti D, et al. Benign paroxysmal positional vertigo: diagnostic criteria. *J Vestib Res.* (2015) 25:105–17. doi: 10.3233/VES-150553

23. Halmagyi GM, Chen L, MacDougall HG, Weber KP, McGarvie LA, Curthoys IS. The video head impulse test. *Front Neurol.* (2017) 8:1. doi: 10.3389/fneur.2017.00258

24. Fujimoto C, Kawahara T, Yagi M, Murofushi T. Association between vestibular dysfunction and findings of horizontal head-shaking and vibration-induced nystagmus. *J Vestib Res.* (2020) 30:319–27. doi: 10.3233/VES-200721

25. Von Brevern M, Zeise D, Neuhauser H, Clarke AH, Lempert T. Acute migrainous vertigo: clinical and oculographic findings. *Brain.* (2005) 128:365–74. doi: 10.1093/brain/awh351

26. Rosengren SM, Colebatch JG, Young AS, Govender S, Welgampola MS. Vestibular evoked myogenic potentials in practice: methods, pitfalls and clinical applications. *Clin Neurophysiol Pract.* (2019) 4:47–68. doi: 10.1016/j.cnp.2019.01.005

frontiers | Frontiers in Neurology

TYPE Brief Research Report
PUBLISHED 09 November 2022
DOI 10.3389/fneur.2022.999419

OPEN ACCESS

EDITED BY
Miriam Welgampola,
The University of Sydney, Australia

REVIEWED BY
Maurizio Versino,
Humanitas Mater Domini, Italy
Yuka Shibata,
Hokkaido University, Japan
Philippe A. Salles,
Universidad de Santiago, Chile

*CORRESPONDENCE
Chong Kun Cheon
chongkun@pusan.ac.kr

SPECIALTY SECTION
This article was submitted to Neuro-Otology, a section of the journal Frontiers in Neurology

RECEIVED 21 July 2022
ACCEPTED 19 October 2022
PUBLISHED 09 November 2022

CITATION
Choi J-H, Kim HS, Oh EH, Lee JH and Cheon CK (2022) Cerebello-brainstem dominant form of X-linked adrenoleukodystrophy with intrafamilial phenotypic variability. *Front. Neurol.* 13:999419. doi: 10.3389/fneur.2022.999419

Cerebello-brainstem dominant form of X-linked adrenoleukodystrophy with intrafamilial phenotypic variability

Jae-Hwan Choi[1,2], Hyun Sung Kim[1], Eun Hye Oh[1], Jae Hyeok Lee[1,2] and Chong Kun Cheon[2,3]*

[1]Department of Neurology, Pusan National University School of Medicine, Pusan National University Yangsan Hospital, Yangsan, South Korea, [2]Research Institute for Convergence of Biomedical Science and Technology, Pusan National University Yangsan Hospital, Yangsan, South Korea, [3]Division of Medical Genetics and Metabolism, Department of Pediatrics, Pusan National University School of Medicine, Pusan National University Children's Hospital, Yangsan, South Korea

Objectives: This study aimed to describe the clinical and radiological characteristics of a cerebello-brainstem dominant form of X-linked adrenoleukodystrophy (X-ALD).

Methods: Three affected members from a family with cerebellar ataxia received full neurological, laboratory and radiological examinations. Genetic diagnoses were confirmed using whole-exome sequencing and protein structural modeling.

Results: All affected members presented with slurred speech, ataxia, and spasticity, but showed obvious differences in phenotypic severity and radiological findings. The levels of very long-chain fatty acids (VLCFA) were elevated in each member, while only one had adrenal dysfunction. Genetic analysis identified a hemizygous missense mutation (c.887A>G, p.Tyr296Cys) of the ATP-binding cassette subfamily D member 1 gene (*ABCD1*) in all affected members, which is likely to destabilize the overall structure of the ABCD1 protein.

Conclusions: We report a cerebello-dominant form of X-ALD caused by a missense variant in *ABCD1*. This report highlights intrafamilial phenotypic variability in X-ALD.

KEYWORDS

adrenoleukodystrophy, *ABCD1*, cerebellar ataxia, very long-chain fatty acids, phenotype

Introduction

X-linked adrenoleukodystrophy (X-ALD) is the most common peroxisomal disorder caused by mutations in the ATP-binding cassette subfamily D member 1 gene (*ABCD1*) of Xq28 (1). *ABCD1* encodes a peroxisomal membrane ABC transporter that is responsible for delivering very long-chain fatty acids (VLCFAs) into the peroxisomes for degradation (1, 2). Thus, defects in *ABCD1* lead to impaired peroxisomal β-oxidation and a subsequent accumulation of saturated VLCFAs in the blood and various tissues, including the adrenal cortex and nervous system.

Patients with ALD present various phenotypes depending on the tissues affected (1). Adrenomyeloneuropathy (AMN) and childhood cerebral ALD (CCALD) are the most common phenotypes. AMN is characterized by adult-onset slow progressive spastic paraplegia due to the involvement of the spinal cord and peripheral nerves, while the onset of CCALD occurs during childhood, with rapid neurological deterioration and progressive cerebral demyelination, which lead to a vegetative state within a few years. There are several additional ALD phenotypes, including adult cerebral ALD (ACALD), cerebello-brainstem dominant ALD, and isolated adrenocortical insufficiency (Addison-only). The cerebello-brainstem dominant form, in which the infratentorial structures are mainly involved, has been estimated to account for 1–2% of ALD, but may be underdiagnosed because patients present with progressive cerebellar dysfunction that mimics multiple system atrophy (MSA) or idiopathic late-onset cerebellar ataxia (ILOCA) (3–12). In addition, various phenotypes can be observed even within the same family, making it difficult to diagnose ALD (13–15).

Here, we present a cerebello-brainstem dominant form of X-ALD with diverse clinical and radiological manifestations in a Korean family.

Materials and methods

Subjects and clinical evaluation

Three members from two consecutive generations of a Korean family with ataxia were enrolled at Pusan National University Yangsan Hospital (Figure 1). Three affected members (proband, II-3, and II-6) received full neurological and neuro-otological evaluations by the authors (H.S.K and J.H.L). Eye movements including nystagmus, saccades, smooth pursuit, and vestibulo-ocular reflex (VOR) were recorded using three-dimensional video-oculography (SLMED, Seoul, Korea). Laboratory evaluations including thyroid and adrenal function, vitamin B12, and paraneoplastic antibody tests, a VLCFA assay, and radiological studies such as brain and spine MRI were performed to determine the etiology of cerebellar ataxia. Adrenal function was evaluated by measuring plasma adrenocorticotropic hormone (ACTH) and cortisol concentrations, and performing a rapid ACTH stimulation test. Nerve conduction studies (NCSs), pure tone audiogram (PTA), and fundus examinations were also conducted.

Molecular analysis

Whole-exome sequencing

Since gene tests for spinocerebellar ataxia types 1–3, 6, 7, and 17, dentatorubropallidoluysian atrophy, fragile X syndrome, and Friedreich's ataxia were all negative, we performed whole-exome sequencing as the next step. Pure genomic DNA was isolated from the peripheral blood leukocytes of the affected members using the QIAamp DNA Blood Midi Kit (Qiagen, Hilden, Germany) according to the manufacturer's protocols. Most of the exonic regions of∼22,000 human genes were captured using one of the following three kits, depending on when the patient was enrolled: Agilent Sure Select kit (version C2, December 2018), Twist capture kit (Twist Bioscience, San Francisco, CA, USA), or xGen Exome Research Panel v2 (Integrated DNA Technologies, Coralville, IA, USA). Sequencing was performed using a NovaSeq6000 device (Illumina, San Diego, CA, USA) with 150 bp paired-end reads. The binary base call sequence files generated by the NovaSeq6000 device were converted and demultiplexed to FASTQ files, which were aligned to the human reference genome (GRCh37/19 from NCBI, February 2009) to generate BAM files using BWAMEM (version 0.7.17). Aligned BAM files were sorted and extracted using the samtools stats software (version 1.9). Variant calling files were generated following the GATK Best Practices (GATK version 3.8). The mean coverage depth was 125X ($>$ 20 X $=$ 97%). Variant classification and interpretation were largely based on guidelines recommended by the American College of Medical Genetics and Genomics (ACMG). Mutation nomenclature was based on the cDNA reference sequences for *ABCD1* (NM_000033.4).

Validation by Sanger sequencing

Sanger sequencing was used to confirm the causative variants. All causative variants were bi-directionally sequenced using the PRISM BigDye Terminator Kit (version 3.1, Applied Biosystems, Foster City, CA, USA). The sequencing products were resolved on a PRISM 3130XL sequencer (Applied Biosystems) and the chromatograms were analyzed using Sequencher software (version 4.9, Gene Codes, Ann Arbor, MI, USA).

Protein structural modeling

Protein structural modeling was performed for *ABCD1* variants. The crystal structures of the wild-type *ABCD1* domains were generated using SWISS-MODEL (https://swissmodel.

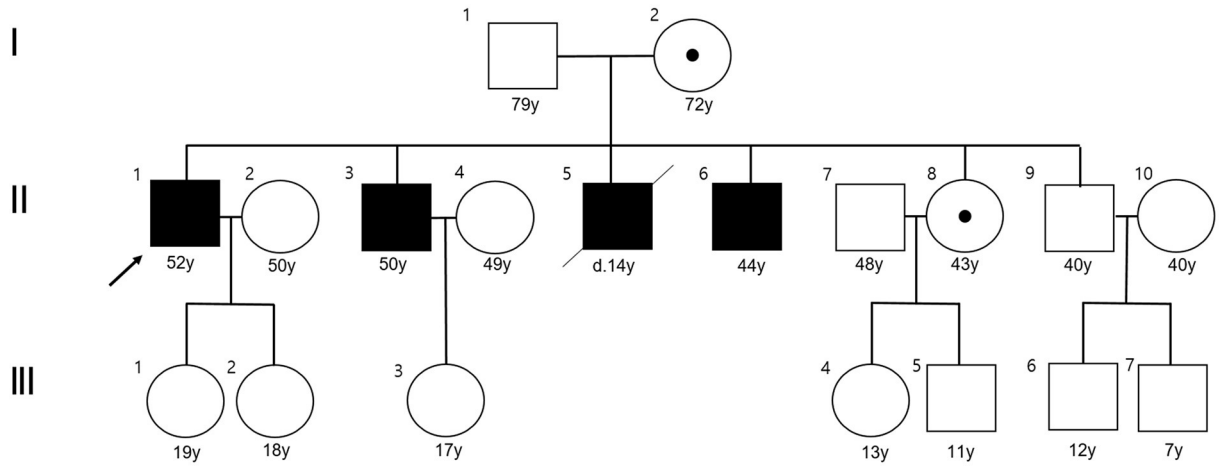

FIGURE 1
Pedigree of the present family. The proband is indicated by an arrow. Affected males are designated by filled symbols and the carrier female by circle with dot (squares for males and circles for females).

expasy.org/). Structural images were generated using PyMOL (version 29, https://pymol.org/2/).

Results

Clinical analysis

The clinical characteristics of the three affected members are listed in Table 1. Another member (II-5) had progressive gait disturbance and limb weakness from the age of 10 years, and died at 14 years.

The proband was a 52-year-old male who presented with dizziness, unsteadiness and dysarthria for 2 years, with gradual onset and progression. Neurological examinations indicated mild dysarthria and bilateral dysmetria in the upper and lower limbs. He was able to stand and walk without support, but had difficulties in tandem walking. Ocular motor tests revealed spontaneous right-beating horizontal nystagmus, hypermetric saccades, and abnormal smooth pursuit in bilateral horizontal directions, but normal VOR functions. He had bilateral spasticity and hyperreflexia in the lower limbs, but not cognitive impairment, motor weakness, sensory disturbance, or urinary dysfunction. Laboratory evaluations revealed a defective rise of the cortisol level in the ACTH stimulation test, and elevated levels of VLCFAs such as C26:0, and in the C24:0/C22:0 and C26:0/C22.0 ratios. There was a mild degree of right sensorineural hearing loss (SNHL) in PTA. NCS results were normal. Brain MRI showed symmetric T2-weighted hyperintensities in the dentate nuclei and the surrounding cerebellar white matter, but spine MRI results were unremarkable (Figure 2).

The younger brother of the proband (II-3) was a 50-year-old male with a 16-year history of gait disturbance and cognitive impairment. He developed unsteadiness, dysarthria, and left lower limb weakness at the age of 34 years, which gradually progressed over time, and became wheelchair-bound at 37 years. Brain MRI performed at 37 years old revealed brainstem and cerebellar atrophy with asymmetric T2-weighted hyperintensities in the middle cerebellar peduncles, cerebral peduncles, posterior limbs of the internal capsules, and periventricular white matter of the frontal lobe (Figure 2). An initial diagnosis of multiple sclerosis (MS) was made based on the symptoms and MRI findings. He visited our hospital at the age of 50 years, and the Mini-Mental State Examination applied at admission revealed difficulties in maintaining attention, performing calculations, and recalling registered three words. Neurological examinations showed bilateral dysmetria and pyramidal signs including spasticity and hyperreflexia that were severe in the left side. He had also dystonia in the left hand and weakness in the left lower limb. Laboratory evaluations indicated elevated VLCFA levels but normal adrenal function. PTA showed bilateral SNHL, especially at high frequencies. NCS results were normal. At the follow-up MRI performed when he was 49 years old, new white-matter hyperintensities were observed in the bilateral parieto-occipital lobes, but spine MRI results were unremarkable.

Another younger brother (II-6) was a 44-year-old male who presented with a 1-year history of progressive dizziness, unsteadiness, and dysarthria. Neurological examinations showed severe dysarthria and dysmetria in all limbs, and difficulties in standing and walking without support. Similar to the proband, ocular motor tests indicated spontaneous right-beating horizontal nystagmus, hypermetric saccades, and abnormal smooth pursuit. He had bilateral lower limb weakness (MRC grade 4) with spasticity and hyperreflexia, and urinary dysfunction, but not cognitive impairment or

10.3389/fneur.2022.999419

TABLE 1 Clinical characteristics of patients with X-linked adrenoleukodystrophy.

	Proband (II-1)	II-3	II-6
Sex/age (years)	Male/52	Male/50	Male/44
Age at onset (years)	50	34	43
Symptoms and signs			
MMSE	25/30	20/30	29–30
Dysarthria	(+)	(+)	(+)
Ocular motor dysfunction	Spontaneous right-beating nystagmus Hypermetric saccades Bilateral saccadic pursuit	(-)	Spontaneous right-beating nystagmus Hypermetric saccades Bilateral saccadic pursuit
Ataxia	(+)	(+)	(+)
SARA score	13.5	16	24
Motor weakness	(-)	(+), left lower limb	(+), both lower limbs
Spasticity	(+)	(+)	(+)
Extrapyramidal symptom	(-)	(+), left hand dystonia	(-)
Sensory disturbance	(-)	(-)	(-)
Urinary dysfunction	(-)	(-)	(+)
Hyperreflexia	(+)	(+)	(+)
VLCFA ratio			
C22:0 (μmol/L, normal range ≤96.3)	30.64	40.87	35.65
C24:0 (μmol/L, normal range ≤91.4)	64.24	76.93	61.34
C26:0 (μmol/L, normal range ≤1.3)	3.96	3.71	3.51
C24:0/C22:0 (normal range ≤1.39)	2.10	1.88	1.72
C26:0/C22:0 (normal range ≤0.023)	0.129	0.091	0.098
Adrenal impairment	Abnormal result for rapid ACTH test	(-)	(-)
Pure tone audiometry	Right SNHL (mild)	Both SNHL (high frequency)	Right SNHL (mild)
Nerve conduction study	No peripheral neuropathy	No peripheral neuropathy	Distal sensory neuropathy in upper limbs
Brain MRI	T2-weighted hyperintensities around the dentate nuclei (at the age of 52 years)	T2-weighted hyperintensities in the corticospinal tract and middle cerebellar peduncle (at the age of 37 years)	Diffuse T2-weighted hyperintensities in the midbrain, pons, middle cerebellar peduncle and cerebellum (at the age of 44 years)

ACTH, adrenocorticotropic hormone; MMSE, mini-mental state examination; SARA, scale for assessment and rating of ataxia; SNHL, sensorineural hearing loss.

sensory disturbance. Laboratory evaluations revealed elevated VLCFA levels but normal adrenal function. PTA indicated a mild right SNHL, and the NCS revealed distal sensory neuropathy in the upper limbs. Brain MRI showed diffuse T2-weighted hyperintensities in the midbrain, pons, middle cerebellar peduncle and cerebellum, while spine MRI results were unremarkable (Figure 2).

With patients only taking Lorenzo's oil for several months, it is still difficult to find improvements in neurological symptoms.

Molecular and structural impact of the variant proteins related to X-ALD

The whole-exome sequencing results revealed that the affected family members carried a hemizygous missense variant (c.887A>G, p.Tyr296Cys) of *ABCD1*, which was confirmed by Sanger sequencing (Figure 3A). The same variant was detected in a heterozygous state in the asymptomatic female carriers (I-2 and II-8). This variant has been previously reported in patients with X-ALD, and classified as pathogenic according to the ACMG criteria, but no functional evidence for this variation was found in the ClinVar database (16, 17).

The p.Tyr296 residue is located on ABC transporter transmembrane region 2. Protein crystallization revealed that the p.Tyr296Cys variant might affect the formation of weak hydrogen bonds between the surrounding residues (Figure 3B). Moreover, the p.Tyr296Cys variant was found to be causing changes in the vibration-related entropy change upon mutation, increasing molecular flexibility ($\Delta\Delta S_{vib}$ ENCoM: 0.121 kcal.mol^{-1}.K^{-1}), which might affect switching mechanism for providing different kinetic control for different transporters (Figure 3C).

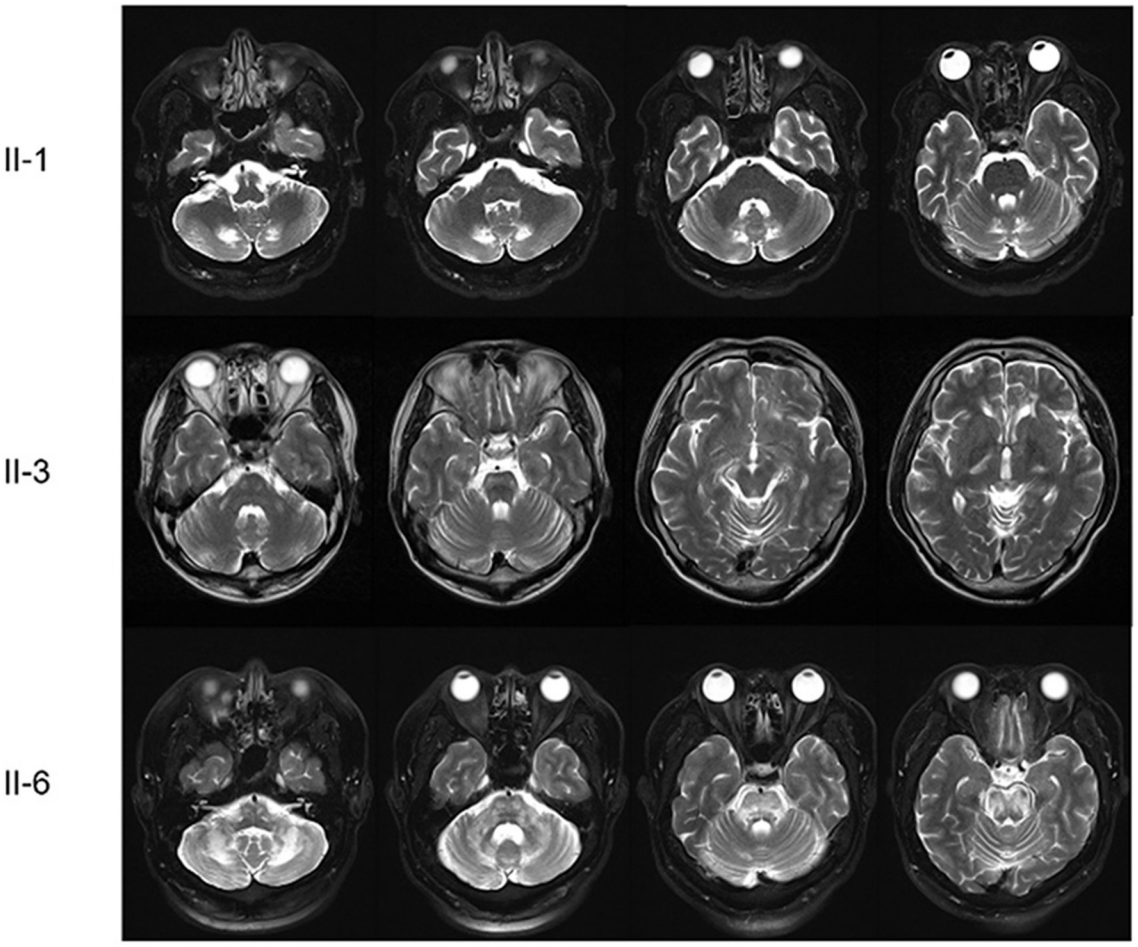

FIGURE 2
Brain MRI scans of the patients. The proband (II-1) had symmetric T2-weighted hyperintensities in the dentate nuclei and the surrounding cerebellar white matter. The first younger brother (II-3) presented brainstem and cerebellar atrophy with asymmetric T2-weighted hyperintensities in the middle cerebellar peduncles, cerebral peduncles, posterior limbs of the internal capsules, and periventricular white matter of the frontal lobe. The third younger brother (II-6) had diffuse T2-weighted hyperintensities in the midbrain, pons, middle cerebellar peduncle and cerebellum.

Discussion

All of the affected members in this family presented with slurred speech, ataxia, and spasticity with or without paraplegia, which were similar to the clinical manifestations of spastic ataxia or spinocerebellar ataxia. Although there were different findings on brain MRI among the affected members, an ALD diagnosis was suspected based on high VLCFA levels in the plasma, and finally confirmed by the detection of the *ABCD1* mutation.

ALD has a wide range of phenotypes according to the involved lesions (1). The cerebello-brainstem dominant form mainly involves the cerebellum and brainstem, and has been referred to by various names such as spinocerebellar variant, olivopontocerebellar form, and ataxic variant (3–12). This phenotype has been rarely reported in the literature, and is estimated to account for 1–2% of ALD cases. However, it may be underdiagnosed because the clinical features can resemble those seen in patients with MSA, ILOCA, and MS. Indeed, some patients who received antemortem clinical diagnose of olivopontocerebellar atrophy, MSA, MS, or schizophrenia were diagnosed with ALD at autopsy (3, 9–11). According to a review of 34 cases with the adult-onset cerebello-brainstem dominant form of ALD, the age at onset was 33 ± 11 years (mean ± SD), which was younger than that of MSA or ILOCA (3). The common clinical manifestations were cerebellar ataxia, gait disturbance, slurred speech, and pyramidal signs. About half of the patients had a family history of ALD or Addison's disease. VLCFA levels were elevated in all of these patients, and more than two-thirds of them presented adrenal insufficiency. T2-weighted hyperintensities in the internal capsule, brainstem, and/or cerebellum might be helpful in diagnosing this rare phenotype, but some patients

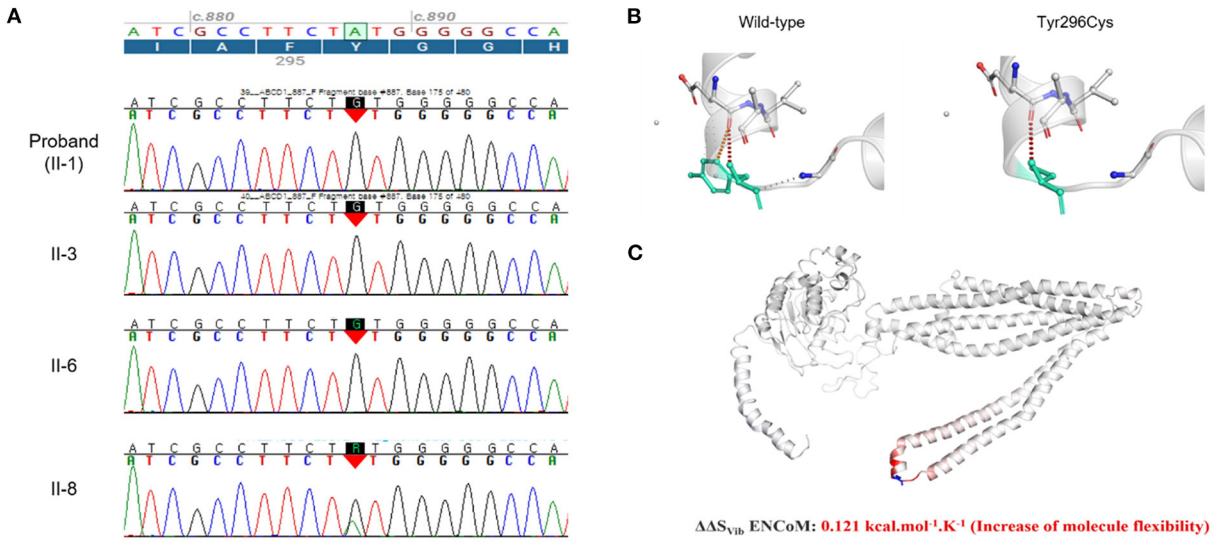

FIGURE 3
(A) Sanger sequencing confirmed a hemizygous missense variant (c.887A>G, p.Tyr296Cys) of the ATP-binding cassette subfamily D member 1 gene (*ABCD1*) (NM_000033.4) that had been identified using whole-exome sequencing for the genome of the affected members (II-1, II-3, and II-6). The same variant was detected in a heterozygous state in the asymptomatic female carrier (II-8). **(B)** Wild-type and mutant residues (p.Tyr296Cys) in the ABCD1 protein are colored light-green and represented as sticks alongside the surrounding residues, which were involved in any interaction type. Red dots are hydrogen bonds, with orange representing weak ones. The crystal structure of the domain from wild-type ABCD1 isoform 1 was generated using SWISS-MODEL (https://swissmodel.expasy.org/) and is depicted as a cartoon representation. **(C)** Results obtained using other predictive tools (NMA based and other structure-based approaches) are also displayed, which predict the effect of the mutation using the DynaMut web-server with the normal mode analysis function (http://biosig.unimelb.edu.au/dynamut/). Visual representation of the Δ vibrational entropy energy in which the amino acids are colored according to the vibrational entropy change upon mutation. Blue regions indicate rigidification and red regions indicate an increase in flexibility.

have been reported with brainstem or cerebellar atrophy but without typical T2-weighted hyperintensities on MRI.

Despite the presence of the same *ABCD1* mutation, there could be several different phenotypes within a family (13–15). A literature review found that about 38% of sibling pairs presented with different clinical types of ALD, and the degree of similarity between ages at onset was 55–60%, regardless of how closely related the family members were (13). In the present family, three affected members mainly showed the cerebello-brainstem dominant form of ALD, but had different clinical characteristics such as age at onset, disease severity, cognitive impairment, and motor weakness. The location and severity of T2-weighted hyperintensities also differed markedly among the family members. It was particularly interesting that the younger brothers (II-6 and II-8) displayed a far worse clinical phenotype than the proband (II-1) (the oldest brother) in terms of neurological symptoms and brain lesions, even though most of their VLCFA levels and ratios were lower than those of the proband. Therefore, it may be difficult to accurately reflect the severity of the disease based on only biochemical findings (1). The deceased member (II-5) was also suspected to have CCALD based on the early-onset and rapid neurological deterioration of their condition. Indeed, the same *ABCD1* mutation has been reported in other ALD phenotypes including CCALD, ACALD, and AMN (16, 17). The range of phenotypic expression, disease severity, and prognosis were unpredictably variable, and there were no obvious correlations between the phenotypes and genotypes of ALD. All of these findings suggest that modifier genes or epigenetic or environmental factors could underlie the high variability of clinical manifestations. A previous study found that decreased expression levels of another peroxisomal transporter gene (*ABCD4*) and VLCFA synthetase gene (*BG1*) tended to be correlated with disease severity in ALD (17). However, we could not detect any variant in modifier genes such as *ABCD2*, *ABCD3*, *ABCD4*, *BG1*, and *VLCS*. The molecular basis for the allelic heterogeneity of X-ALD is currently poorly understood. In order to explain the various clinical phenotypes in patients within the same household in detail, RNA sequencing-based transcriptome profiling analysis, bisulfite sequencing-based methylome profiling or ATAC-Seq-based open chromatin profiling analysis will be needed.

In conclusion, we have presented a cerebello-dominant form of X-ALD caused by a missense variant in *ABCD1*. This report highlights intrafamilial phenotypic variability in X-ALD, suggesting the existence of modifier genes or epigenetic or environmental factors. In addition, the cerebello-dominant form of X-ALD should be considered as a differential diagnosis of cerebellar ataxia, especially in cases with T2-weighted hyperintensities or atrophy in the brainstem or cerebellum on MRI.

Data availability statement

The datasets presented in this study can be found in online repositories. The name of the repository and accession numbers can be found below: National Center for Biotechnology Information (NCBI) GenBank, https://www.ncbi.nlm.nih.gov/genbank/Banklt2611441, OP204635-OP204637.

Ethics statement

All experiments followed the tenets of the Declaration of Helsinki, and written informed consent was obtained from the participants after the nature and possible consequences of this study had been explained. This study was approved by the institutional review boards of Pusan National University Yangsan Hospital (05-2022-157).

Author contributions

J-HC contributed to the collection, interpretation of the data, and wrote the manuscript. HSK, JHL, and EHO contributed to the interpretation and analysis of data. CKC conducted the design and conceptualization of the study, interpretaion of the data, and revised the manuscript. All authors contributed to the article and approved the submitted version.

Conflict of interest

The authors declare that the research was conducted in the absence of any commercial or financial relationships that could be construed as a potential conflict of interest.

Publisher's note

All claims expressed in this article are solely those of the authors and do not necessarily represent those of their affiliated organizations, or those of the publisher, the editors and the reviewers. Any product that may be evaluated in this article, or claim that may be made by its manufacturer, is not guaranteed or endorsed by the publisher.

References

1. Raymond GV, Moser AB, Fatemi A. X-Linked adrenoleukodystrophy. In: Adam MP, Mirzaa GM, Pagon RA, Wallace SE, Bean LJH, Gripp KW, Amemiya A, editors. *GeneReviews®*. Seattle, WA: University of Washington (1999).

2. Morita M, Shimozawa N, Kashiwayama Y, Suzuki Y, Imanaka T, ABC. subfamily D proteins and very long chain fatty acid metabolism as novel targets in adrenoleukodystrophy. *Curr Drug Targets.* (2011) 12:694–706. doi: 10.2174/138945011795378577

3. Ogaki K, Koga S, Aoki N, Lin W, Suzuki K, Ross OA, et al. Adult-onset cerebello-brainstem dominant form of X-linked adrenoleukodystrophy presenting as multiple system atrophy: case report and literature review. *Neuropathology.* (2016) 36:64–76. doi: 10.1111/neup.12230

4. Li JY, Hsu CC, Tsai CR. Spinocerebellar variant of adrenoleukodystrophy with a novel ABCD1 gene mutation. *J Neurol Sci.* (2010) 290:163–5. doi: 10.1016/j.jns.2009.12.002

5. Suda S, Komaba Y, Kumagai T, Yamazaki M, Katsumata T, Kamiya T, et al. Progression of the olivopontocerebellar form of adrenoleukodystrophy as shown by MRI. *Neurology.* (2006) 66:144–5. doi: 10.1212/01.wnl.0000191329.34585.15

6. Vianello M, Manara R, Betterle C, Tavolato B, Mariniello B, Giometto B. X-linked adrenoleukodystrophy with olivopontocerebellar atrophy. *Eur J Neurol.* (2005) 12:912–4. doi: 10.1111/j.1468-1331.2005.01134.x

7. Tan EK, Lim SH, Chan LL, Wong MC, Tan KP. X-linked adrenoleukodystrophy: spinocerebellar variant. *Clin Neurol Neurosurg.* (1999) 101:137–40. doi: 10.1016/S0303-8467(99)00028-1

8. Chen Y, Zhang J, Wang J, Wang K, A. Novel variant in ABCD1 gene presenting as adolescent-onset atypical adrenomyeloneuropathy with spastic ataxia. *Front Neurol.* (2018) 9:271. doi: 10.3389/fneur.2018.00271

9. Kuroda S, Hirano A, Yuasa S. Adrenoleukodystrophy-cerebello-brainstem dominant case. *Acta Neuropathol.* (1983) 60:149–52. doi: 10.1007/BF00685361

10. Takada K, Onoda K, Takahashi K, Nakamura H, Taketomi T. An adult case of adrenoleukodystrophy with features of olivo-ponto-cerebellar atrophy: I. Clinical and pathological studies. *Jpn J Exp Med.* (1987) 57:53–8.

11. Tateishi J, Sato Y, Suetsugu M, Takashiba T. Adrenoleukodystrophy with olivopontocerebellar atrophy-like lesions. *Clin Neuropathol.* (1986) 5:34–9.

12. Chen YH, Lee YC, Tsai YS, Guo YC, Hsiao CT, Tsai PC, et al. Unmasking adrenoleukodystrophy in a cohort of cerebellar ataxia. *PLoS ONE.* (2017) 12:e0177296. doi: 10.1371/journal.pone.0177296

13. Shibata Y, Matsushima M, Matsukawa T, Ishiura H, Tsuji S, Yabe I. Adrenoleukodystrophy siblings with a novel ABCD1 missense variant presenting with phenotypic differences: a case report and literature review. *J Hum Genet.* (2021) 66:535–7. doi: 10.1038/s10038-020-00866-x

14. Ozdemir Kutbay N, Ozbek MN, Sarer Yurekli B, Demirbilek H. A distinct clinical phenotype in two siblings with X-linked adrenoleukodystrophy. *Neuro Endocrinol Lett.* (2019) 40:36–40.

15. Mehrpour M, Gohari F, Dizaji MZ, Ahani A, Malicdan MC, Behnam B. An ABCD1 mutation (c253dupC) caused diverse phenotypes of adrenoleukodystrophy in an iranian consanguineous pedigree. *J Mol Genet Med.* (2016) 10:222. doi: 10.4172/1747-0862.1000222

16. Takano H, Koike R, Onodera O, Sasaki R, Tsuji S. Mutational analysis and genotype-phenotype correlation of 29 unrelated Japanese patients with X-linked adrenoleukodystrophy. *Arch Neurol.* (1999) 56:295–300. doi: 10.1001/archneur.56.3.295

17. Asheuer M, Bieche I, Laurendeau I, Moser A, Hainque B, Vidaud M, et al. Decreased expression of ABCD4 and BG1 genes early in the pathogenesis of X-linked adrenoleukodystrophy. *Hum Mol Genet.* (2005) 14:1293–303. doi: 10.1093/hmg/ddi140

frontiers | Frontiers in Neurology

TYPE Original Research
PUBLISHED 29 November 2022
DOI 10.3389/fneur.2022.1022362

OPEN ACCESS

EDITED BY
Alexander A. Tarnutzer,
University of Zurich, Switzerland

REVIEWED BY
Michael C. Schubert,
Johns Hopkins University,
United States
Sergio Carmona,
INEBA Institute of Neurosciences
Buenos Aires, Argentina

*CORRESPONDENCE
Xu Yang
yangxu2011@163.com

†These authors have contributed equally to this work and share first authorship

SPECIALTY SECTION
This article was submitted to Neuro-Otology, a section of the journal Frontiers in Neurology

RECEIVED 18 August 2022
ACCEPTED 08 November 2022
PUBLISHED 29 November 2022

CITATION
Feng Y, Zhao T, Wu Y, Ling X, Zhang M, Song N, Kim J-S and Yang X (2022) The diagnostic value of the ocular tilt reaction plus head tilt subjective visual vertical (±45°) in patients with acute central vascular vertigo. *Front. Neurol.* 13:1022362. doi: 10.3389/fneur.2022.1022362

The diagnostic value of the ocular tilt reaction plus head tilt subjective visual vertical (±45°) in patients with acute central vascular vertigo

Yufei Feng[1,2†], Tongtong Zhao[1,2†], Yuexia Wu[1], Xia Ling[1], Menglu Zhang[1,2], Ning Song[1], Ji-Soo Kim[3,4] and Xu Yang[1*]

[1]Department of Neurology, Aerospace Center Hospital, Peking University Aerospace School of Clinical Medicine, Beijing, China, [2]Department of Neurology, The First Affiliated Hospital of Jinzhou Medical University, Jinzhou, China, [3]Department of Neurology, Seoul National University College of Medicine, Seoul, South Korea, [4]Dizziness Center, Seoul National University Bundang Hospital, Seongnam, South Korea

Objectives: To investigate the localization diagnostic value of the ocular tilt reaction (OTR) plus head tilt subjective visual vertical (SVV) in patients with acute central vascular vertigo (ACVV).

Methods: We enrolled 40 patients with acute infarction, 20 with unilateral brainstem infarction (BI) and 20 with unilateral cerebellar infarction (CI). We also included 20 patients with unilateral peripheral vestibular disorders (UPVD) as the control group. The participants completed the OTR and SVV during head tilt (±45°) within 1 week of symptom onset.

Results: In patients with ACVV, including that caused by lateral medullary infarction (100%, 2/2), partial pontine infarction (21%, 3/14), and cerebellum infarction (35%, 7/20), we observed ipsiversive OTR, similar to that seen in UPVD patients (80.0%, 16/20). Some of the patients with medial medullary infarction (50%, 1/2), partial pons infarction (42%, 6/14), midbrain infarction (100%, 2/2), and partial cerebellum infarction (30.0%, 6/20) showed contraversive OTR. The skew deviation (SD) of the BI group with ACVV was significantly greater than that of the UPVD group (6.60 ± 2.70° vs. 1.80 ± 1.30°, $Z = -2.50$, $P = 0.012$), such that the mean SD of the patients with a pons infarction was 9.50° and that of patients with medulla infarction was 5.00°. In ACVV patients with no cerebellar damage, the area under the curve of the receiver operating characteristic curve corresponding to the use of SD to predict brainstem damage was 0.92 (95%CI: 0.73–1.00), with a sensitivity of 100% and a specificity of 80% when SD ≥ 3°. We found no statistical difference in SD between the UPVD and CI groups (1.33 ± 0.58° vs. 1.80 ± 1.30°, $Z = -0.344$, $P = 0.73$). Compared with the UPVD patients, the ACVV patients with a partial pons infarction (43%, 6/14, $\chi^2 = 13.68$, $P = 0.002$) or medulla infarction (25%, 1/4, $\chi^2 = 4.94$, $P = 0.103$) exhibited signs of the ipsiversive E-effect with the contraversive A-effect, while those with a partial medulla infarction (50%, 2/4), pons infarction (43%, 6/14), or cerebellar infarction (60%, 12/20) exhibited a pathological symmetrical increase in the E-effect.

Conclusions: The evaluation of OTR plus head tilt SVV (±45°) in vertigo patients is helpful for identifying and diagnosing ACVV, especially when SD is ≥ 3° or the E-effect is symmetrically increased.

KEYWORDS

central vascular vertigo, ocular tilt reaction, subjective visual vertical, skew deviation, A/E-effect, unilateral peripheral vestibular disorders

Introduction

Clinically, the incidence of dizziness/vertigo is high (1). According to population-based questionnaires, about 20–30% of people have experienced dizziness/vertigo (2). Studies have shown that at least 4 million patients in the United States visit the emergency department for acute dizziness/vertigo each year (3). Of these, about 1 million patients are routinely overtested to exclude malignant events such as stroke, even though one-third of strokes remain misdiagnosed (4, 5). The early and accurate identification of acute central vascular vertigo (ACVV) is thus an important issue for clinicians.

In recent years, with the rapid development of vestibular science, including clinical theories and related evaluation methods, it has become increasingly possible to accurately locate and diagnose vertigo/vestibular diseases. Studies have shown that evaluations based on the function of the otolith pathway, such as the ocular tilt reaction (OTR) test, are of great value in localizing and diagnosing vertigo-related issues affecting the central and peripheral areas (6). The OTR test includes head tilt (HT), skew deviation (SD), ocular torsion (OT), and subjective visual vertical (SVV) tilt. In previous studies, the rates of abnormal HT, SD, abnormal OT, and abnormal SVV in patients with acute peripheral vestibular syndrome were 4–20%, 14–29%, 19–82%, and 50.6–94% (7–11), respectively. The rates of abnormal HT, SD, abnormal OT, and abnormal SVV in ACVV patients were 3–38%, 29–31%, 57–83%, and 74.1–94% (12–14), respectively. The SVV is known to be the most sensitive index in the OTR. Although the degree of SD in the OTR has been found to be important in recent years, especially in the differentiation of peripheral and central diseases, its diagnostic value in assessing cerebellar damage is unclear. Furthermore, the prevalence of SD is low in both patients with peripheral and central vestibular disorders (12, 15). Korda et al. showed that the incidence of SD was 24% in patients with acute vestibular syndrome and 29% in those with stroke and that an SD > 3.3° had a high diagnostic value in identifying ACVV.

Head tilt SVV has also been found to be helpful in the localization and diagnosis of vertigo/vestibular diseases (16). However, whether it can be combined with the OTR to improve the localization and lateral diagnosis of peripheral and central damage has not been established. To address this, we assessed the diagnostic value of the traditional OTR plus head tilt SVV (±45°) in ACVV patients, including those with brainstem infarction (BI) and those with cerebellum infarction (CI). Our goal was to provide clinical evidence to facilitate the accurate diagnosis of ACVV.

Materials and methods

Participants and protocol

A prospective, cross-sectional study design was implemented in a tertiary hospital with an advanced vertigo center from April 8, 2021 to May 20, 2022. The target population was patients presenting for acute dizziness or vertigo. The inclusion criteria were: 1) Acute dizziness or vertigo; 2) Continuous dizziness or vertigo at the time of examination; 3) Age ≥ 18 years. The exclusion criteria were: 1) Dizziness or vertigo attributed to head trauma, orthostatic hypotension, or a known medical or neurologic disorder (e.g., hepatic encephalopathy, hydrocephalus); 2) Benign paroxysmal positional vertigo; 3) Severe new-onset with large lesions in MRI which could not cooperate with SVV and OTR tests; 4) Not cooperative to complete brain MRI; 5) Ophthalmoplegia which caused by lesions involving the oculomotor or trochlear nucleus, oblique neck, scoliosis or pelvic tilt that may affect the results of OTR/ head tilt SVV evaluation; 6) Incomplete data. Forty patients with ACVV (33 men, mean age 59.32, range: 38–75 years old) were finally enrolled (20 patients with acute unilateral BI and 20 patients with acute unilateral CI). Twenty patients with unilateral peripheral vestibular disorders (UPVD) (13 men, mean age 51.8, range: 28–66 years old) were also included as a control group. We also recruited 30 healthy subjects (16 men, mean age, 31.9 years old, range 22–63 years old) as the healthy control group. The diagnosis of BI and CI were confirmed by diffusion-weighted MRIs with an onset time ≤7 days. The diagnosis of UPVD was based on caloric canal paresis (CP) > 25%, indicating unilateral horizontal semicircular canal hypofunction, and onset time of spontaneous vertigo ≤7 days. All evaluations of OTR/ head tilt SVV (±45°) were performed during the acute phase (within 7 days from the symptom onset) with a mean interval of 4 days. To ensure the safety and reliability of the assessment, OTR/ head tilt

SVV (±45°) were evaluated by two experienced neurologists. The patient sat in the back of a chair seat (in the outpatient clinic or ward). One examiner helped the patient maintain the appropriate head position, and the other evaluated the patient in the order of HT, SD, head upright SVV, head tilt SVV (±45°), and OT. The time required to complete the above assessments is 15–25 min.

This study was approved by the Ethics Committee of Peking University Aerospace Clinic School of Medicine and was conducted in accordance with the Declaration of Helsinki.

HT

Before measurement, the patient was required to keep the body and head straight as far as possible while the examiner observed the patient's posture. If the height of the patient's shoulders was not at the same level, the patient was verbally prompted to adjust the height of the shoulders to keep the shoulders at the same level. After the adjustment, the examiner measured the angle between the sagittal axis of the patient's head and gravity with the protractor of the iPhone, which was the degree of head tilt. HT $> 2^{\circ}$ was defined abnormal (9).

OT

Fundus photography was performed using a Nonmyd α-DIII retinal camera (Kowa American Corporation). Before capturing the image, the patient was instructed to adapt to the darkroom for 5 min to ensure their pupils were enlarged. Their head was required to be completely upright, and fixation was required while capturing the image. After photographing one eye, the patient was instructed to rest for 3 min with his or her eyes closed. After pupil recovery, the other eye was photographed in the same way. Ocular torsion was determined by measuring the angle formed by a horizontal meridian running through the center of the disc and a straight line passing through the center of the disc and the fovea. A difference in the torsional degree between the two eyes $\geq 8.8^{\circ}$ was considered abnormal (12).

SD

A Maddox rod was placed in front of the patient's right eye, and they were asked to focus both eyes on a light source located 33 cm away.

If SD was absent, the points and lines were seen to coincide; If an SD was presented, it was abnormal, and the patients could detect the separation of the points and lines. When separation was detected, we capped the prism for quantification. When the point and the line of separation overlap, the degree of the prism was taken as the patient's SD (15).

SVV

The SVV was measured using VertiSVV (ZT-SVV-I, Shanghai ZEHNIT Medical Technology Co., Ltd., Shanghai, China). The system consists of a pair of Virtual Reality (VR) goggles, a wireless controller, and a laptop computer. The VR goggles display a luminous line in a completely dark background without visual cues. The VR goggles created a black visual field, and a yellow light bar with a length of 60 cm was projected into this field 2 meters away. The initial position was set to within ±25° (0° reflects the direction of gravity), and the participant adjusted the line's orientation by turning the knob of the wireless controller clockwise or counter-clockwise. Once the participant judges the luminous line to be aligned with true vertical, he or she confirms the position by pressing the confirm button on the wireless controller. The SVV angle and the head position of the subject were then recorded by the PC software (VertiPACS, ZEHNIT, Shanghai, China). We measured SVV in the head upright position, the head tilted to the right ear down 45° position (+45°), and the head tilted to the left ear down 45° position (−45°). The precision of the wireless controller was ± 0.1°. The examiner fixed the patient's head with both hands to complete the SVV measurements from all angles and controlled the change amplitude of the patient's head within ±1°. Each subject completed nine adjustments of the luminous line in each head position. After the subjects practiced the test twice, the test values were recorded and saved during the third trial to eliminate the influence of visual memory. The SVV adjustments were finally retained 7 times and averaged. In the healthy controls, the SVV was defined as positive when the tilt was rightward from the participant's perspective. However, to find the consistency between the SVV tilt side and the lesion side from the results of patients with left- and right-sided lesions, this paper specifies that positive SVV equates to roll-tilt toward the affected side ("ipsilesional"). In contrast, negative SVV is toward the patients' healthy side ("contralesional"). The head-upright SVV (HU-SVV) exceeding the range (−2.5 to +2.5°) was defined abnormal (17). We obtained the head tilt SVV(HT-SVV) errors by subtracting the SVV in the head upright position from that in the head tilted (±45°) positions. In both controls and patients, errors in HT-SVV were defined as negative values when the shift was in the opposite direction of head tilt, indicating the E-effect. Likewise, the errors in HT-SVV were defined as positive values when the shift induced by a head tilt in the same direction, indicating the A-effect (18). OTR was defined positive if a patient had any component of OTR (HT, SD, OT, and SVV).

TABLE 1 Prevalence of the components of OTR in three groups patients.

	BI($n = 20$)	CI($n = 20$)	UPVD($n = 20$)	P^*
Abnormal HT	20.0% (4/20)	5.0%(1/20)	25.0%(5/20)	0.305
SD	25.0%(5/20)	15.0%(3/20)	25.0%(5/20)	0.789
Abnormal OT	40.0%(8/20)	20.0%(4/20)	60.0%(12/20)	0.042
Abnormal HU-SVV	70.0%(14/20)	55.0%(11/20)	75.0%(15/20)	0.481
Ipsiversive OTR	25.0%(5/20)	35%(7/20)	80%(16/20)	0.001
Contraversive OTR	45.0%(9/20)	30%(6/20)	5%(1/20)	0.011

BI, brainstem infarction; CI, cerebellum infarction; HT, head tilt; HU-SVV, head upright subjective visual vertical; OT, ocular torsion; OTR, ocular tilt reaction; SD, skew deviation; UPVD, unilateral peripheral vestibular disorders. *based on Chi-square test.

Statistical analyzes

Statistical analyzes were performed using SPSS software (version 25.0, IBM SPSS Statistics, N.Y., USA). Continuous variables were expressed as the mean ± SD. Categorical variables were expressed as percentages. Data normality was determined using the Shapiro-Wilk test. We used an independent sample *t*-test or nonparametric Mann-Whitney test to compare the groups. The Chi-square (χ^2) test was also used for group comparisons, and Yates' continuity correction or Fisher's exact test was performed if necessary. All data were tested using two-sided tests, and $P < 0.05$ was considered statistically significant.

Results

Prevalence and lateralization of the OTR

The prevalence of abnormal HT, SD, abnormal OT, and abnormal HU-SVV tilt was 20.0, 25.0, 40.0, and 70.0%, respectively, in the BI group, 5.0, 15.0%, 20.0, and 55.0%, respectively, in the CI group, 25.0, 25.0, 60.0, and 75.0%, respectively, in the UPVD group (Table 1). The prevalence of abnormal OT in the UPVD group was significantly higher than in the CI group (60.0 vs. 20.0%, $\chi^2 = 6.997$, $P = 0.042$, Pearson Chi-square test). The prevalence of abnormal HT, SD, and abnormal HU-SVV tilt was not significantly different among the three groups ($P > 0.05$, Pearson Chi-square test, Figure 1).

OTR was ipsiversive in 25% (5/20) of the patients with BI (lateral medullary infarction (LMI) 2, pontine infarction 3), 35% (7/20) of the patients with CI (tonsil and biventer lobule 5, biventer lobule and inferior semilunar lobule 1, cerebellar middle peduncles 1), and in 80% (16/20) of the patients with UPVD. OTR was contraversive in 45% (9/20) of the patients with BI (medial medullary infarction (MMI) 1, pontine infarction 6, midbrain infarction 2), 30% (6/20) of the patients with CI (tonsils, biventer lobule, and inferior semilunar lobules 2, posterior paravermis 1, dentate nucleus 2, nodulus 1), and in 5% (1/20) of the patients with UPVD (Figure 2). The direction of the OTR was significantly correlated with the lesion side (Kappa = 0.862, $P < 0.05$, McNemar test).

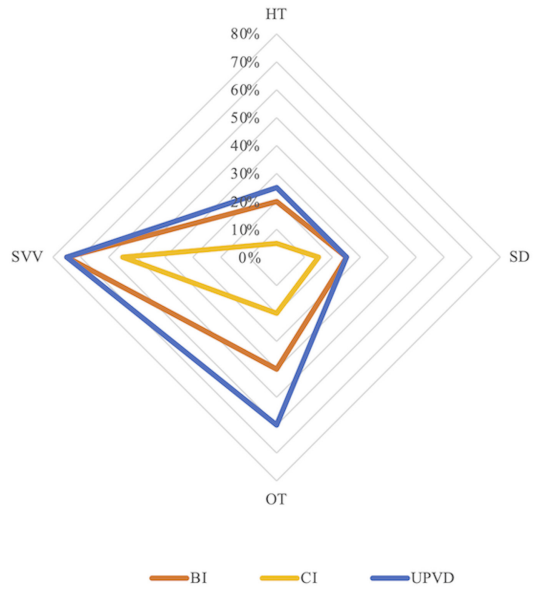

FIGURE 1
Prevalence of skew deviation (SD), ocular torsion (OT), head tilt (HT), and subjective visual vertical (SVV) tilt in the three groups. BI, brainstem infarction; CI, cerebellum infarction; UPVD, unilateral peripheral vestibular disorders.

Localization of the OTR

The SD in the BI group was significantly greater than that in the UPVD group (6.6 ± 2.7° vs. 1.8 ± 1.3°, $Z = -2.50$, $P = 0.012$, Mann-Whitney test). Further, the mean SD of the pontine infarction in the BI group was 9.5°, and that of the medullary infarction was 5.0°, which was significantly greater than that in the UPVD group ($Z = -2.10$, $P = 0.044$; $Z = -2.03$, $P = 0.042$, Mann-Whitney test). We found no statistical difference in SD between the UPVD and CI groups (1.3 ± 0.6° vs. 1.8 ± 1.3°, $Z = -0.344$, $P = 0.73$; Figure 3). Furthermore, the OT in the CI group was significantly smaller than that in the UPVD group (10.3 ± 10.4° vs. 5.6 ± 7.4°, $Z = -2.93$, $P = 0.03$, Mann-Whitney test), but the OT was not statistically different between the BI and the UPVD groups (10.3 ± 10.4° vs. 12.6 ± 9.7°, $Z = -1.011$, $P = 0.312$, Mann-Whitney test) and between the BI and the CI groups (10.3 ± 10.4° vs. 5.6 ± 7.4°, $Z = -0.624$, $P = 0.533$, Mann-Whitney test). There were no statistical differences in HT (5.1 ± 1.7° vs. 5.3 ± 1.9° vs. 4.0°, $H = 1.580$, $P = 0.450$, Kruskal-Wallis H test) or the degree of HU-SVV tilt (4.6 ± 5.5° vs. 3.1 ± 3.0° vs. 6.7 ± 5.7 °, $F = 1.17$, $P = 0.318$, one-way ANOVA) among the three groups (Table 2). To evaluate the

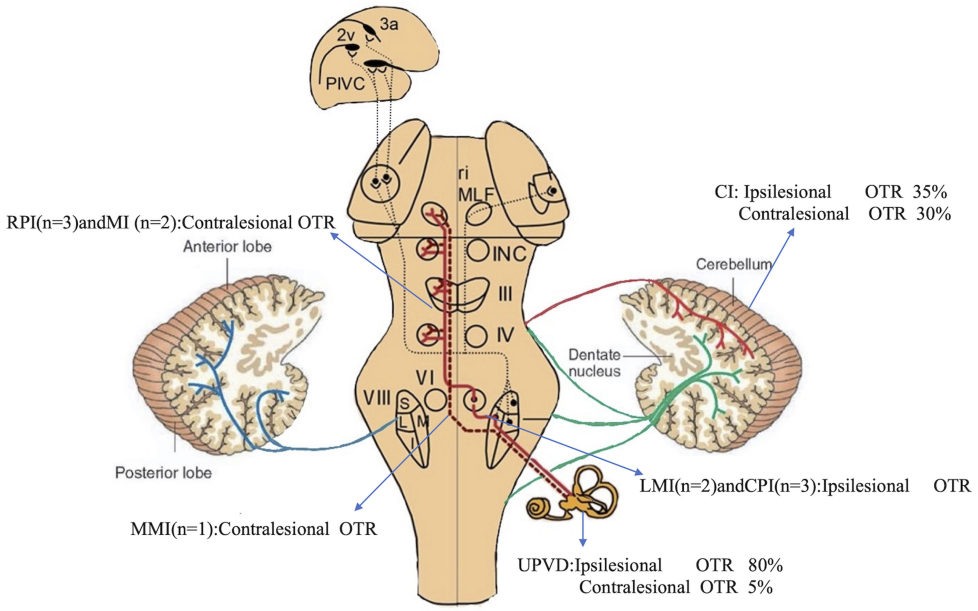

FIGURE 2
Incidence and direction of pathological OTR caused by different structural injuries. Pathways from the utricles and vertical semicircular canals mediate graviceptive function in the frontal roll plane. These pathways ascend from the vestibular nuclei (VIII) to the ocular motor nuclei, including the trochlear nucleus (IV), oculomotor nucleus (III), and abducens nucleus (VI). From here, they travel to the supranuclear centers of the interstitial nucleus of Cajal (INC), and the rostral interstitial nucleus of the medial longitudinal fasciculus (riMLF) in the midbrain tegmentum. RPI, rostral pontine infarction; CPI, caudal pontine infarction; MI, midbrain infarction; blue line, vestibulocerebellar fibers; green line, reticulocerebellar fibers; red line, pontocerebellar fibers [modified from Dieterich and Brandt (19)].

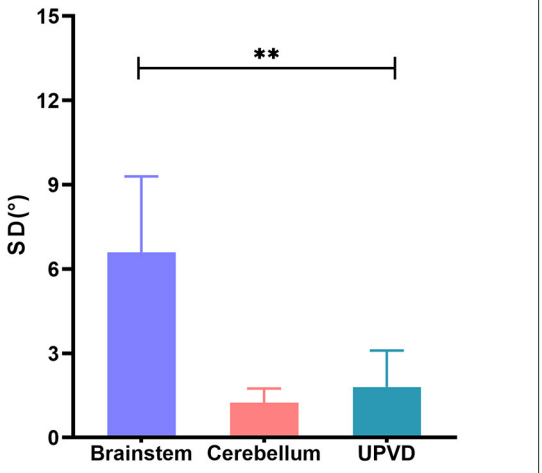

FIGURE 3
Comparison of SD of brainstem, cerebellum, and UPVD groups. SD, skew deviation; UPVD, unilateral peripheral vestibular disorders. **p < 0.05.

ability of SD to predict BI, we constructed receiver operating characteristic (ROC) curves and calculated the area under the curve (AUC) (Figure 4).

TABLE 2 Test results of components of OTR in three patient groups.

	BI	CI	UPVD	*p*
HT	$5.1 \pm 1.7°(n = 4)$	$4.0°(n = 1)$	$5.3 \pm 1.9°(n = 5)$	0.450[a]
SD	$6.6 \pm 2.7°(n = 5)$	$1.3 \pm 0.6°(n = 3)$	$1.8 \pm 1.3°(n = 5)$	0.012[b]
OT	$10.3 \pm 10.4°(n = 20)$	$5.6 \pm 7.4°(n = 20)$	$12.6 \pm 9.7°(n = 20)$	0.042[b]
HU-SVV	$4.6 \pm 5.5°(n = 20)$	$3.1 \pm 3.0°(n = 20)$	$6.7 \pm 5.7°(n = 20)$	0.318[c]

BI, brainstem infarction; CI, cerebellum infarction; HT, head tilt; HU- SVV, head upright subjective visual vertical; n, number of patients; OT, ocular torsion; SD, skew deviation; UPVD, unilateral peripheral vestibular disorders. [a]based on Kruskal-Wallis H test, [b]based on Mann-Whitney test, and [c]based on one-way ANOVA.

HT- SVV and E-effect/A-effect

In the individuals with pontine infarction ($N = 14$), the HT-SVV errors on the ipsilateral side were $-7.6 \pm 10.8°$, and that on the contralateral was $2.3 \pm 14.9°$. The incidence of bilateral E-effect, ipsiversive E-effect with contraversive A-effect, contraversive E-effect with ipsiversive A-effect, and bilateral A-effect were 43.0, 43.0, 0, and 14.0%, respectively. In the medullary infarction group ($N = 4$), the incidence of bilateral E-effect, ipsiversive E-effect with contraversive A-effect, contraversive E-effect with ipsiversive A-effect, and bilateral

A-effect were 50, 25.0, 0, and 25.0%, respectively. In the CI group, the ipsilateral HT-SVV errors were −7.9 ± 12.2°, and that of the contralateral side was −8.2 ± 10.9°. The incidences of bilateral E-effect, ipsiversive E-effect with contraversive A-effect, contraversive E-effect with ipsiversive A-effect, and bilateral A-effect were 60, 5, 15, and 20%, respectively. In the UPVD group, the ipsilateral HT-SVV errors were 1.8 ± 9.6°, and that on the contralateral side was −8.0 ± 10.1°. The overall performance indicated the presence of the contraversive E-effect with ipsiversive A-effect. The incidences of bilateral E-effect, ipsiversive E-effect with contraversive A-effect, contraversive E-effect with ipsiversive A-effect, and bilateral A-effect were 45.0, 0, 35.0, and 20.0%, respectively. We compared the differences in the incidence of the A/E-effects of HT-SVV (±45°) in the ACVV and UPVD groups using the Chi-square test. We found that 35% of the patients with UPVD (7/20) showed ipsiversive A-effect and contraversive E-effect while 43% of the patients with pontine infarction (6/14) and 25% of patients with medullary infarction (1/4) had ipsiversive E-effect and contraversive A-effect. The incidence of the ipsiversive E-effect with contraversive A-effect in patients with pontine infarction was significantly higher than that in the UPVD group ($\chi^2 = 13.68$, $P = 0.002$, Pearson Chi-square test; Figure 5).

Since most of the ACVV (75%, 15/20) and some of the UPVD (45%, 9/20) patients exhibited bilateral E-effects, we further analyzed the absolute value and symmetry of the bilateral E-effect in these patients. Specifically, in patients and healthy controls, the symmetry of the E-effect of HT-SVV when the head tilted to both sides is the intra-group comparison. The absolute value of the E-effect of patients with head tilt to both sides was compared with the mean of the absolute value of the E-effect of the healthy control group between groups. In the healthy control group, the range of the E-effect was 0.1–9.5°, and the mean absolute value of the bilateral E-effect was 4.5 ± 2.1°. The absolute value of the bilateral E-effect in the three groups was significantly higher than that in the healthy control group. Among the groups, the absolute value of the ipsilesional E-effect in the UPVD group was significantly higher than that of the contralesional E-effect, indicating an asymmetric E-effect. However, we found no significant difference in the absolute value of the bilateral E-effect between the BI and CI groups, showing a symmetrical increase in the pathological E-effect (Figure 6 and Table 3).

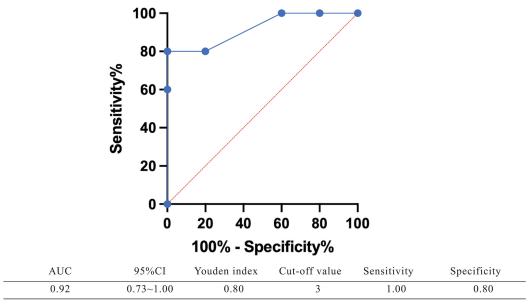

AUC	95%CI	Youden index	Cut-off value	Sensitivity	Specificity
0.92	0.73–1.00	0.80	3	1.00	0.80

FIGURE 4
The receiver operating characteristic (ROC) curve of using SD predicting brainstem damage. The area under the curve (AUC) of the receiver operating characteristic curve was 0.92 (95%CI: 0.73–1.00), with a sensitivity of 100% and a specificity of 80% when SD ≥ 3°.

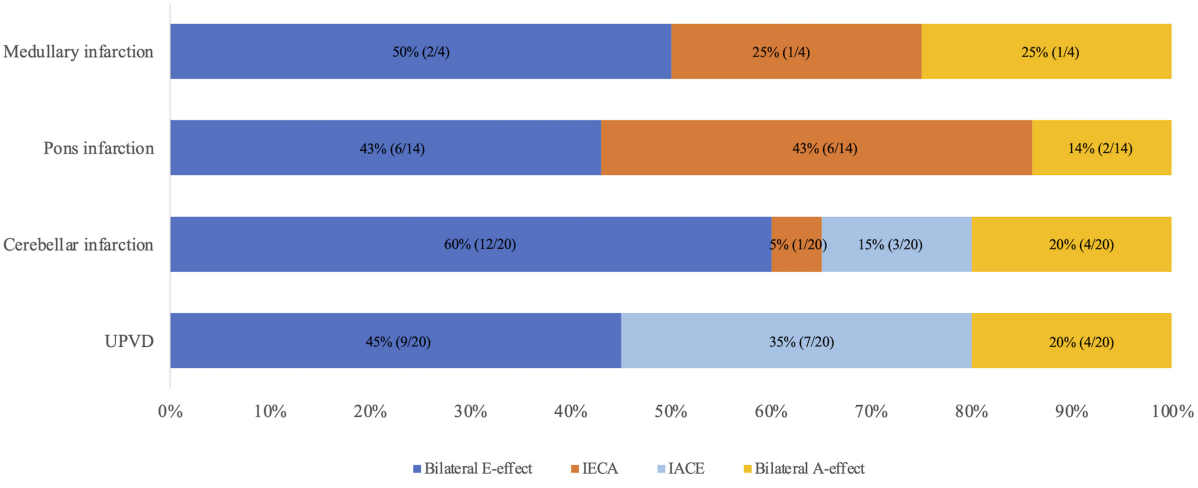

FIGURE 5
Distribution of A/E-effects of head tilt SVV (±45°) in medullary, pons, cerebellum, and UPVD groups. IECA, Ipsilesional E-effect contralesional A-effect; IACE, Ipsilesional A-effect contralesional E-effect; UPVD, unilateral peripheral vestibular disorders.

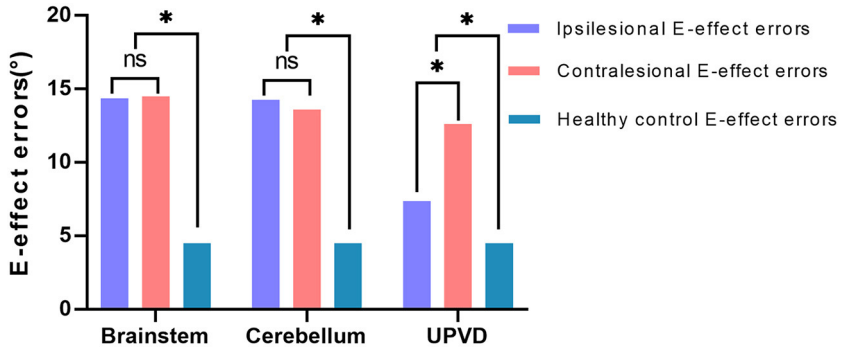

FIGURE 6
Difference analysis of the mean value of the bilateral E-effect in three patient groups. *$P < 0.05$. UPVD, unilateral peripheral vestibular disorders.

TABLE 3 Absolute values and symmetry analysis of the bilateral E-effect according to injury.

	Ipsilesional E-effect errors(°)	Contralesional E-effect errors(°)	*t*	*P*
BI ($n = 8$)	14.38 ± 8.91[a]	14.51 ± 8.59[a]	0.194	0.852
t	3.152	2.982		
P	0.016	0.020		
CI ($n = 12$)	14.27 ± 10.84[a]	13.61 ± 9.81[a]	0.310	0.762
t	3.135	3.230		
P	0.009	0.008		
UPVD($n = 9$)	7.38 ± 3.64[a]	12.63 ± 6.37[a]	2.391	**0.044**[b]
t	2.365	3.619		
P	0.041	0.006		

[a]There is a significant difference in the absolute value of the E-effect compared with the healthy control group.
[b]There is a significant difference in the absolute value of the E-effect between the ipsilesional and the contralesional sides. BI, brainstem infarction; CI, cerebellum infarction; UPVD, unilateral peripheral vestibular disorders.
The bold value means $P < 0.05$.

Discussion

As with UPVD patients, we found that certain patients with ACVV, including that caused by LMI (100%, 2/2), pontine infarction (21%, 3/14), and cerebellar infarction (35%, 7/20), showed ipsiversive OTR. However, other patients with ACVV caused by MMI (50%, 1/2), partial pontine infarction (42%, 6/14), midbrain infarction (100%, 2/2), and cerebellar infarction (30.0%, 6/20) showed contraversive OTR. The graviceptive brainstem pathways originate from the vestibular nuclei (VN), cross the midline at the pontine level, and ascend in the medial longitudinal fascicle to the interstitial nucleus of Cajal (INC) in the midbrain. Therefore, lesions involving the medulla or those caudal to the pons before decussation cause ipsiversive OTR, whereas lesions affecting the region rostral to the pons and midbrain cause contraversive OTR (10). The direction of OTR is often uncertain in patients with lesions at the pontomedullary junction (20–22). There are several reasons for this. First, the precise anatomical localization of the level of the crossing of the graviceptive pathways has not been conducted (23). Second, medullary lesions, such as medial and lateral lesions of the medulla, involve different vestibular structures (VN, nucleus prepositus hypoglossi, inferior cerebellar peduncle, etc.) and thus lead to different OTR patterns (20).

Of the patients with ipsiversive OTR, 2 had lesions of the lateral medulla, and 3 had lesions of the caudal pons. Of the patients with contraversive OTR, 2 had lesions of the midbrain, and 6 had lesions of the rostral pons, which is consistent with the previous theories regarding OTR (10). However, 1 patient with MMI had a different OTR pattern compared with the patients with LMI, and showed isolated contraversive SVV tilt without HT, SD, and OT. Previous studies have shown that contraversive SVV tilt can be observed in patients with isolated MMI, which may indicate a unilateral lesion of the graviceptive brainstem pathways after decussation at the pontomedullary junction (24).

Of the 6 patients with pontine infarction showing contraversive OTR, only 1 (16%) had isolated SVV tilt, and 5 (83%) had at least 2 (including SVV tilt and OT) or more components of the OTR. Of the 4 patients (20%) with brainstem infarction showing a complete OTR, 2 had lesions of the lateral medulla with ipsiversive OTR, 1 had a lesion of the pons and showed contraversive OTR with internuclear ophthalmoplegia, and 1 had a lesion of the midbrain and showed contraversive OTR. Brandt et al. (10) examined patients with acute unilateral brainstem infarctions. They revealed that pathological tilts of SVV (94%) and ocular torsion (83%) were the most sensitive tests, such that only 20% of the patients showed complete OTR, consistent with our results.

Studies have shown that the OTR of patients with cerebellar lesions does not have a directionality according to the lesion side. There are three possible reasons for this. First, lesions involving the nodulus/uvula may lead to contraversive OTR because of a

loss of inhibition over the ipsilesional VN (12, 25). Second, there are inhibitory projections from the dentate nucleus to the VN, and lesions of the dentate nucleus may lead to an increase in tonic resting activity in the ipsilesional VN because of a loss of inhibition. This could thus induce contraversive OTR (13). Third, as the lesions were mostly associated with the biventer lobule and inferior semilunar lobule when researchers observed ipsiversive signs of OTR, the disruption of inhibitory GABAergic efferents from the cerebellar cortex may enhance activity in the intact dentate nucleus and thus decrease tonic resting activity in the VN (13). This could lead to an ipsiversive OTR. Of the 6 patients with cerebellar infarcts showing contraversive OTR in our study, 1 had lesions of the unilateral nodulus/uvula and 2 had lesions of the dentate nucleus. This supports the hypothesis that lesions involving the dentate nucleus or nodulus/uvula may lead to disinhibition of the ipsilesional vestibular nuclear complex and result in contraversive OTR. The contraversive OTR observed in the 2 patients with large infarcts in the posterior inferior cerebellar artery (PICA) territory may be explained by damage to the afferent or efferent pathways to and from the dentate nucleus or nodulus/uvula (12, 13). We found that 1 patient with an isolated lesion in the posterior paravermis showed only contraversive SVV tilt. This suggests that midline structural components of the cerebellum other than the nodule/uvula and dentate nucleus may be involved in processing otolithic signals. Of the 7 patients with cerebellar infarction showing ipsiversive OTR in our study, 6 had lesions in the PICA territory, mostly involving the tonsils, biventer lobule, and inferior semilunar lobule, and 1 had a lesion of the middle cerebellar peduncle involving the anterior inferior cerebellar artery (AICA) territory. Hypoperfusion of the AICA might lead to infarction of its branch labyrinth artery, thus inducing ipsiversive OTR (26). Further studies are needed with a larger sample size to explore the precise localization of key cerebellar structures related to the OTR.

Recent studies have shown that SD is the only specific but non-sensitive (40%) sign of pseudoneuritis (27), and this has been incorporated into the bedside eye movement assessment (HINTS) conducted to differentiate between central and peripheral acute vestibular syndrome (28). Our study found that the frequency of SD was not high in ACVV patients. Instead, a minority of patients [brain stem infarction (25%, 5/25), cerebellar infarction (15%, 3/20), and UPVD (25%, 5/20)] had SD. Korda et al. (11) found that the SD prevalence was 24% in AUVP patients and 29% in stroke patients, consistent with our findings.

We used the monocular Maddox rod to examine SD and added a prism to correct vertical diplopia. In a previous study of 7 patients with acute vestibular neuronitis, all patients had a subtle 1 prism diopter hyperphoria that was only measurable with a Maddox rod test (15). This is consistent with our findings that UPVD patients have a small SD amplitude. The SD of the BI group was significantly greater than that of the UPVD group, and the AUC of the receiver operating characteristic curve corresponding to the use of SD to predict brainstem damage was 0.92, with a sensitivity of 100% and a specificity of 80% when SD $\geq 3^{\circ}$. In a previous study having adopted video-oculography to quantify SD, an SD greater than 3.3° corresponded to a specificity for predicting stroke of 98.1% and a sensitivity of 8.3%, similar to our findings (11). Patients with SD and central lesions have been found to exhibit impaired neural integration related to Listing's law, while there is no such related evidence for patients with peripheral lesions (29). This may be one of the reasons why the SD amplitude is larger in central lesion patients.

Our results indicate that SD has limited diagnostic value for patients with cerebellar lesions in ACVV. In a previous study of 27 patients with acute unilateral cerebellar infarction, no patients showed SD. In our study, only 3 patients (15%) with cerebellar infarcts showed SD, and the degree of SD was not different from that observed in UPVD patients. SD has been attributed to an afferent imbalance of utricular signals in oculomotor neurons through the brainstem or polysynaptic transmission through the cerebellum (30–32). Primary afferents arising from the utricle project to the second-order neurons in the VN, which then carry signals *via* the medial longitudinal fasciculus to the oculomotor and trochlear nuclei in the brainstem. The cerebellum also mediates the utricle-ocular reflex *via* a polysynaptic pathway, and primary utricular afferents have strong direct projections to the VN, cerebellar nodulus, and ventral uvula, with weaker projections to the anterior vermis, fastigial nuclei, and the flocculus and ventral paraflocculus (32, 33). There is an extensive projection network of otolithic signals within the cerebellum, and the cerebellum plays a critical role in sensorimotor signal transformation in the otolith-ocular pathway by computing an internal estimate of gravity (34, 35). Therefore, differences in SD in ACVV patients may be caused by differences in utricle-ocular reflex pathways involved in brainstem/cerebellar lesions.

SVV errors reflect challenges encountered by the brain in maintaining a common reference frame based on sensory information encoding eye, head, and body positions. Physiologically, SVV errors are biased toward the direction of the body position at tilt angles greater than 60° (known as the Aubert or A-effect). At tilt angles less than 60°, SVV errors are often biased in the opposite direction of the body position (known as the Müller or E-effect) (36). Otolithic inputs play a dominant role in the perception of verticality during small angle head tilts. Although prior studies have examined the mechanisms of the E- and A-effects, the origins of these effects are not well understood (18, 37).

In our study, we found that compared with the 35% of patients with UPVD (7/20) who showed an ipsiversive A-effect with a contraversive E-effect, among ACVV patients, the head tilt SVV ($\pm 45^{\circ}$) of 43% of the patients with pons infarction (6/14) and 25% of the patients with medulla infarction (1/4) exhibited the ipsiversive E-effect with a contraversive A-effect. The utricle responds to roll tilts and side-to-side translation of

the head, and the hair cells for opposing polarization are aligned on either side of the striola. The hair cells are oriented toward the striola, with a 3:1 preponderance of the units with ipsilaterally directed vectors (18). The medial and lateral portions of the utricle respond differently according to the vectors generated by different degrees of head tilt. When the head is tilted in the direction of the axis of polarity of a hair cell unit, that cell depolarizes and excites the afferent vestibular fibers (18). During linear acceleration of the head, some hair cells are depolarized while others on the opposite side of the striola are hyperpolarized (cross-striolar inhibition) (38). Small angle head tilts mainly excite the lateral portion of the utricle and induce a small deflection in the hair cells in the opposite direction of head movements. This can contribute to the E-effect (18). When a patient with UPVD slightly tilts their head to the ipsilesional side, afferent signals from the lateral portion of the ipsilesional utricle cannot be generated, while simultaneous inhibition through the commissural inhibition of the utricle in the ipsilesional ear does not occur. Thus, the disinhibited neuronal activities from the lateral portion of the contraversive utricle deviate the SVV in the direction of the head tilt, resulting in the A-effect (18). In ACVV patients with pontine or medullary lesions, we observed a contralateral A-effect. This may have been caused by the afferent signals the crossed to the contralateral side from the primary utricle through the medial longitudinal fasciculus at the pontomedulla junction.

In this study, we found that a considerable proportion of UPVD (35%, 7/20) and ACVV patients exhibited bilaterally pathological E-effects. Interestingly, compared with healthy subjects, UPVD patients showed an asymmetric increase in the pathological E-effect, such that the absolute value of the contraversive E-effect was significantly higher than the ipsiversive one. In contrast, ACVV patients exhibited a symmetrical increase in the pathological E-effect. The asymmetric increase in the E-effect in UPVD patients might have been related to the loss of one utricle, such that the remaining one becomes bidirectionally sensitive (this process is thought to occur within 6–10 weeks). In this case, hypersensitivity of the contraversive utricle makes the absolute value of the contraversive E-effect higher than the ipsiversive one (39). Consistent with our findings, a chronic unilateral vestibular hypofunction study found that the adjustment errors of ±45° SVV was asymmetric, leading the authors to reject the hypothesis that a constant offset is added to physiological deviations in SVV adjustments when roll-tilting occurs (40). Tarnutzer et al. (41) examined 6 patients with central vestibular pathway lesions and compared SVV measurements in different roll orientations (0°, ±45°, and ±90°) in the subacute state (4–33 day). They found that two patients with cerebellar lesions exhibited a bilateral increased E-effect, consistent with our findings of bilateral symmetrical E-effects in patients with cerebellar lesions. Vestibulo-cerebellar lesion-induced loss of inhibitory function in the vestibular graviceptive pathway might have resulted in a bilateral E-effect because of overestimation of the direction of gravity. We also found that in ACVV patients with LMI, the direction of the OTR was similar to that for patients with peripheral lesions. However, the SD and ±45°SVV showed a central pattern.

This is presumably because the secondary neurons in the vestibular nucleus directly receive the primary afferents from the utricle but are also involved in the central modulation and integration of these signals. Thus, the lesions in our patients appear to be characterized by a mixed pattern of peripheral and central vestibular dysfunction.

Limitations

There are some limitations to this study. First, we did not perform a follow-up assessment because of the cross-sectional design. Moreover, the sample size of this study was small, and it was a single-center study with the possibility of a selection bias. Further studies with a larger sample size are needed to explore the diagnostic value of OTR plus head tilt SVV (±45°) in ACVV patients.

Conclusions

The evaluation of OTR plus head tilt SVV (±45°) in vertigo patients is helpful for identification and diagnosis of ACVV, especially when SD $\geq$ 3° and the the E-effects are symmetrically increased.

Data availability statement

The original contributions presented in the study are included in the article/supplementary material, further inquiries can be directed to the corresponding authors.

Ethics statement

The studies involving human participants were reviewed and approved by Ethics Committee of Aerospace Center Hospital, Peking University Aerospace School of Clinical Medicine. The patients/participants provided their written informed consent to participate in this study.

Author contributions

XY designed the study. YF, TZ, YW, NS, and MZ performed the experiments and analyzed the data. YF and TZ drafted and prepared the manuscript. J-SK and XL corrected this manuscript. All authors read and approved the final manuscript.

Funding

This study was supported by the Hygiene and Health Development Scientific Research Fostering Plan of Haidian District Beijing (HP2021-03-50703).

Conflict of interest

The authors declare that the research was conducted in the absence of any commercial or financial relationships that could be construed as a potential conflict of interest.

Publisher's note

All claims expressed in this article are solely those of the authors and do not necessarily represent those of their affiliated organizations, or those of the publisher, the editors and the reviewers. Any product that may be evaluated in this article, or claim that may be made by its manufacturer, is not guaranteed or endorsed by the publisher.

References

1. Zwergal A, Dieterich M. Vertigo and dizziness in the emergency room. *Curr Opin Neurol.* (2020) 33:117–25. doi: 10.1097/WCO.0000000000000769

2. Geser R, Straumann D. Referral and final diagnoses of patients assessed in an academic vertigo center. *Front Neurol.* (2012) 3:169. doi: 10.3389/fneur.2012.00169

3. Kerber KA, Brown DL, Lisabeth LD, Smith MA, Morgenstern LB. Stroke among patients with dizziness, vertigo, and imbalance in the emergency department: a population-based study. *Stroke.* (2006) 37:2484–7. doi: 10.1161/01.STR.0000240329.48263.0d

4. Saber Tehrani AS, Coughlan D, Hsieh YH, et al. Rising annual costs of dizziness presentations to U.S. emergency departments. *Acad Emerg Med.* (2013) 20:689–96. doi: 10.1111/acem.12168

5. Newman-Toker DE, McDonald KM, Meltzer DO. How much diagnostic safety can we afford, and how should we decide? *A health economics perspective. BMJ Qual Saf.* (2013) 22 (Suppl 2):ii11–ii20. doi: 10.1136/bmjqs-2012-001616

6. Finke C, Ploner CJ. Pearls & oy-sters: vestibular neuritis or not?: the significance of head tilt in a patient with rotatory vertigo. *Neurology.* (2009) 72:e101–2. doi: 10.1212/WNL.0b013e3181a60a44

7. Strupp M. Otolith dysfunction in vestibular neuritis: recovery pattern and a predictor of symptom recovery. *Neurology.* (2008) 71:1928–9. doi: 10.1212/01.wnl.0000339401.71837.90

8. Faralli M, Ricci G, Manzari L, Zambonini G, Lapenna R, Pettorossi VE. Different time course of compensation of subjective visual vertical and ocular torsion after acute unilateral vestibular lesion. *Eur Arch Otorhinolaryngol.* (2021) 278:2269–76. doi: 10.1007/s00405-020-06312-0

9. Hirvonen TP, Jutila T, Aalto H. Subjective head vertical test reveals subtle head tilt in unilateral peripheral vestibular loss. *Eur Arch Otorhinolaryngol.* (2011) 268:1523–6. doi: 10.1007/s00405-011-1560-8

10. Brandt T, Dieterich M. Vestibular syndromes in the roll plane: topographic diagnosis from brainstem to cortex. *Ann Neurol.* (1994) 36:337–47. doi: 10.1002/ana.410360304

11. Korda A, Zamaro E, Wagner F, Morrison M, Domenico Caversaccio M, Sauter TC, et al. Acute vestibular syndrome: is skew deviation a central sign?. *J Neurol.* (2022) 269:1396–403. doi: 10.1007/s00415-021-10692-6

12. Choi SY, Lee SH, Kim HJ, Kim JS. Impaired modulation of the otolithic function in acute unilateral cerebellar infarction. *Cerebellum.* (2014) 13:362–71. doi: 10.1007/s12311-013-0544-1

13. Baier B, Bense S, Dieterich M. Are signs of ocular tilt reaction in patients with cerebellar lesions mediated by the dentate nucleus?. *Brain.* (2008) 131(Pt 6):1445–54. doi: 10.1093/brain/awn086

14. Glasauer S, Dieterich M, Brandt T. Neuronal network-based mathematical modeling of perceived verticality in acute unilateral vestibular lesions: from nerve to thalamus and cortex. *J Neurol.* (2018) 265(Suppl 1):101–12. doi: 10.1007/s00415-018-8909-5

15. Green KE, Gold DR. HINTS examination in acute vestibular neuritis: do not look too hard for the skew. *J Neuroophthalmol.* (2021) 41:e672–8. doi: 10.1097/WNO.0000000000001013

16. Yagi C, Morita Y, Kitazawa M, Nonomura Y, Yamagishi T, Ohshima S, et al. Head roll-tilt subjective visual vertical test in the diagnosis of persistent postural-perceptual dizziness. *Otol Neurotol.* (2021) 42:e1618–24. doi: 10.1097/MAO.0000000000003340

17. Sakagami M, Wada Y, Shiozaki T, Ota I, Kitahara T. Results of subjective visual vertical tests in patients with vertigo/dizziness. *Auris Nasus Larynx.* (2022) 49:342–6. doi: 10.1016/j.anl.2021.08.010

18. Kim SH, Kim JS. Effects of head position on perception of gravity in vestibular neuritis and lateral medullary infarction. *Front Neurol.* (2018) 9:60. doi: 10.3389/fneur.2018.00060

19. Dieterich M, Brandt T. Perception of verticality and vestibular disorders of balance and falls. *Front Neurol.* (2019) 10:172. doi: 10.3389/fneur.2019.00172

20. Cho KH, Kim YD, Kim J, Ye BS, Heo JH, Nam HS. Contraversive ocular tilt reaction after the lateral medullary infarction. *Neurologist.* (2015) 19:79–81. doi: 10.1097/NRL.0000000000000015

21. Yang TH, Oh SY, Kwak K, Lee JM, Shin BS, Jeong SK. Topology of brainstem lesions associated with subjective visual vertical tilt. *Neurology.* (2014) 82:1968–75. doi: 10.1212/WNL.0000000000000480

22. Kim SH, Park SH, Kim HJ, Kim JS. Isolated central vestibular syndrome. *Ann N Y Acad Sci.* (2015) 1343:80–9. doi: 10.1111/nyas.12712

23. Zwergal A, Cnyrim C, Arbusow V, et al. Unilateral INO is associated with ocular tilt reaction in pontomesencephalic lesions: INO plus. *Neurology.* (2008) 71:590–3. doi: 10.1212/01.wnl.0000323814.72216.48

24. Kim JS, Choi KD, Oh SY, Park SH, Han MK, Yoon BW, et al. Medial medullary infarction: abnormal ocular motor findings. *Neurology.* (2005) 65:1294–8. doi: 10.1212/01.wnl.0000180627.80595.10

25. Kim HA, Lee H, Yi HA, Lee SR, Lee SY, Baloh RW. Pattern of otolith dysfunction in posterior inferior cerebellar artery territory cerebellar infarction. *J Neurol Sci.* (2009) 280:65–70. doi: 10.1016/j.jns.2009.02.002

26. Naoi T, Morita M, Kawakami T, Fujimoto S. Ipsiversive ocular torsion, skew deviation, and hearing loss as initial signs of anterior inferior cerebellar artery infarction. *Intern Med.* (2018) 57:1925–7. doi: 10.2169/internalmedicine.0283-17

27. Cnyrim CD, Newman-Toker D, Karch C, Brandt T, Strupp M. Bedside differentiation of vestibular neuritis from central "vestibular pseudoneuritis". *J Neurol Neurosurg Psychiatry.* (2008) 79:458–60. doi: 10.1136/jnnp.2007.123596

28. Kattah JC, Talkad AV, Wang DZ, Hsieh YH, Newman-Toker DE. HINTS to diagnose stroke in the acute vestibular syndrome: three-step bedside oculomotor examination more sensitive than early MRI diffusion-weighted imaging. *Stroke.* (2009) 40:3504–10. doi: 10.1161/STROKEAHA.109.551234

29. Fesharaki M, Karagiannis P, Tweed D, Sharpe JA, Wong AM. Adaptive neural mechanism for Listing's law revealed in patients with skew deviation caused by brainstem or cerebellar lesion. *Invest Ophthalmol Vis Sci.* (2008) 49:204–14. doi: 10.1167/iovs.07-0292

30. Chandrakumar M, Blakeman A, Goltz HC, Sharpe JA, Wong AM. Static ocular counterroll reflex in skew deviation. *Neurology.* (2011) 77:638–44. doi: 10.1212/WNL.0b013e3182299f71

31. Schlenker M, Mirabella G, Goltz HC, Kessler P, Blakeman AW, Wong AM. The linear vestibulo-ocular reflex in patients with skew deviation. *Invest Ophthalmol Vis Sci.* (2009) 50:168–74. doi: 10.1167/iovs.08-2254

32. Wong AM. New understanding on the contribution of the central otolithic system to eye movement and skew deviation. *Eye (Lond).* (2015) 29:153–6. doi: 10.1038/eye.2014.243

33. Brodsky MC, Donahue SP, Vaphiades M, Brandt T. Skew deviation revisited. *Surv Ophthalmol.* (2006) 51:105–28. doi: 10.1016/j.survophthal.2005.12.008

34. MacNeilage PR, Glasauer S. Gravity perception: the role of the cerebellum. *Curr Biol.* (2018) 28:R1296–8. doi: 10.1016/j.cub.2018.09.053

35. Dakin CJ, Peters A, Giunti P, Day BL. Cerebellar degeneration increases visual influence on dynamic estimates of verticality. *Curr Biol.* (2018) 28:3589–3598.e3. doi: 10.1016/j.cub.2018.09.049

36. Kheradmand A, Winnick A. Perception of upright: multisensory convergence and the role of temporo-parietal cortex. *Front Neurol.* (2017) 8:552. doi: 10.3389/fneur.2017.00552

37. Saeys W, Herssens N, Verwulgen S, Truijen S. Sensory information and the perception of verticality in post-stroke patients. Another point of view in sensory reweighting strategies. *PLoS ONE.* (2018) 13:e0199098. doi: 10.1371/journal.pone.0199098

38. Uchino Y, Sato H, Kushiro K, Zakir M, Imagawa M, Ogawa Y, et al. Cross-striolar and commissural inhibition in the otolith system. *Ann N Y Acad Sci.* (1999) 871:162–72. doi: 10.1111/j.1749-6632.1999.tb09182.x

39. Lempert T, Gianna C, Brookes G, Bronstein A, Gresty M. Horizontal otolith-ocular responses in humans after unilateral vestibular deafferentation. *Exp Brain Res.* (1998) 118:533–40. doi: 10.1007/s002210050309

40. Müller JA, Bockisch CJ, Tarnutzer AA. Spatial orientation in patients with chronic unilateral vestibular hypofunction is ipsilesionally distorted. *Clin Neurophysiol.* (2016) 127:3243–51. doi: 10.1016/j.clinph.2016.07.010

41. Tarnutzer AA, Schuknecht B, Straumann D. Verticality perception in patients with lesions along the graviceptive pathways: acute deficits and subsequent compensation. *Schweizer Arch fur Neurol und Psychiatr.* (2011) 162:60–5. doi: 10.4414/sanp.2011.02242

Frontiers in Neurology

Explores neurological illness to improve patient care

The third most-cited clinical neurology journal explores the diagnosis, causes, treatment, and public health aspects of neurological illnesses. Its ultimate aim is to inform improvements in patient care.

Discover the latest Research Topics

See more →

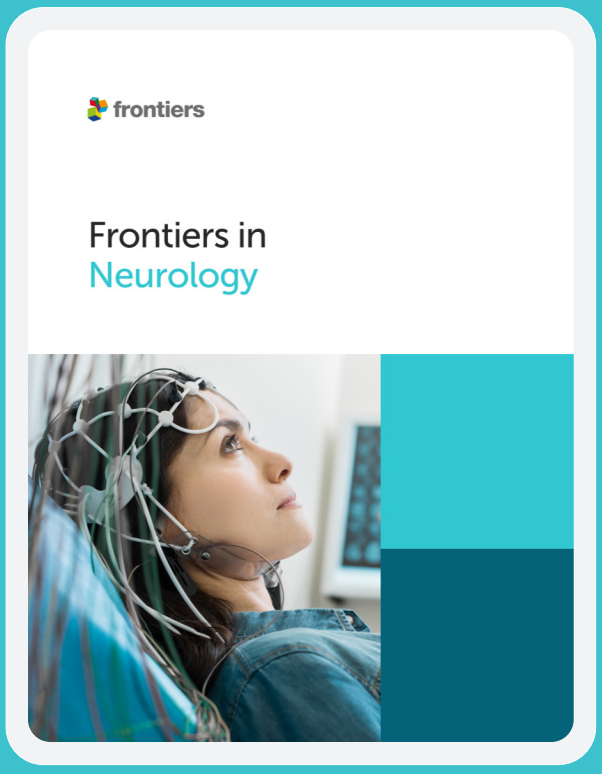

Frontiers

Avenue du Tribunal-Fédéral 34
1005 Lausanne, Switzerland
frontiersin.org

Contact us

+41 (0)21 510 17 00
frontiersin.org/about/contact